

NATIONAL  
SPACE  
SCIENCE  
DATA  
CENTER

IN-70-TM  
100035  
1980-70

WORLD DATA CENTER A for ROCKETS AND SATELLITES

86-04

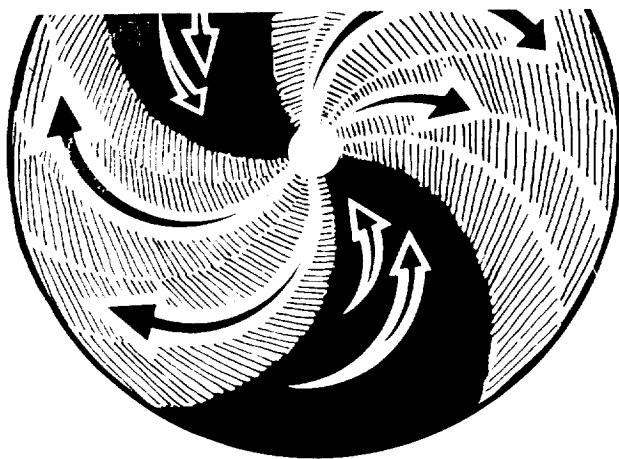
NASA-TM-89683

# Interplanetary Medium Data Book – Supplement 3, 1977–1985

(NASA-TM-89683) INTERPLANETARY MEDIUM DATA  
ECC. SUPPLEMENT 3: 1977-1985 (NASA) 246 p  
CSCL 03B

N89-10772

Unclassified  
G3/90 0114970



April 1986



National Aeronautics and  
Space Administration

Goddard Space Flight Center



*Interplanetary Medium Data Book - Supplement 3*

1977 - 1985

By

David A. Couzens

and

Joseph H. King

April 1986

National Space Science Data Center (NSSDC)/  
World Data Center A for Rockets and Satellites (WDC-A-R&S)  
National Aeronautics and Space Administration  
Goddard Space Flight Center  
Greenbelt, Maryland 20771



ACKNOWLEDGMENTS

The continuation of this Data Book series would be impossible if not for the sustained efforts of the GSFC, MIT, LANL and JPL groups in carefully analyzing and reducing their data and in making these data available to the NSSDC and hence to the solar terrestrial physics community.

Much of the computer programming for this supplement was performed by Howard A. Leckner. His thoroughness and perseverance are greatly appreciated.

PRECEDING PAGE BLANK NOT FILMED



## TABLE OF CONTENTS

	Page
Acknowledgments .....	iii
Introduction .....	1
Data Sources for This Supplement .....	1
Systematic and Random Differences Between Data Sets .....	2
Time Shifting of ISEE 3 Data .....	3
Cross-Normalization of Data Sets .....	21
Data Coverage .....	28
Data Presentation .....	28
Additional Data Availability .....	28
Intensity Versus Time Profiles .....	32

## LIST OF TABLES

Table 1. Data Sources for This Supplement .....	2
Table 2. Summary of Hourly Z-Function Information .....	18
Table 3. Scatter Function Ratios for ISEE 3 vs. IMP 8 Plasma Parameters .....	19
Table 4. MIT vs. LANL Scatter Functions - IMP 8 .....	20
Table 5. IMP 8 vs. ISEE 3 IMF Regression Parameters .....	21
Table 6. Flow Speed Regressions .....	23
Table 7. Density Regressions .....	24
Table 8. Temperature Regressions .....	25
Table 9. Normalization Parameters for N and T .....	26

LIST OF FIGURES

Figure 1. Scatter plot and best fit regression line for IMP 8 and ISEE 3 $B_z$ 5-min values, Feb. 6 - Mar. 7, 1979 .....	4
Figure 2. Scatter functions, corotation shift, 5-min analysis .....	6
Figure 3. Histograms of scatter function ratios .....	8
Figure 4. Scatter functions, corotation shift, 1-hr. analysis .....	10
Figure 5. Scatter plot and best fit regression line for IMP 8 and ISEE 3 $B_x$ hourly averages, Aug. 78 - June 79 .....	11
Figure 6. Scatter plot and best fit regression line for IMP 8 and ISEE 3 $B_y$ hourly averages, Aug. 78 - June 79 .....	12
Figure 7. Scatter plot and best fit regression line for IMP 8 and ISEE 3 $B_z$ hourly averages, Aug. 78 - June 79 .....	13
Figure 8. Scatter plot and best fit regression line for IMP 8 and ISEE 3 hourly averaged field magnitudes, Aug. 78 - June 79 .....	14
Figure 9. Scatter plot and best fit regression line for IMP 8 and ISEE 3 hourly averaged speeds, Aug. 78 - Feb. 80 .....	15
Figure 10. Scatter plot and best fit regression line for IMP 8 and ISEE 3 logarithms of hourly averaged densities, Aug. 78 - Feb. 80 .....	16
Figure 11. Scatter plot and best fit regression line for IMP 8 and ISEE 3 logarithms of hourly averaged temperature, Aug. 78 - Feb. 80 .....	17
Figure 12. Plot of yearly IMP(MIT) and IMP(LANL) plasma parameter averages .....	27
Figure 13. Histogram of IMF and plasma parameter coverage from 1963 to 1985 .....	29

INTERPLANETARY MEDIUM DATA BOOK - SUPPLEMENT 3

1977 - 1985

ABSTRACT

The updating of the hourly resolution near-Earth solar wind data compilation is discussed. Data plots and listings are then presented. In the text, the time shifting of ISEE 3 magnetic field and plasma data, using corotation delay is explained in detail. Normalizations of IMP(MIT), ISEE 3, and ISEE 1 temperatures and densities to equivalent IMP(LANL) values are also discussed. The levels of arbitrariness in combining data sets, and of random differences between data sets, are elucidated.



## Introduction

In previous issues of this series, hourly averaged interplanetary magnetic field and plasma parameters have been listed and plotted. These parameters have come from a number of spacecraft in the near-Earth solar wind. Data for 1963-1975 were contained in the *Interplanetary Medium Data Book* (NSSDC/WDC-A-R&S 77-04, 1977), data for 1975-1978 were published in the *Interplanetary Medium Data Book - Supplement 1* (NSSDC/WDC-A-R&S 79-08, 1979) and data for 1978-1982 were published in the *Interplanetary Medium Data Book - Supplement 2* (NSSDC/WDC-A-R&S 83-01, 1983). This third supplement represents an extension of the earlier compilations to 1985. Supplement 3 supersedes Supplement 2 in terms of both the data and the discussion. It begins in 1977 in order to incorporate ISEE 1 data, and corrects previously announced errors published in Supplement 2 which affected values of  $B_y$  (GSM) and  $B_z$  (GSM) in 1980 to 1982 and some  $B_y$  (GSE) values in mid-1980. Because of its size, this supplement has been published in two volumes. The first volume (Supplement 3) contains descriptive information and 27-day plots of various parameters. Listings of selected parameters are contained in Supplement 3A. Copies of all the books in this series, as well as the parent OMNI tape from which the listings and plots are generated, are available from the National Space Science Data Center (NSSDC). These data (from 1976 onward) are also accessible online through the NSSDC VAX. Access procedures are described subsequently.

## Data Sources for this Supplement

Data for this supplement come from the IMP 8, ISEE 3 and ISEE 1 spacecraft. IMP 8 was launched on October 26, 1973, and is in a low eccentricity,  $\sim 30\text{Re} \times 40\text{ Re}$ , 12.5-day geocentric orbit. IMP 8 is in the solar wind for a duration of 6 to 8 days per orbit. ISEE 3 was launched on August 12, 1978. Until mid-1982 it orbited the Earth-sun libration point approximately 240 Earth radii sunward of the earth, ranging up to 100 Re from the Earth-sun line. ISEE 3 was then redirected into the Earth's geotail. It sampled the solar wind for a large portion of 1982 and for portions of 1983. Launched on October 22, 1977, ISEE 1 has a highly elliptical orbit with an apogee of 23 Re and a period of about 57 hours. Usually ISEE 1 only enters the solar wind from August through December where it can spend up to 30 or more hours of each orbit in the interplanetary medium. As of early 1986, IMP 8 and ISEE 1 continue to provide near-Earth data.

The six data sets folded into this compilation are identified in Table 1. Some of the plasma data attributed to Los Alamos IMP 8 actually were provided as a mix of Los Alamos IMP 6, IMP 7 and IMP 8 data. All ISEE 1 and IMP 8 plasma parameters are based on ion measurements. ISEE 3 plasma parameters are based on ion measurements through day 48, 1980 (at which time the ion portion of the instrument failed), and electron measurements after this time. When both ISEE 3 and IMP 8 (field or plasma) data were available for a given hour, the IMP data were used in this compilation due to IMP's greater proximity to the Earth. When both MIT and LANL IMP 8 plasma data were available, the MIT data were chosen for historical reasons. ISEE 3 plasma data were chosen preferentially to ISEE 1 plasma data because of the availability of additional statistical and flow direction parameters.

TABLE 1. Data Sources for this Supplement

Spacecraft		Principal Investigator	Time Span (YR/DOY)
Magnetic Fields	IMP 8	N. F. Ness (GSFC)	73/302 --- 85/091
	ISEE 3	E. J. Smith (JPL)	78/225 --- 83/365
Plasma	IMP 8	H. S. Bridge (MIT)	73/334 --- 85/107
	IMP 8	S. J. Bame (LANL)	71/076 --- 84/357
	ISEE 3	S. J. Bame (LANL)	78/228 --- 82/279
	ISEE 1	S. J. Bame (LANL)	77/303 --- 79/365

\* Key scientists associated with the reduction of these data include R. P. Lepping, B. T. Tsurutani, J. D. Sullivan, A. J. Lazarus, J. A. Gosling, W. C. Feldman, and R. D. Zwickl.

#### Systematic and Random Differences Between Data Sets

The principal task in interspersing data from different sources is to make the data sets as compatible as possible. Thus, a data compilation is desired in which small amplitude, long term changes, and larger amplitude, short term changes may be studied with relatively high confidence levels. Absolute values of parameters, and small amplitude, hourly changes are less accurately determined, especially when more than one data source is involved.

There may be random differences and systematic differences between data sets. Systematic differences result from calibration errors in one or both data sets. In this context, "calibration" implies the whole process of transforming the electrical output of a sensor or sensors measuring some physical parameter to a declaration of what the physical parameter value is.

Random differences occur at least in part because two instruments may be measuring at different times or places, in the presence of temporal evolution or spatial gradients in the parameter being measured. In the case of hourly averages, differing parts of an hour may have been measured by two experiments. Random differences may also arise from the use of the differing instrumentation and data analysis technique, which has been discussed by Neugebauer (*Sp. Sci. Rev.*, 33, 127, 1982).

When a regression analysis is performed between two data sets of "simultaneously measured" parameter values, the deviation of the regression line from  $Y = X$  gives a measure of the systematic difference between data sets, and the scatter of data points about the regression line gives a measure of the random difference. For the case of ISEE 3, data must first be time shifted to expected Earth arrival times. If this is not done, the random differences found by regressing IMP 8 and ISEE 3 parameters are not irreducible. This is because the ISEE 3 to IMP 8 transit time is comparable to the hourly time resolution used in this compilation.

For those parameters for which systematic differences are comparable to or greater than the random differences, a cross-normalization of data sets is performed. It has been found that only density and temperature need to be

cross-normalized. That is, IMF parameters and flow speed had systematic differences significantly less than random differences. The decisions as to which data set to normalize to which other data set involved a certain arbitrariness, which was discussed in the original Data Book and Supplement 1.

#### Time Shifting of ISEE 3 Data

Either or both of two approaches to time-shifting ISEE 3 fine scale data may be expected to yield statistically irreducible random errors. (There are random differences between two sets of observations and random errors between either set of observations and the "true" values.) These approaches are corotation and convection. Consider initially the first of these. The corotation delay equation is:

$$\tau = \frac{X}{V} \left\{ \frac{1 + \frac{V}{R\Omega} \frac{Y}{X}}{1 - \frac{V_e}{R\Omega}} \right\}$$

In this equation,  $\tau$  is the time shift,  $X$  and  $Y$  are the ecliptic plane projections of the geocentric ISEE 3 position vector along and across the Earth-sun line,  $V$  is the measured solar wind speed (assumed radial),  $R\Omega$  is the equivalent speed of solar rotation at 1 AU (~428 km/s), and  $V_e$  is the orbital speed of the Earth (~30km/s).

Use of the corotation delay equation would be completely correct if the constant-phase surfaces of all solar wind variations were normal to the ecliptic plane and aligned with the ideal spiral interplanetary magnetic field (IMF) direction, and if solar wind variations had no temporal evolution on the ISEE-to-Earth transit time scale nor spatial gradients transverse to the Earth-sun line on scales less than  $\sim 100$  Re. None of these required conditions is satisfied by all solar wind variations. Thus, random errors are an inevitable part of the inference of near-Earth solar wind parameter values from ISEE 3 data and the corotation delay equation.

A study of these errors was begun by comparing "simultaneous" 5-min-averaged ISEE 3 and IMP 8 field and plasma data. Simultaneity here implies that the IMP 8 time is within 2.5 min of the corotation-shifted ISEE 3 time. In this analysis, the  $X$  and  $Y$  of the corotation delay equation relate to the ISEE-IMP separation vector rather than to the geocentric ISEE position vector.

Figure 1 shows a scatter plot of simultaneous, 5-min averaged ISEE 3 and IMP 8 measurements of the  $Z$ (GSE) component of the IMF. These data were taken between day 36 and 66 of 1979, when ISEE 3 was within 50  $R_e$  of the Earth-sun line. There are 1867 data points included. The regression line determined by minimizing the sum of squares of perpendicular distances between data points and regression line is shown on the figure. That the regression line is not  $Y = X$  relates to systematic differences and will be addressed in the next section. Of principal interest here is the scatter of points about the regression line. The rms perpendicular distance between data points and regression line (labelled RMS PERP DIST OF PTS ABT LINE on the plot and called the "scatter function" for convenience in the following) is 1.35 nanoTeslas (nT). This means that for a given ISEE 3 5-min observation of  $B_z$ , IMP 8 would

PARAMETER : BZ - GSE  
TIME SPAN IS: 79036 TO 79066  
NO. OF PTS: 1867  
SHIFT TYPE: COROTATION  
AVERAGES: IMP 0.76 ±5.05  
: ISEE 0.77 ±5.18

$$BZ-IMP = 0.01 (\pm 0.03) + 0.97 (\pm 0.01) \times BZ-ISEE$$

RMS PERP DIST OF PTS ABT LINE: 1.35

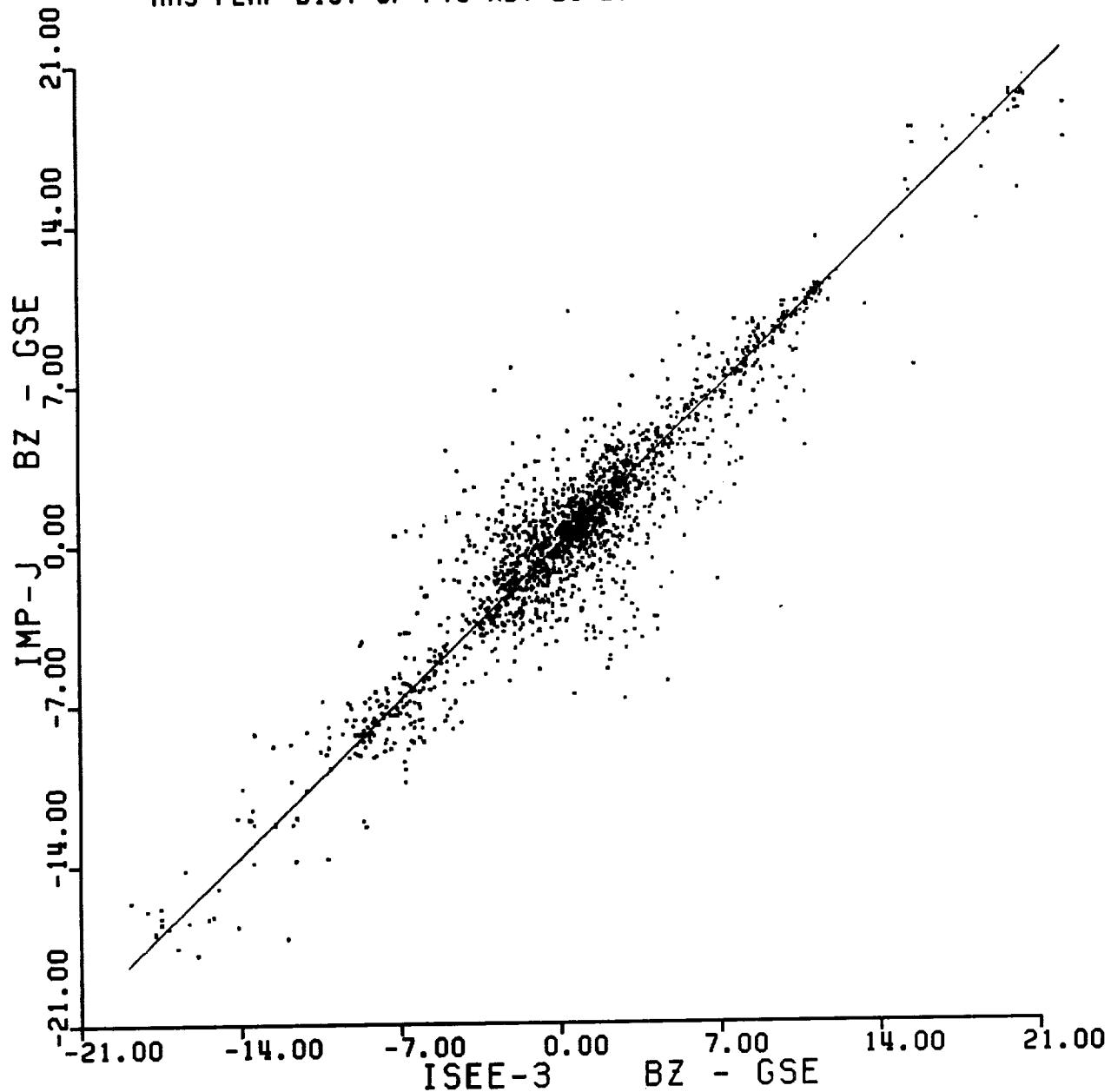


Figure 1. Scatter plot and best fit regression line for  
IMP 8 and ISEE 3 B<sub>Z</sub> 5-min values, Feb. 6 - Mar. 7, 1979

measure, over the five corresponding corotation-shifted minutes, a value of  $B_z$  in the range given by the ISEE 3 value, plus or minus  $\sqrt{2} * 1.35$  nT, with a probability of ~68%. (The  $\sqrt{2}$  factor enters because 1.35 nT is a distance normal to the regression line, while for the present purpose we need an equivalent distance parallel to the ordinate. Regression line slopes are close enough to unity that  $\sqrt{2}$  is an adequate approximation throughout.)

Using 5-min data, regression lines and scatter functions have been determined for each of seven interplanetary parameters, for each of eight (magnetic field) or thirteen (plasma) time periods, for each of three approaches to time-shifting ISEE 3 data. (Time periods after day 48, 1980, were treated separately since 5-min resolution plasma data were not available. The method used to time shift these later time periods is explained toward the end of this section.) The parameters analyzed are field Cartesian components ( $B_x$ ,  $B_y$ ,  $B_z$ ), field magnitude ( $B_m$ ), flow speed ( $V$ ), proton density ( $N$ ), and temperature ( $T$ ). Because  $N$  and  $T$  are distributed more logarithmically than linearly,  $\log N$  and  $\log T$  were used in the regression analysis.

The time periods for which analyses were performed were defined by the ISEE 3 orbital phase:  $|Y(\text{ISEE})| < 50 R_e$ ;  $-50 R_e < Y(\text{ISEE}) < 50 R_e$ ;  $50 R_e < |Y(\text{ISEE})|$ . Most intervals so defined had durations between 30 and 60 days, and contained between 1000 and 3000 ISEE/IMP 5-min data points. Note that because IMP 8 covers the range  $-40 R_e < Y < 40 R_e$  during each 12.5 day orbit, there is some overlap of  $|Y(\text{ISEE}) - Y(\text{IMP})|$  between  $|Y(\text{ISEE})| < 50 R_e$  and  $|Y(\text{ISEE})| > 50 R_e$  periods.

The three time shifts used for ISEE data were corotation (delay equation given above), convection [delay =  $(X(\text{ISEE}) - X(\text{IMP})) / V$ ], and no shift. Convection is expected to yield smaller random errors than corotation if the constant-phase surfaces of interplanetary variations are more nearly normal to a heliocentric radius vector than they are aligned with the ideal spiral IMF direction, by a statistically significant amount. The no-shift case was included to estimate the level of reduction of the random differences produced by time-shifting ISEE data.

Figure 2 summarizes the scatter function information for all physical parameters and time periods, for the case of corotation-shifting of the ISEE 3 data. Note that scatter functions separately computed for individual Cartesian components of the IMF have been averaged. Note also that scatter functions computed for  $|Y(\text{ISEE})| < 50 R_e$  and  $|Y(\text{ISEE})| > 50 R_e$  intervals are distinguished. Lines have been drawn connecting the  $|Y(\text{ISEE})| < 50 R_e$  intervals.

Several points may be noted in Figure 2. First, there is variability from one interval to the next. For the IMF components, the scatter functions are larger for the  $|Y(\text{ISEE})| > 50 R_e$  intervals than for the  $|Y(\text{ISEE})| < 50 R_e$  intervals. This is less clearly true for the field magnitude, and is not true for the plasma parameters. These statements are also true when convective shifting of ISEE data is considered. This behavior is consistent with the transverse scale of plasma parameter variations being greater than 50 to 100  $R_e$ , and with the scale for field component (or direction) variations being comparable to or less than 50 to 100  $R_e$ . Field magnitude variation scales seem to be intermediate.

## Scatter Functions, Corotation Shift, 5 min. Analysis

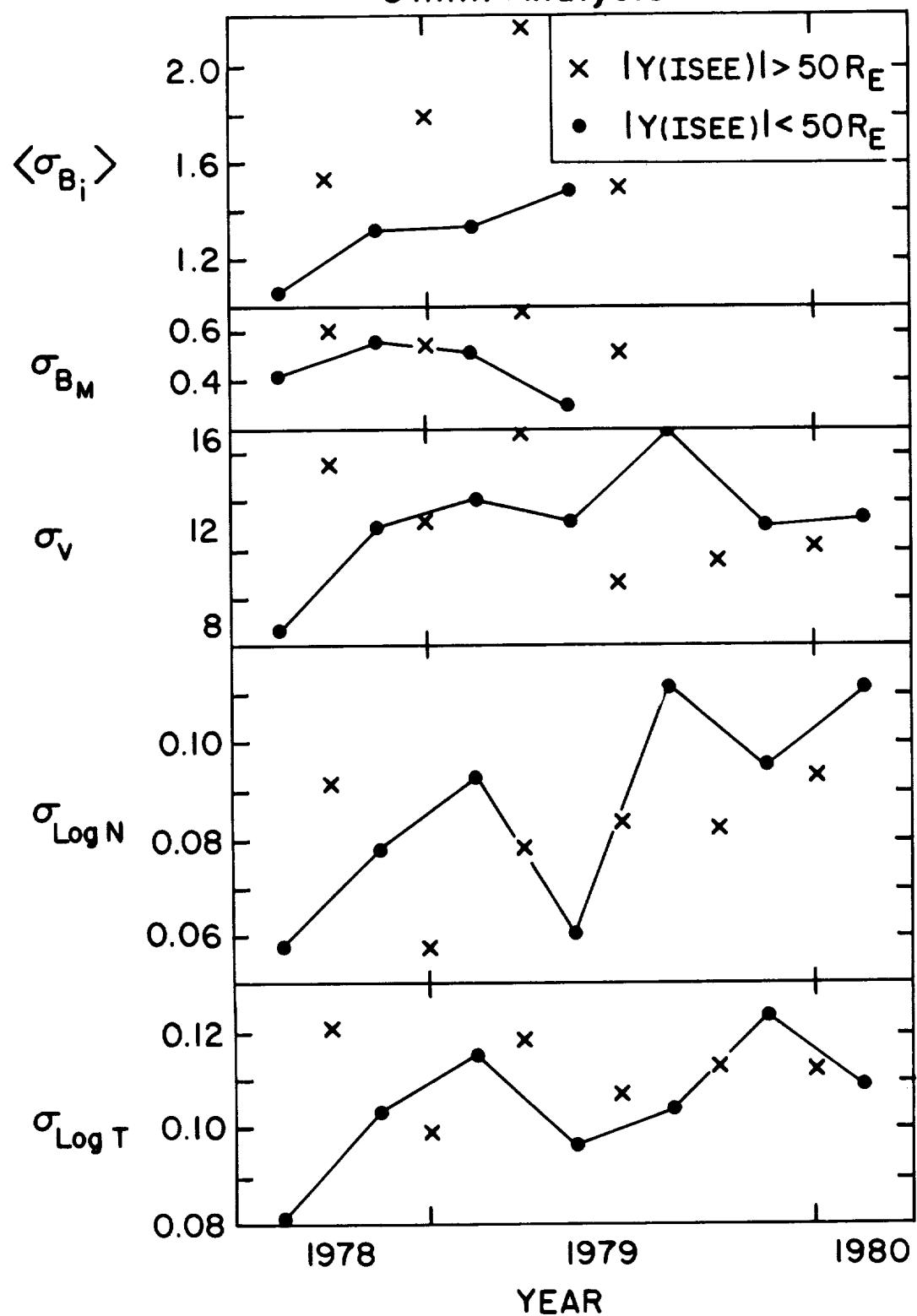


Figure 2. Scatter functions, corotation shift, 5-min analysis

Note that the scatter functions for field magnitude are significantly smaller than scatter functions for field components. This is consistent with a preponderance of constant-field-intensity Alfvénic fluctuations in the solar wind.

As averaged over all time periods, the mean scatter functions for the five panels of Figure 2 are 1.52 nT, 0.51 nT, 12.4 km/s, 0.084, and 0.108. Recall the above discussion of Figure 1 concerning the relation of these values to the inference of near-Earth parameter values from ISEE observations. Note that the last two of these five mean scatter functions correspond to one-sigma uncertainties in near-Earth density and temperatures values of 30% and 40%, given ISEE 3 observations.

Next we compare these results, based on corotation shifting, with the results of convective shifting and no shifting. Figure 3 (left and center panels) contains histograms of ratios of scatter functions for these latter analyses to those illustrated in Figure 2. Note that  $|Y(\text{ISEE})| < 50 R_E$  and  $|Y(\text{ISEE})| > 50 R_E$  cases are again distinguished.

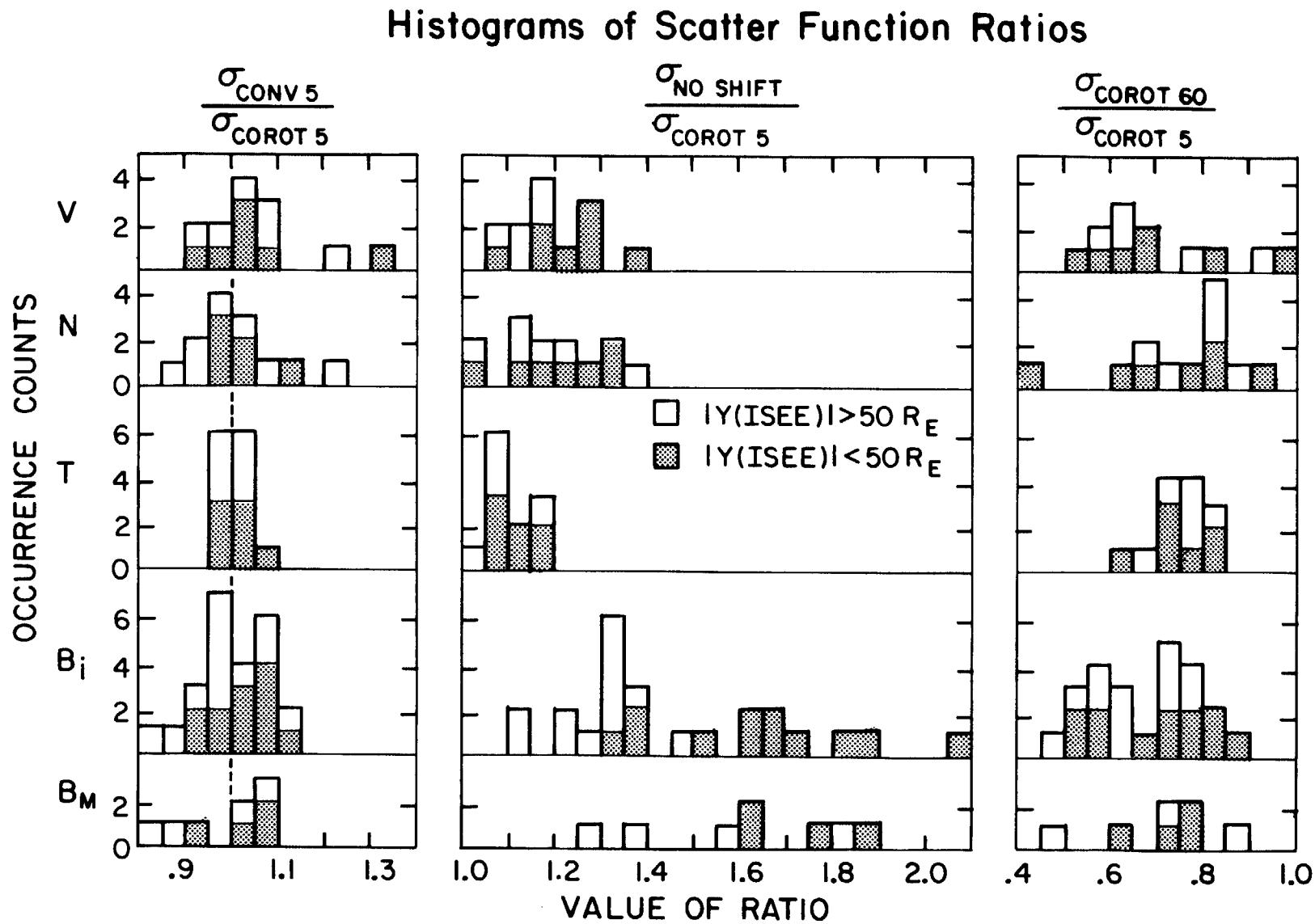
From the convection-to-corotation histogram, it is apparent that very similar scatter functions are obtained with corotation and convection. Very seldom do the convection and corotation scatter functions differ by more than 10% for a given physical parameter and time period. When all time periods and parameters are considered, it is found that the convective scatter function exceeds the corotation scatter function in 55% of the cases (39 out of 71). Even for the  $|Y(\text{ISEE})| > 50 R_E$  cases when the corotation and convection analyses might be expected to exhibit the greatest differences (owing to the greater delay differences), there is no statistically significant difference between the corotation and convection cases. From this it may be concluded that the distribution of constant-phase surfaces of interplanetary variations is peaked neither along the ideal IMF spiral direction nor perpendicular to a heliocentric radius vector. Our choice of time shifting by corotation rather than by convection is seen to be a basically arbitrary choice.

Given this statistical equivalence of convective and corotational time shifting of ISEE 3 data, it may be asked whether these shifts give a statistically significant improvement (reduction of random differences, or scatter functions) relative to not shifting ISEE data at all. From the no-shift to corotation-shift histogram of Figure 3 (center panel), it is clear that time shifting does indeed make a difference. The extent of the difference depends on both the physical parameter and on  $|Y(\text{ISEE})|$ .

Time shifting reduces the random differences by anywhere between 0% and 40% for plasma parameters, and up to a factor of 2 for field parameters. The greater improvement in field parameters results from these parameters' smaller scale lengths. That is, a greater portion of the random differences between (no-shift) simultaneous ISEE 3 and IMP 8 field parameters results from the temporal-spatial displacement of these spacecraft than is the case for plasma parameters, and this displacement is at least partially compensated for by the time-shifting.

Time shifting also reduces the scatter functions by a greater amount for the  $|Y(\text{ISEE})| < 50 R_E$  intervals than for the  $|Y(\text{ISEE})| > 50 R_E$  intervals; this effect is more pronounced for the field parameters than for the plasma data.

Figure 3. Histograms of scatter function ratios



This is an effect of transverse spatial gradients in interplanetary variations and the existence of a distribution of constant-phase orientations. These become increasingly significant as  $|Y(ISEE)|$  increases, and they are handled only imperfectly with a simple time shift which assumes a uniform constant-phase orientation.

All the foregoing discussion has concerned 5-min resolution analysis. It is expected that coarser time resolution would yield smaller random differences, since finer scale structures which probably contribute significantly to the 5-min-resolution random differences would be averaged out. This expectation is realized.

ISEE 3 hourly averages, constructed from corotation-shifted 5-min averages, have been compared to corresponding IMP 8 hourly averages. The scatter functions determined in this analysis have been compared to those obtained in the 5-min resolution analysis. Ratios of hour-based scatter functions to 5-min-based scatter functions are also shown in Figure 3 (right panel). The process of taking hourly averages of 5-min averages reduces the random difference between data sets by up to a factor of 2. There is no major dependence on which physical parameter is involved, nor on  $|Y(ISEE)|$ . There is a weak suggestion that the reduction in scatter function is slightly greater for flow speed and for field components than for the other parameters.

In Figure 4 are presented the scatter function values themselves, as obtained from the hourly resolution analysis. The format and scaling are the same as for Figure 2, although the scales have been translated to account for the smaller hourly based scatter functions. There were typically between 300 and 600 pairs of "corotation-simultaneous" ISEE and IMP hourly averages in each time period.

Again, variability is observed from one interval to the next, although for most parameters the amplitude of the variability is reduced relative to Figure 2. Again, scatter functions for field components are smaller at  $|Y(ISEE)| < 50 R_E$  than at  $|Y(ISEE)| > 50 R_E$ ; this  $|Y(ISEE)|$  dependence is less apparent for field magnitude and is not apparent for plasma parameters.

As discussed in the next section, a single cross-normalization will be applied to each parameter for all time. It is of interest to determine random differences between ISEE and IMP for each parameter over the full span of the simultaneously available data. Figures 5-11 contain scatter plots, regression lines and scatter functions for all seven physical parameters, based on all available "corotation-simultaneous" hourly averages.

### Scatter Functions, Corotation Shift, 1hr. Analysis

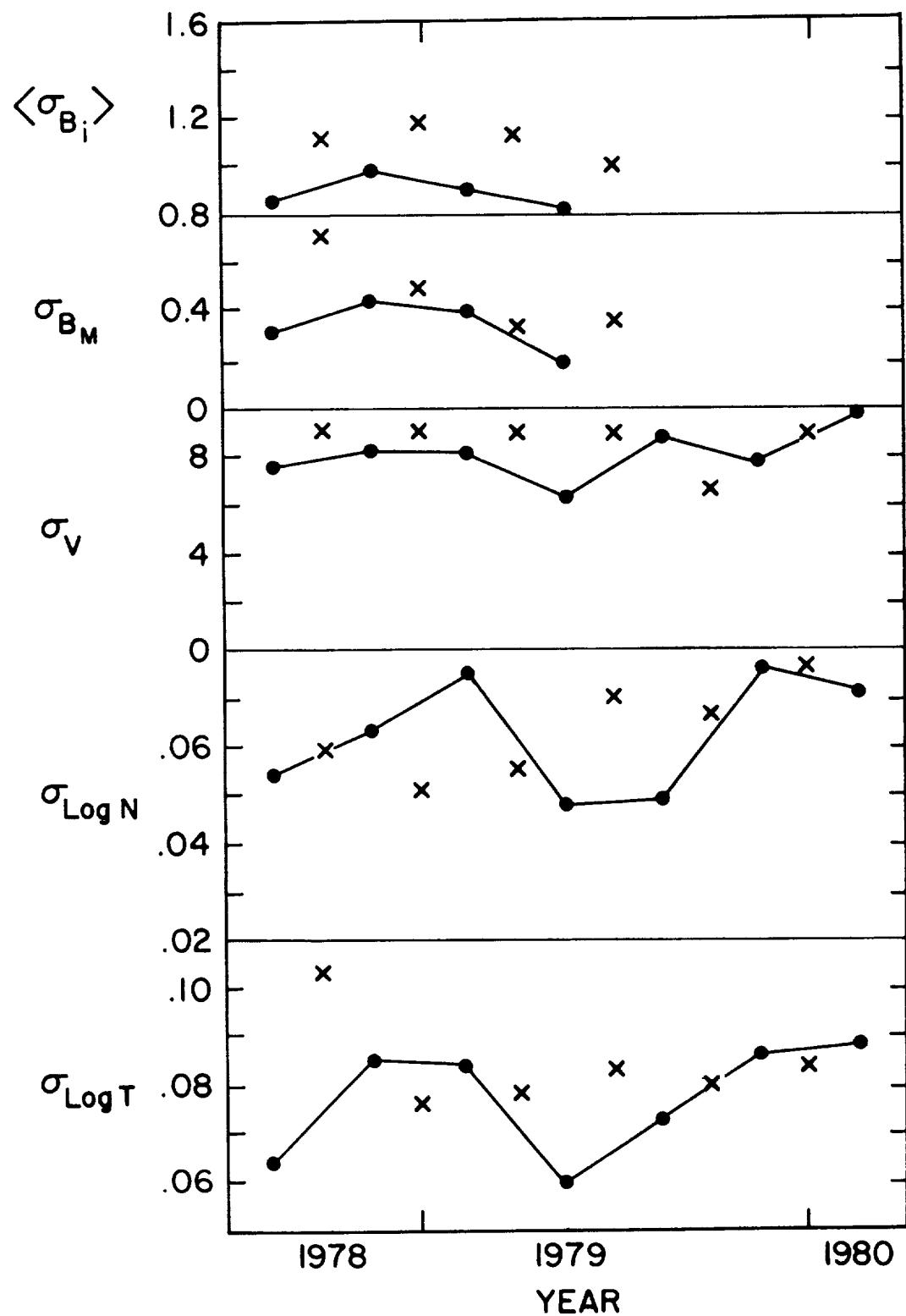


Figure 4. Scatter functions, corotation shift, 1-hr. analysis

PARAMETER : BX - GSE  
TIME SPAN IS: 78224 TO 79178  
NO. OF PTS: 3400  
SHIFT TYPE: COROTATION  
AVERAGES: IMP 0.24 ±4.14  
: ISEE 0.20 ±4.22

$$BX-\text{IMP} = 0.04 (\pm 0.02) + 0.98 (\pm 0.01) \times BX-\text{ISEE}$$

RMS PERP DIST OF PTS ABT LINE: 0.97

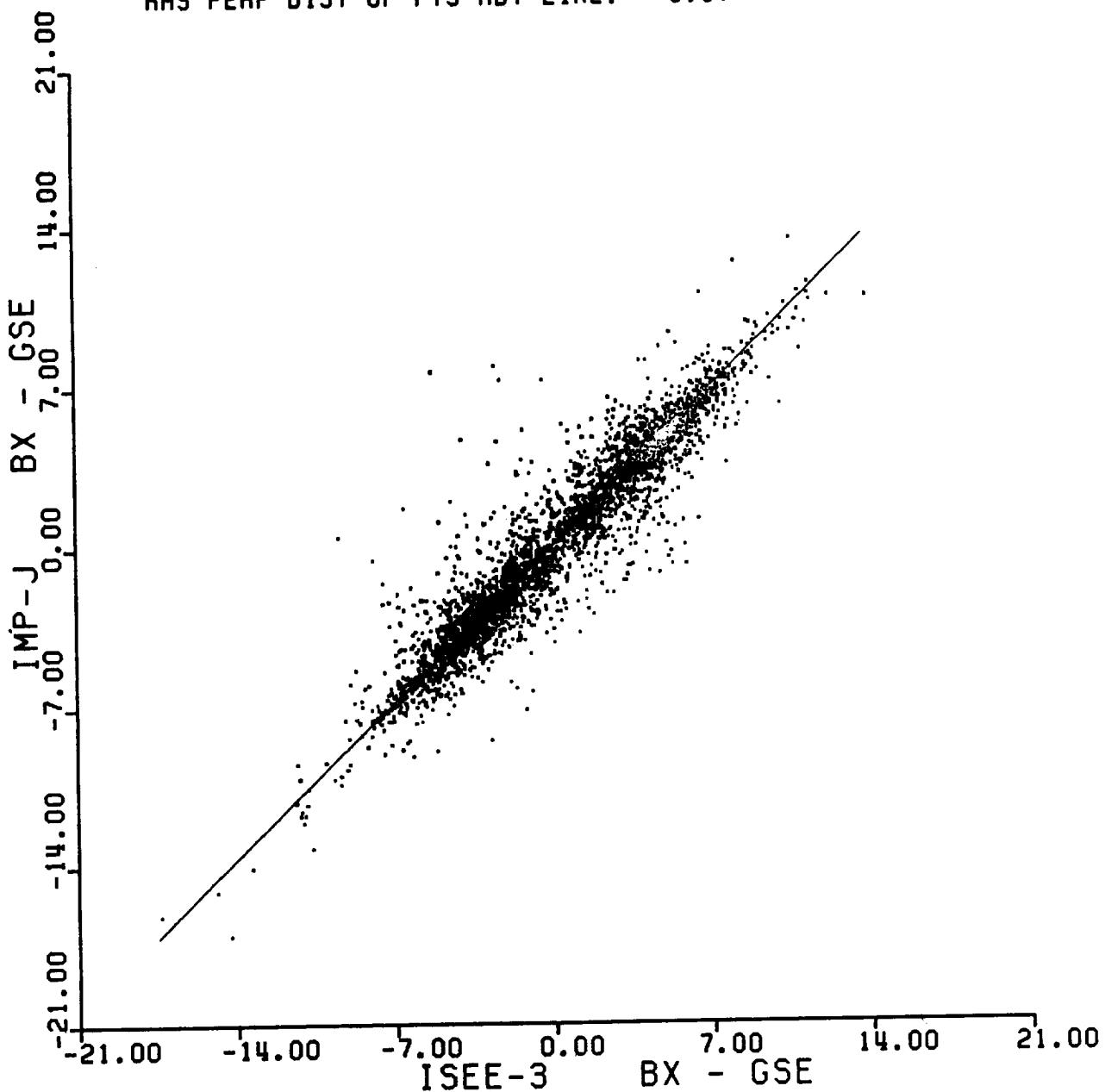


Figure 5. Scatter plot and best fit regression line for IMP 8 and ISEE 3  $B_x$  hourly averages, Aug. 78 - June 79

PARAMETER : BY - GSE  
TIME SPAN IS: 78224 TO 79178  
NO. OF PTS: 3400  
SHIFT TYPE: COROTATION  
AVERAGES: IMP -0.15 ±4.73  
: ISE -0.15 ±4.87

$$\text{BY-IMP} = -0.00 (\pm 0.02) + 0.97 (\pm 0.01) \times \text{BY-ISEE}$$

RMS PERP DIST OF PTS ABT LINE: 1.01

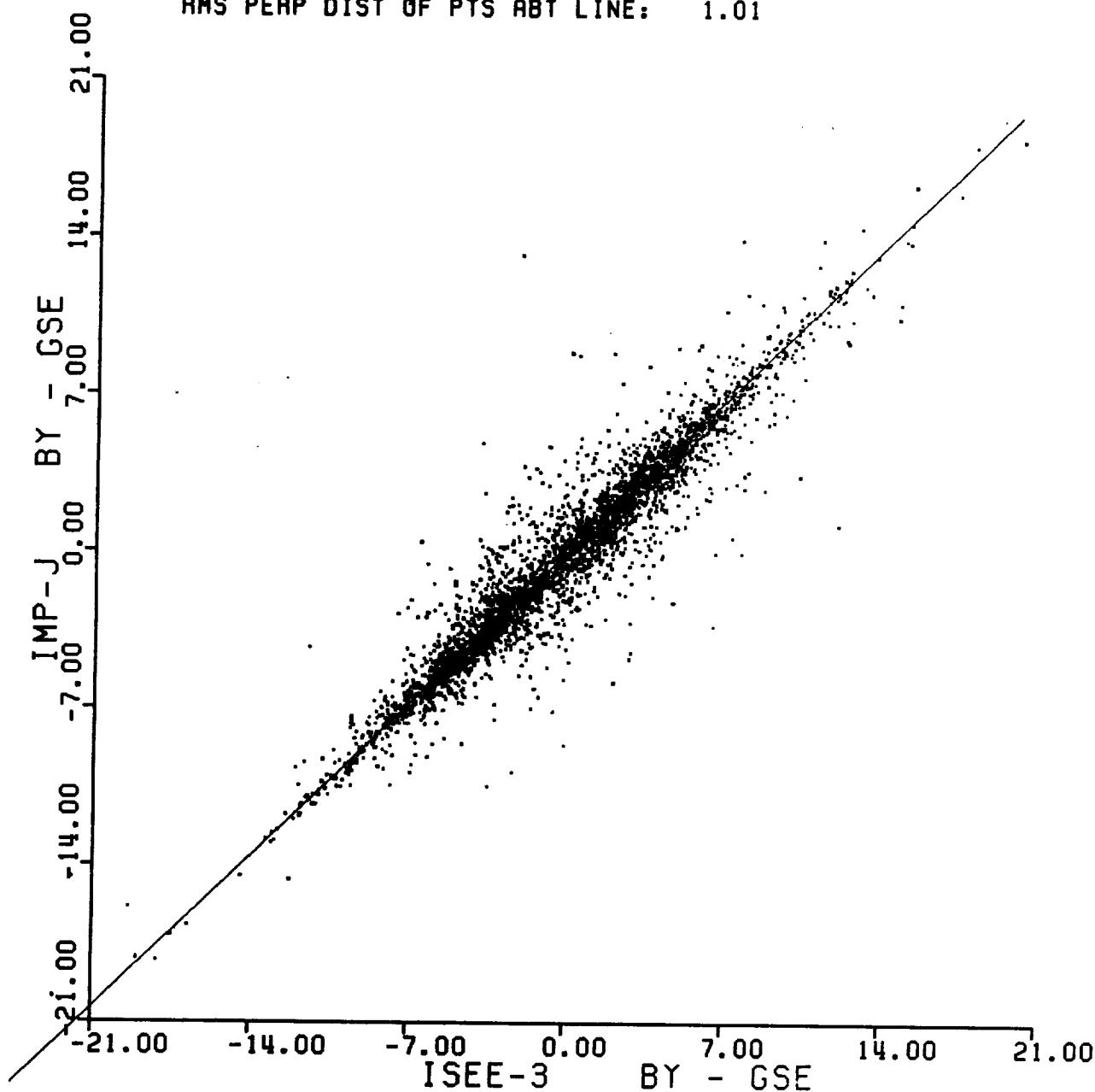


Figure 6. Scatter plot and best fit regression line for IMP 8 and ISEE 3  $B_y$  hourly averages, Aug. 78 - June 79

PARAMETER : BZ - GSE  
TIME SPAN IS: 78224 TO 79178  
NO. OF PTS: 3400  
SHIFT TYPE: COROTATION  
AVERAGES: IMP -0.23 ±3.55  
: ISEE -0.30 ±3.47

$$BZ-IMP = 0.07 (\pm 0.02) + 1.03 (\pm 0.01) \times BZ-ISEE$$

RMS PERP DIST OF PTS ABT LINE: 1.12

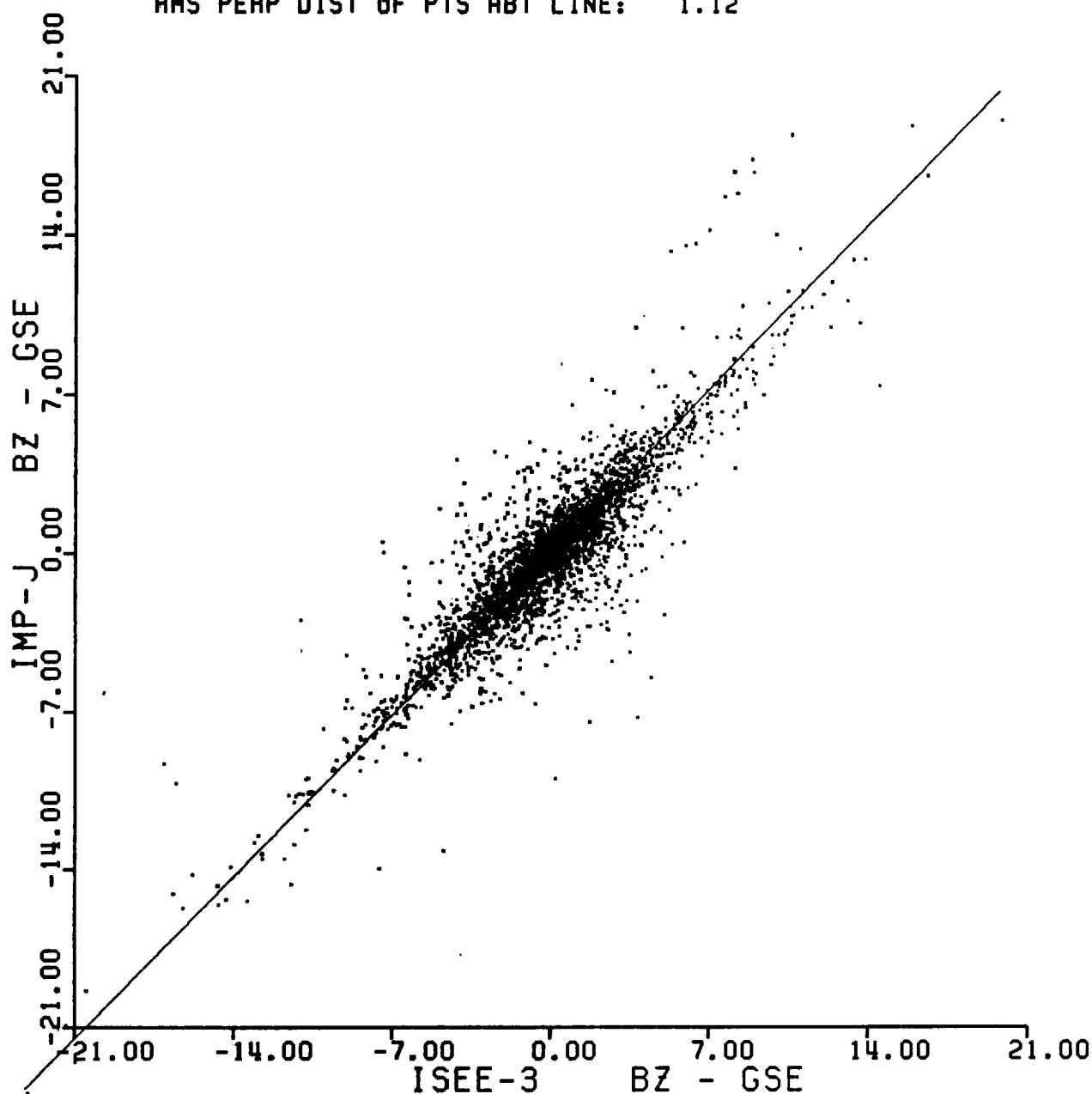


Figure 7. Scatter plot and best fit regression line for IMP 8 and ISEE 3 B<sub>z</sub> hourly averages, Aug. 78 - June 79

PARAMETER : B-MAGNITUDE  
TIME SPAN IS: 78224 TO 79178  
NO. OF PTS: 3400  
SHIFT TYPE: COROTATION  
AVERAGES: IMP 7.30 ±3.08  
: ISEE 7.42 ±3.08

$$\text{MAG-IMP} = -0.13 (\pm 0.01) + 1.00 (\pm 0.00) \times \text{MAG-ISEE}$$

RMS PERP DIST OF PTS ABT LINE: 0.48

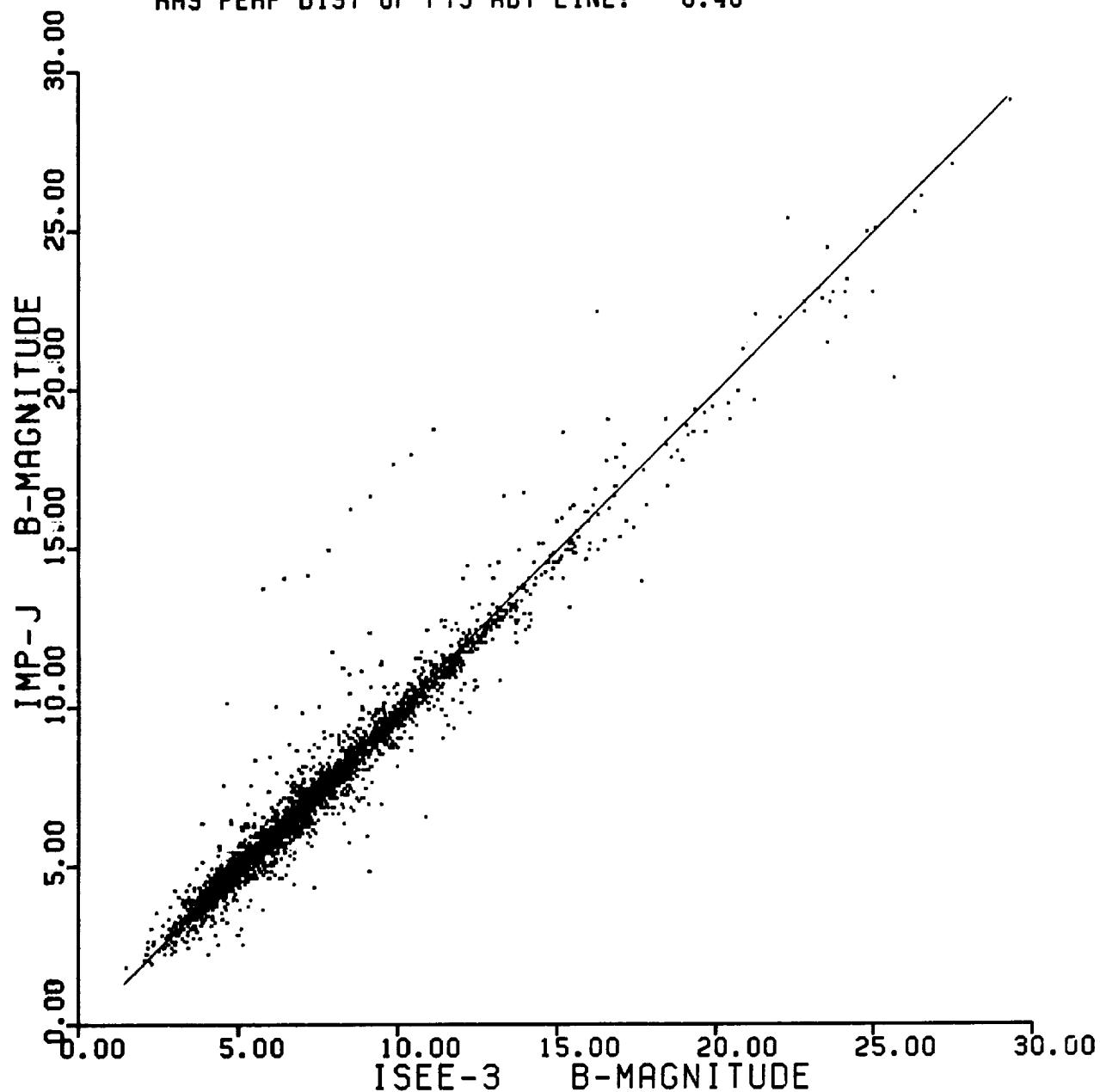


Figure 8. Scatter plot and best fit regression line for  
IMP 8 and ISEE 3 hourly averaged field magnitudes,  
Aug. 78 - June 79

PARAMETER : SPEED  
TIME SPAN IS: 78228 TO 80049  
NO. OF PTS: 5000  
SHIFT TYPE: COROTATION  
AVERAGES: IMP 417 ±81  
: ISEE 410 ±81

$$V - \text{IMP} = 5.97 (\pm 0.05) + 1.00 (\pm 0.00) \times V - \text{ISEE}$$

RMS PERP DIST OF PTS ABT LINE: 8.44

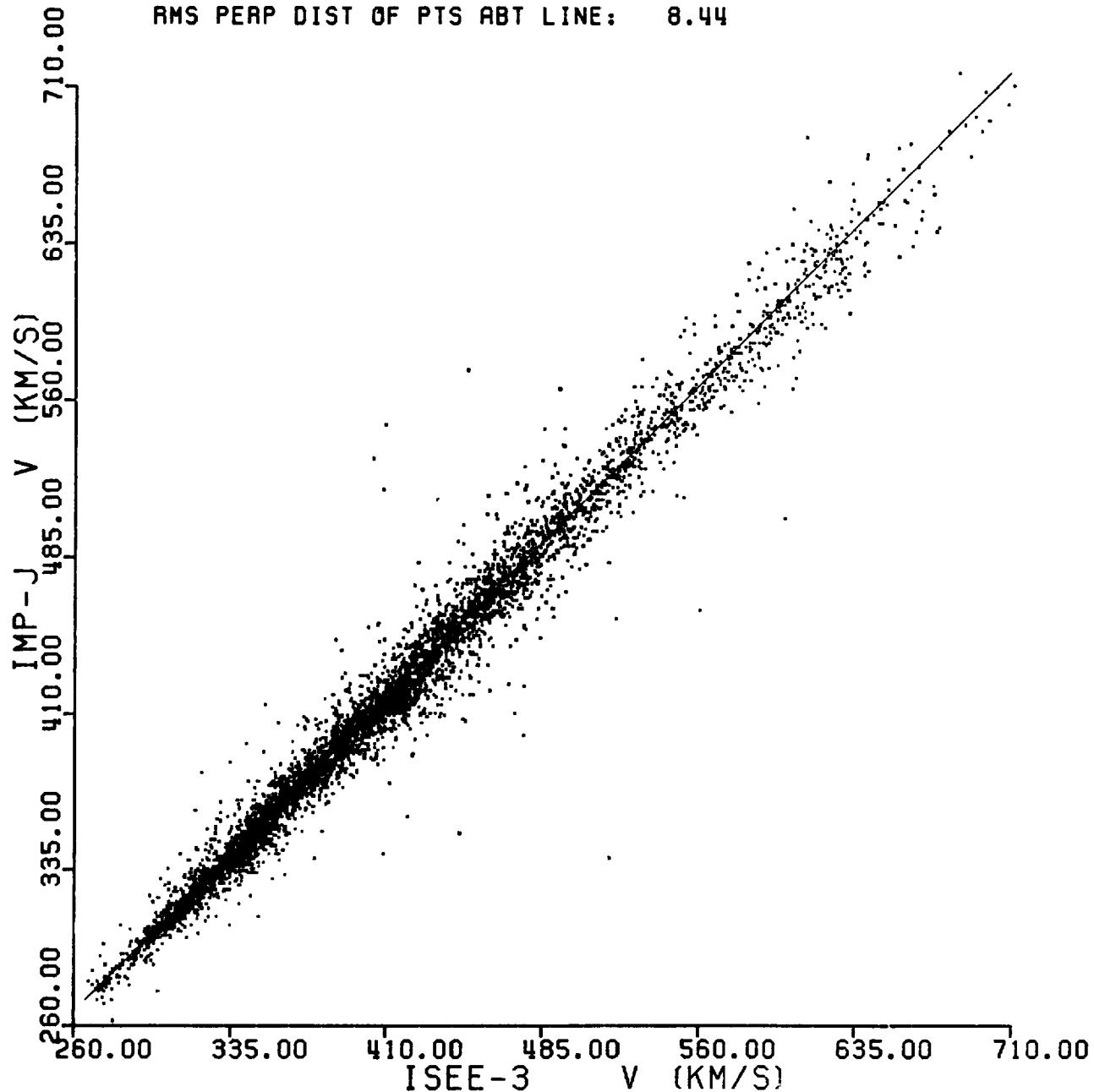


Figure 9. Scatter plot and best fit regression line for IMP 8 and ISEE 3 hourly averaged speeds, Aug. 78 - Feb. 80

PARAMETER : LOG DENSITY  
TIME SPAN IS: 78228 TO 80049  
NO. OF PTS: 5000  
SHIFT TYPE: COROTATION  
AVERAGES: IMP 0.82 ±0.32  
: ISEE 0.79 ±0.32

LOG-N-IMP = 0.04 (±0.00) + 1.00 (±0.00) × LOG-N-ISEE

RMS PERP DIST OF PTS ABT LINE: 0.07

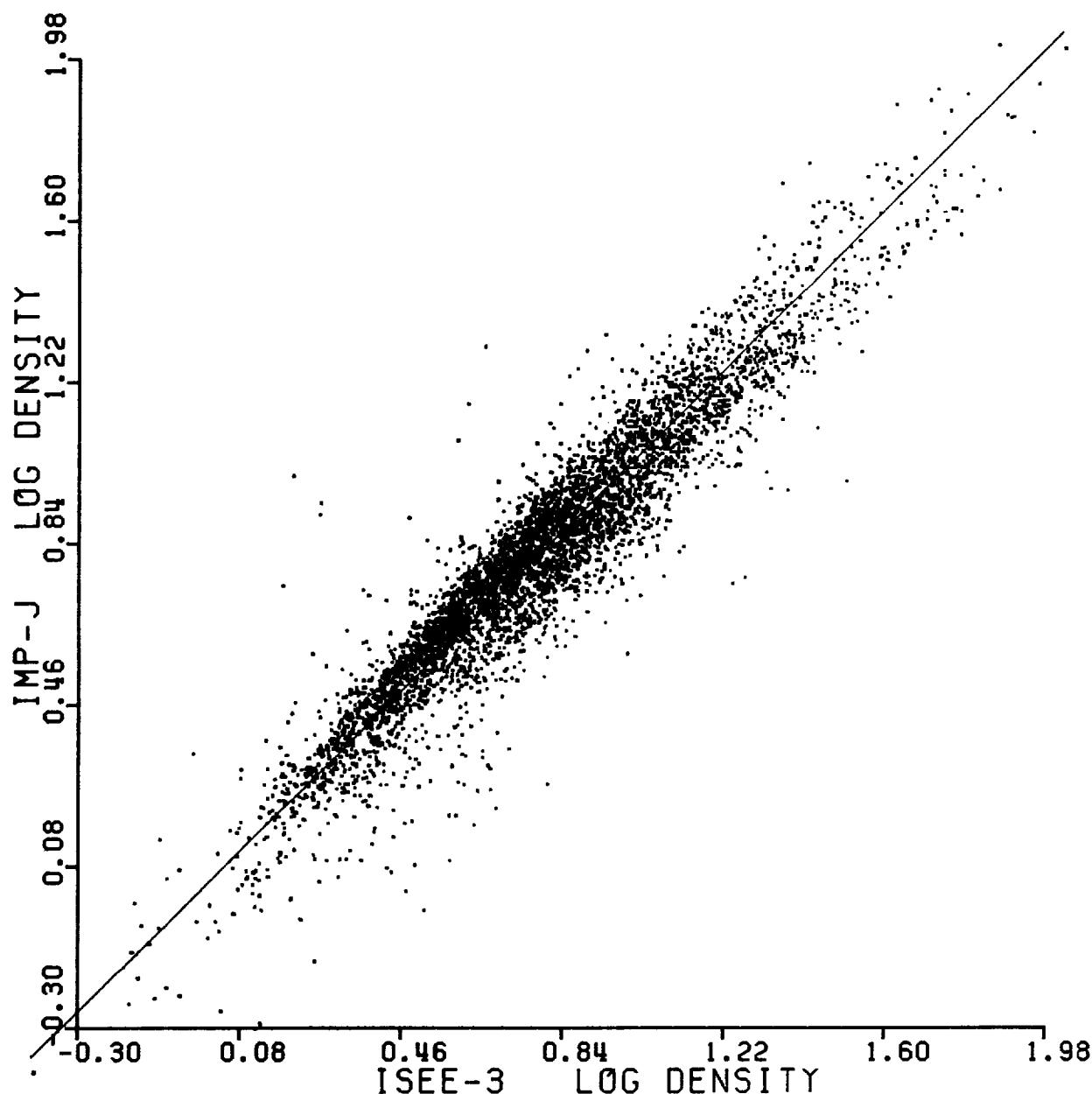


Figure 10. Scatter plot and best fit regression line for IMP 8 and ISEE 3 logarithms of hourly averaged densities, Aug. 78 - Feb. 80

PARAMETER : LOG TEMP  
TIME SPAN IS: 78228 TO 80049  
NO. OF PTS: 5000  
SHIFT TYPE: COROTATION  
AVERAGES: IMP 4.95 ±0.30  
: ISEE 4.90 ±0.29

$$\text{LOG-T-IMP} = -0.08 (\pm 0.01) + 1.03 (\pm 0.01) \times \text{LOG-T-ISEE}$$

RMS PERP DIST OF PTS ABT LINE: 0.09

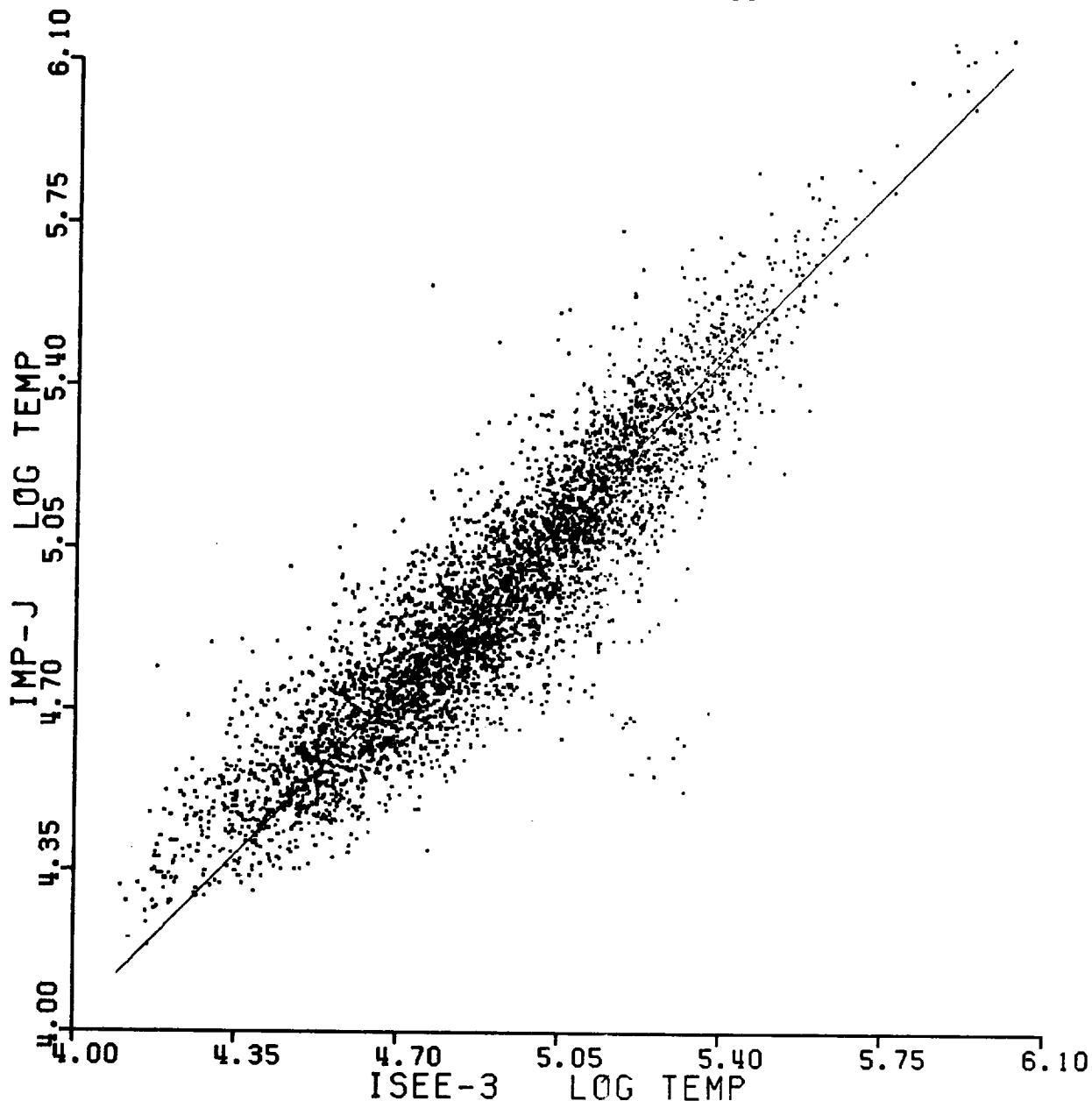


Figure 11. Scatter plot and best fit regression line for  
IMP 8 and ISEE 3 logarithms of hourly averaged  
temperature, Aug. 78 - Feb. 80

The scatter function information contained on those figures may be summarized by the first part of Table 2 below and the statement:

If an hourly averaged value of X is obtained for parameter Y from remotely measured but corotation-shifted ISEE 3 fine-scale data, then the near-Earth IMP 8 would measure a value for parameter Y in the range  $X \pm Z$  with a 1-sigma ( $\sim 68\%$ ) confidence level, where the Z functions are given below.

TABLE 2. Summary of Hourly Z-Function Information

Y	5-min ion-based speeds used for $\tau$ calculation (1978-1980)	Hourly electron-based speeds for $\tau$ calculation (1979-1983)
Z	Z	Z
$B_x$	1.37 nT	1.63
$B_y$	1.43	1.80
$B_z$	1.58	1.88
$B_m$	0.68	0.75
V	11.9 km/sec	29.3 km/sec
log N	0.10	0.14
log T	0.13	no ion tempera- tures available

Note that the Z factors differ from the scatter functions by  $\sqrt{2}$ , as explained previously. We take these values to represent the irreducible random differences arising from the interspersal of ISEE 3 and IMP hour averages. (The right-hand column in Table 2 is discussed below.)

All of the above discussion of time shifting concerned data that were collected prior to day 48, 1980, and used originally in Supplement 2. After this time, the ISEE 3 plasma data available were hourly averaged parameters based on electron observations. The LANL group has carefully normalized their densities and velocities to their ion-based data by comparing parameters when both ion and electron measurements were taken. Nonetheless, we should bear in mind that errors associated with electron-based parameters are somewhat higher than those associated with ion-based parameters.

After day 48, 1980, time shifting of ISEE 3 IMF data was effected using the hourly resolution ISEE 3 speeds. (For late 1982 and 1983 when ISEE 3 IMF data were available but ISEE 3 plasma data were not, hourly resolution IMP 8 speeds were used.) Note that for portions of 1982 and 1983, ISEE 3 was actually tailward of the earth and thus time shift values can be positive or negative. Using the time-shifted ISEE 3 IMF hourly values, regression lines and scatter functions for ISEE 3 vs. IMP 8 were determined for  $B_x$ ,  $B_y$ ,  $B_z$  and  $B_m$ . The scatter functions are summarized in Table 2.

IMF scatter functions calculated when only hourly averaged speeds were available have slightly higher values than those calculated when 5 minute averaged speeds were used for time shifting. This result is not totally unexpected especially when one recalls that the hourly averaged speeds are based on electron measurements. It is also important to point out that the two separate analyses (5-min ion-based speeds and hourly electron-based speeds used for time shifting) were performed on different time intervals. The scatter functions do vary somewhat from year to year and this may account for much of the differences.

In the absence of 5-min resolution plasma data, time shifting of the post day 48, 1980, plasma data involved a much less straightforward procedure than that which was done previously. Each ISEE 3 hourly averaged density and speed was shifted to the Earth using the observed ISEE 3 speed and the corotation delay equation. Typically an ISEE hour (e.g., 0200-0300) shifted to a non-integral Earth hour (e.g., 0245-0345). Earth-time hourly averages (e.g., for 0300-0400) were then built as averages of ISEE values which shifted into the desired Earth hour, weighted by their relative contribution to that hour.

In order to determine the value of the weighted average approach to time shifting, a regression analysis was done between IMP 8 plasma data and ISEE 3 plasma data which were not time shifted. Scatter functions calculated for the "no shift" case were compared with those calculated where weighted averages were used in the time-shifting scheme. Table 3 displays the ratio of these two scatter functions by year for speeds (V) and densities (N). Ratios greater than 1 indicate that the scatter is reduced by time shifting using weighted averages. Also listed in Table 3 are the yearly averages (as measured by ISEE 3) of the solar wind speed and density. We note that the importance of time shifting increases when solar wind speeds are low or when densities are high. Since higher solar wind speeds imply smaller  $\tau$ 's, neglecting  $\tau$  (by not time shifting) would introduce greater error for low-speed intervals. These results also imply that variability exists in solar wind speeds even when the average speed is low. On the other hand, as evident by the density scatter function ratios, periods of high average density appear to be more variable than low average density intervals.

TABLE 3. Scatter Function Ratios for ISEE 3 vs. IMP 8 Plasma Parameters

Year	# points	$\frac{\sigma}{\sigma}$ NO SHIFT		ISEE 3 Averages	
		V	N	V	N
1979	1148	1.23	1.41	390	6.64
1980	1752	1.34	1.57	378	7.24
1981	1542	1.16	1.10	432	6.01
1982	1112	1.12	2.00	482	8.68

Values of the actual plasma parameter functions are shown in Table 2. Density scatter functions determined using electron-based weighted averages are about 40% higher than those found when 5-min averaged ion-based densities were used. The velocity scatter functions differ by almost a factor of 3. These differences have three possible sources: (1) using electron-based plasma parameters in lieu of ion-based parameters, (2) constructing hourly averages by the method of weighted averages instead of collecting 5-min averages, and (3) the fact that the time periods compared are not the same. Regressing ISEE 3 hourly averaged ion-based densities and velocities to their ISEE 3 electron-based counterparts for 1978 through 1980 results in a Z of .17 for log density and a Z of 33 km/sec for velocity based on 11,770 hours of overlapping data. Hence, we conclude that most of the differences between the density and velocity scatter functions can be attributed to the somewhat larger errors associated with electron-based parameters.

In order to estimate what fraction of the irreducible differences results from the remoteness of ISEE 3, it is of interest to compare the scatter functions from Table 2 with those obtained in cross-normalizing pairs of near-Earth data sets. A special case is the pair of IMP 8 plasma data sets provided by MIT and LANL. Virtually all of these data are from IMP 8 with the exception of some 1977 LANL IMP 7 data. Table 4 summarizes the scatter function data obtained upon cross-normalizing these data sets for 1977 through 1984. A comparison of the Z functions to those of Table 2 suggests that 1/3 to 1/2 of the irreducible differences between ISEE 3 and IMP 8 V and log N values, and a yet smaller fraction for log T, may result from the remoteness of ISEE 3. Note the somewhat greater scatter in the 1980-1982 era.

TABLE 4. MIT vs. LANL Scatter Functions - IMP 8

Year	Number of Hours	Scatter Functions			Z Functions		
		V	log N	log T	V	log N	log T
1977	4465	4.1	.04	.07	5.8	.05	.10
1978	2267	4.9	.04	.10	6.9	.06	.14
1979	2213	4.0	.05	.09	5.7	.06	.13
1980	1938	4.5	.06	.10	6.3	.08	.14
1981	1575	5.5	.07	.12	7.8	.10	.16
1982	1235	6.2	.05	.10	8.7	.08	.14
1983	2400	4.6	.04	.09	6.6	.06	.13
1984	1616	4.9	.03	.08	7.0	.04	.11

In the original *Interplanetary Medium Data Book* of 1977, scatter functions for plasma and field parameters were listed for several pairs of data sets obtained from near-Earth spacecraft between 1963 and 1975. These scatter functions ranged between 7.5 and 17.8 km/s ( $V$ ), 0.04 to 0.10 (Log- $N$ ), and 0.06 to 0.20 (Log- $T$ ). There has been a trend towards decreasing random differences between data sets with time, due at least in part to the increasing number of instrument energy channels from whose count rates bulk flow parameters are determined. For magnetic field components, the scatter functions were typically in the 0.7 to 1.1 nT range, while for field magnitudes the scatter functions were either in the 0.3 to 0.6 nT range (8 cases) or 0.9 to 1.1 nT range (4 cases). Unlike the IMP 8 plasma case, there has been no recent case of two magnetometers flown on the same spacecraft. We conclude that the irreducible differences between the IMP 8 and corotationally shifted ISEE 3 hourly averaged IMF data sets are not significantly different statistically from the irreducible differences between non-time-shifted hourly data sets obtained for a pair of near-Earth spacecraft. In this sense, adding corotation-shifted ISEE 3 IMF data to our 1 AU, hourly average data compilation does not significantly diminish the reliability of the compilation.

#### Cross-Normalization of Data Sets

We consider next the systematic differences between individual data sets. Such differences are in contrast to the previously discussed random differences between data sets, and are reflected in the extent to which "best fit" regression lines deviate from  $Y=X$ . Here the concern is to make the data sets contributing to this supplement as mutually consistent as possible, and separately to make these 1977-1985 data as consistent with earlier data as possible. Recall that while all parameters have been cross-compared in the past, only density and temperature have been normalized.

Table 5 summarizes the ISEE 3 versus IMP 8 IMF regression results. In this Table,  $\sigma$  is the scatter function. The "1- $\sigma$  range" column gives the range of  $P(\text{ISEE}3)$  over which the regression line lies within one sigma (parallel to ordinate) of  $Y=X$ . Typical field components and magnitude values are almost always deep within these ranges. Therefore, concluding that there would be no statistically significant gain in cross-normalizing the field data sets, we have not normalized them.

TABLE 5. IMP 8 vs. ISEE 3 IMF Regression Parameters

P	$P_{\text{IMP}} = a + b P_{\text{ISEE } 3}$				
	a	b	$\sigma$	1- $\sigma$ range	
$B_x$	.04	.98	.97	-66 to 70nT	5-minute ion-based
$B_y$	.00	.97	1.01	-47 to 47nT	speeds used for $\tau$
$B_z$	.07	1.03	1.12	-55 to 50nT	calculation
$B_m$	-.13	1.00	0.48	0 to nT	1978-79
$B_x$	.01	.98	1.16	-102 to 103nT	hourly electron
$B_y$	.02	.98	1.27	-88 to 90nT	based speeds used
$B_z$	.02	1.00	1.33	-388 to 380nT	$\tau$ calculation
$B_m$	.03	.98	.53	0 to 40nT	1979-83

There are four plasma data sets to be cross-compared. Regression results for flow speeds, densities and temperatures are shown in Tables 6, 7 and 8 respectively. In order to ascertain whether or not the regression parameters are time invariant, each comparison has been presented for each year. Also shown are the ranges of V, N and T over which the regression lines for V, log N and log T lie within one sigma of perfect agreement (Y=X).

Flow speed data generally agree to within a few km/sec. There are some yearly variations, but no trends are apparent. Even though for certain years the 1-sigma range for the IMP(LANL) IMP(MIT) velocity regression is not ideal, we have elected not to normalize these data in order to avoid using a time varying normalization. A small but significant number of density and temperature values are measured in the parts of parameter space where the systematic differences are comparable to or greater than random differences. Thus, we shall follow our earlier approach of cross-normalizing the density and temperature data.

ISEE 1 and ISEE 3 plasma data sets were compared to both the LANL and MIT data sets from IMP 8. Chaining of the derived regression equations demonstrates their mutual consistency. For example, the 1977 IMP(LANL) vs. IMP(MIT) and the 1977 IMP(LANL) vs. ISEE 1 relations of Tables 7 and 8 can be combined to yield:

$$\begin{aligned}\log N_{MIT} &= .16 + .84 \log N_{ISEE} 1 \\ \log T_{MIT} &= .85 + .83 \log T_{ISEE} 1\end{aligned}$$

These equations compare favorably to those found from the direct IMP(MIT) vs. ISEE 1 comparison.

It remains to choose what normalization to apply to which data sets. Rather than presume to judge which of the four data sets is more likely to be absolutely correct, we shall normalize all densities and temperatures to IMP(LANL) values for historical consistency. In previous Data Books, the density normalization used for IMP(MIT) data from 1973 to 1978 was:

$$\log N_{LANL} = .12 + .89 \log N_{MIT}$$

This equation is not statistically different from the normalization equation found by cross-comparing data from 1979 to 1984. Hence, we shall normalize the IMP(MIT) density data using the 1973 to 1978 relation.

It is worth noting that although there are yearly variations in the normalization parameters, little is gained by applying a time varying normalization. The sigma values are such that the 1-sigma range calculated against the proposed normalization for any given year usually encompasses virtually all of the relevant parameter space. For 1980 and 1981 this is not true since the IMP(LANL) IMP(MIT) regression line appears to undergo a "lowering". These "anomalous" years will be addressed subsequently in this section.

The IMP(LANL) vs. IMP(MIT) temperature regression results for 1979 to 1984 shown in Table 8 are essentially identical to the 1973-1978 results of

$$\log T_{LANL} = -.62 + 1.11 \log T_{MIT}$$

Hence for historical consistency the previous normalization will be used. Again, it is worth pointing out the year-to-year variations in the regression parameters.

TABLE 6. Flow Speed Regressions

$V_{LANL} = a + b V_{MIT}$  (for IMP 8)

Year	# Points	a	b	$a_L$	1 - $\sigma$ range
1977	4465	-7.0	1.01	4.1	100 to 1000 km/sec
1978	2267	-1.6	1.00	4.9	0 to $\infty$
1979	2213	-0.6	0.99	4.0	0 to 560
1980	1938	0.2	0.99	4.5	0 to 470
1981	1575	4.3	0.98	5.5	0 to 470
1982	1235	-2.7	0.99	6.2	0 to 1000
1983	2400	1.2	0.99	4.6	0 to 560
1984	1616	1.6	0.99	4.9	0 to 590
1979-1984	10,977	0.3	0.99	4.9	0 to 580

$V_{IMP} = a + b V_{ISEE1}$

Year	IMP Instrument	# Points	a	b	$a_L$	1 - $\sigma$ range
1977	LANL	655	3.1	1.01	6.8	0 to 670
1978	LANL	635	-2.0	1.02	11.7	0 to 980
1979	LANL	525	-7.0	1.03	16.9	0 to 1030
1977-1979	LANL	1815	-0.8	1.02	12.1	0 to 1060
1977	MIT	461	12.6	0.99	7.2	220 to 2000
1978	MIT	859	12.8	0.99	9.5	0 to 2300
1979	MIT	921	11.8	1.02	12.3	0 to 330
1977-1979	MIT	2241	17.0	0.99	11.0	120 to 2700

$V_{IMP} = a + b V_{ISEE3}$

Year	IMP Instrument	# Points	a	b	$a_L$	1 - $\sigma$ range
1978	LANL	815	8.0	0.99	6.9	0 to 1200
1979	LANL*	1148	-27.2	1.07	15.6	80 to 750
1980	LANL*	1817	21.4	0.96	24.2	0 to 1300
1981	LANL*	1605	-27.3	1.08	21.1	0 to 710
1982	LANL*	1177	-21.8	1.06	17.0	0 to 760
1980-1982	LANL*	4599	-6.3	1.03	20.8	0 to 1190
1978-1980	MIT	5008	6.0	1.00	8.4	0 to $\infty$
1979	MIT*	1896	-4.2	1.03	13.1	0 to 810
1980	MIT*	3097	3.3	1.02	20.9	0 to 1100
1981	MIT*	2794	-19.5	1.07	15.8	0 to 580
1982	MIT*	1930	-17.7	1.07	19.6	0 to 670
1979-1982	MIT*	9717	-10.0	1.05	18.0	0 to 700

\*Electron-based ISEE 3 parameters used.

TABLE 7. Density Regressions

$$\log N_{\text{LANL}} = a + b(\log N_{\text{MIT}})$$

Year	# Points	a	b	$\alpha$	1- $\sigma$ range (N)	
1977	4465	.09	.92	.04	2.7 to 41	$\text{cm}^{-3}$
1978	2267	.07	.94	.04	1.3 to 150	
1979	2213	.10	.90	.05	2.8 to 57	
1980	1938	.05	.85	.06	0.6 to 7.9	
1981	1575	.08	.82	.07	0.8 to 9.6	
1982	1235	.18	.85	.05	5.1 to 51	
1983	2400	.15	.90	.04	10 to 145	
1984	1616	.18	.87	.03	12 to 55	
1979-198	10,977	.09	.91	.07	0.9 to 110	

$$\log N_{\text{IMP}} = a + b(\log N_{\text{ISEE1}})$$

Year	IMP Instrument	# Points	a	b	$\alpha$	1- $\sigma$ range (N)
1977	LANL	655	.24	.77	.08	3.6 to 30
1978	LANL	635	.14	.92	.09	1.7 to 1200
1979	LANL	525	.16	.88	.10	1.5 to 320
1977-1979	LANL	1815	.18	.85	.09	2.3 to 110
1977	MIT	461	.19	.84	.06	$4 \cdot 10^{-4}$ to $54^{14}$
1978	MIT	859	.06	.99	.07	$10^{-4}$ to $10^{14}$
1979	MIT	921	.04	.98	.07	$10^{-4}$ to $10^8$
1977-1979	MIT	2241	.07	.96	.07	.2 to $10^{14}$

$$\log N_{\text{IMP}} = a + b(\log N_{\text{ISEE3}})$$

Year	IMP Instrument	# Points	a	b	$\alpha$	1- $\sigma$ range (N)
1978	LANL	815	.19	0.85	.09	3.6 to 136
1979	LANL*	1148	.16	0.88	.07	2.8 to 164
1980	LANL*	1817	.07	0.83	.10	0.4 to 16
1981	LANL*	1605	.05	0.85	.09	0.3 to 15
1982	LANL*	1177	.14	0.82	.07	1.8 to 18
1980-1982	LANL*	4599	.06	0.85	.09	0.4 to 20
1978-1980	MIT	5008	.09	0.93	.07	$0.9 \cdot 10^{-4}$ to $740^{11}$
1979	MIT*	1896	.05	0.99	.06	$10^{-4}$ to $10^{11}$
1980	MIT*	3097	.00	0.99	.09	$10^{-20}$ to $10^{20}$
1981	MIT*	2794	.01	0.96	.07	.01 to 660
1982	MIT*	1930	-.09	1.02	.09	.07 to $10^7$
1979-1982	MIT*	9717	.00	0.98	.08	$10^{-5}$ to $10^5$

\*Electron-based ISEE 3 parameters used.

TABLE 8. Temperature Regressions

$$\log T_{\text{LANL}} = a + b(\log T_{\text{MIT}})$$

Year	# Points	a	b	$\alpha$	1- $\sigma$ range (T)	$^{\circ}\text{K}$
1977	4465	-.77	1.15	.07	$2.0 \times 10^{-4}$	to $4.6 \times 10^5$
1978	2267	-.75	1.16	.10	$8.3 \times 10^{-3}$	to $6.6 \times 10^5$
1979	2213	-.87	1.18	.09	$1.5 \times 10^{-4}$	to $3.9 \times 10^5$
1980	1938	-1.14	1.24	.10	$1.3 \times 10^{-4}$	to $1.9 \times 10^5$
1981	1575	-.43	1.11	.11	$3.5 \times 10^{-2}$	to $3.7 \times 10^5$
1982	1235	.25	0.96	.10	$7.1 \times 10^{-2}$	to $4.5 \times 10^5$
1983	2400	-.72	1.15	.09	$1.0 \times 10^{-4}$	to $5.3 \times 10^5$
1984	1616	-.04	1.02	.08	$5.0 \times 10^{-5}$	to $1.3 \times 10^5$
1979-1984	10,977	-.62	1.13	.10	$4.4 \times 10^{-3}$	to $5.2 \times 10^5$

$$\log T_{\text{IMP}} = a + b(\log T_{\text{ISEE}1})$$

Year	IMP	# Points	a	b	$\alpha$	1- $\sigma$ range (T)
Instrument						
1977	LANL	655	.21	0.95	.06	$1.7 \times 10^2$ to $2.1 \times 10^5$
1978	LANL	635	.30	0.93	.09	$2.0 \times 10^2$ to $8.7 \times 10^5$
1979	LANL	525	-.97	1.17	.14	$3.6 \times 10^{-4}$ to $1.2 \times 10^7$
1977-1979	LANL	1815	.14	0.96	.11	$0.4$ to $3.4 \times 10^6$
1977	MIT	461	.81	.84	.08	$1.8 \times 10^{-3}$ to $4.9 \times 10^5$
1978	MIT	859	.80	.83	.11	$6.3 \times 10^{-3}$ to $3.7 \times 10^4$
1979	MIT	921	.46	.86	.14	$10^2$ to $4.6 \times 10^5$
1977-1979	MIT	2241	.85	.80	.14	$2.5 \times 10^{-3}$ to $2.2 \times 10^5$

$$\log T_{\text{IMP}} = a + b(\log T_{\text{ISEE}3})$$

Year	# Points	a	b	$\alpha$	1- $\sigma$ range (T)
1978-1980	5008 (MIT)	-.06	1.04	.08	$.02$ to $1.6 \times 10^5$
1978	815 (LANL)	.34	0.94	.06	$3.3 \times 10^{-4}$ to $2.2 \times 10^7$

Cross-comparisons of ISEE 1 with either IMP instrument were performed on a fairly small number of points. Thus the significance of the year-to-year variations is not easily determined. Chaining the IMP(LANL)-IMP(MIT) with the IMP(MIT)-ISEE 1 equations yields results consistent with the direct IMP(LANL) ISEE 1 equations for both densities and temperatures. Temperatures will not be normalized since the 1977-1979 regression parameters do not differ significantly from Y=X. We do normalize ISEE 1 density as indicated in Table 9.

A cross-comparison of ion-based ISEE 3 densities with IMP(MIT) densities was done for 1978 through day 48, 1980 (Table 7). Similar regression parameters are obtained when ISEE 3 electron-based densities are used for 1979.

The IMP(LANL) ISEE 3 density regression parameters for 1979 and 1982 lie within a  $1-\sigma$  range of the normalization used in Supplement 2 ( $\log N_{\text{LANL}} = .20 + .83 \log N_{\text{ISEE } 3}$ ). However, 1980 and 1981 IMP(LANL) ISEE 3 regression parameters have a different character. The regression line appears to be lowered in a similar manner to that found from the IMP(LANL)-IMP(MIT) cross-comparison. Since IMP(MIT) ISEE 3 regression parameters do not exhibit any anomalies for 1980 and 1981, we assume that any instrumental time variability is in the IMP(LANL) instrument. Thus we normalize all IMP(MIT) and ISEE 3 densities using the same relation that was used in Supplement 2. As explained earlier, IMP(MIT) parameter values are selected preferentially over IMP(LANL) values when both are available for any given hour. Because of this, there is only a small number (~300) of 1980-1981 hours having IMP(LANL) data.

To further support the ignoring of time variations in the normalizations, we depict in Figure 12 the yearly averages of the densities, velocities, and temperatures for the two IMP plasma instruments. These averages are based on the overlapping hours listed in the first part of Tables 6, 7 and 8. Velocities agree quite closely. Average temperatures are not as close, but LANL temperatures are consistently higher than MIT temperatures. The average LANL densities are lower than MIT densities for 1980 and 1981 yet higher for all other years.

Table 9 summarizes the normalizations used in this book.

TABLE 9. Normalization Parameters for N and T

DS	$P = \log N$		$P = \log T$	
	a	b	a	b
IMP-LANL	0	1.00	0	1.00
IMP-MIT	.12	0.89	-.62	1.11
ISEE 3	.20	0.83	-.55	1.07
ISEE 1	.18	0.85	0	1.00

# Yearly IMP Plasma Averages

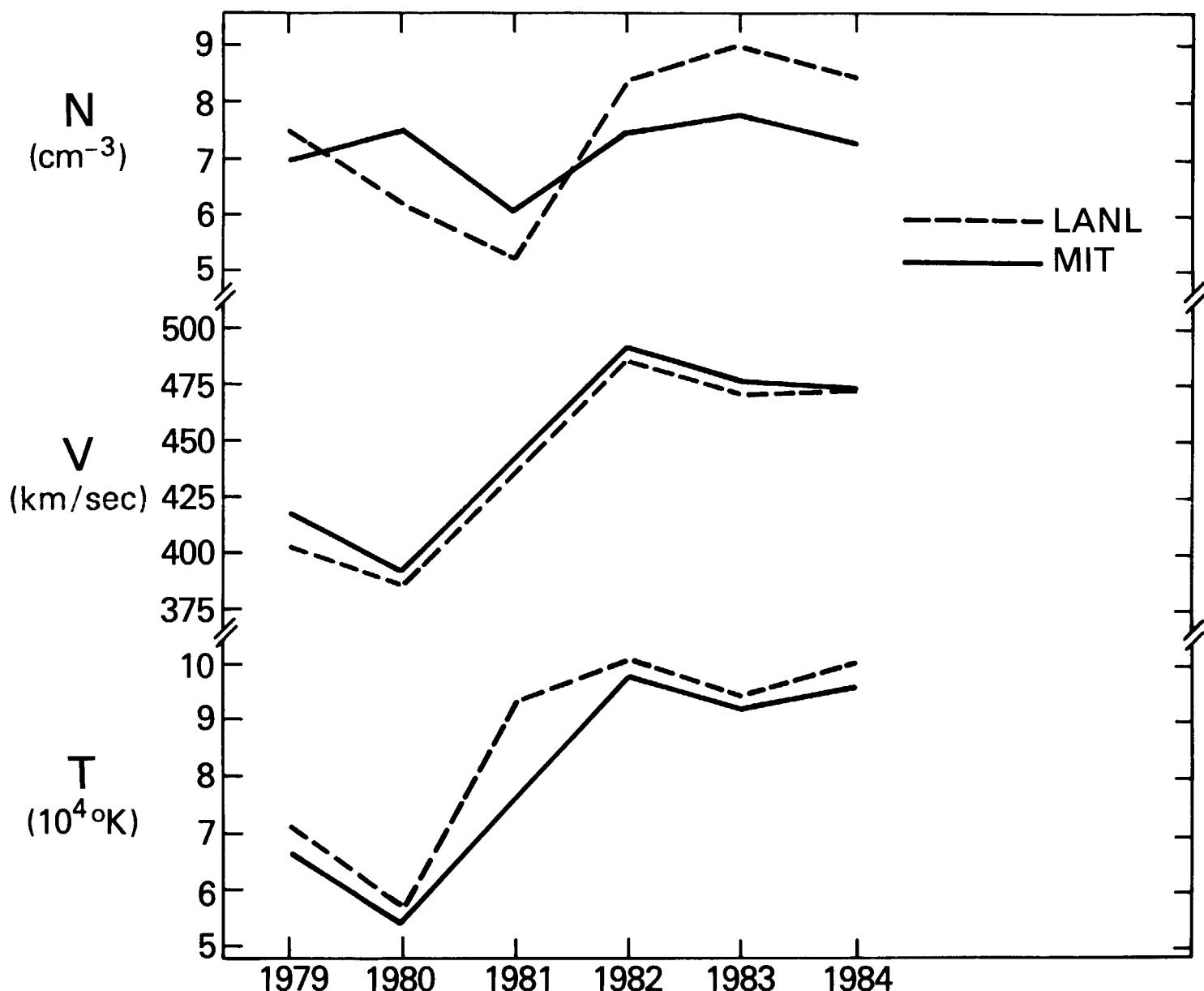


Figure 12

### Data Coverage

The percent of coverage of the composite data set over the 1963 to 1985 time period is shown in Figure 13. Of the 188,568 hours included in Bartels' solar rotations 1783 to 2073, there are 98,771 hours with field and plasma data of which 72,548 hours have field and plasma data from a common spacecraft, 22,031 hours with field data only, 24,960 hours with plasma data only, and 42,806 hours with no interplanetary plasma or field data.

### Data Presentation

This third Data Book Supplement consists of graphical (Volume 3) and tabular (Volume 3A) presentations of some of the parameters of the composite data set. In Volume 3, there are two plots for each solar rotation in which any plasma or field data were obtained. On facing pages, for convenience in lining up features in the data, are found a plot of plasma data (bulk speed, density, and proton temperature) and a plot of field data (average magnitude, geocentric solar magnetospheric (GSM)  $B_z$  component, and geocentric solar ecliptic (GSE) latitude and longitude angles of the average field vector). Note that on those rare occasions when the parameter values exceed the allowed range, a heavy mark is placed near the edge of the plot. For such cases the reader is advised to consult the data listings (Volume 3A) for appropriate numerical values.

### Additional Data Availability

In addition to the parameters listed and plotted herein, the data set from which this Data Book Supplement was generated also contains additional IMF parameters (e.g.,  $B_y$ ,  $B_z$  in GSE coordinates), additional plasma parameters (flow direction), standard deviations in IMF and plasma parameters, and geophysical and solar activity indices ( $K_p$ ,  $C_9$ ,  $Dst$ ,  $R$ ).

This data set is available both online, on the NSSDC VAX, and on magnetic tape. The data set is updated as NSSDC receives additional relevant data, at a typical frequency of every several months. New hardcopy Supplements are issued only every few years.

A word on day-numbering conventions is appropriate. When the first OMNItape was created, most input data used the convention that January 1 is Day 0. This convention was employed for the OMNItape, and has been continued for all subsequent tape versions. However, it is recognized that this is a minority convention. Accordingly, the Data Books and the recently created online "OMNIfile" both use the convention that January 1 is Day 1.

In all versions of this data set, missing parameter values are filled with zeros.

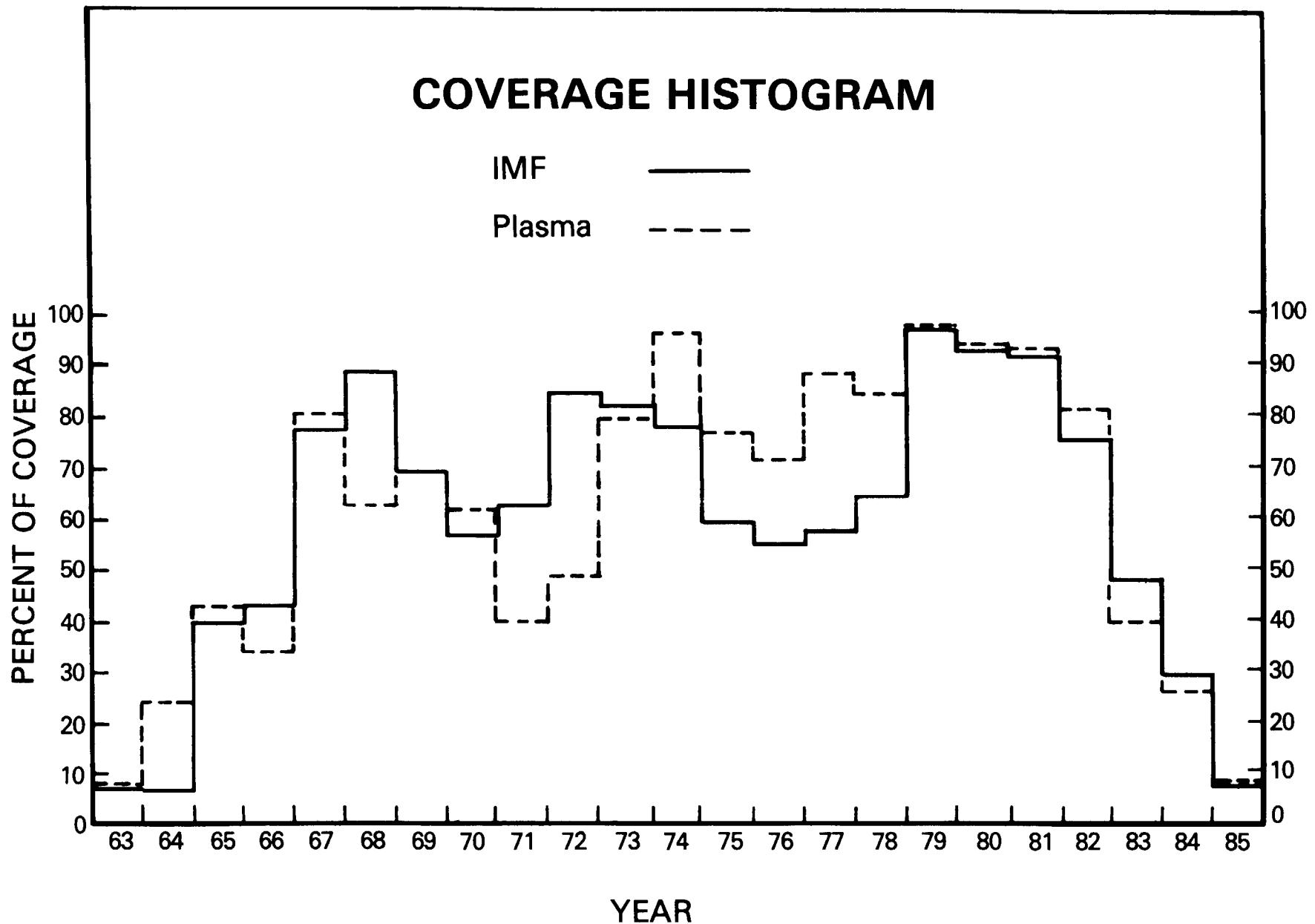


Figure 13  
29

### The Online File

The data set is online from 1976 onward. Earlier portions can be brought online in response to demand. The data set may be accessed over SPAN by \$SET HOST NSSDC, USERNAME=NSSDC. This interface gives a menu of NSSDC online services, one of which is access to the "OMNIfile." Currently, the user may view the file format and may select and list at his terminal any subset of parameters for any days of interest. Additional capabilities, such as linking to an NSSDC-supplied READ subroutine to read OMNIfile records, and creating a subfile for downloading to the user's VAX, are currently being developed.

### The Magnetic Tape

ASCII or IBM/binary magnetic tape versions of the data set from 1963 onward are also available. Copies of either of these tapes (or a reformatted version), with documentation, may be ordered electronically from another menu option of the USERNAME=NSSDC account discussed in the previous paragraph, or by request to:

National Space Science Data Center  
Code 633.4  
NASA/Goddard Space Flight Center  
Greenbelt, MD 20771  
Telephone: (301) 344-6695  
Telex No.: 89675 NASCOM GBLT  
TWX No.: 7108289716

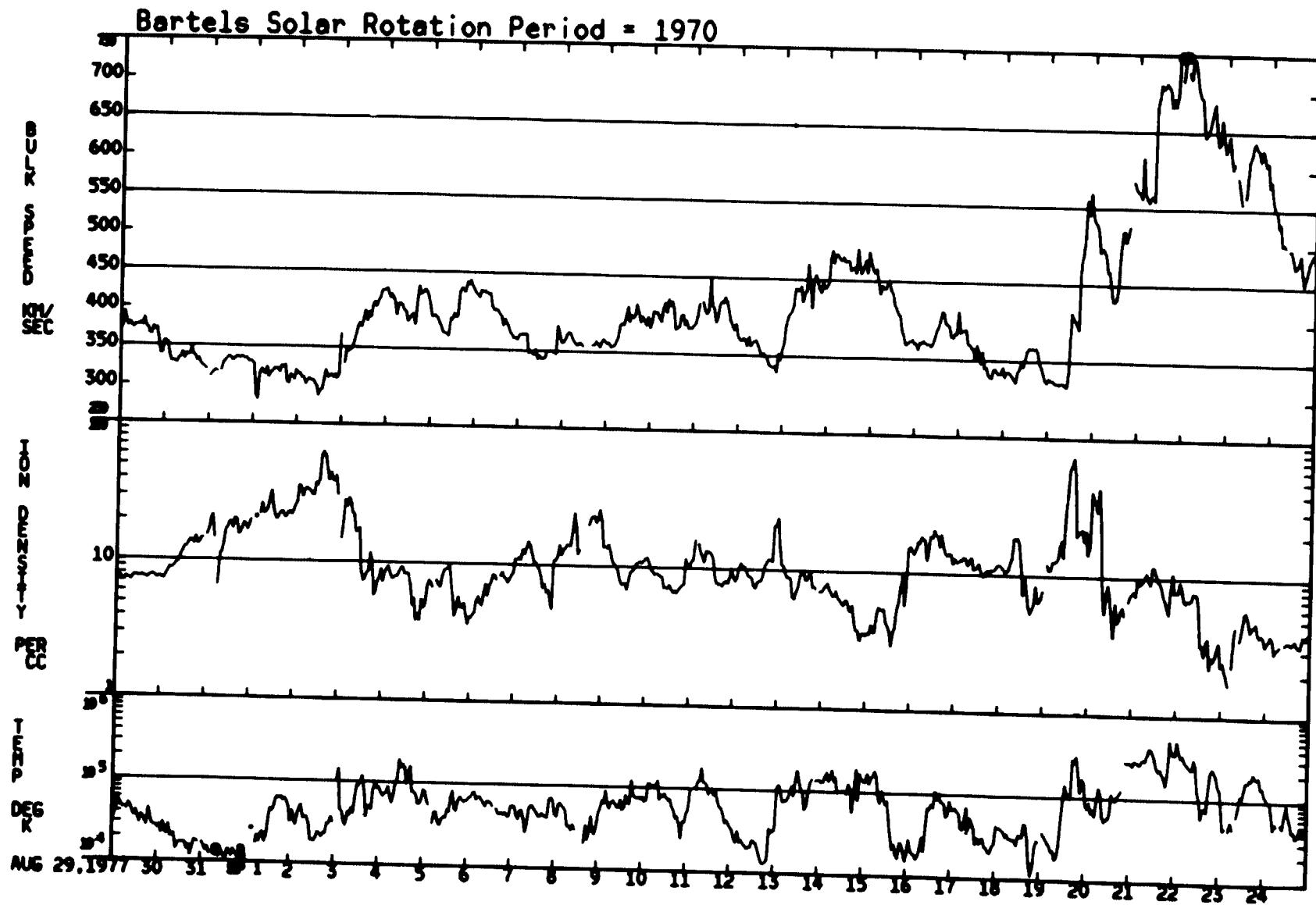
Researchers who reside outside the United States would contact:

World Data Center A for Rockets and Satellites  
Code 630.2  
NASA/Goddard Space Flight Center  
Greenbelt, MD 20771 U.S.A.  
Telephone: (301) 344-6695  
Telex No.: 89675 NASCOM GBLT  
TWX No.: 7108289716

# **Intensity Versus Time Profiles**

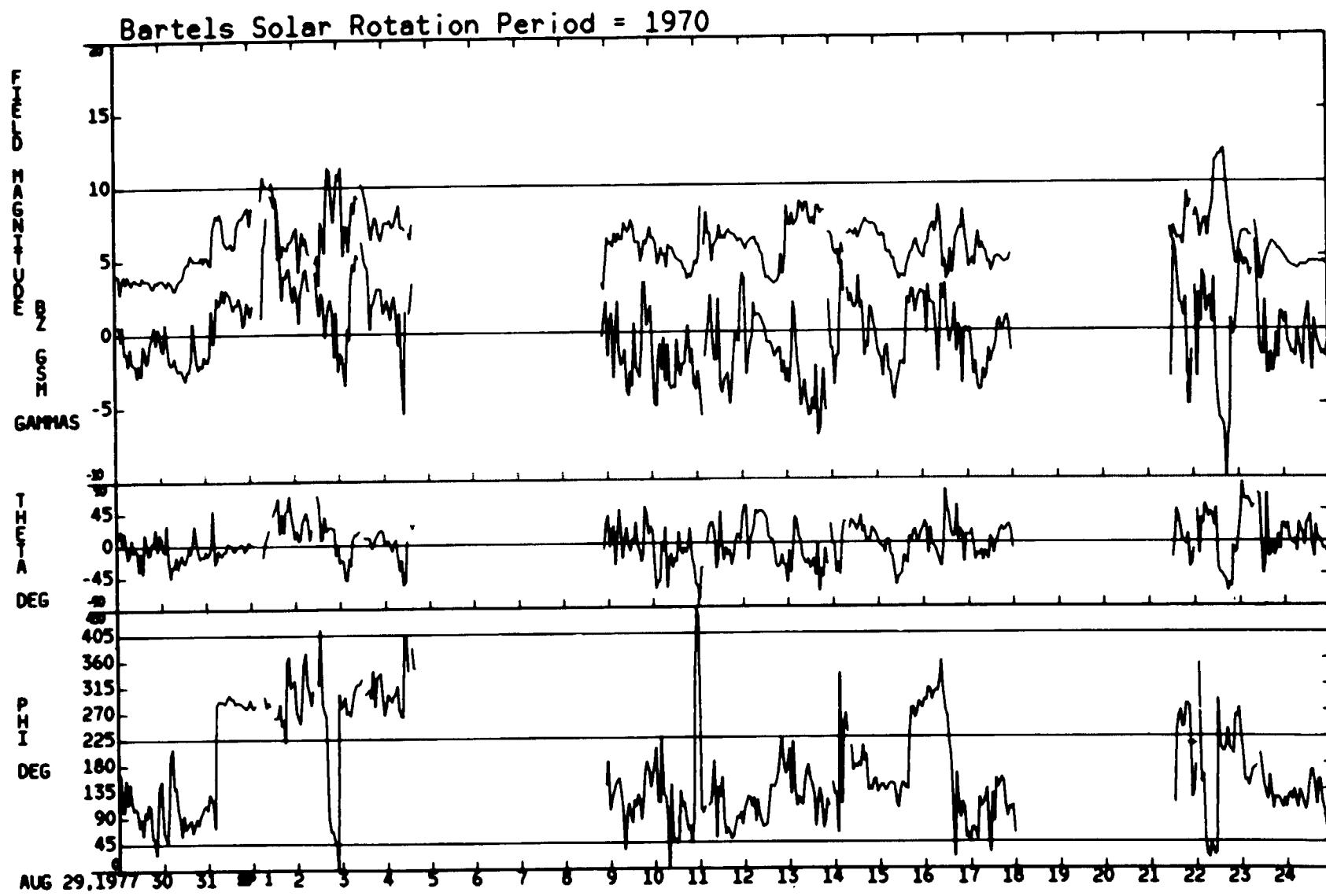
**ORIGINAL PAGE IS  
OF POOR QUALITY**

08/30/77 – 09/24/77

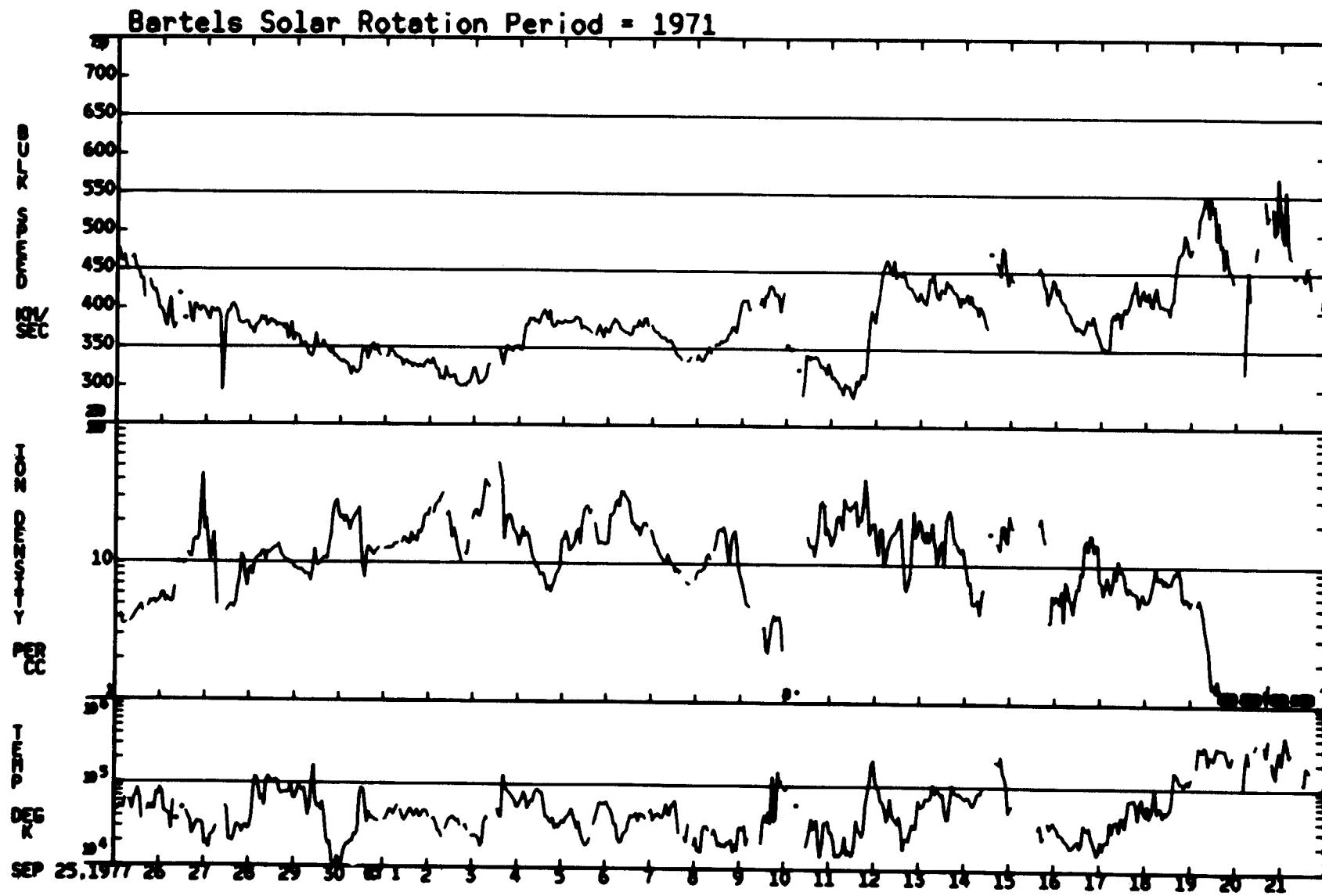


ORIGINAL PAGE IS  
OF POOR QUALITY

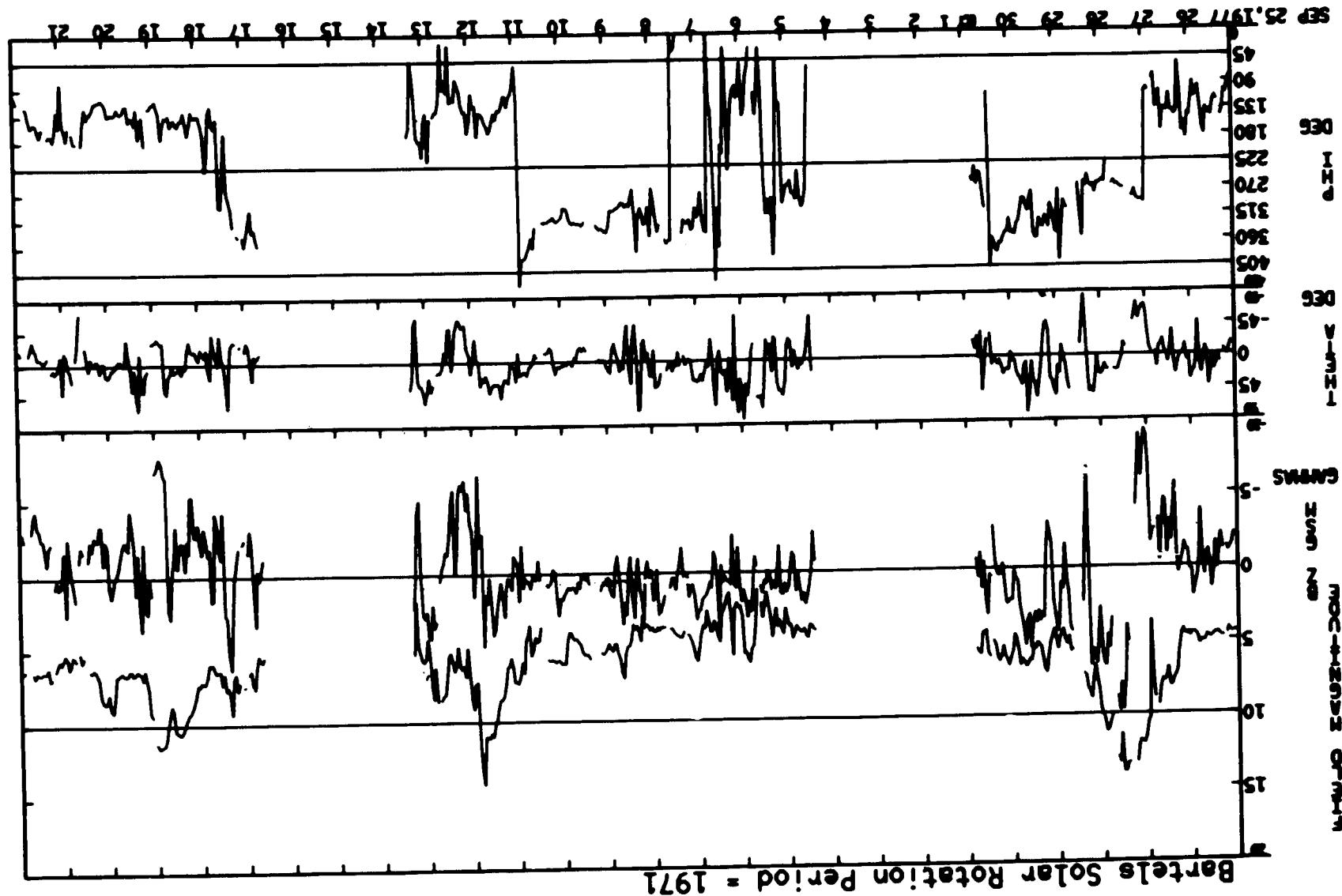
08/30/77 – 09/24/77



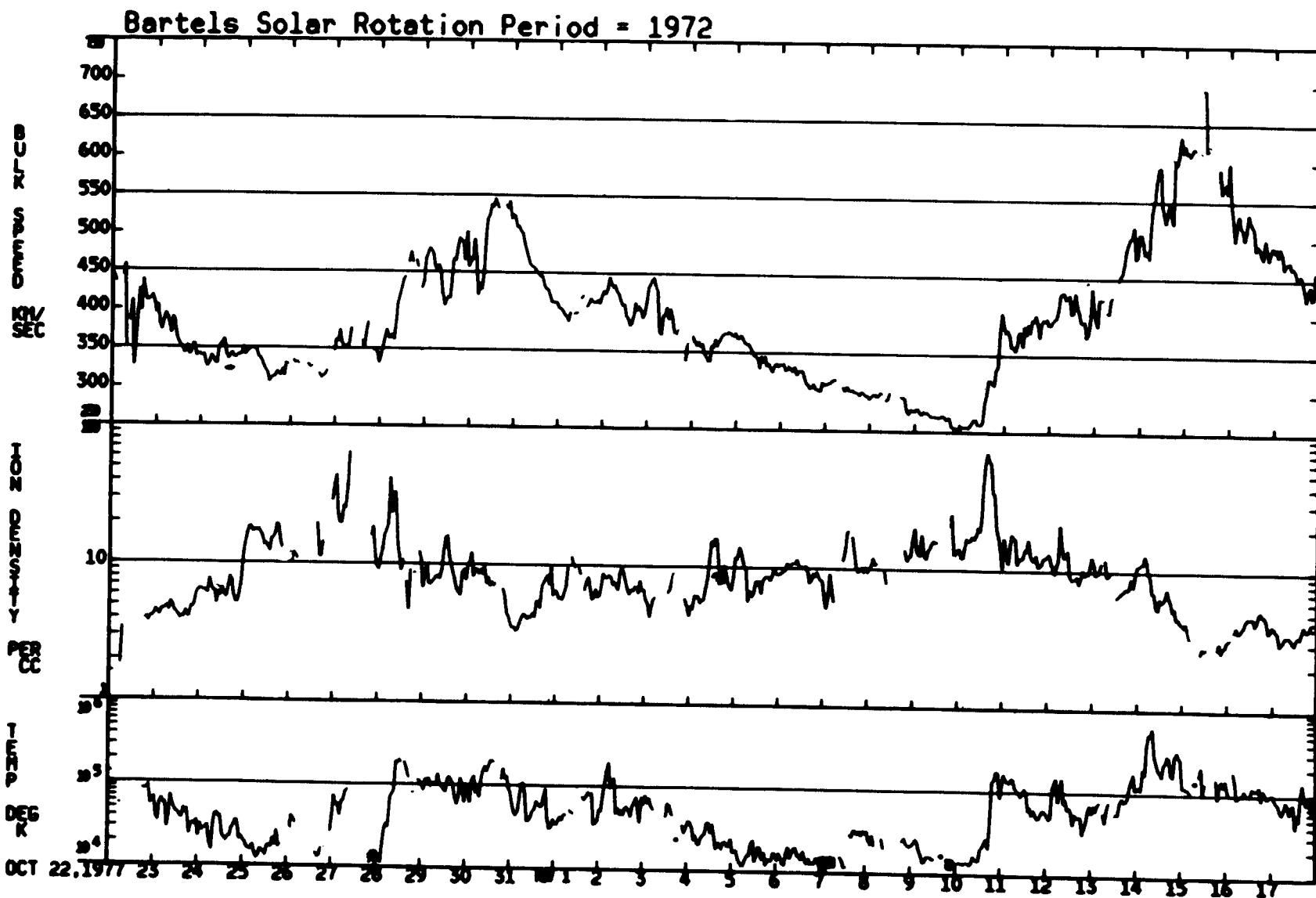
09/25/77 – 10/21/77



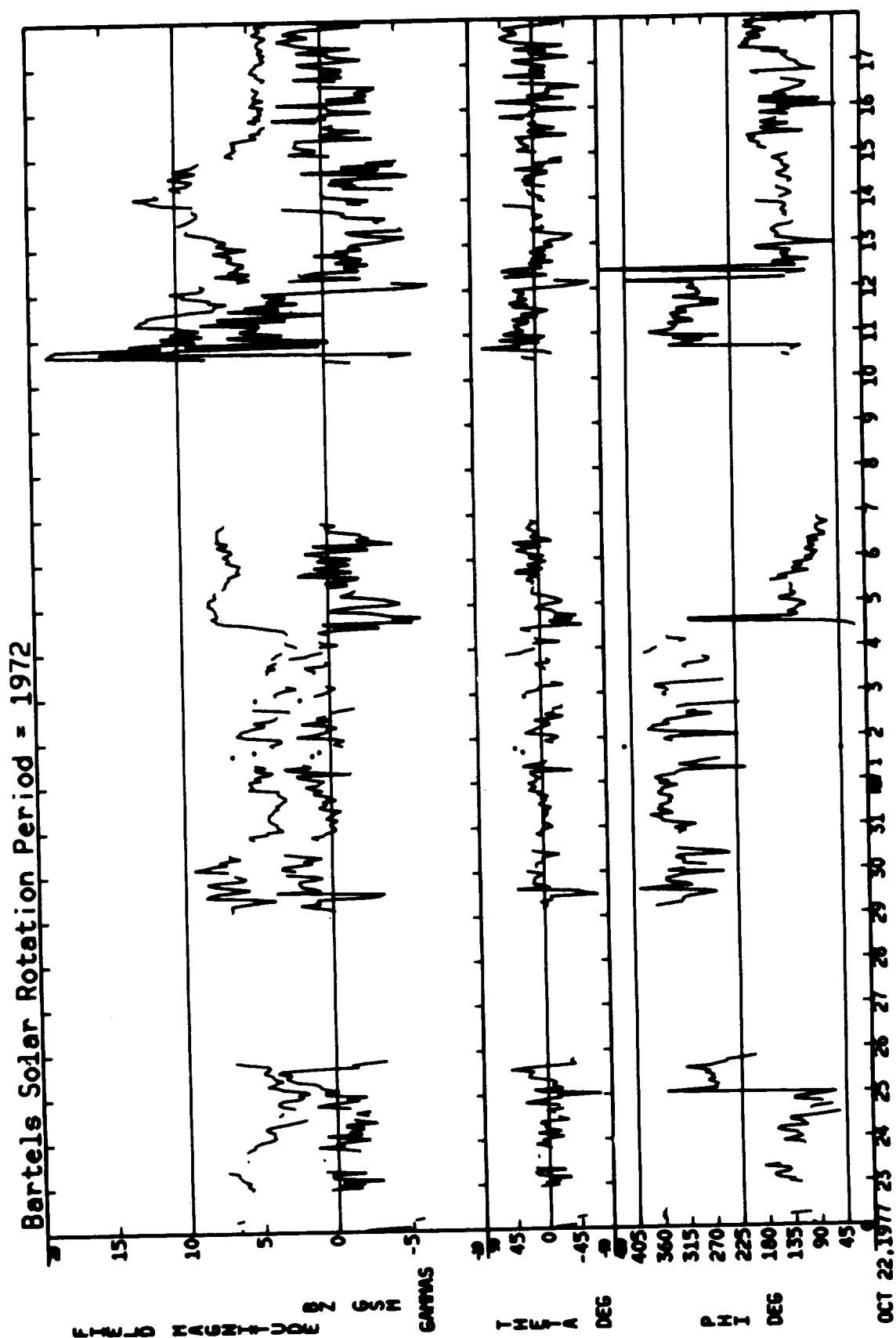
09/25/77 - 10/21/77



10/22/77 - 11/17/77

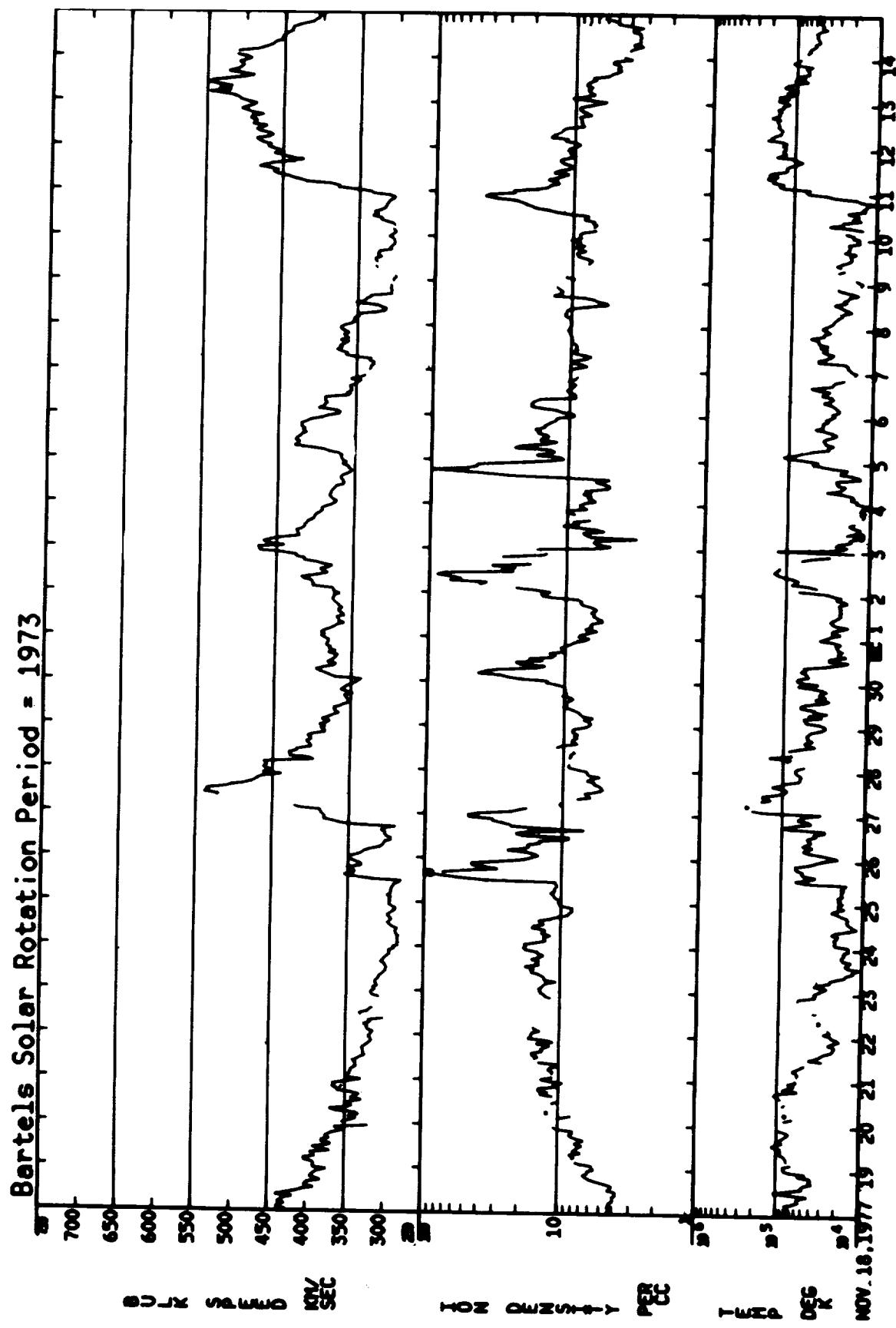


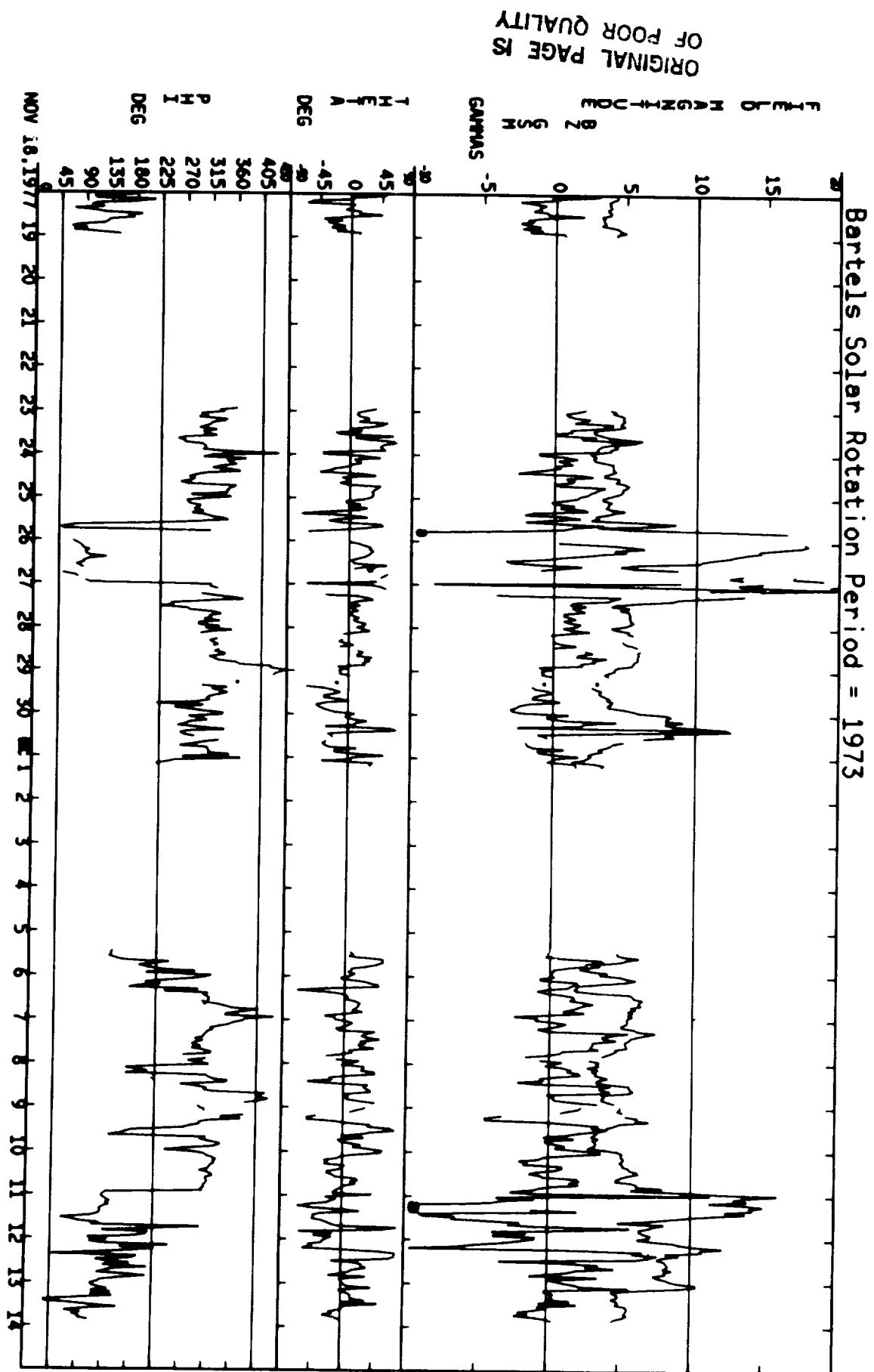
10/22/77 - 11/17/77



ORIGINAL PAGE IS  
OF POOR QUALITY

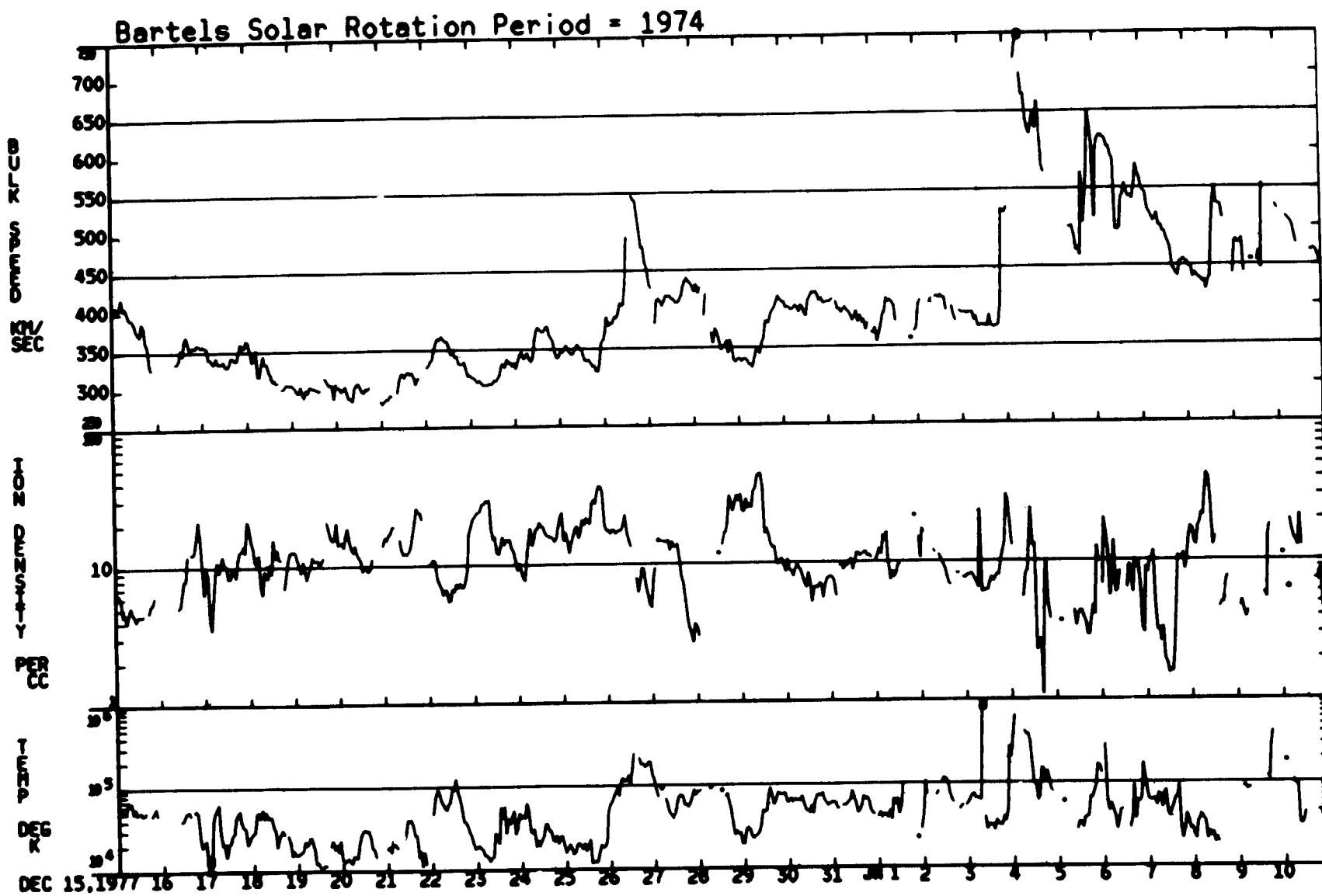
11/18/77 - 12/14/77



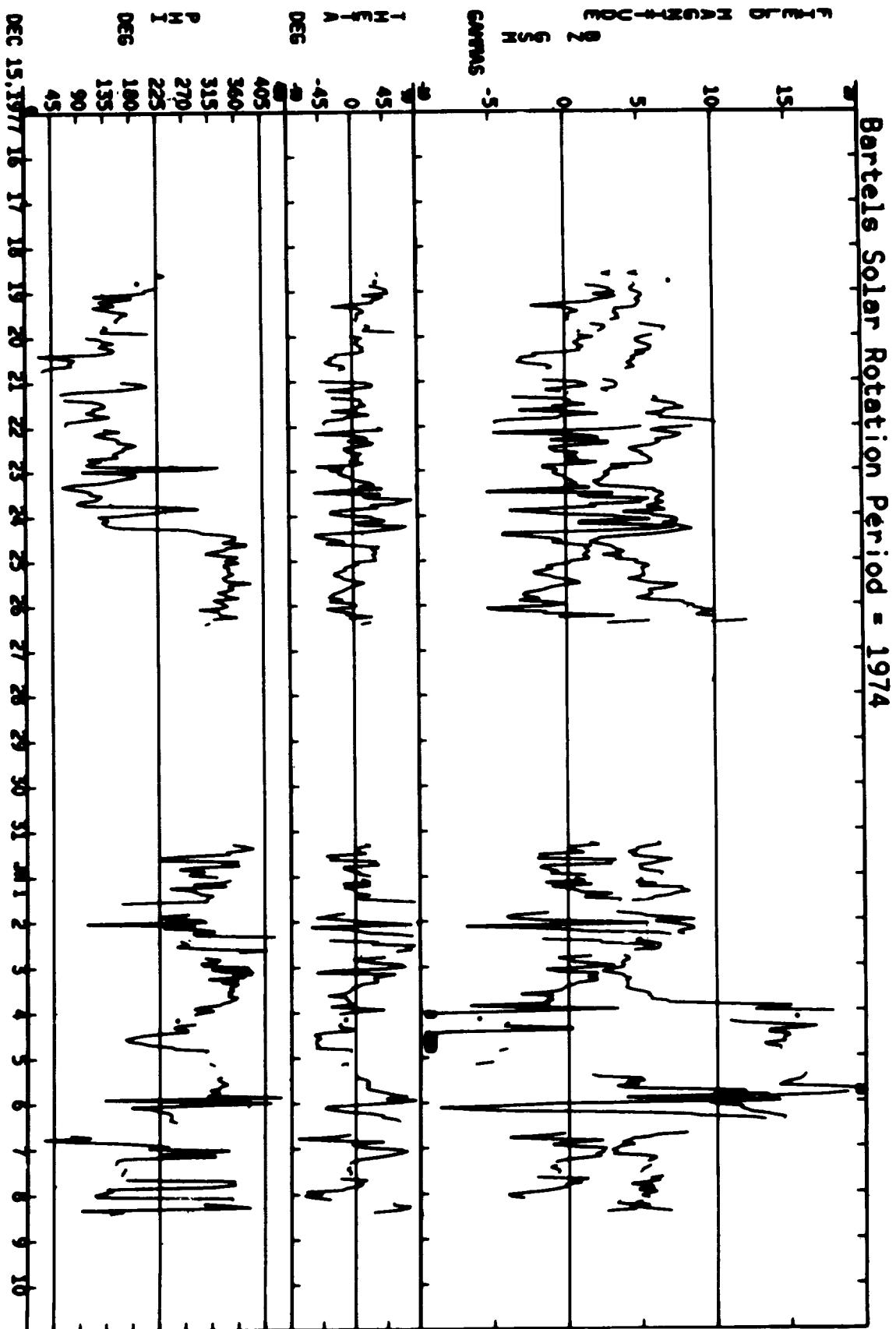


11/18/77 - 12/14/77

12/15/77 – 01/10/78

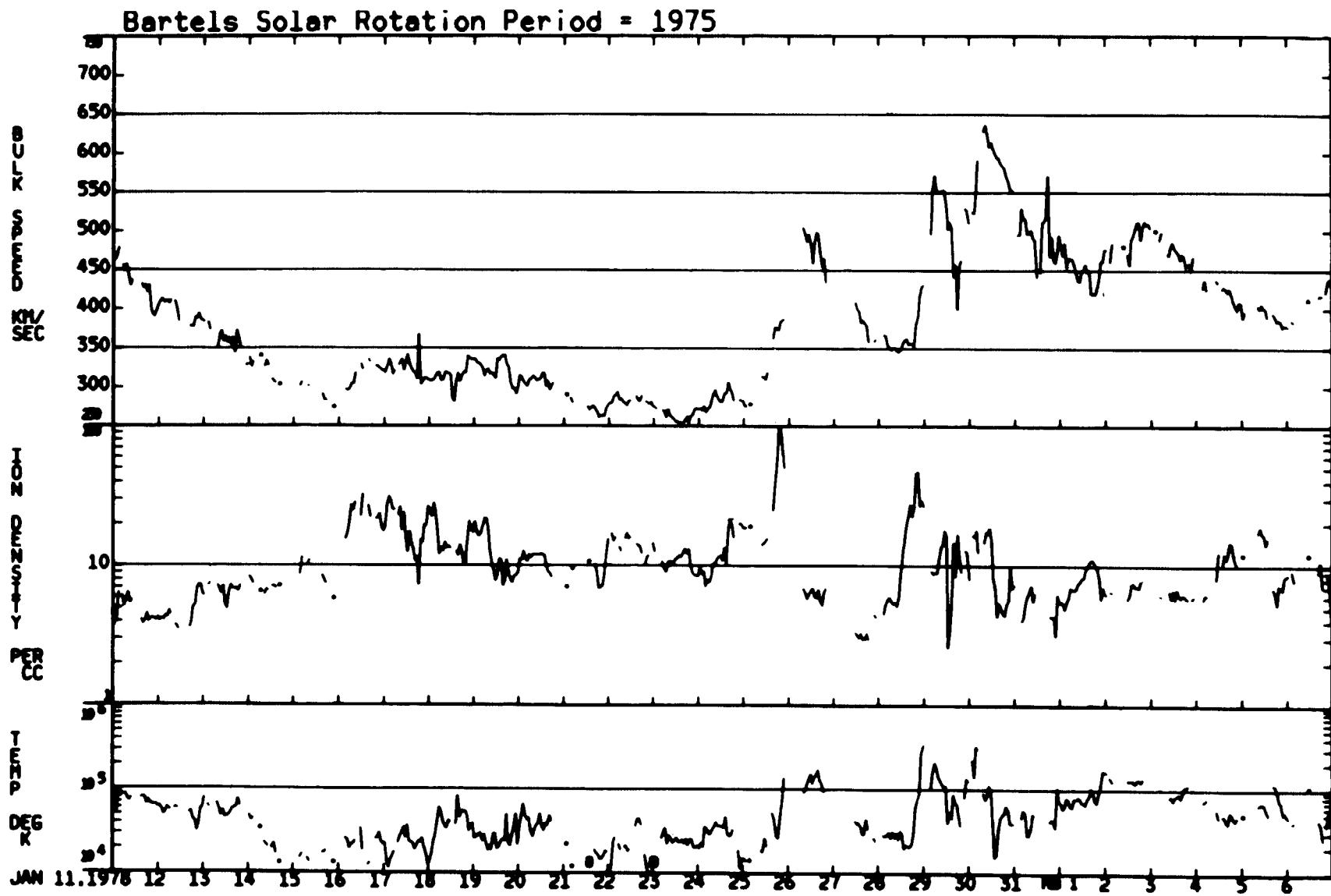


ORIGINAL PAGE IS  
OF POOR QUALITY

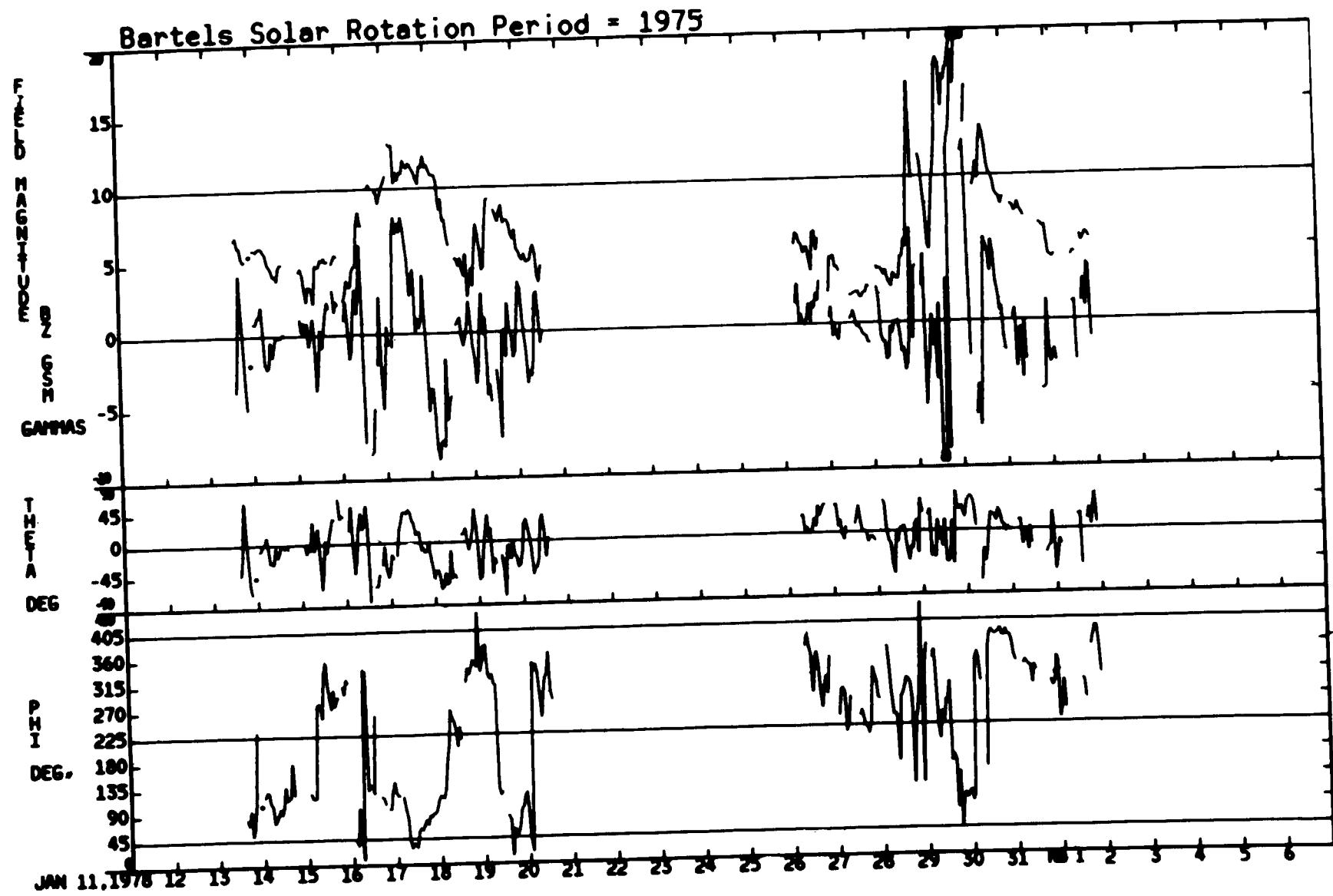


12/15/77 - 01/10/78

01/11/78 – 02/06/78

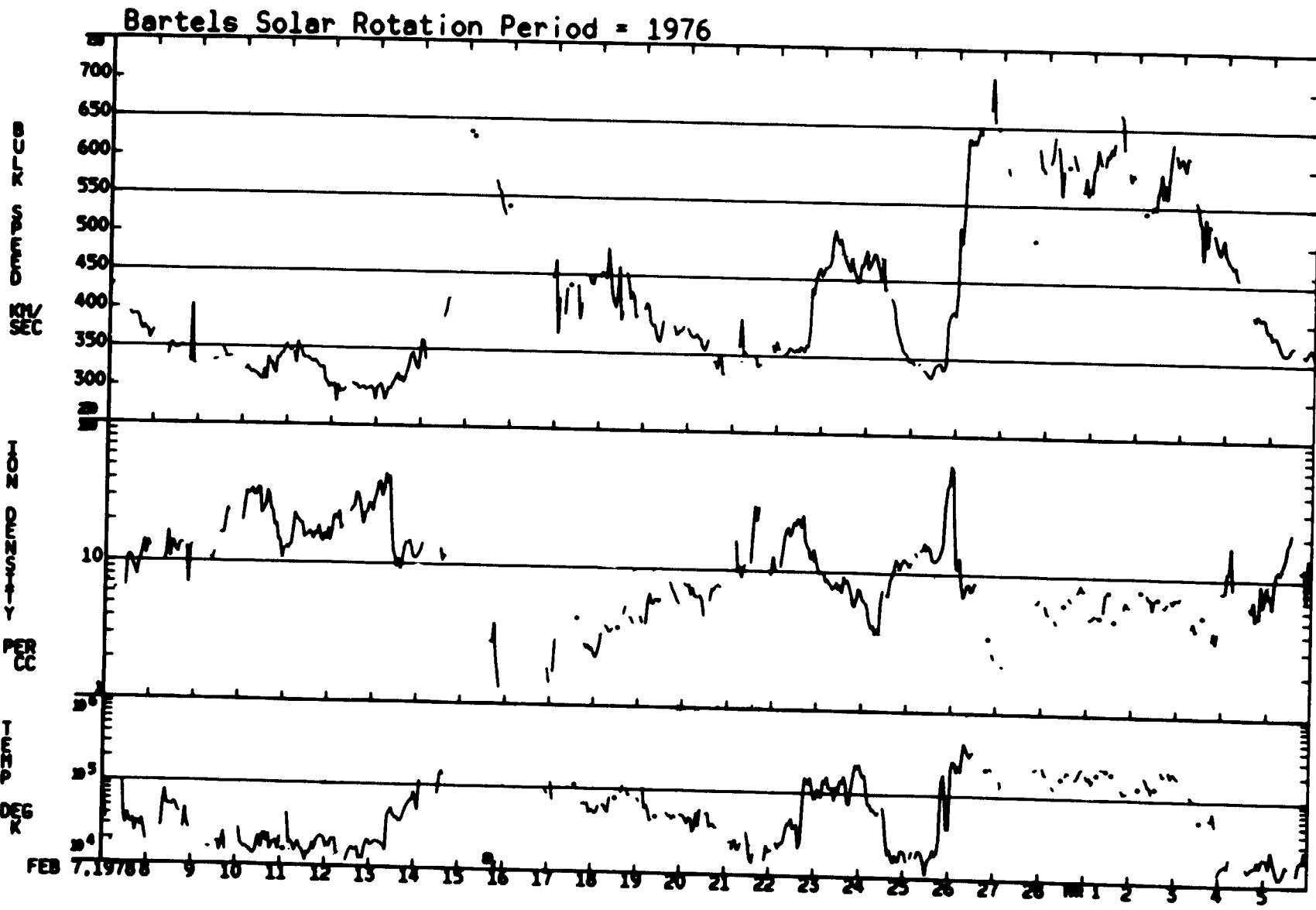


01/11/78 – 02/06/78

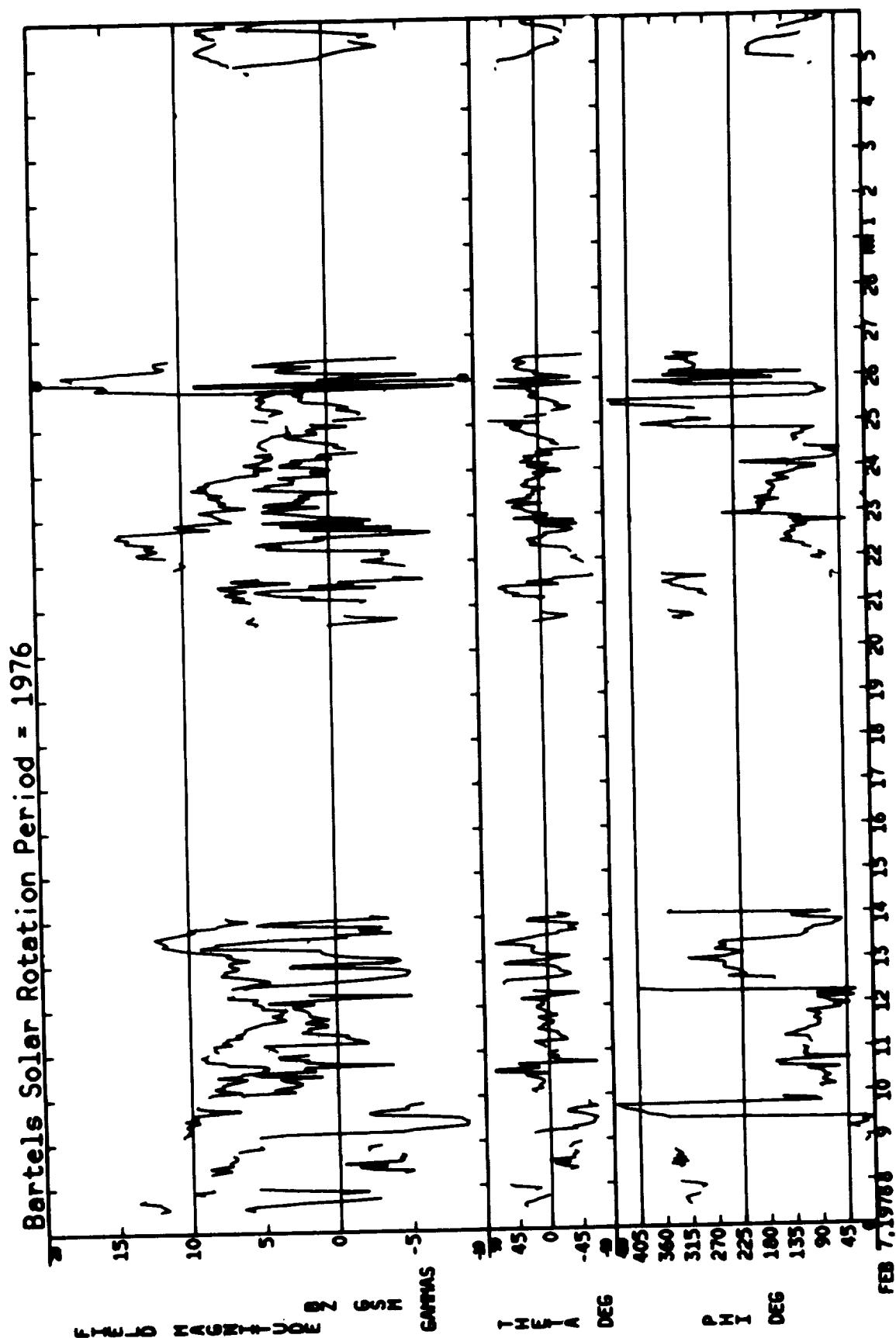


ORIGINAL PAGE IS  
OF POOR QUALITY

02/07/78 – 03/05/78

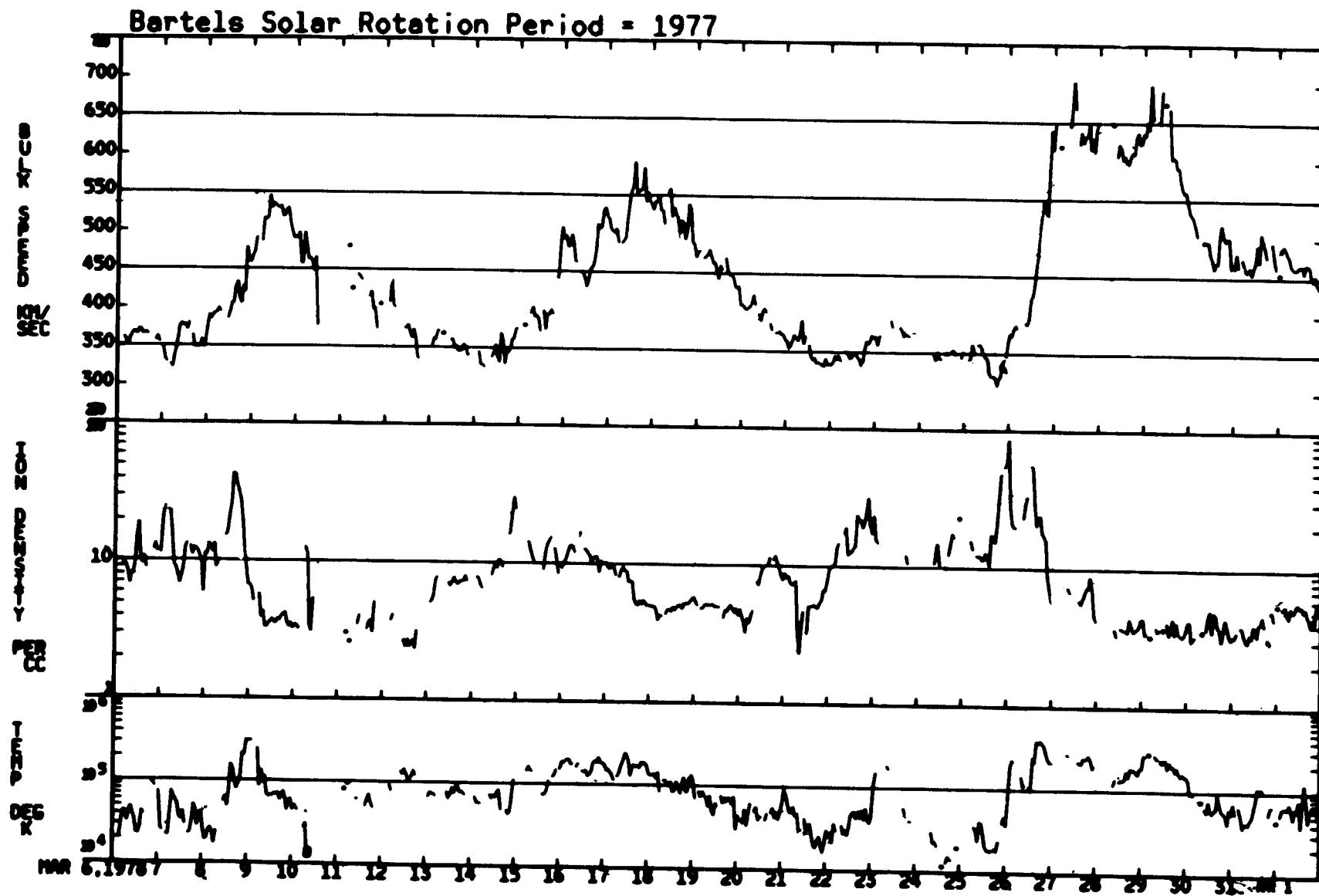


02/07/78 – 03/05/78



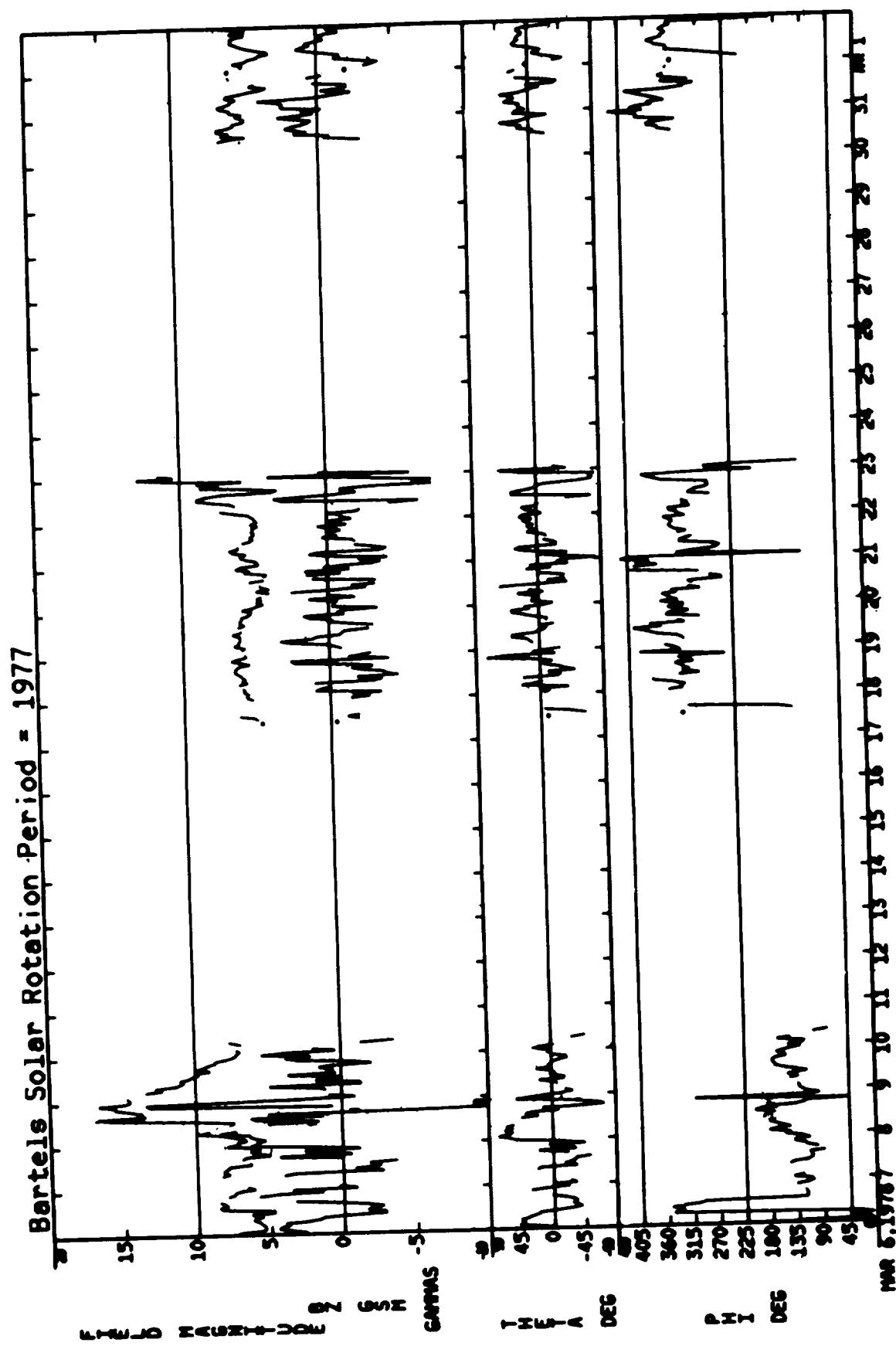
CRIMINAL PAGE IS  
OF POOR QUALITY

03/06/78 — 04/01/78

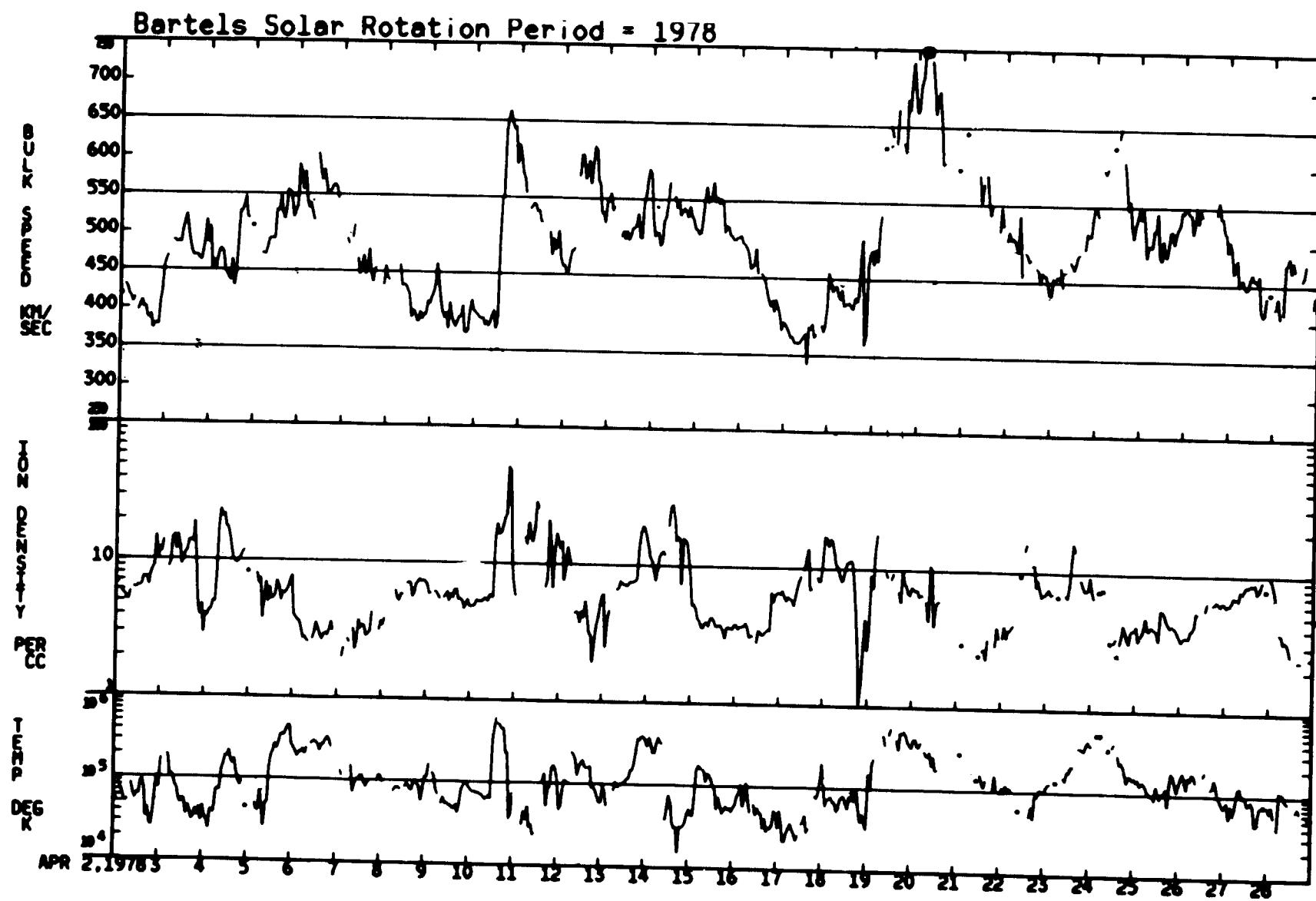


C. THIS PAGE IS  
OF POOR QUALITY.

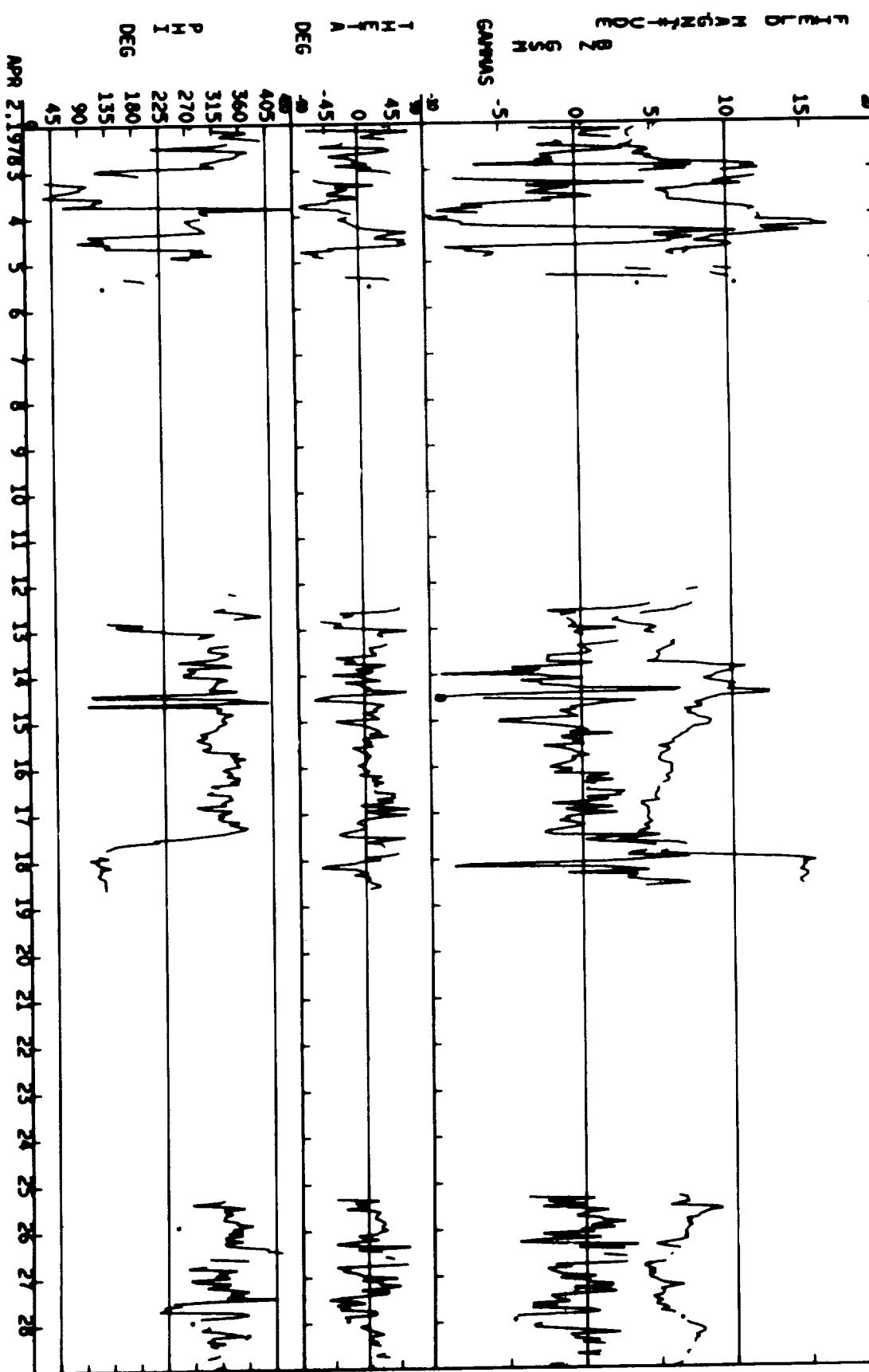
03/06/78 - 04/01/78



04/02/78 – 04/28/78

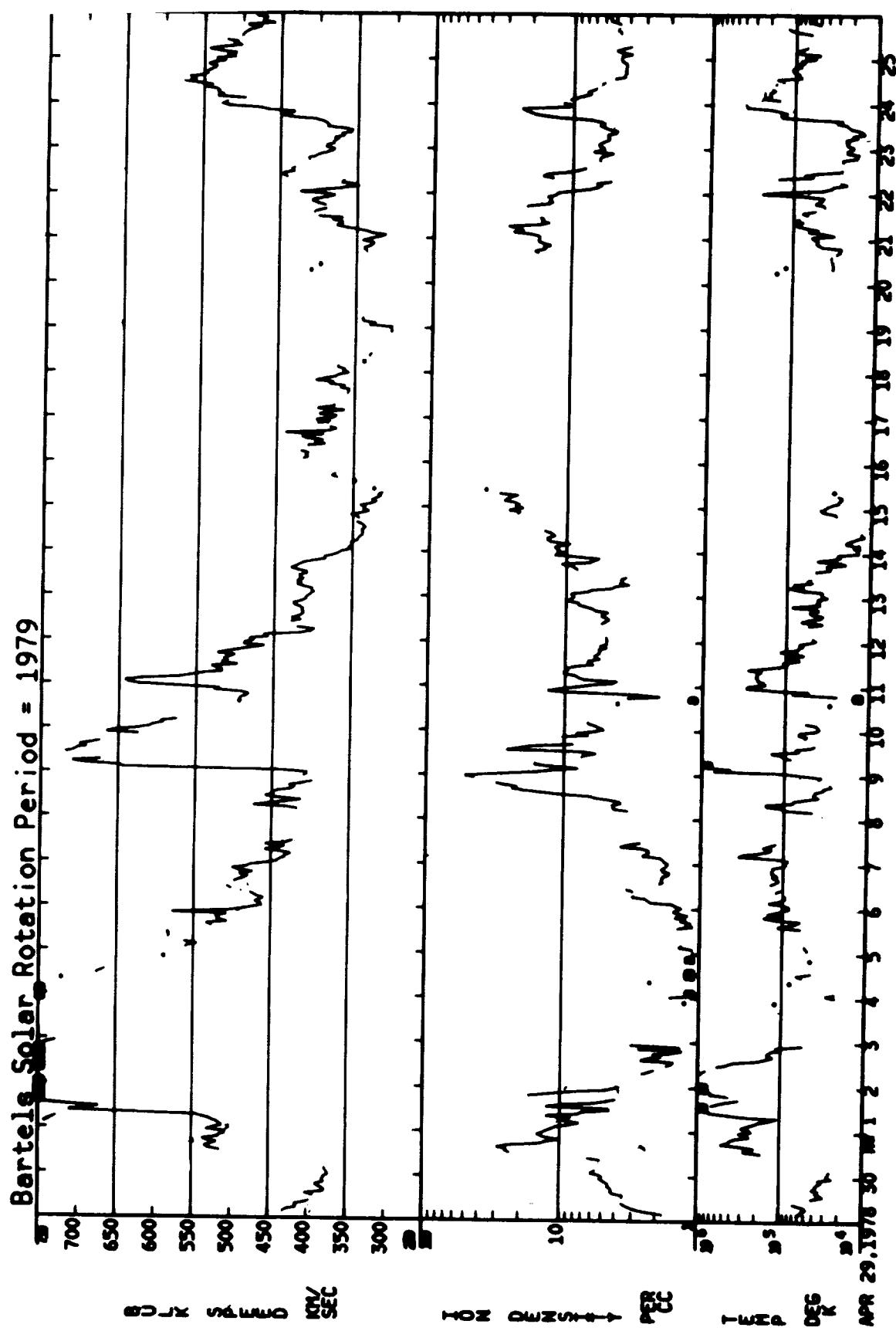


Bartels Solar Rotation Period = 1978



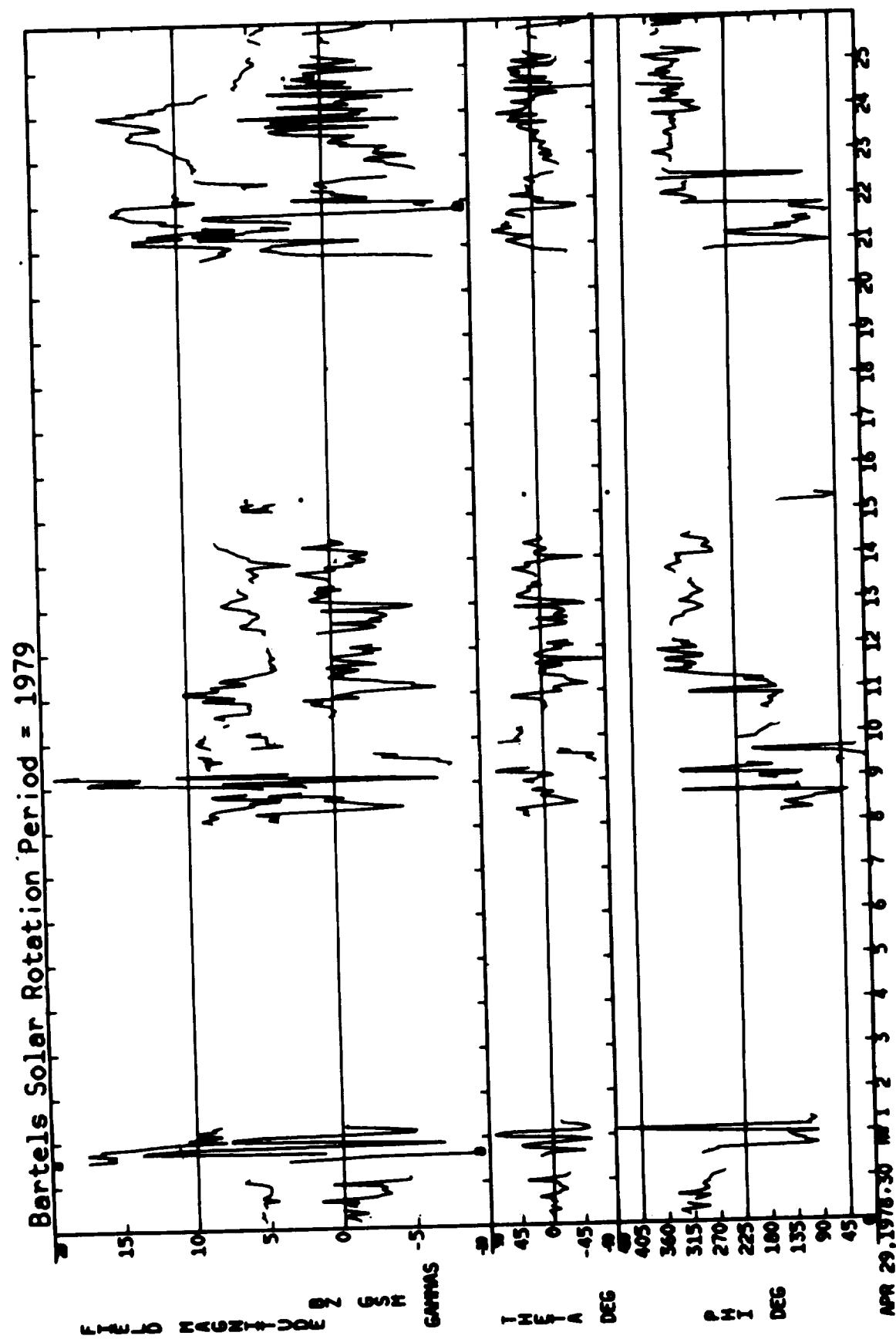
04/02/78 - 04/28/78

04/29/78 — 05/25/78

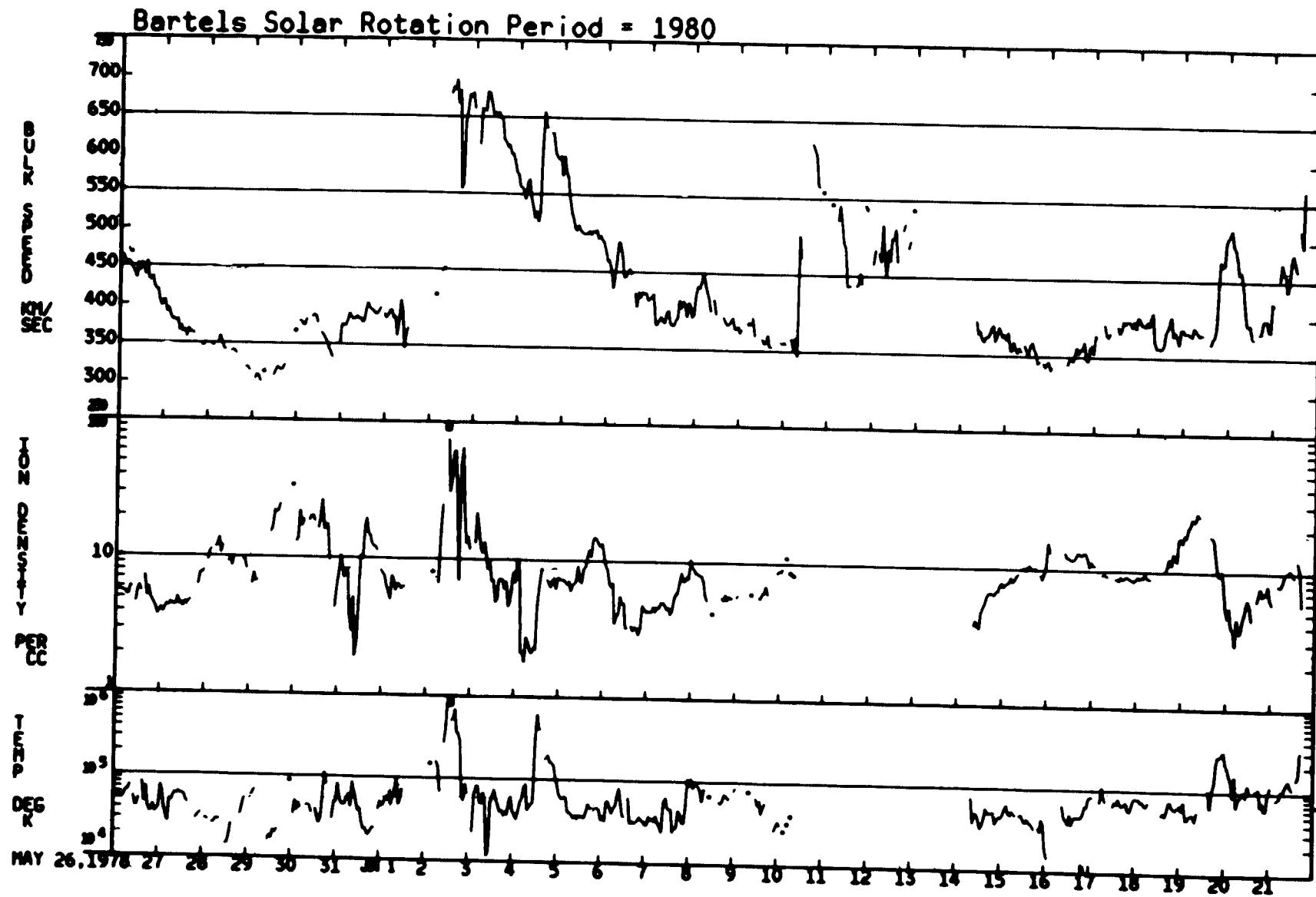


ORIGINAL PAGE IS  
OF POOR QUALITY

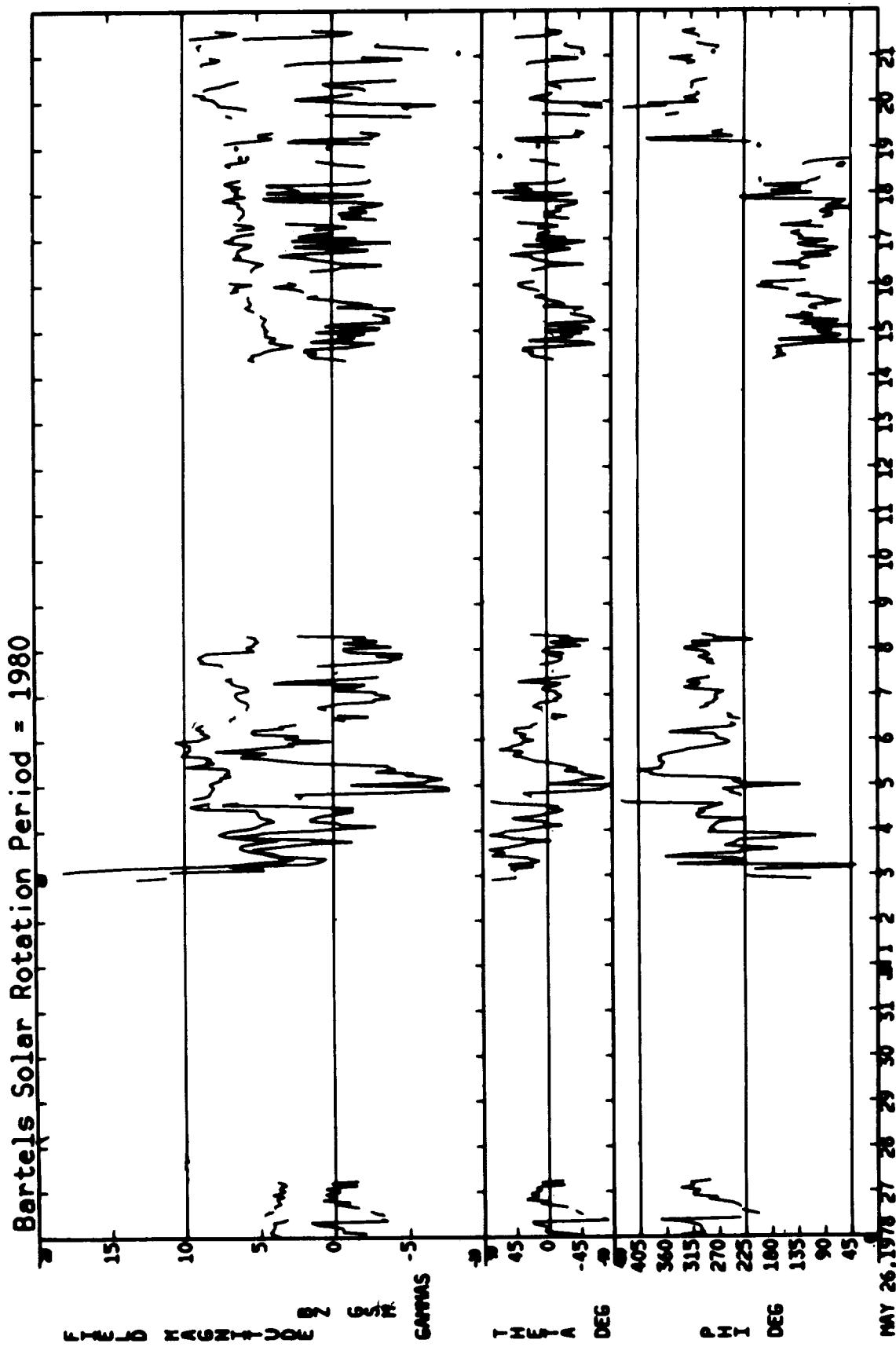
04/29/78 - 05/25/78



05/26/78 – 06/21/78

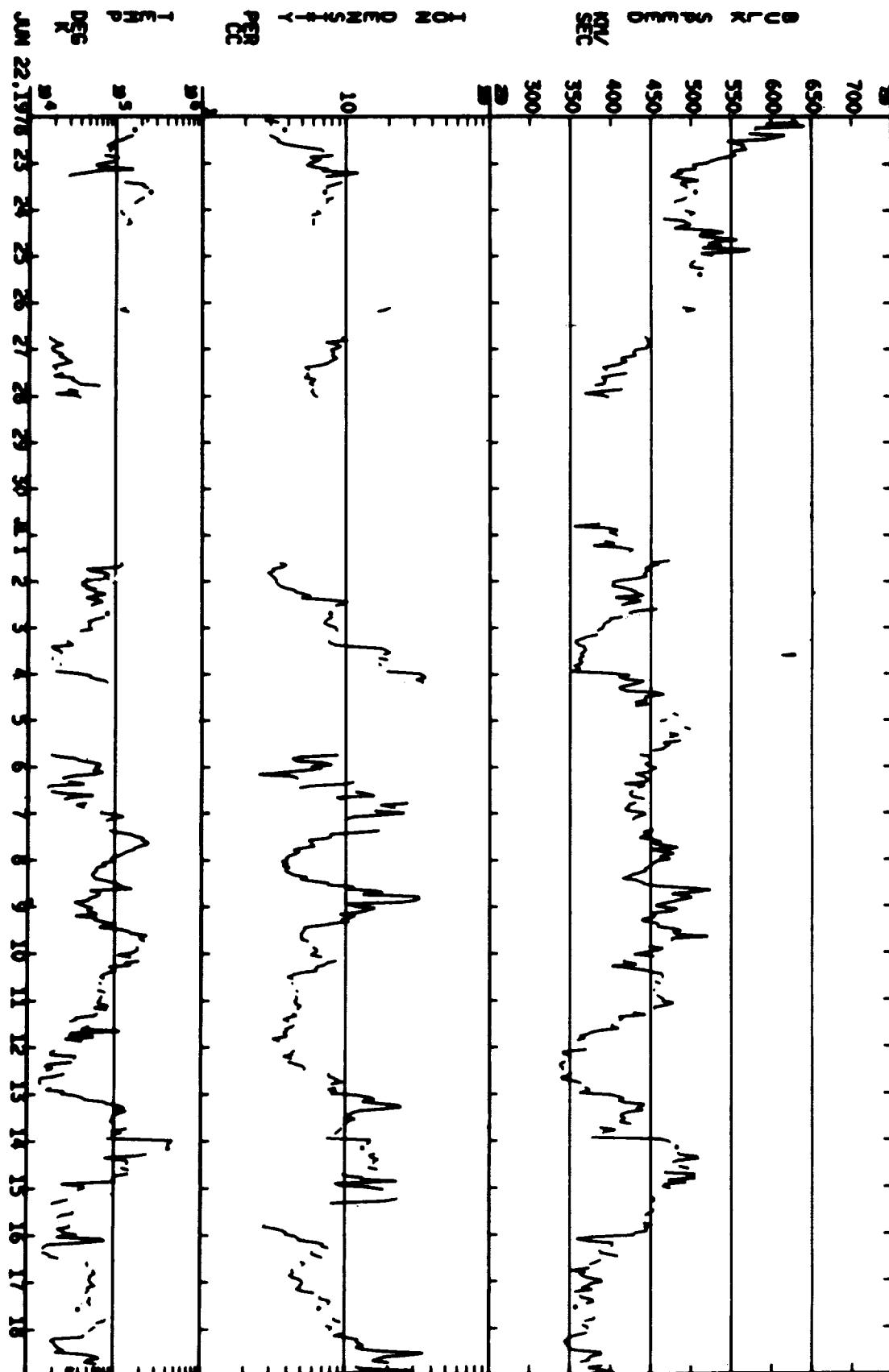


05/26/78 – 06/21/78



ORIGINAL PAGE IS  
OF POOR QUALITY

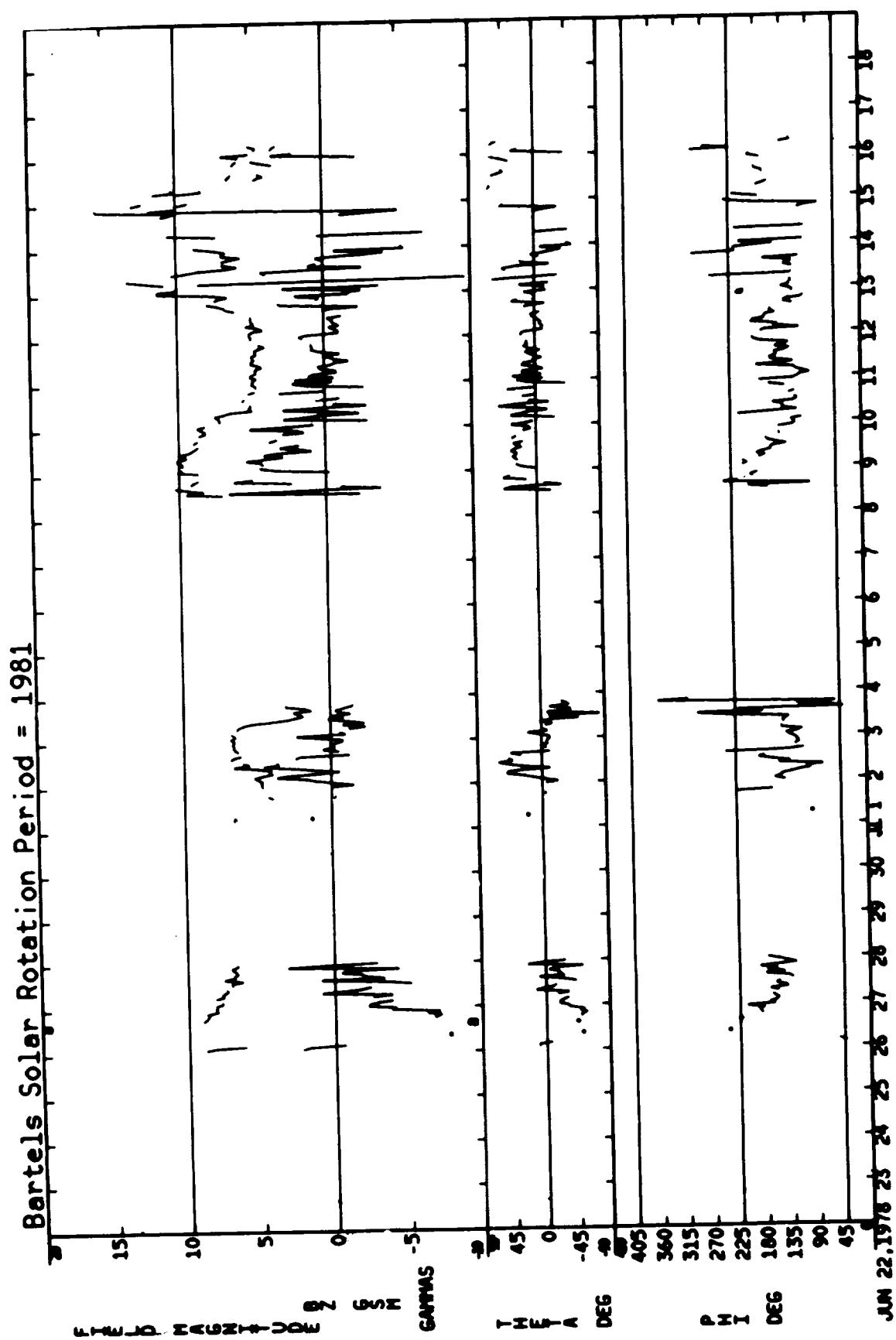
Bartels Solar Rotation Period = 1981



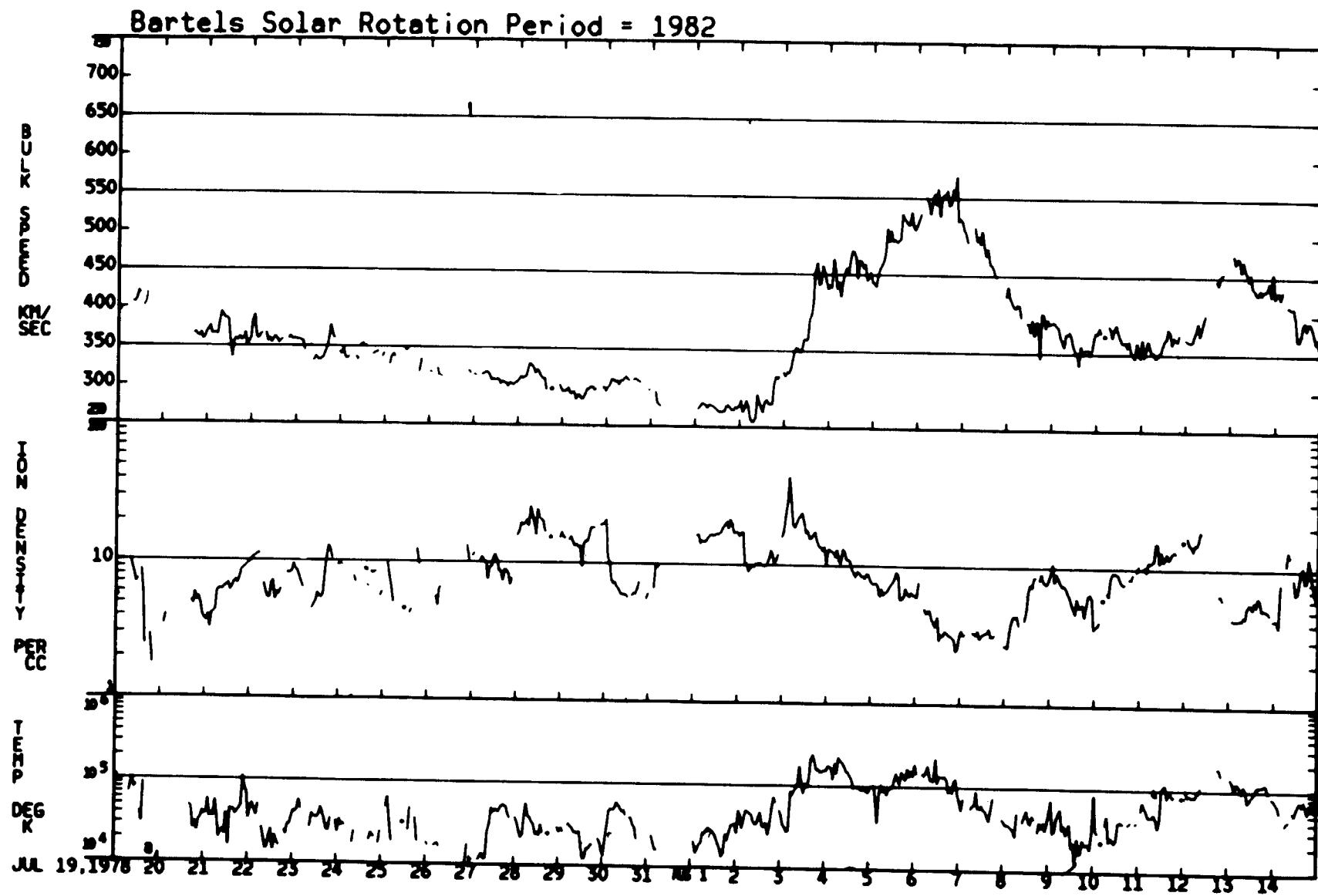
06/22/78 - 07/18/78

ORIGINAL PAGE IS  
OF POOR QUALITY

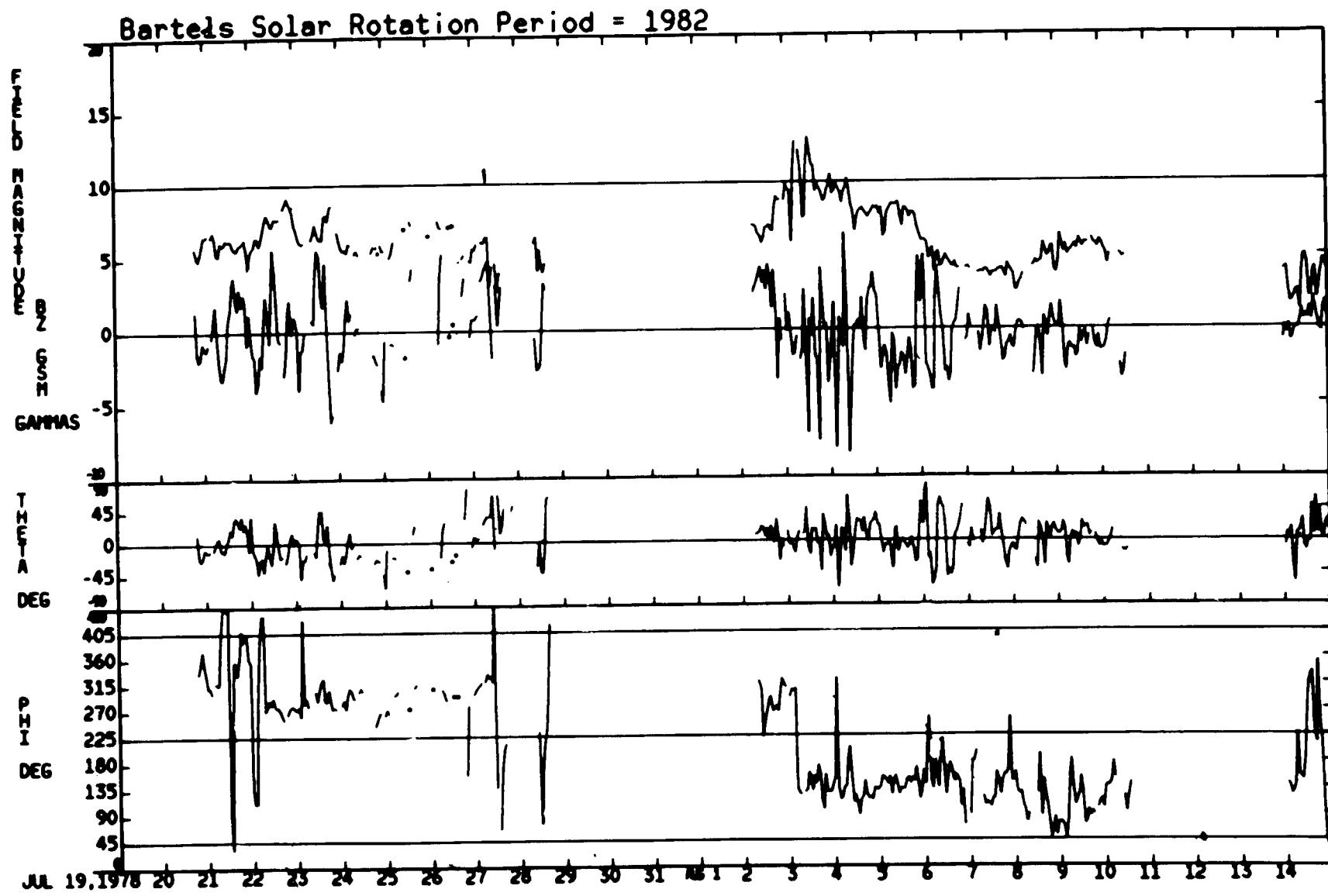
06/22/78 — 07/18/78



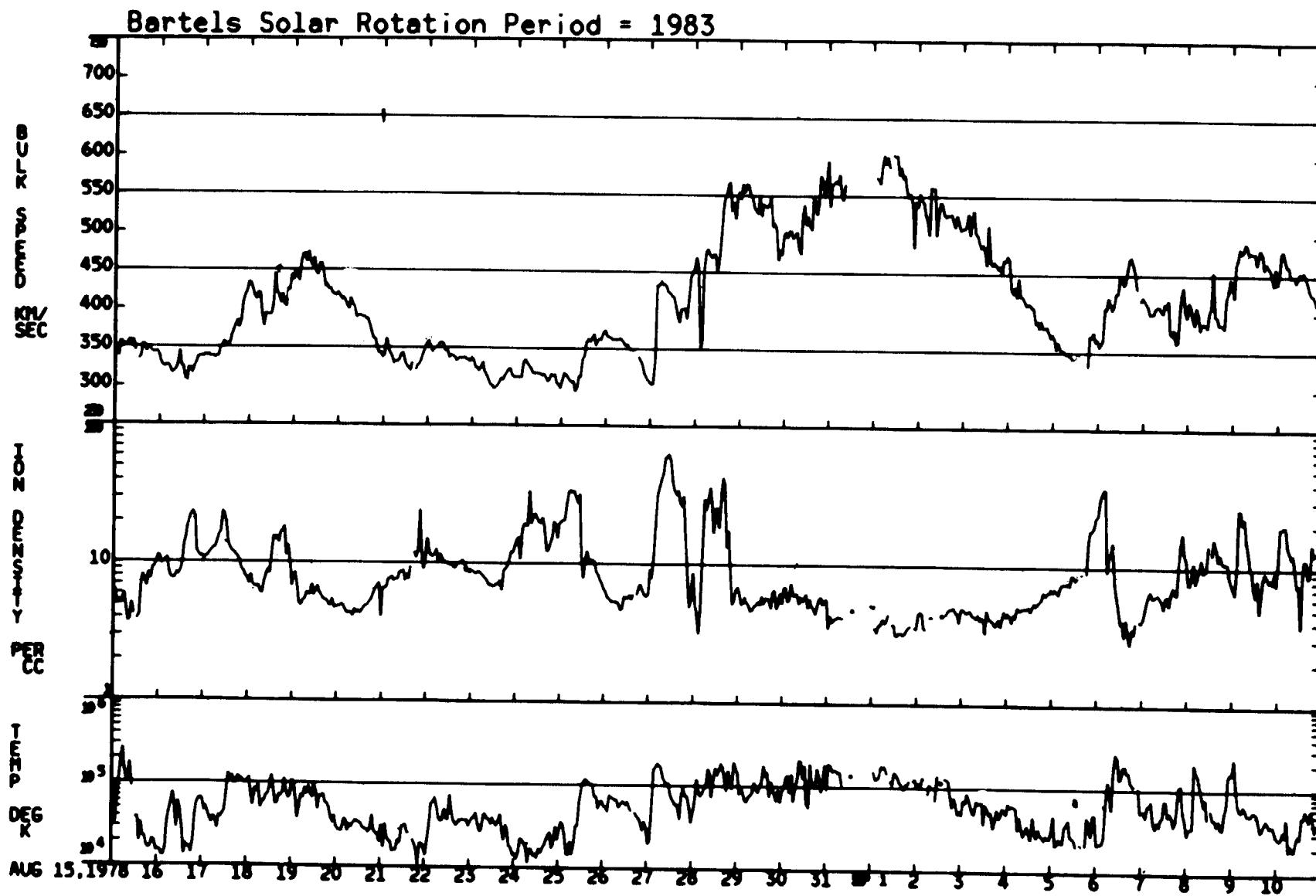
07/19/78 – 08/14/78



07/19/78 – 08/14/78

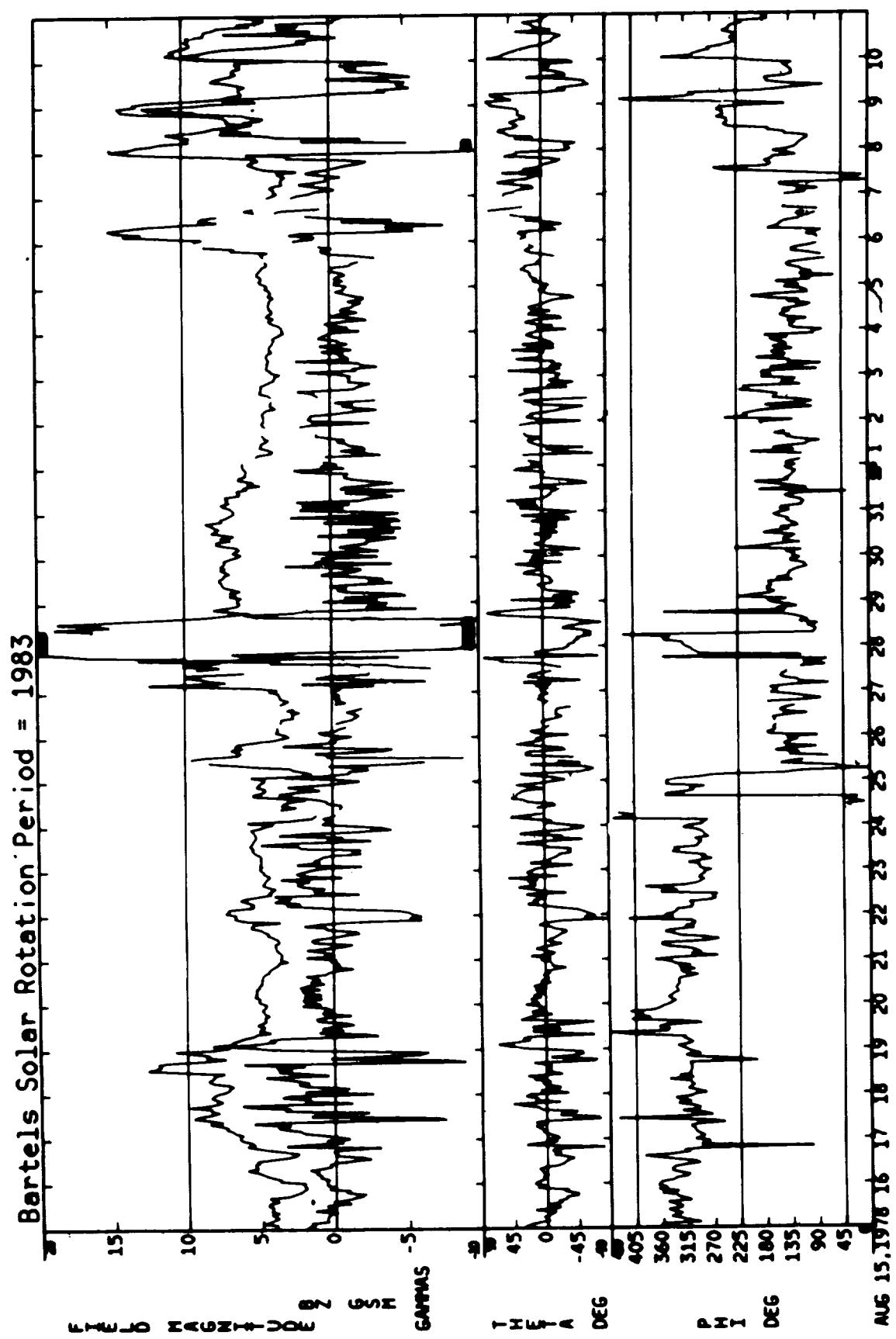


08/15/78 – 09/10/78

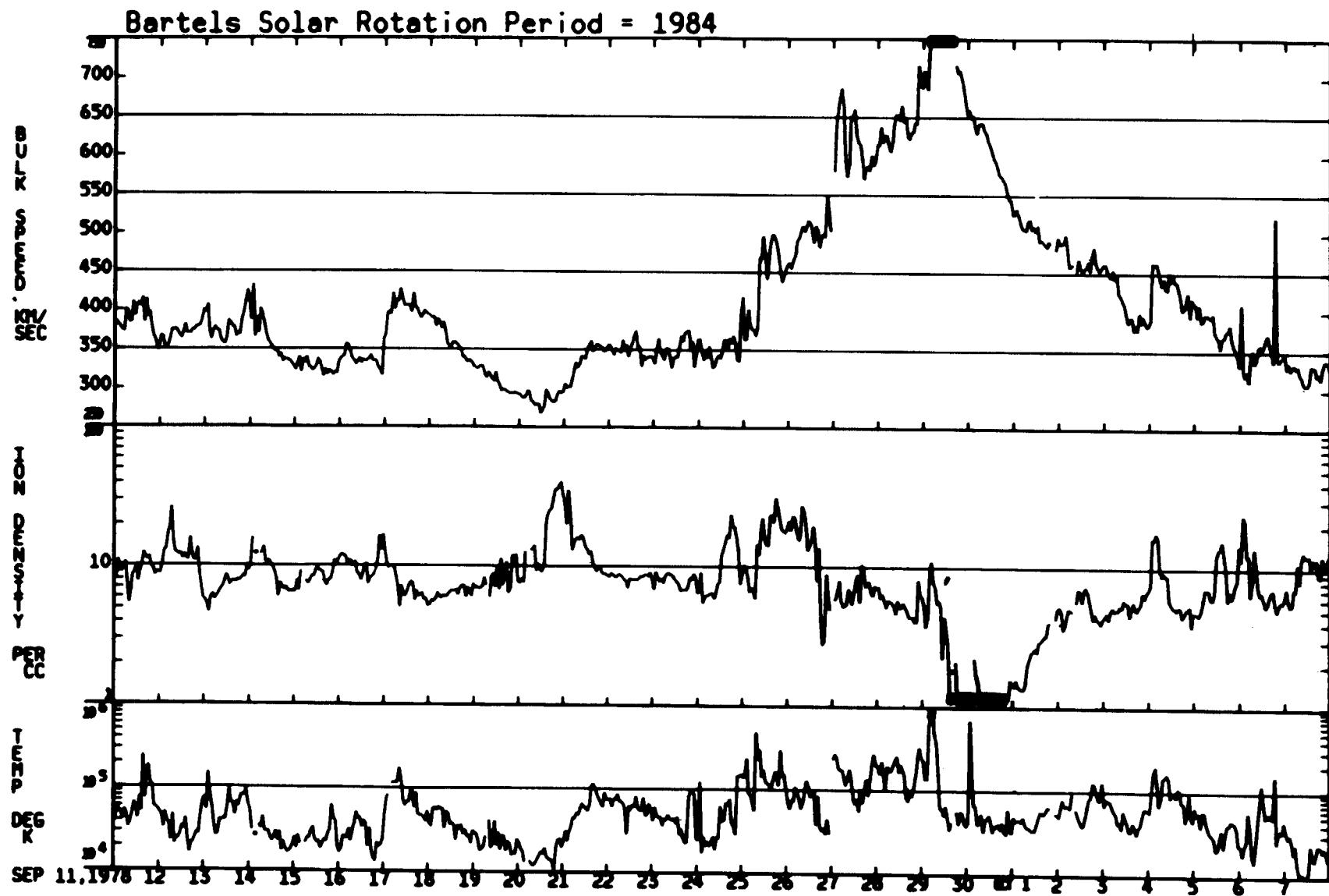


ORIGINAL PAGE IS  
OF POOR QUALITY

08/15/78 — 09/10/78

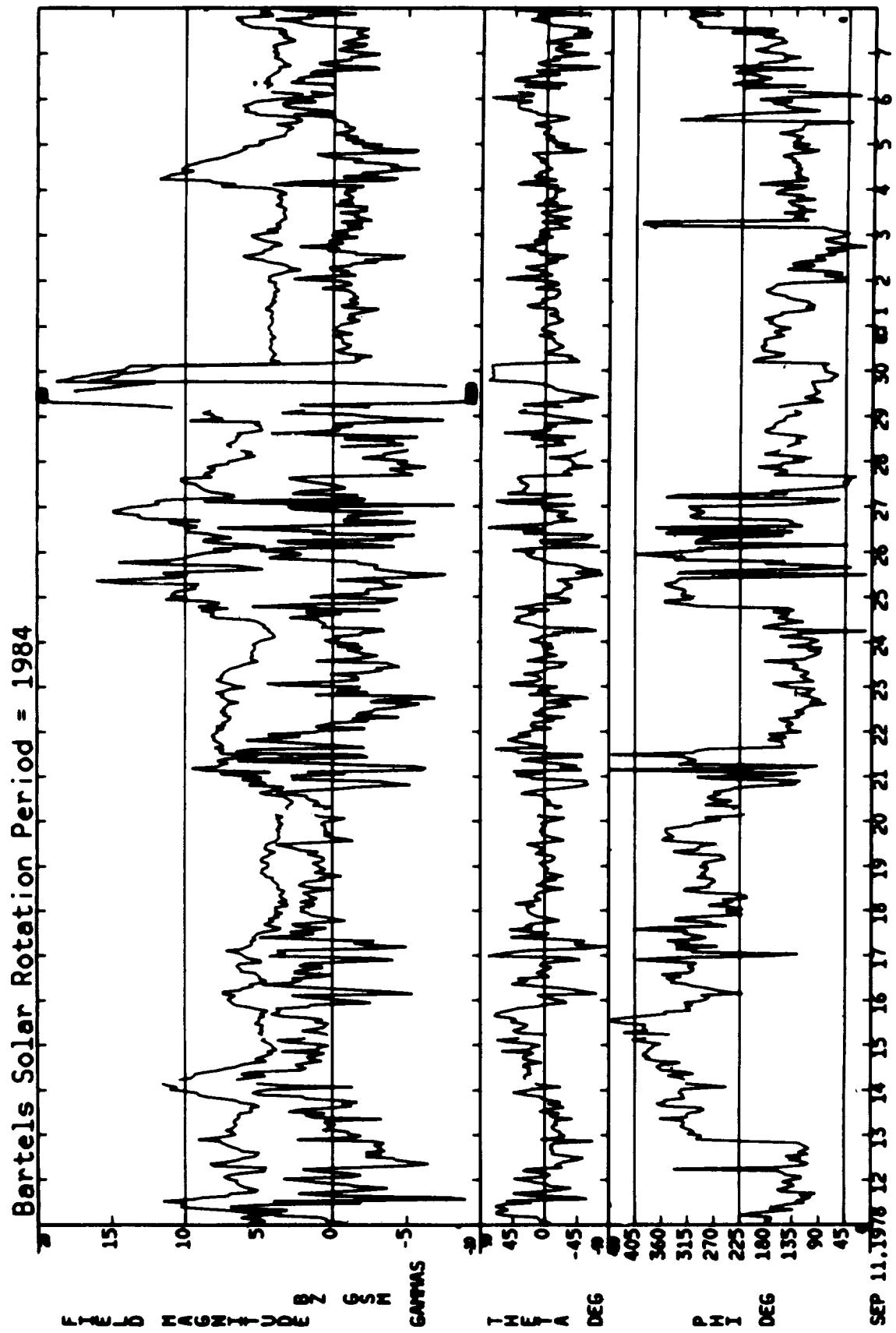


09/11/78 - 10/07/78

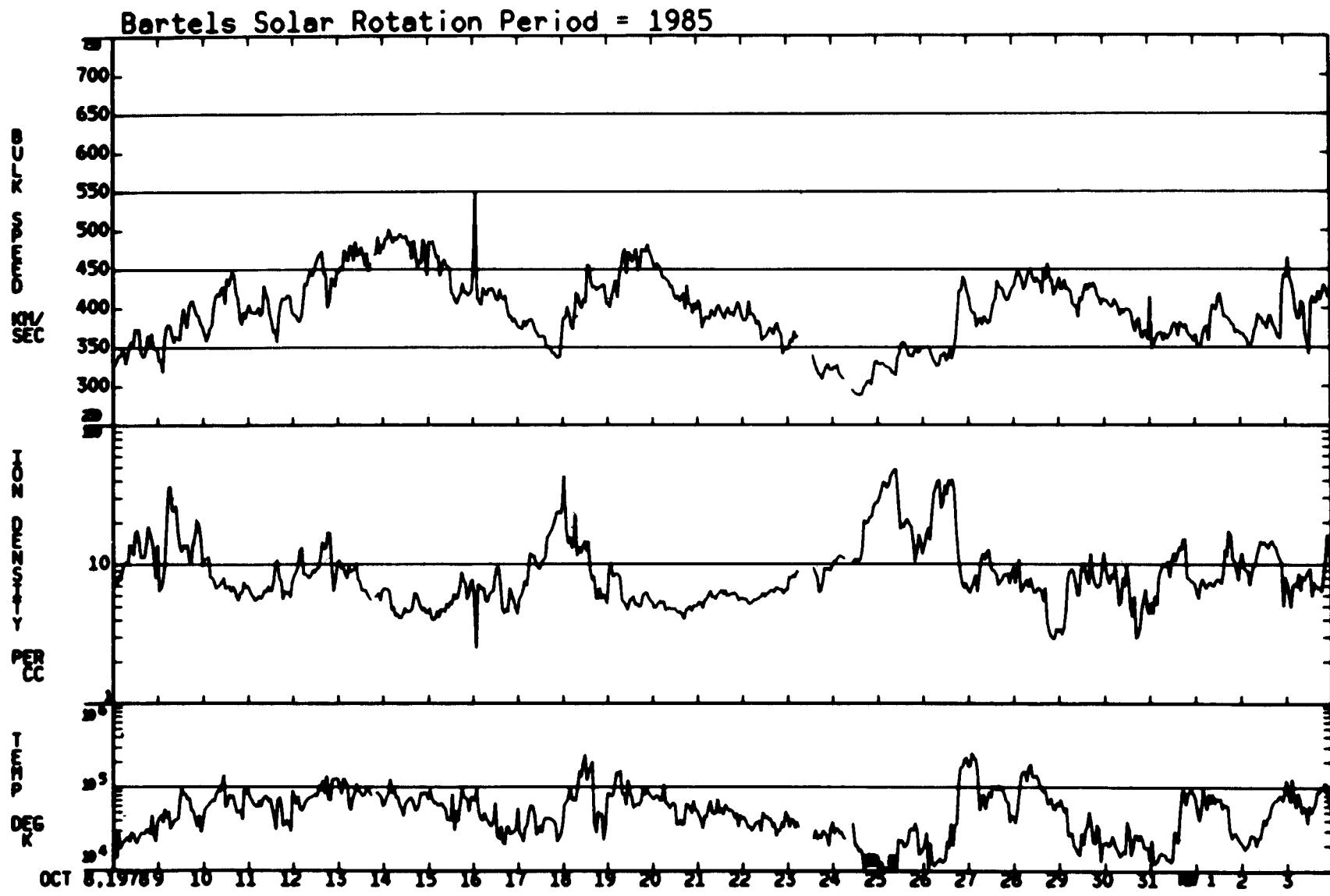


ORIGINAL PAGE IS  
OF POOR QUALITY

09/11/78 - 10/07/78

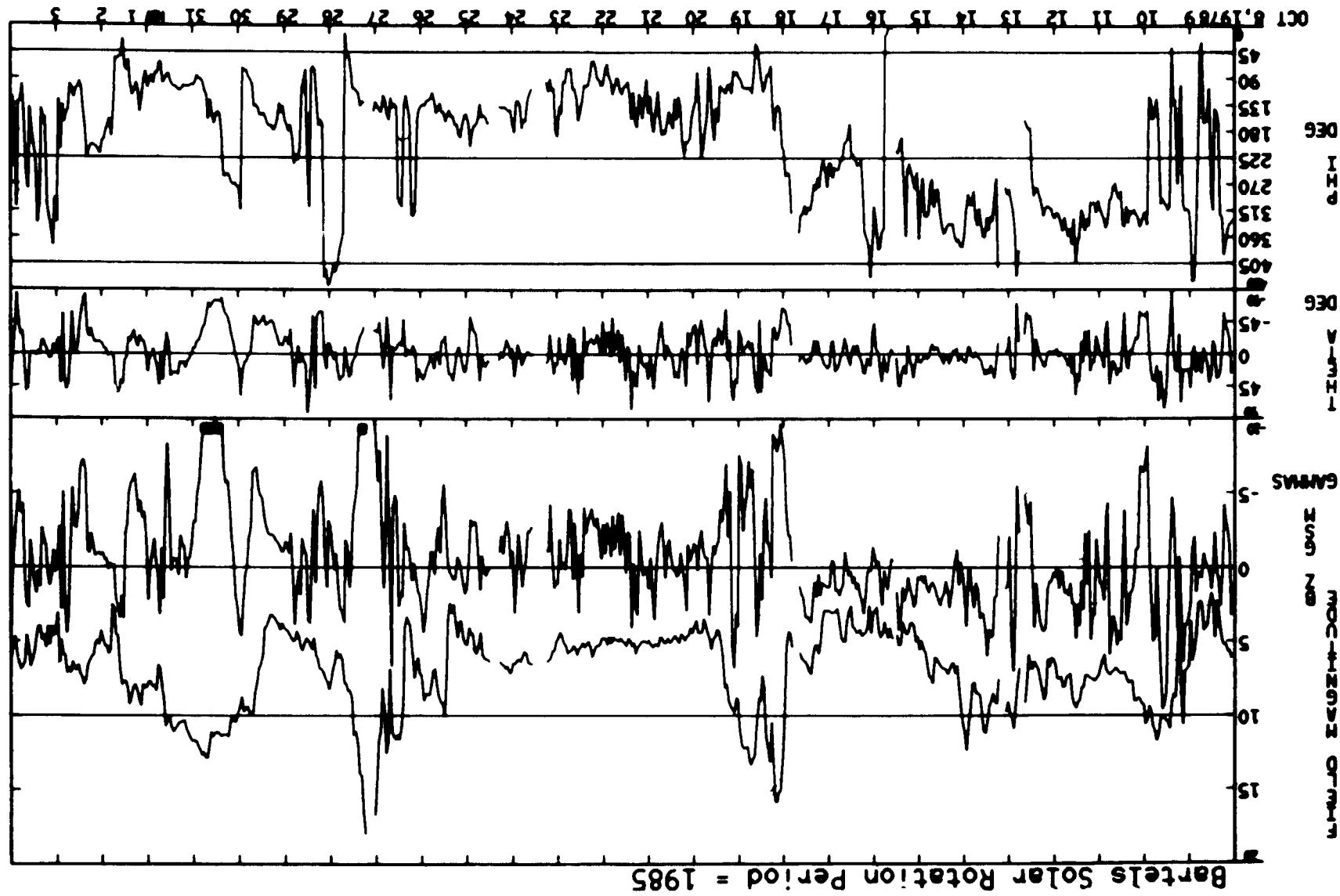


10/08/78 – 11/03/78

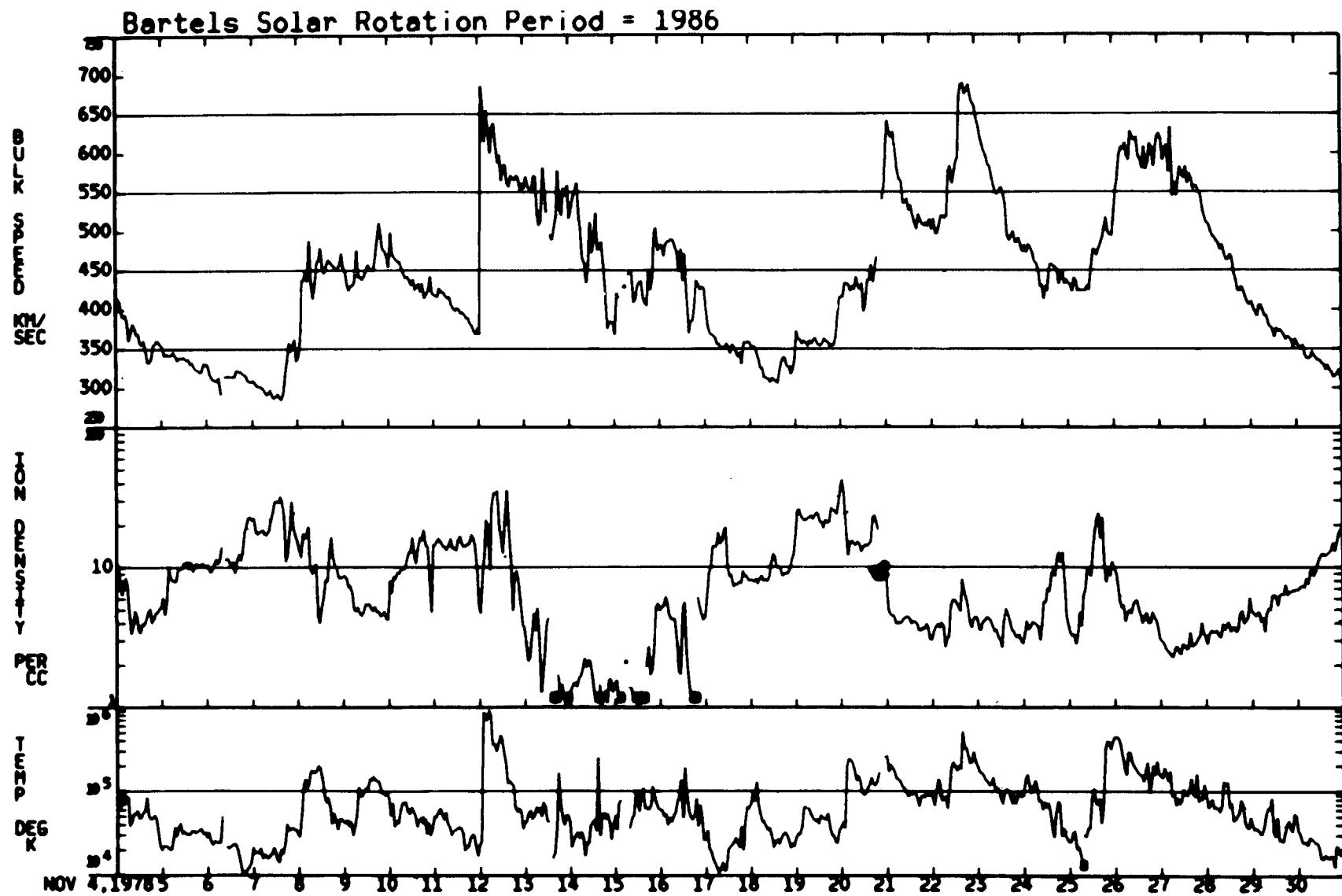


10/08/78 - 11/03/78

ORIGINAL PAGE IS  
OF POOR QUALITY

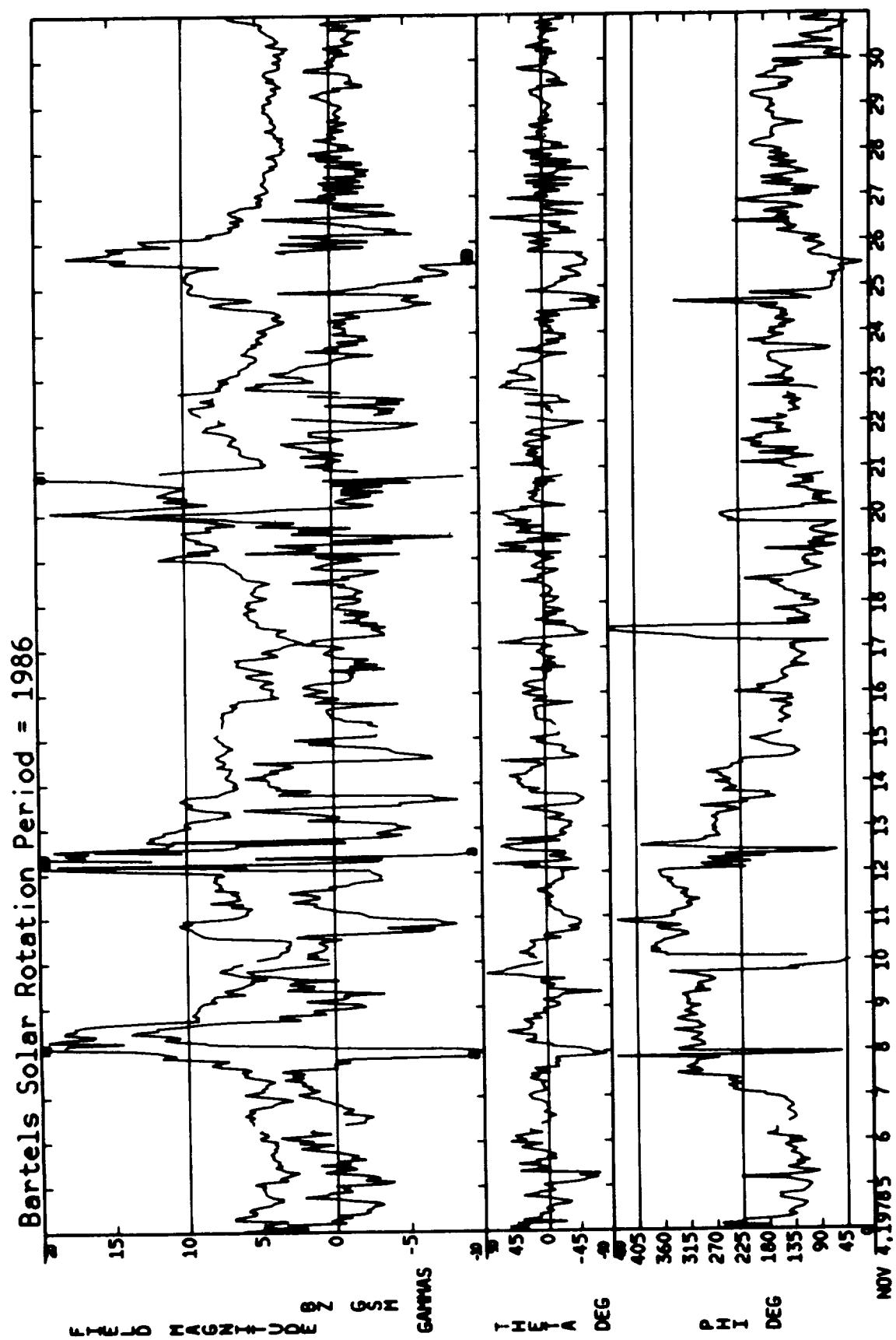


11/04/78 - 11/30/78

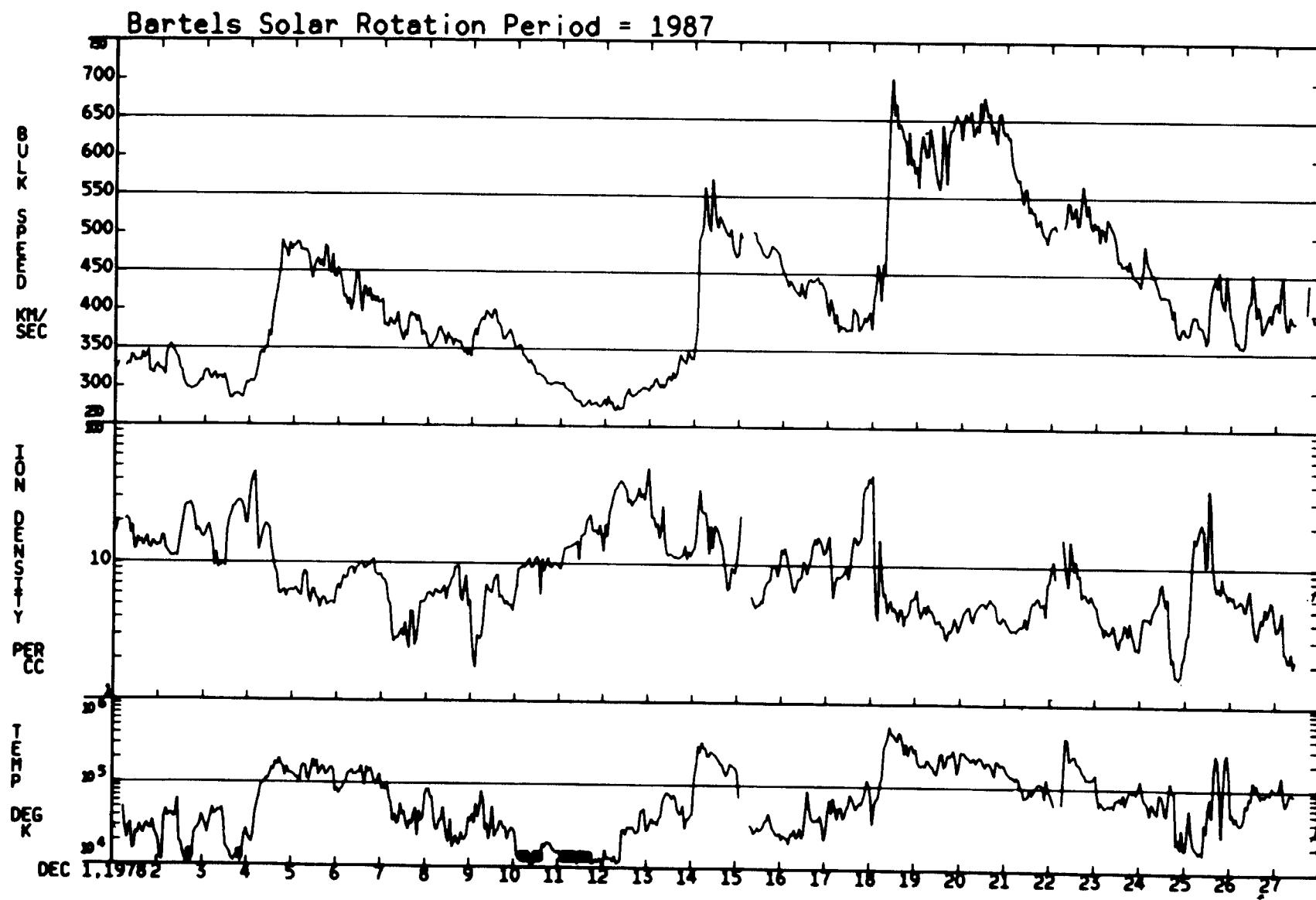


ORIGINAL PAGE IS  
OF POOR QUALITY

11/04/78 - 11/30/78

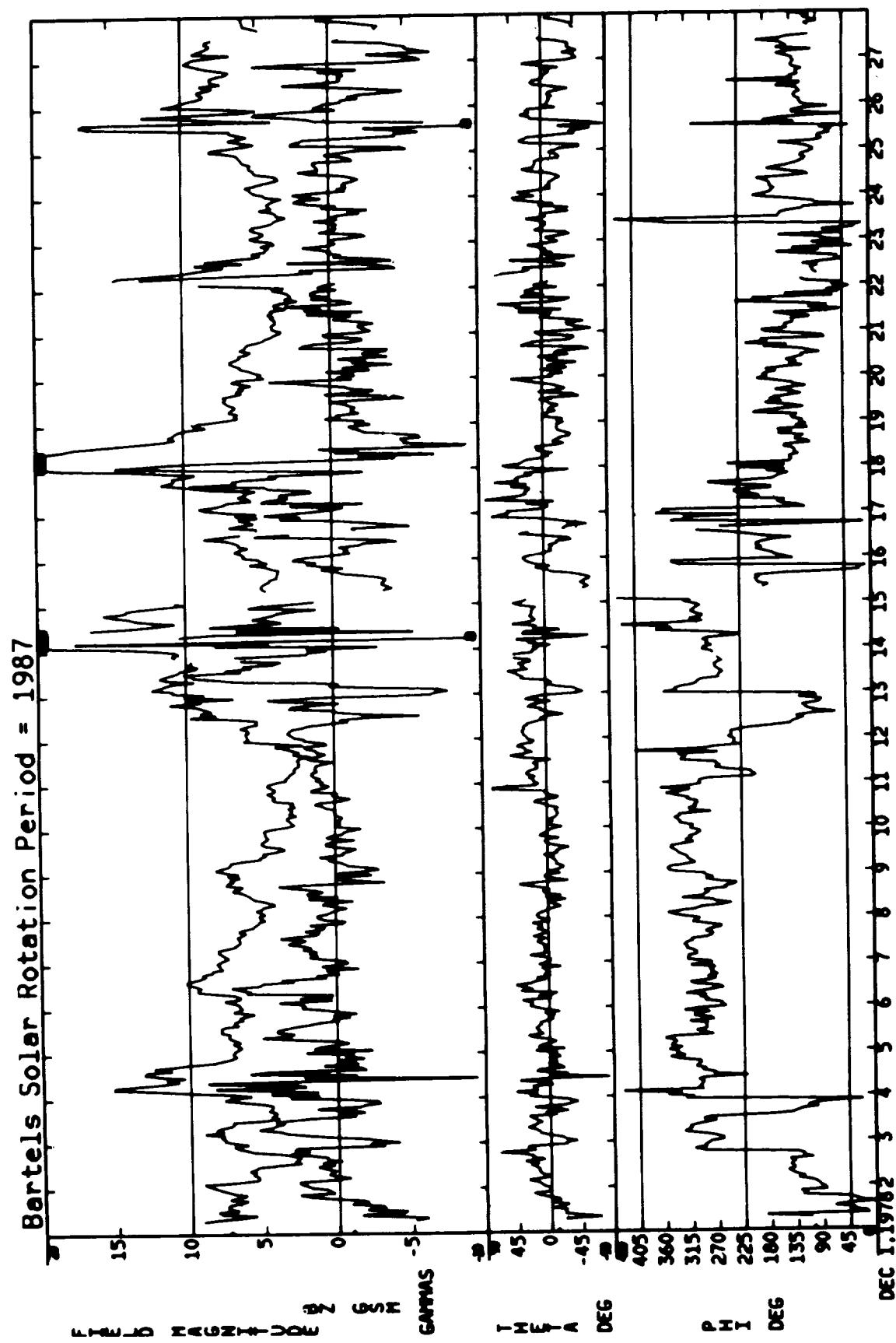


12/01/78 – 12/27/78

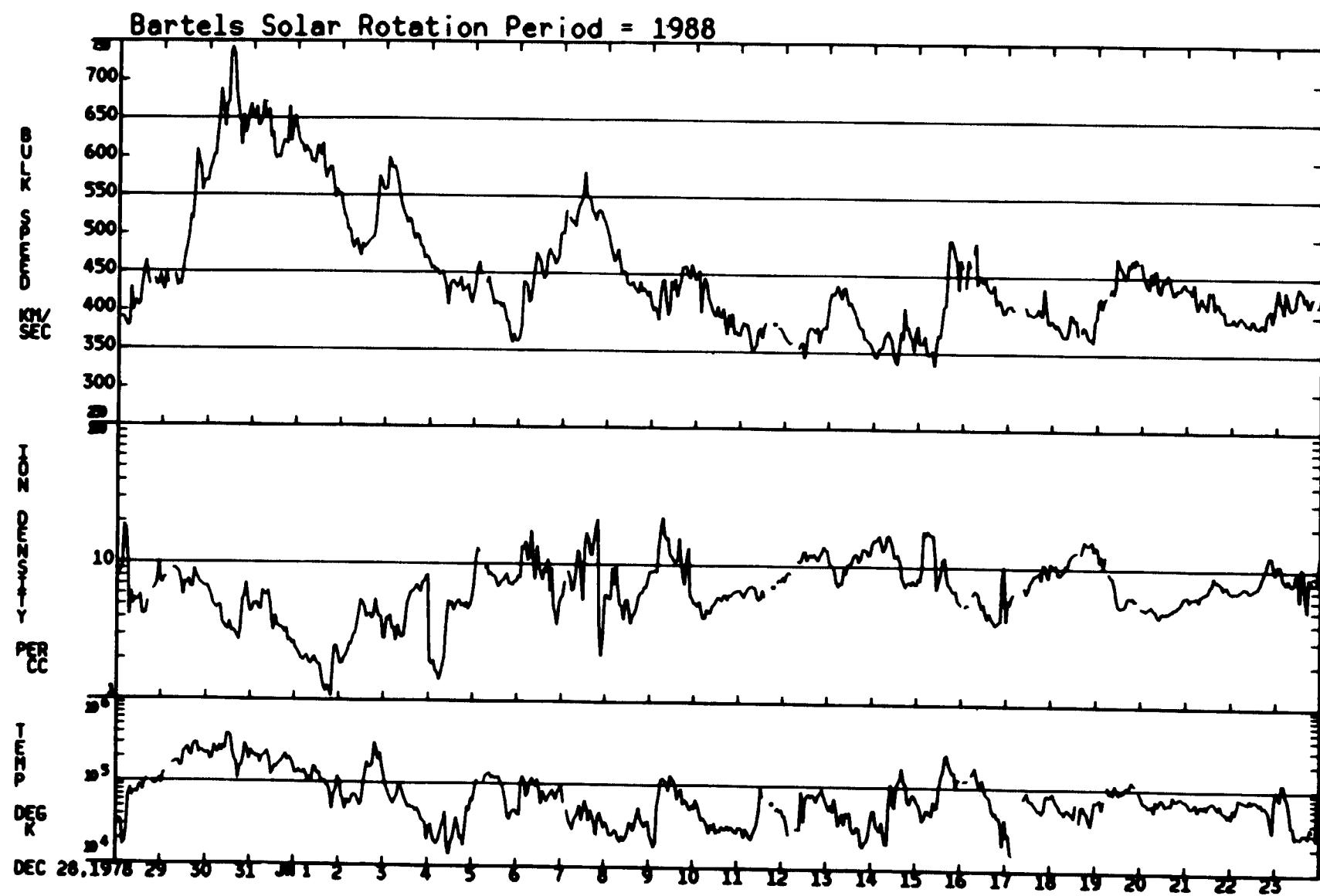


ORIGINAL PAGE IS  
OF POOR QUALITY

12/01/78 — 12/27/78

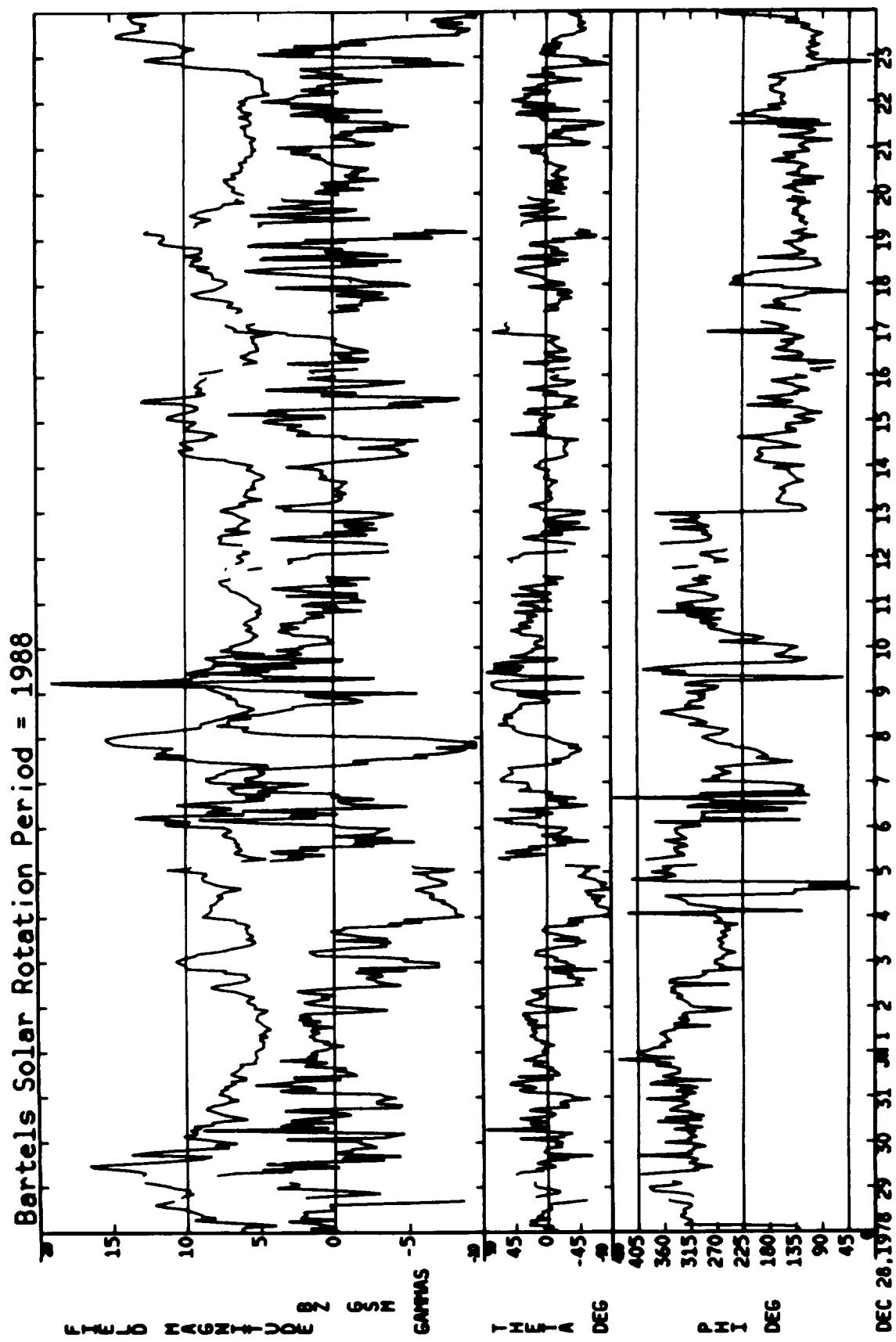


12/28/78 – 01/23/79

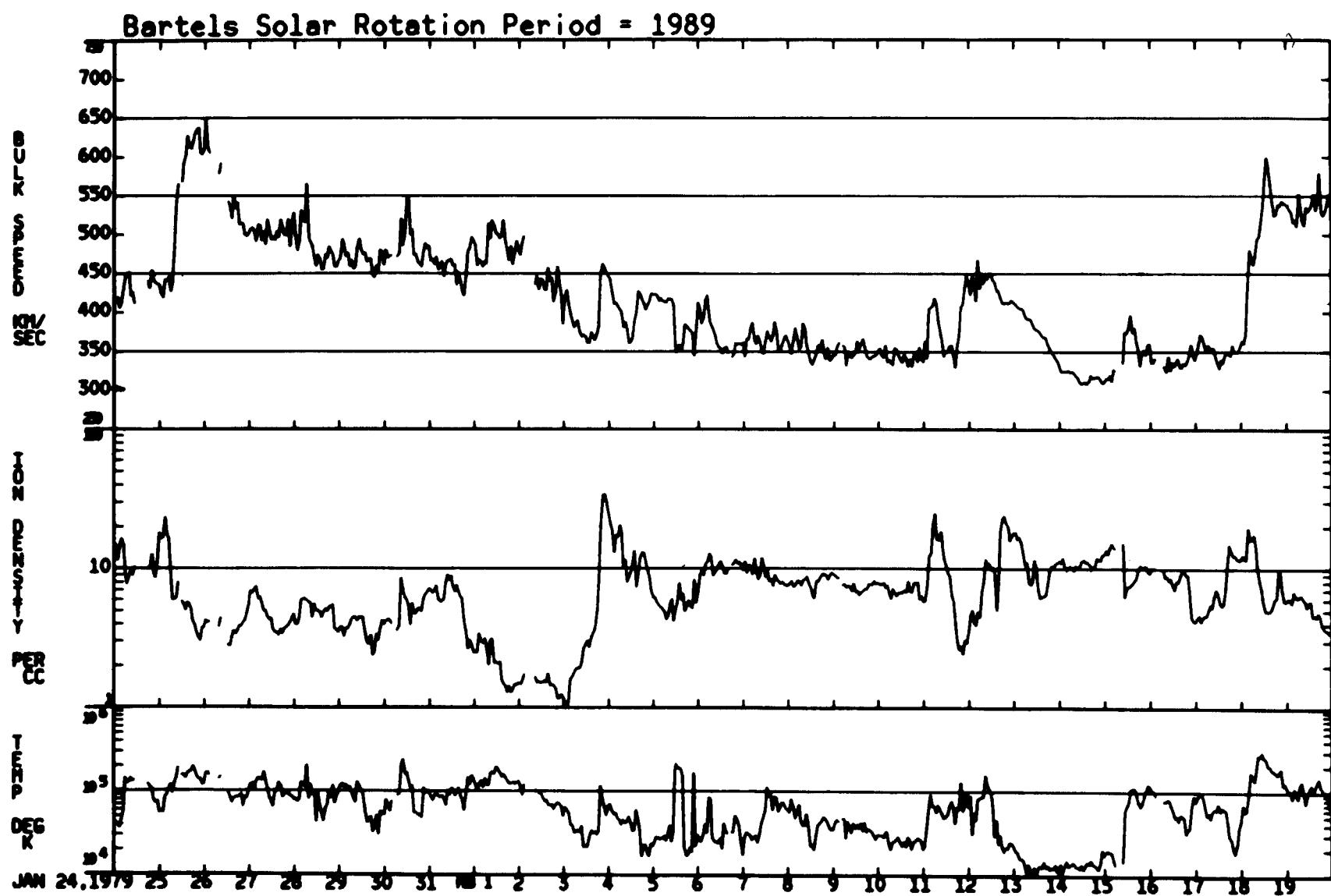


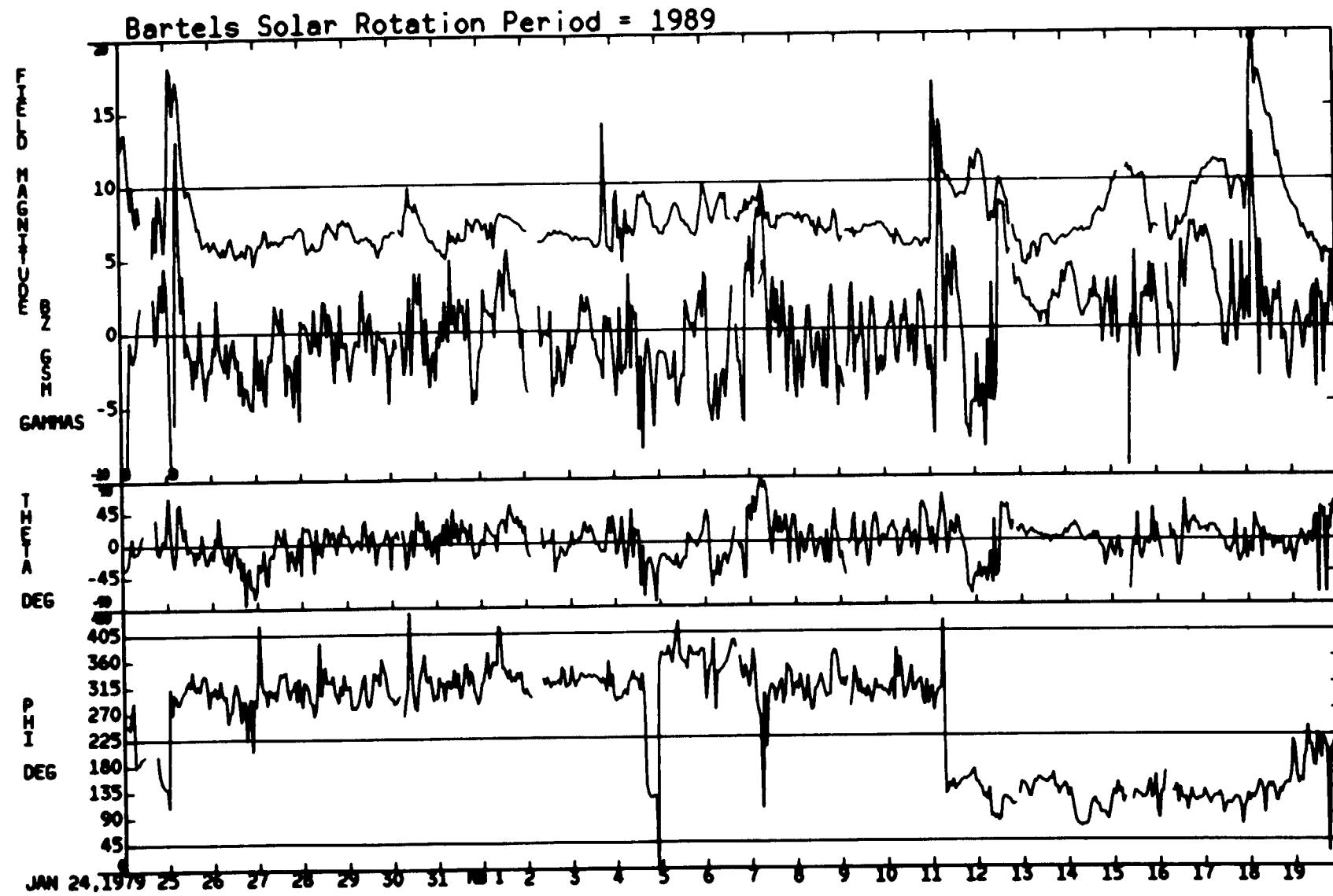
ORIGINAL PAGE IS  
OF POOR QUALITY

12/28/78 – 01/23/79

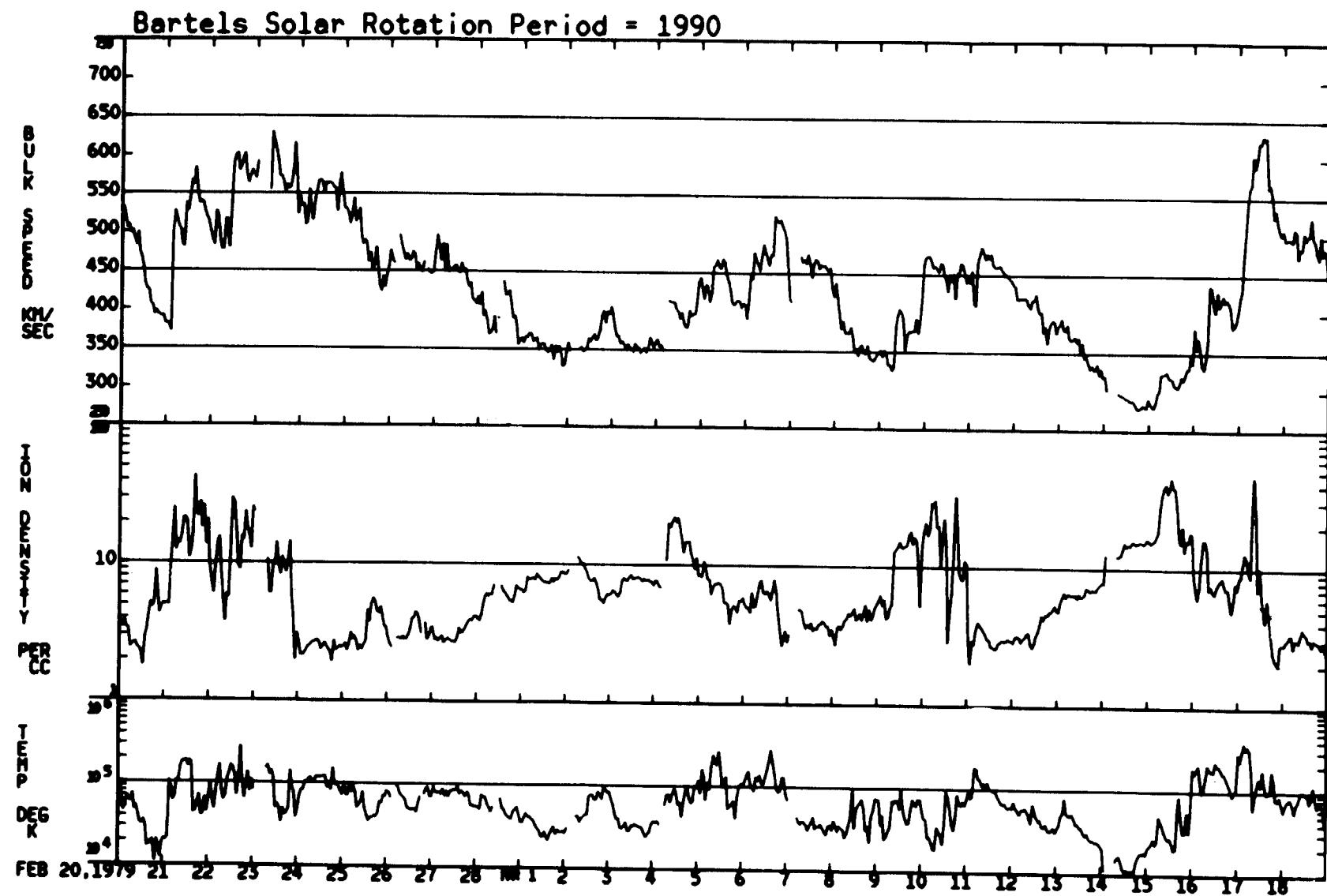


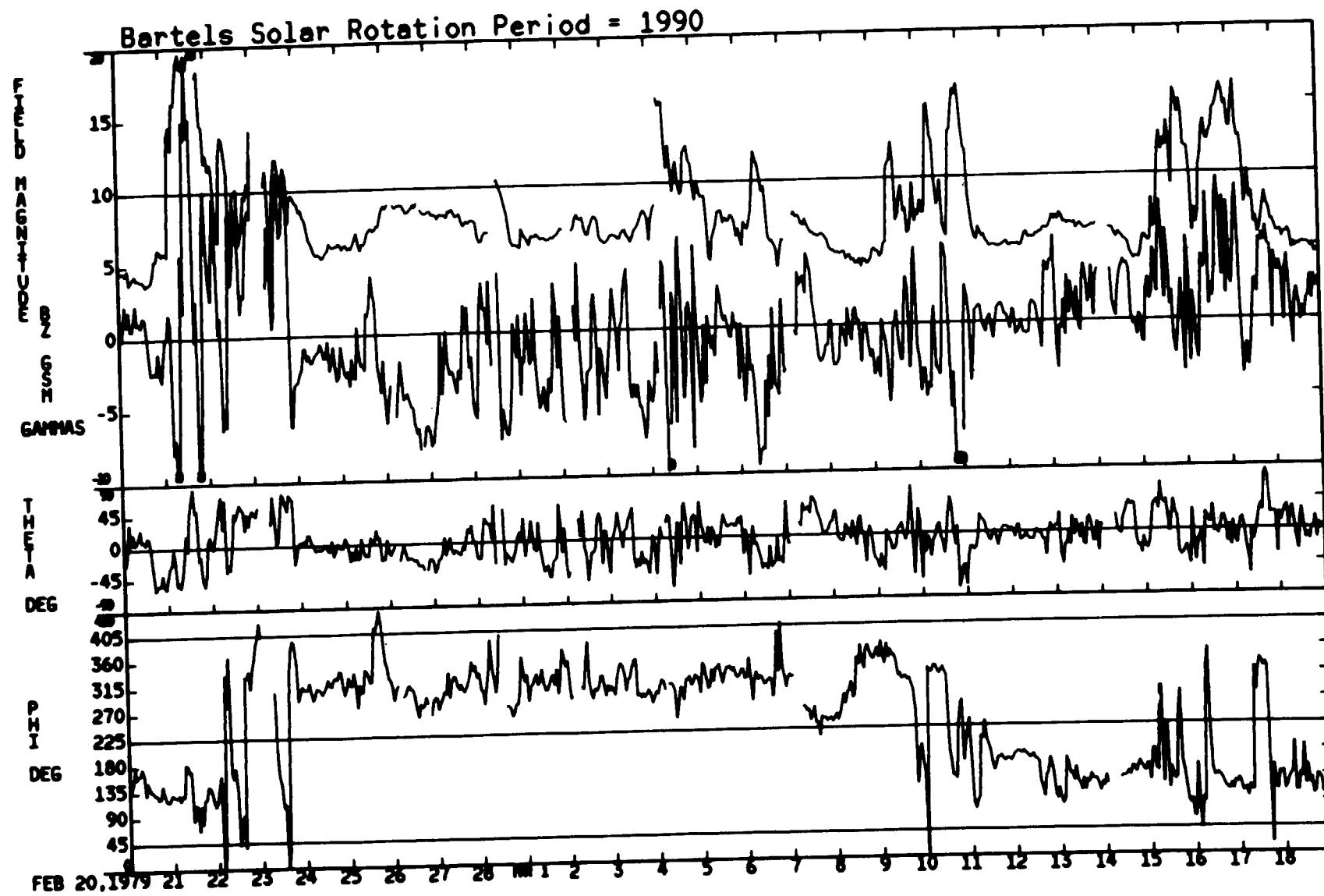
01/24/79 – 02/19/79





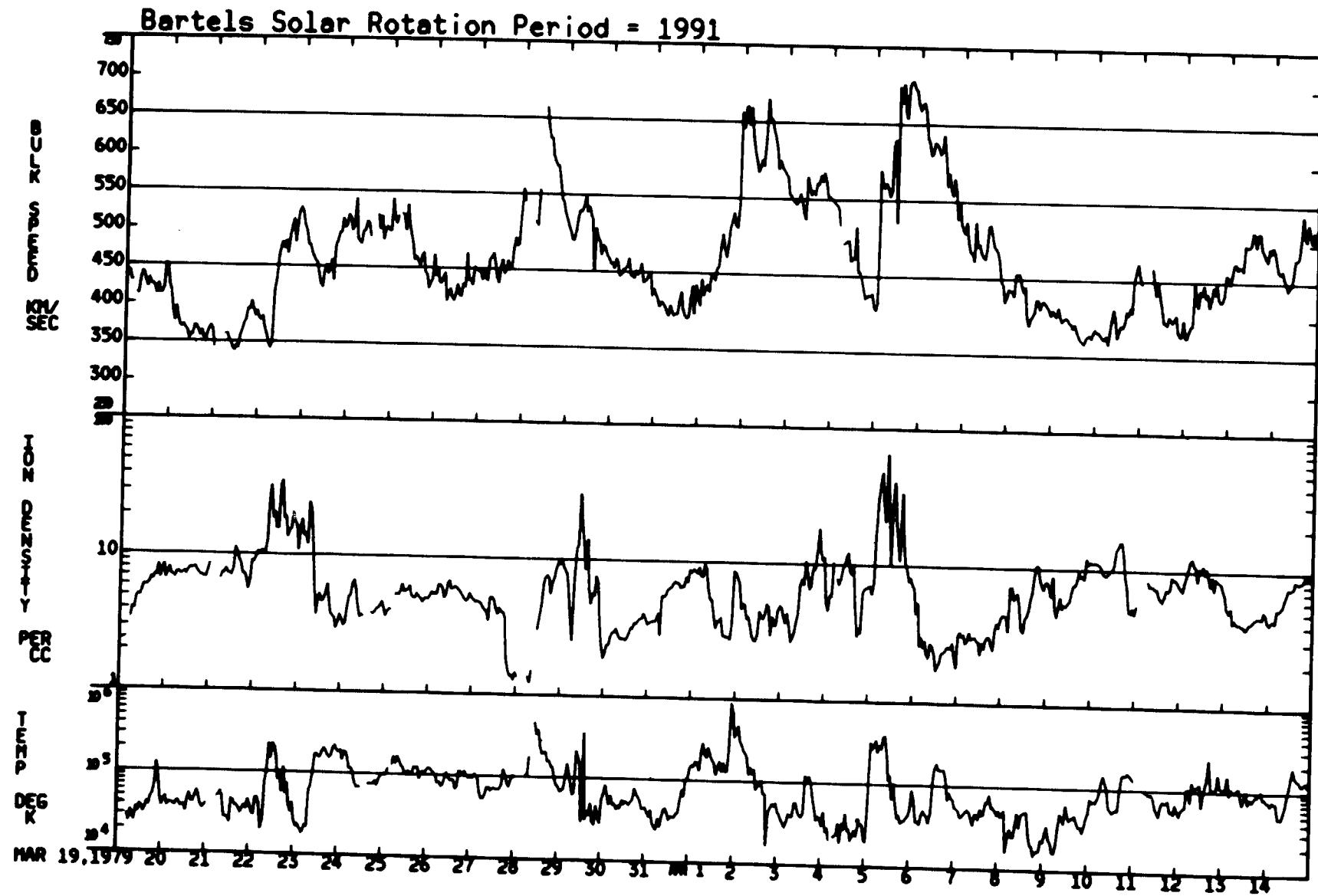
02/20/79 – 03/18/79



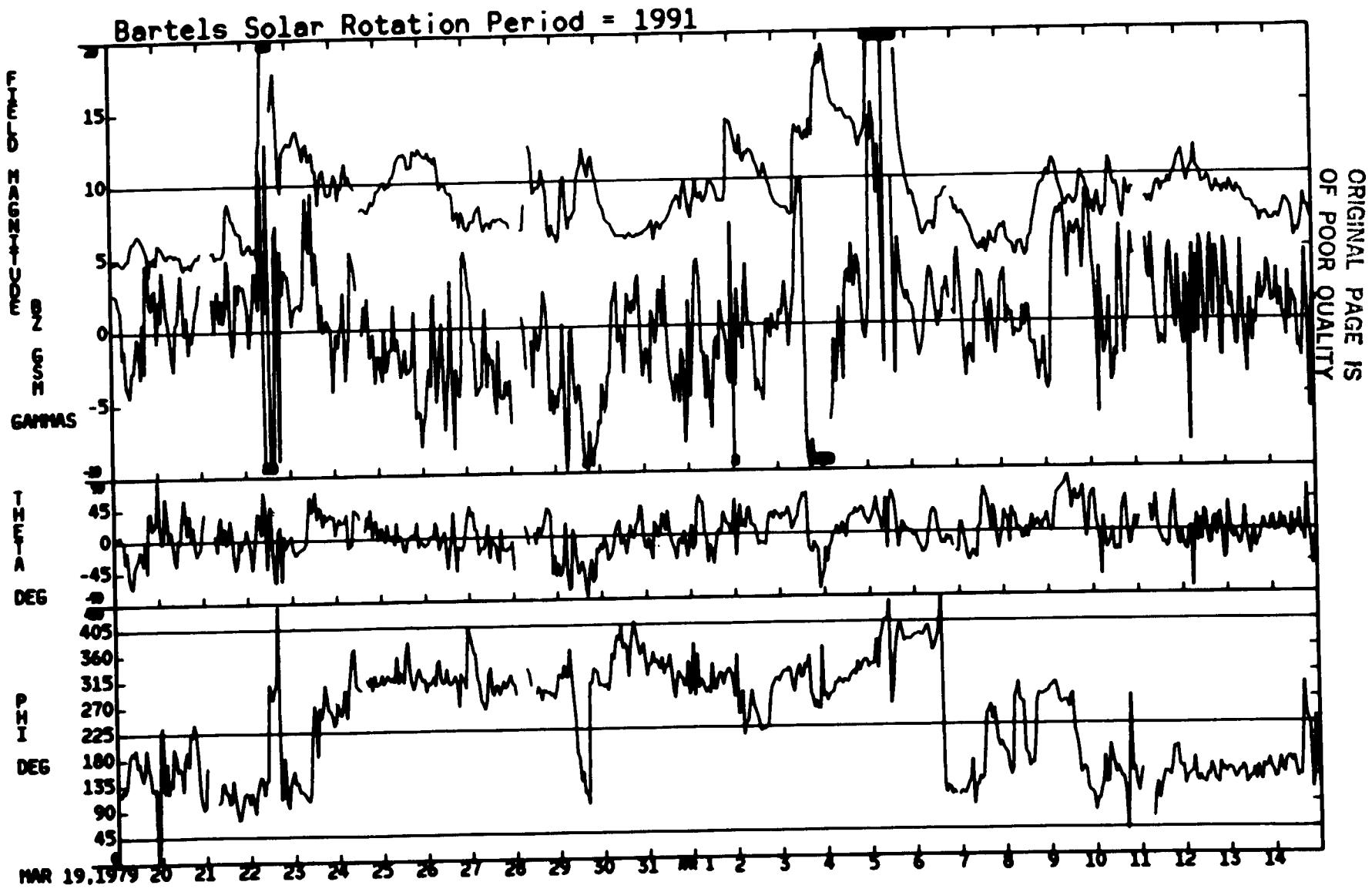


02/20/79 – 03/18/79

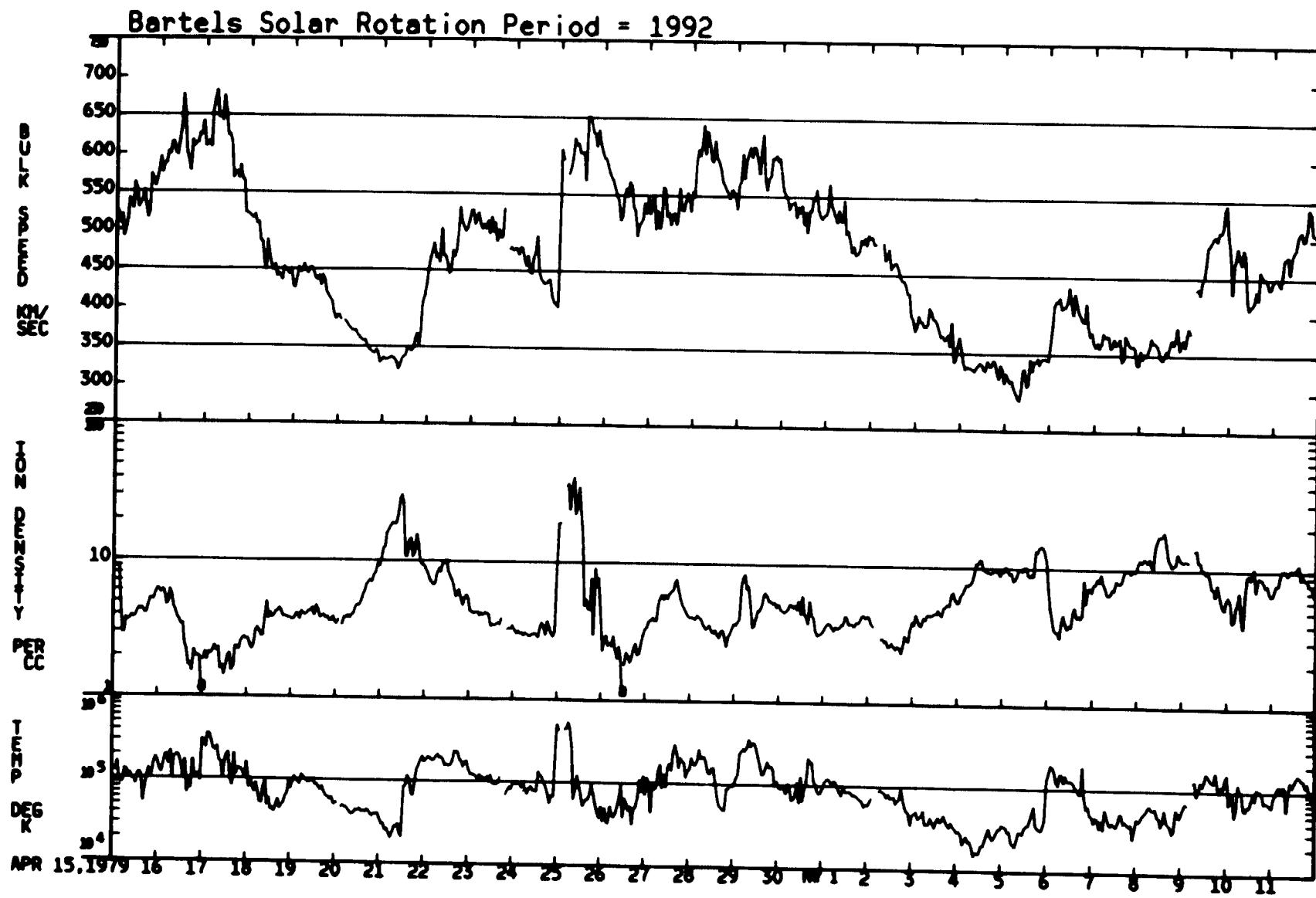
03/19/79 – 04/14/79



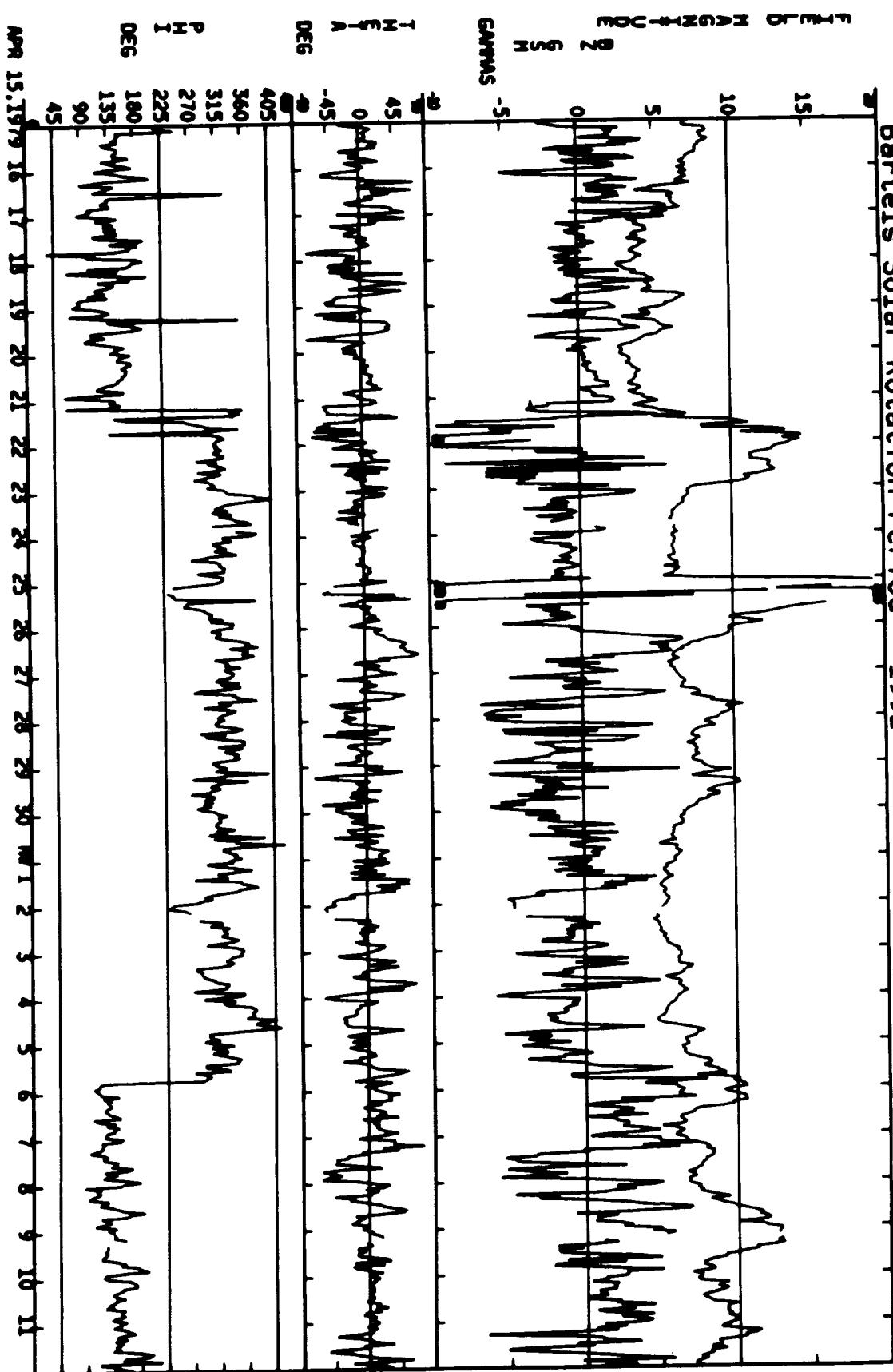
03/19/79 – 04/14/79



04/15/79 – 05/11/79

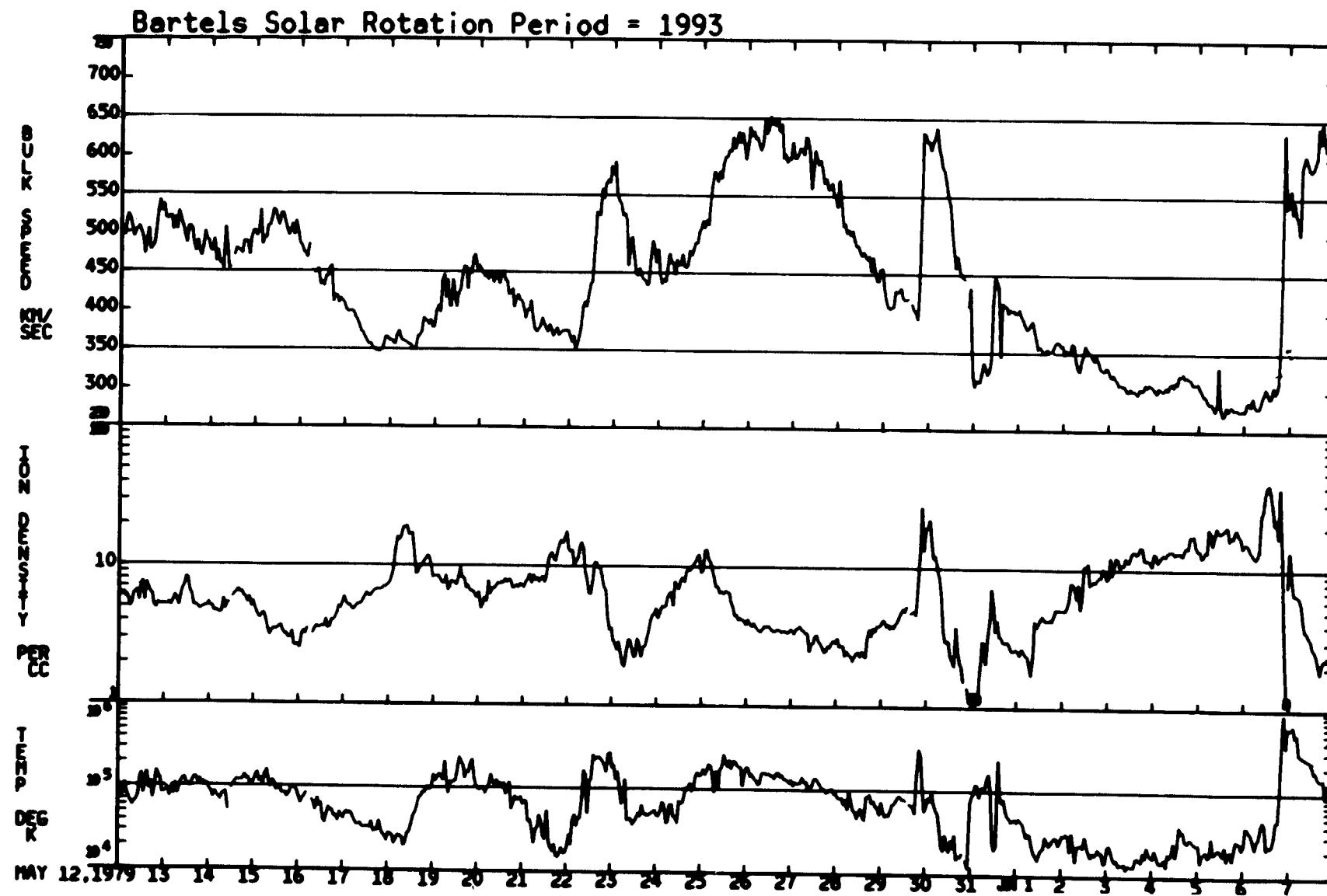


Bartels Solar Rotation Period = 1992



04/15/79 - 05/11/79

05/12/79 – 06/07/79



ORIGINAL PAGE IS  
OF POOR QUALITY

05/12/79 – 06/07/79

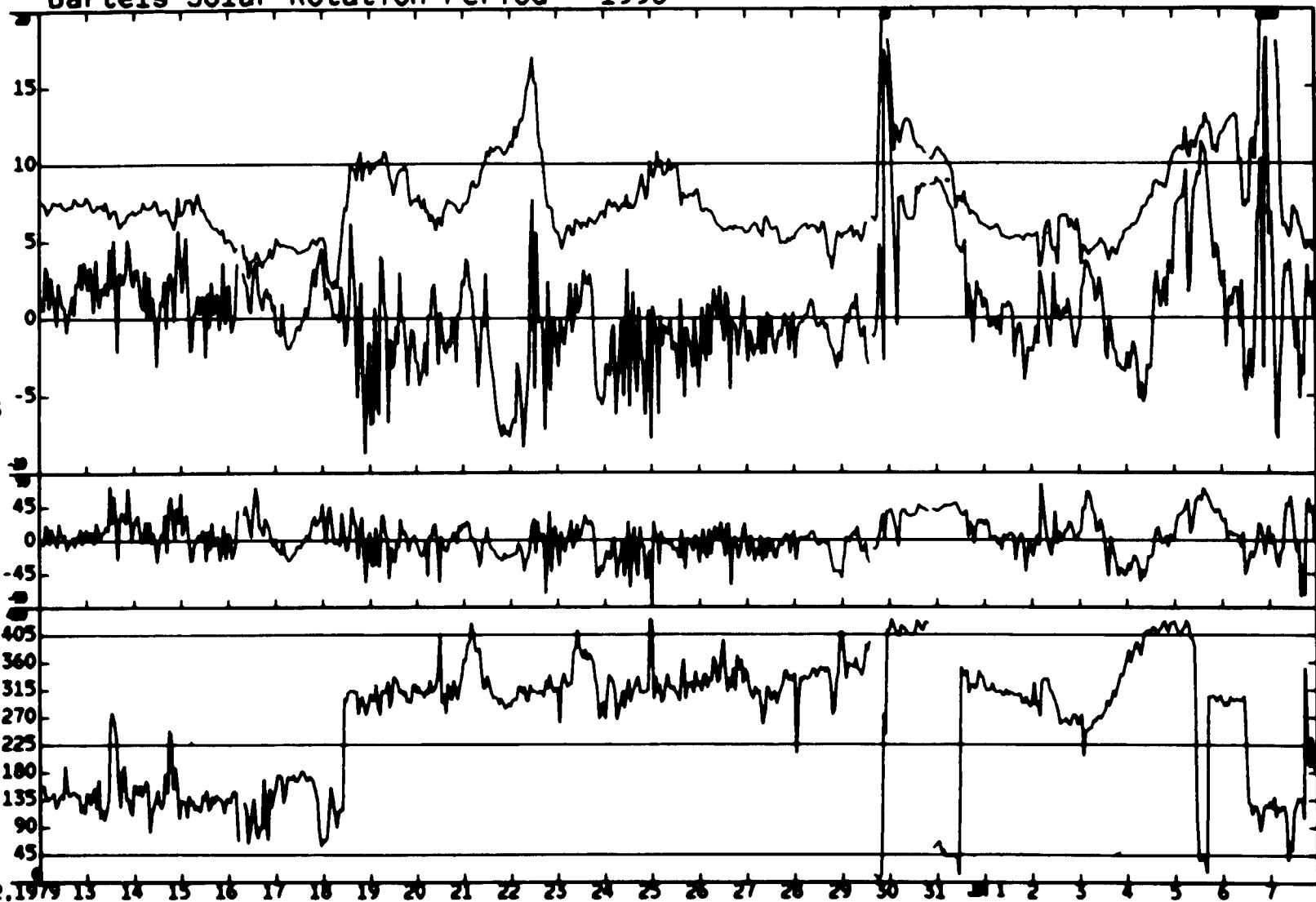
Bartels Solar Rotation Period = 1993

E FIELD MAGNETISM IN GEME  
GAMMAS

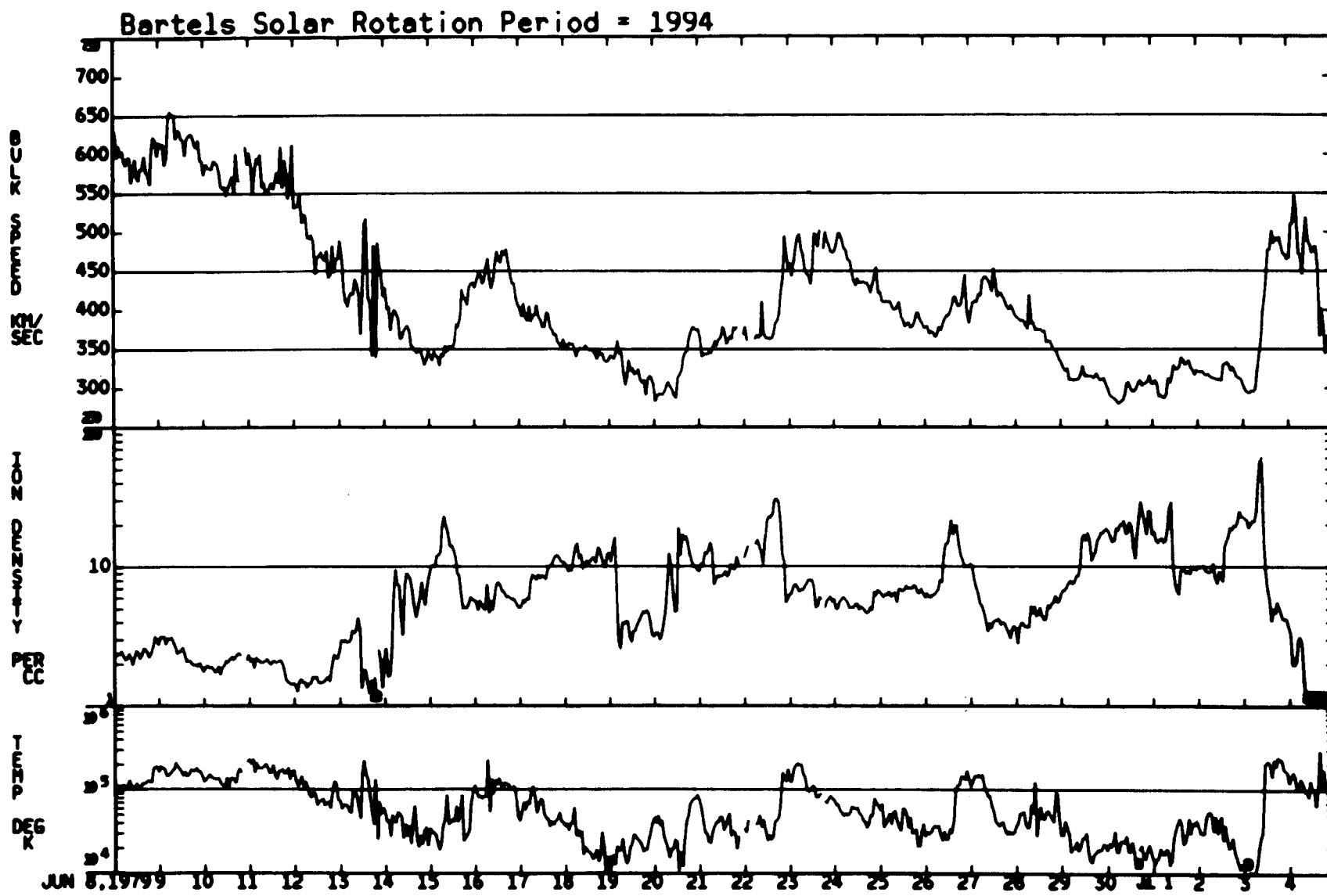
THETA DEG

PHI DEG

MAY 12, 1979 13 14 15 16 17 18 19 20 21 22 23 24 25 26 27 28 29 30 31 1 2 3 4 5 6 7



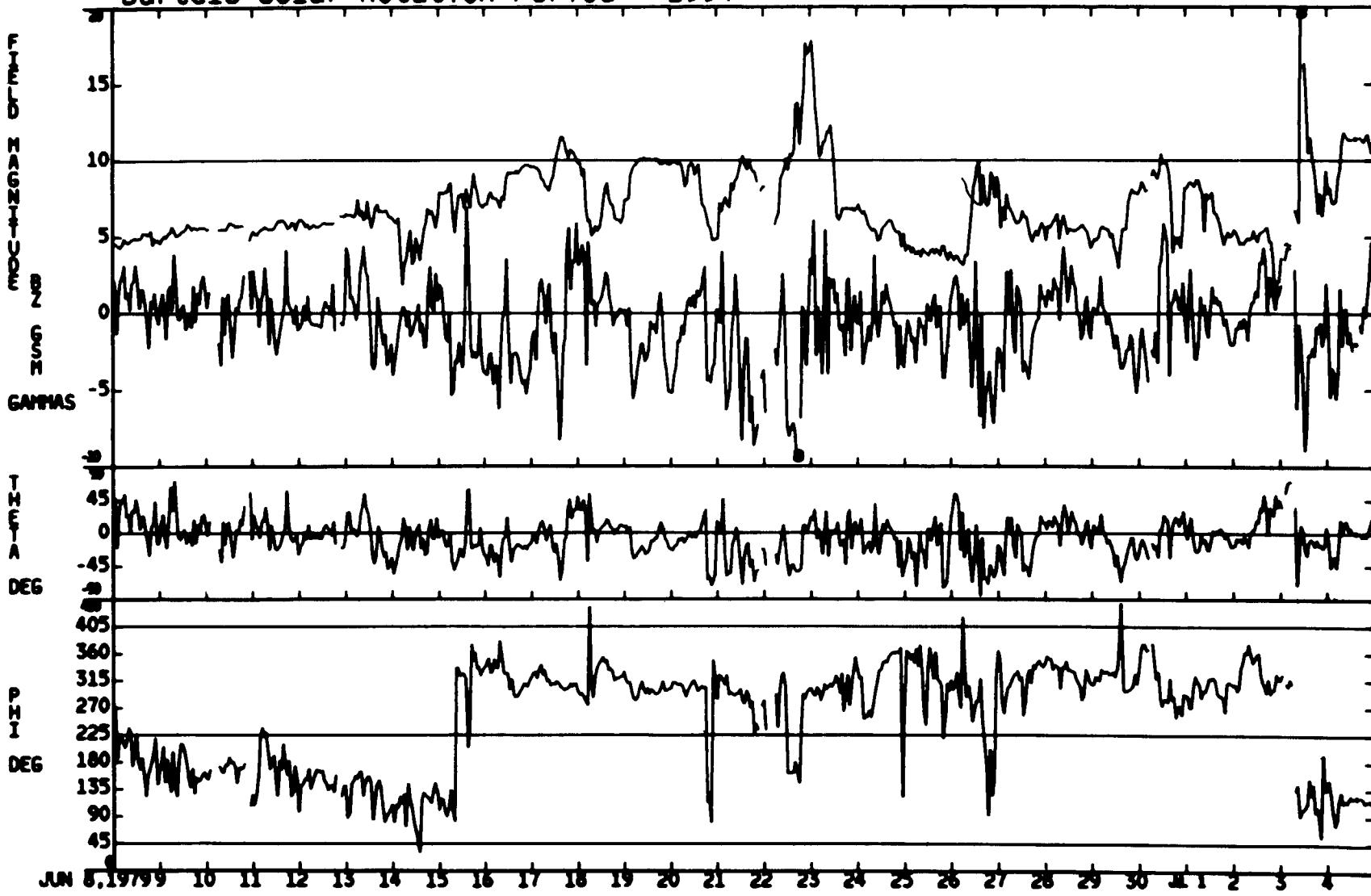
06/08/79 - 07/04/79



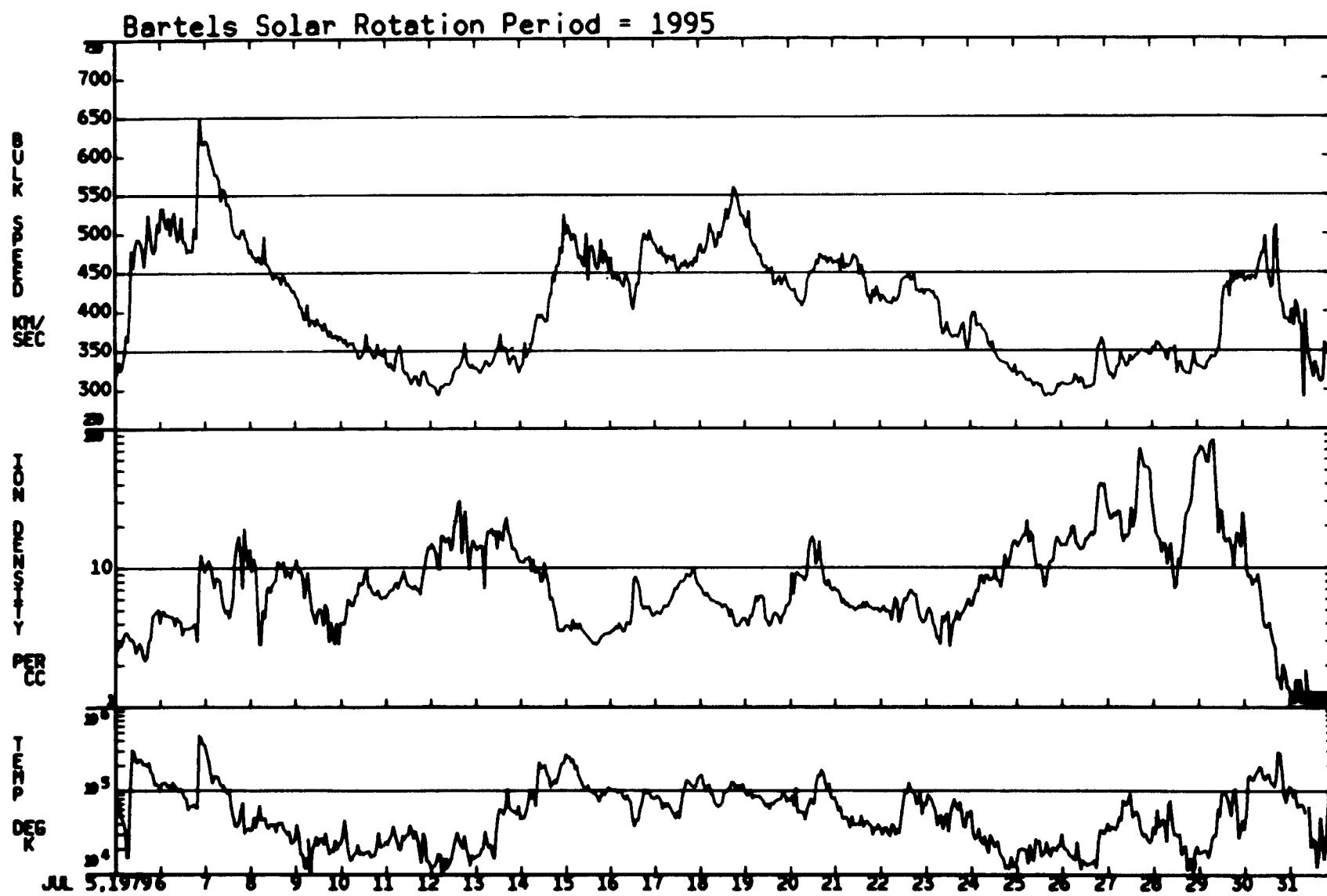
ORIGINAL PAGE IS  
OF POOR QUALITY

06/08/79 – 07/04/79

Bartels Solar Rotation Period = 1994



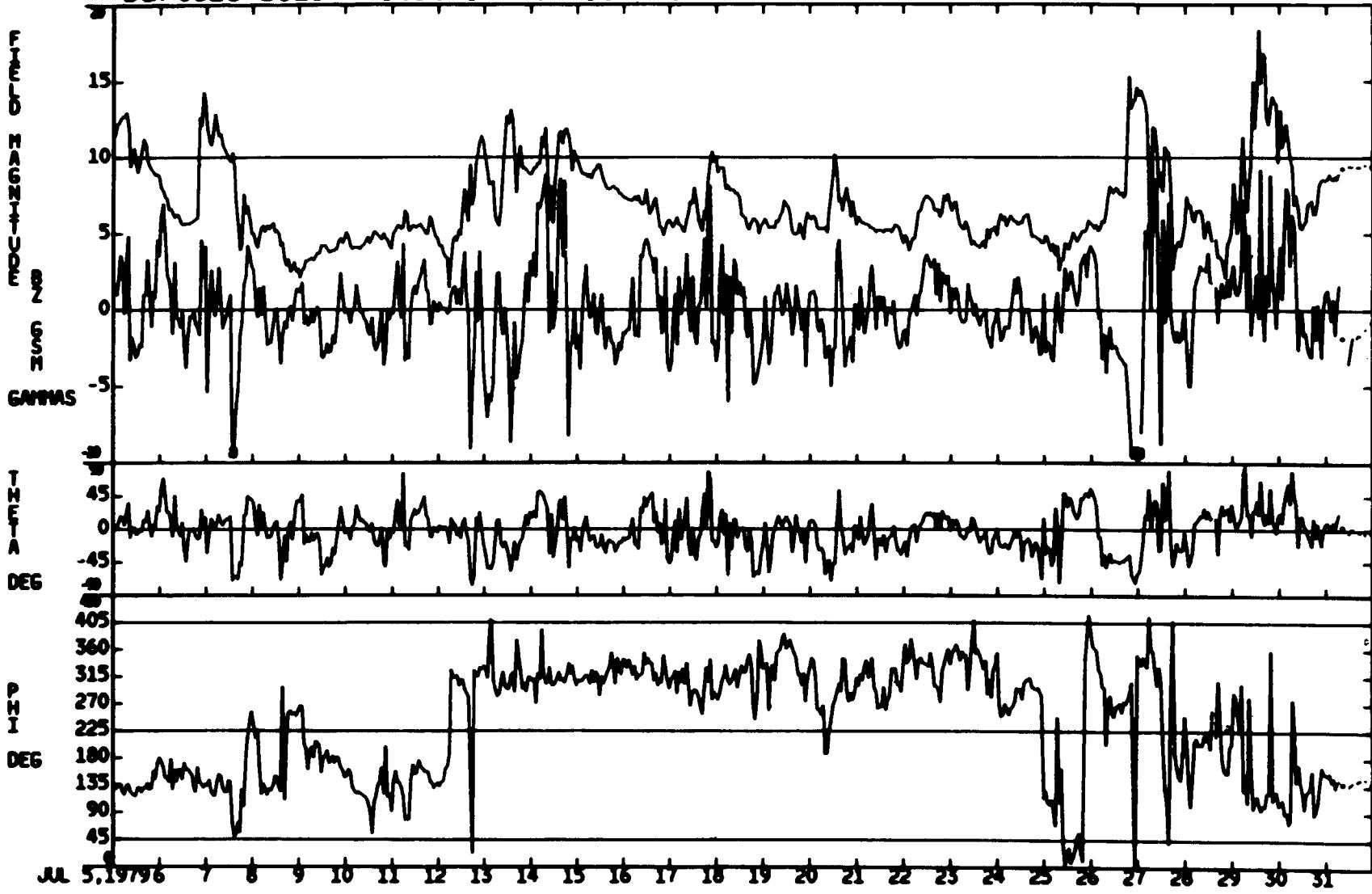
07/05/79 - 07/31/79



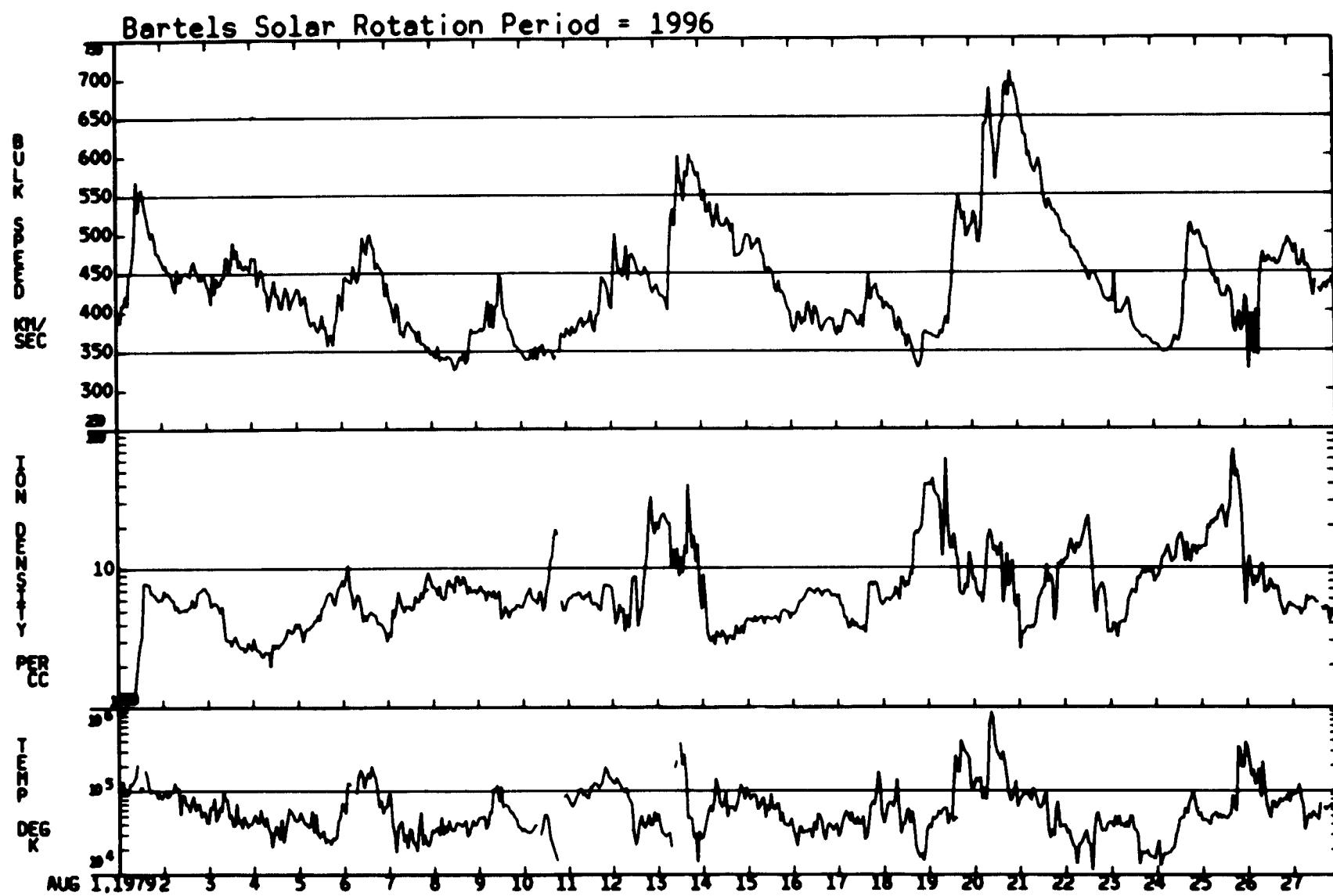
ORIGINAL PAGE IS  
OF POOR QUALITY

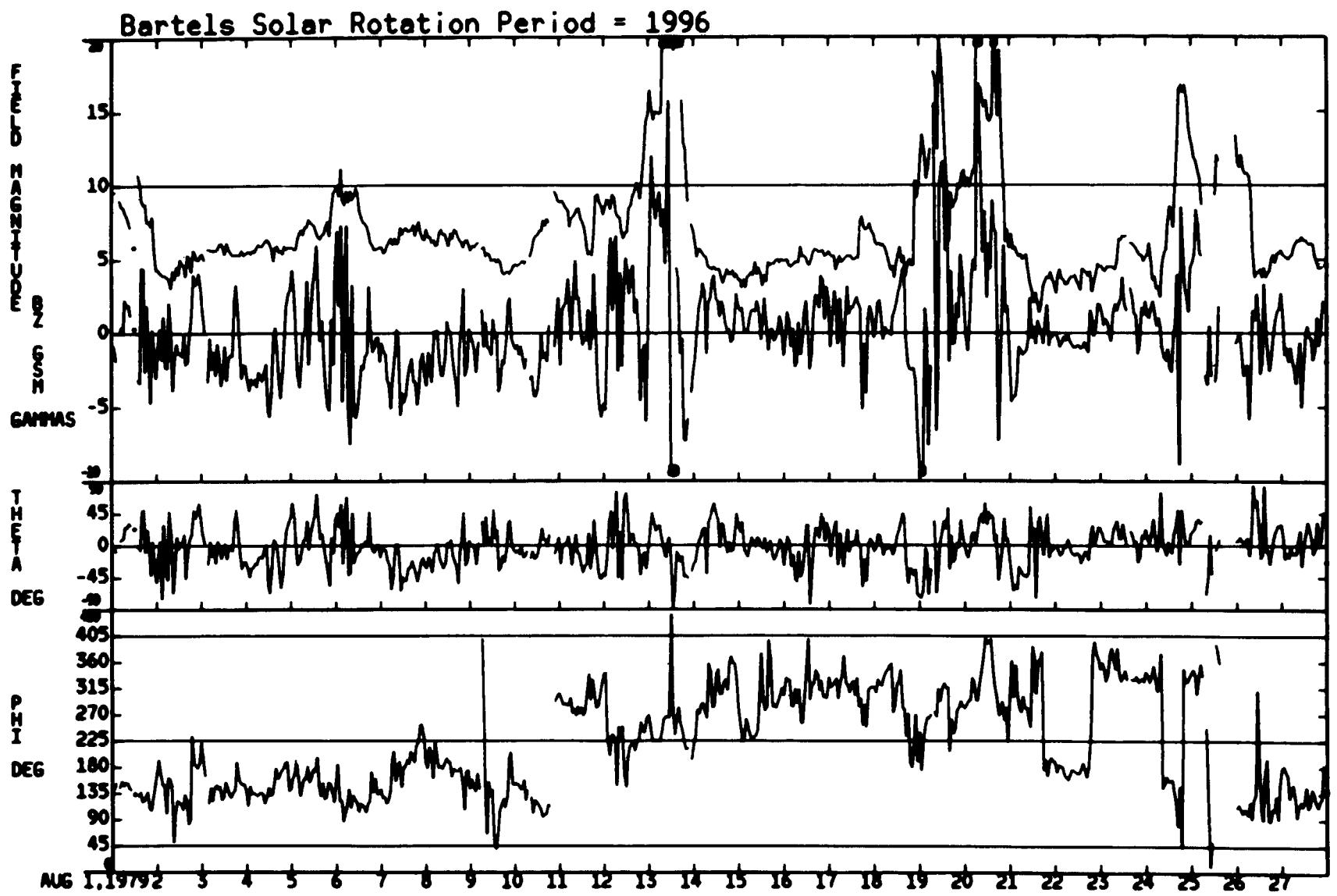
07/05/79 — 07/31/79

Bartels Solar Rotation Period = 1995



08/01/79 – 08/27/79

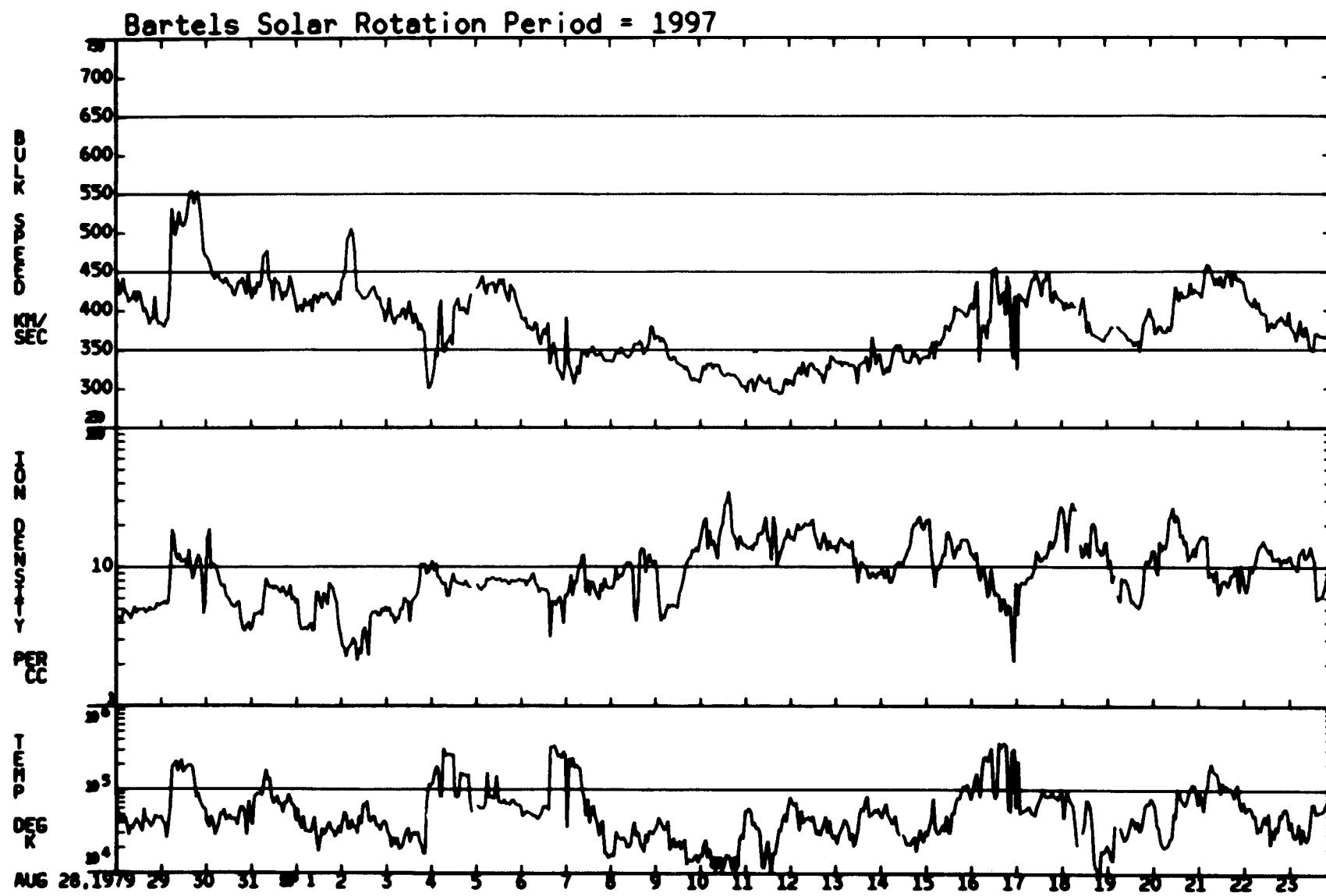




ORIGINAL PAGE IS  
OF POOR QUALITY

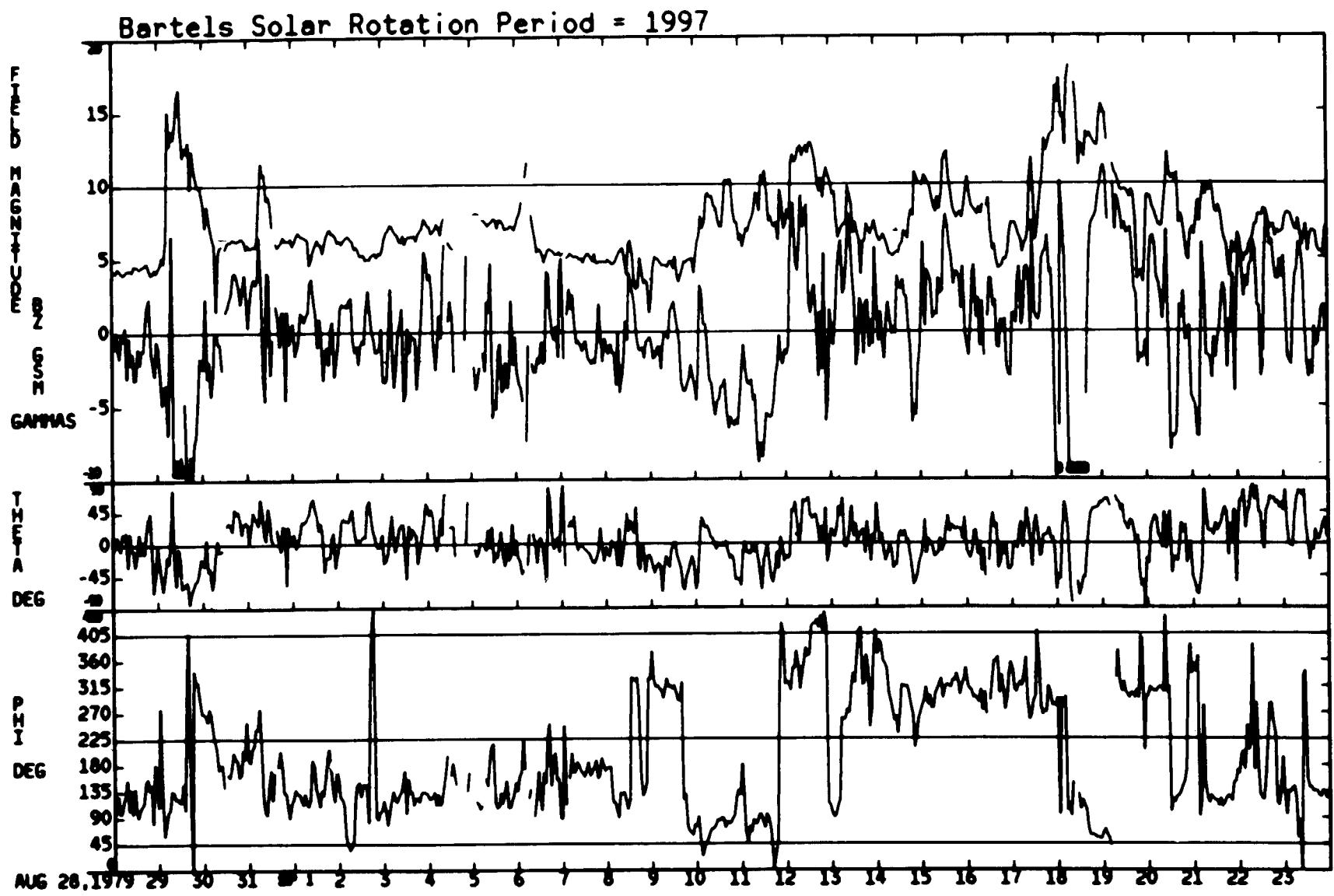
08/01/79 – 08/27/79

08/28/79 – 09/23/79

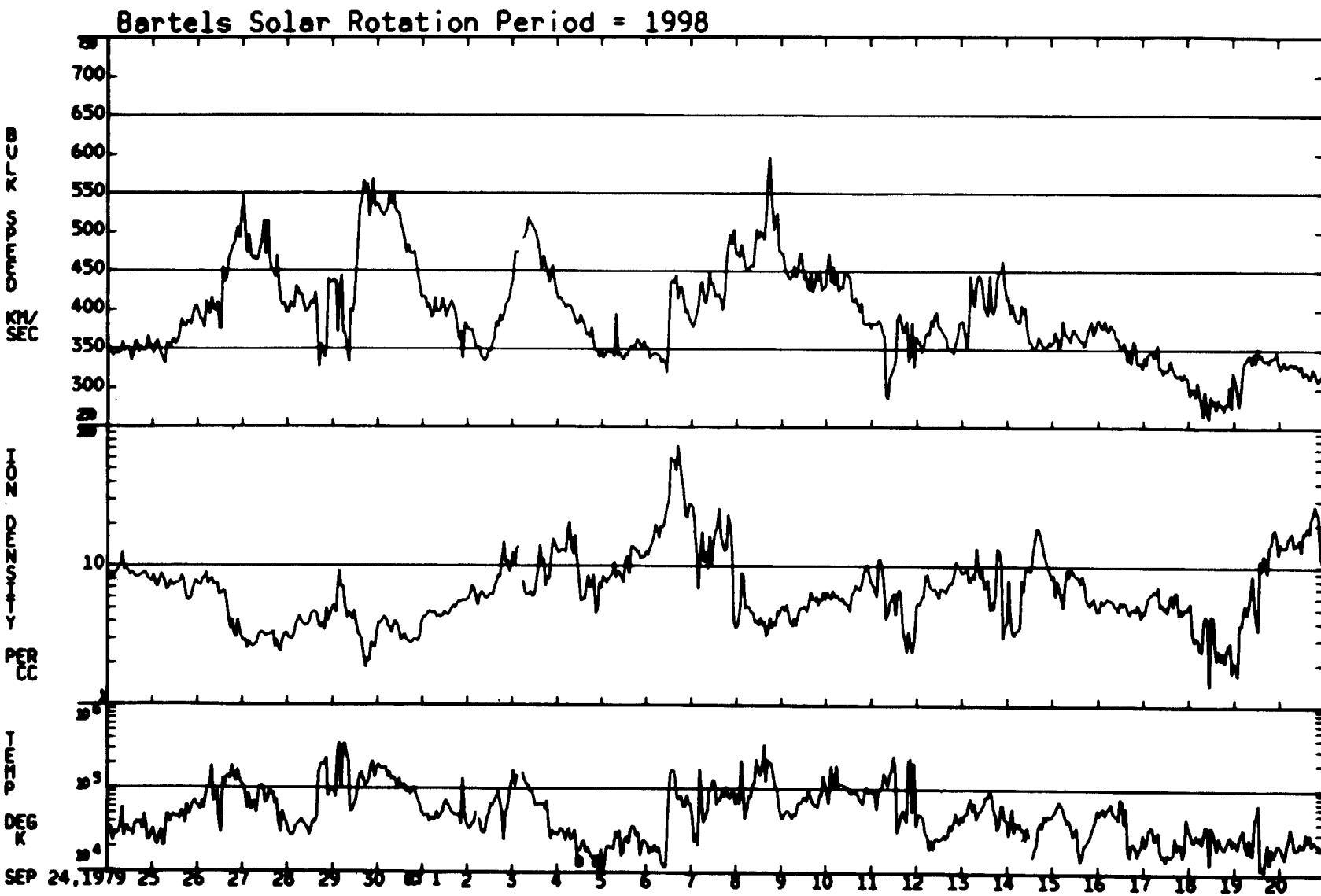


ORIGINAL PAGE IS  
OF POOR QUALITY

08/28/79 – 09/23/79

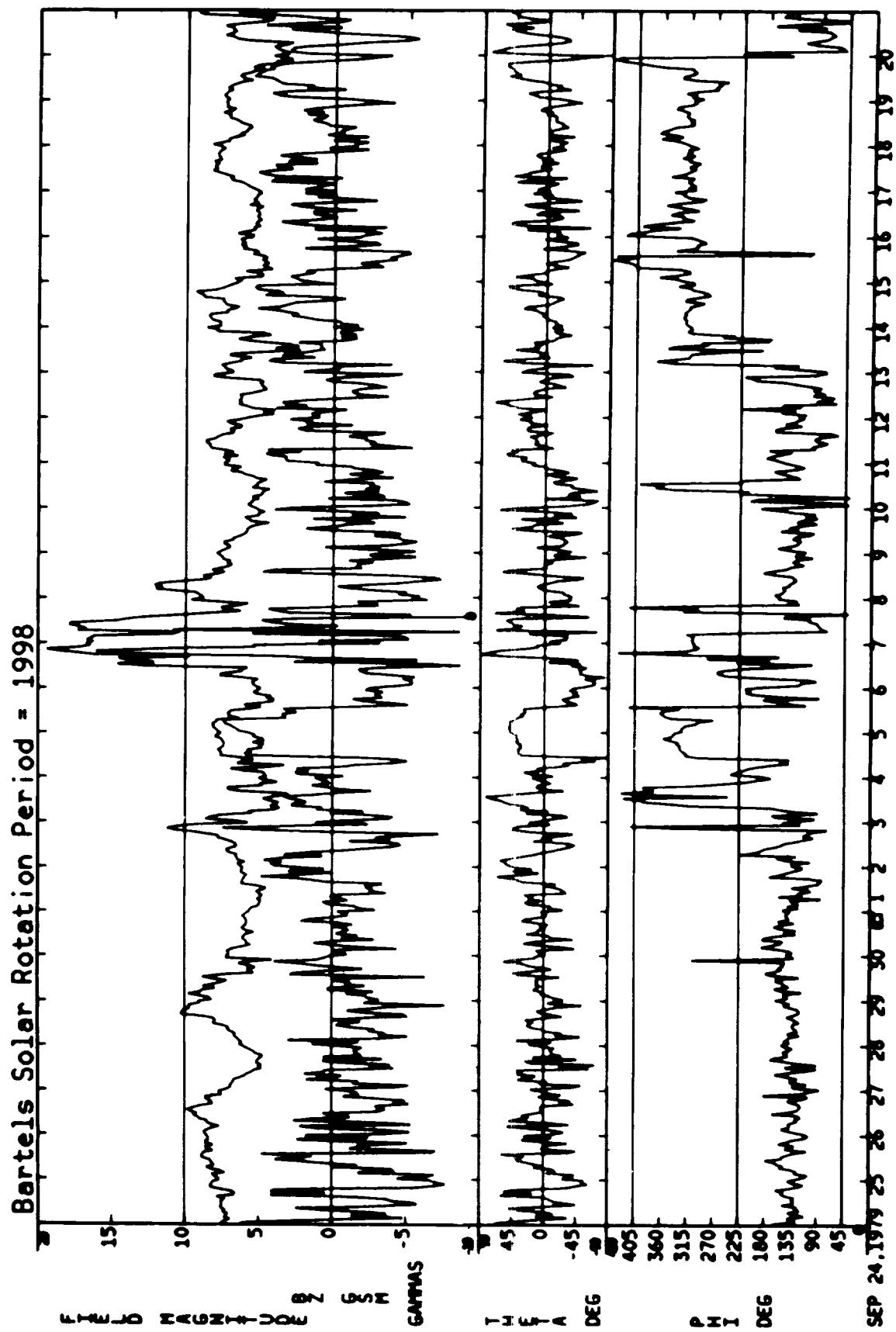


09/24/79 – 10/20/79

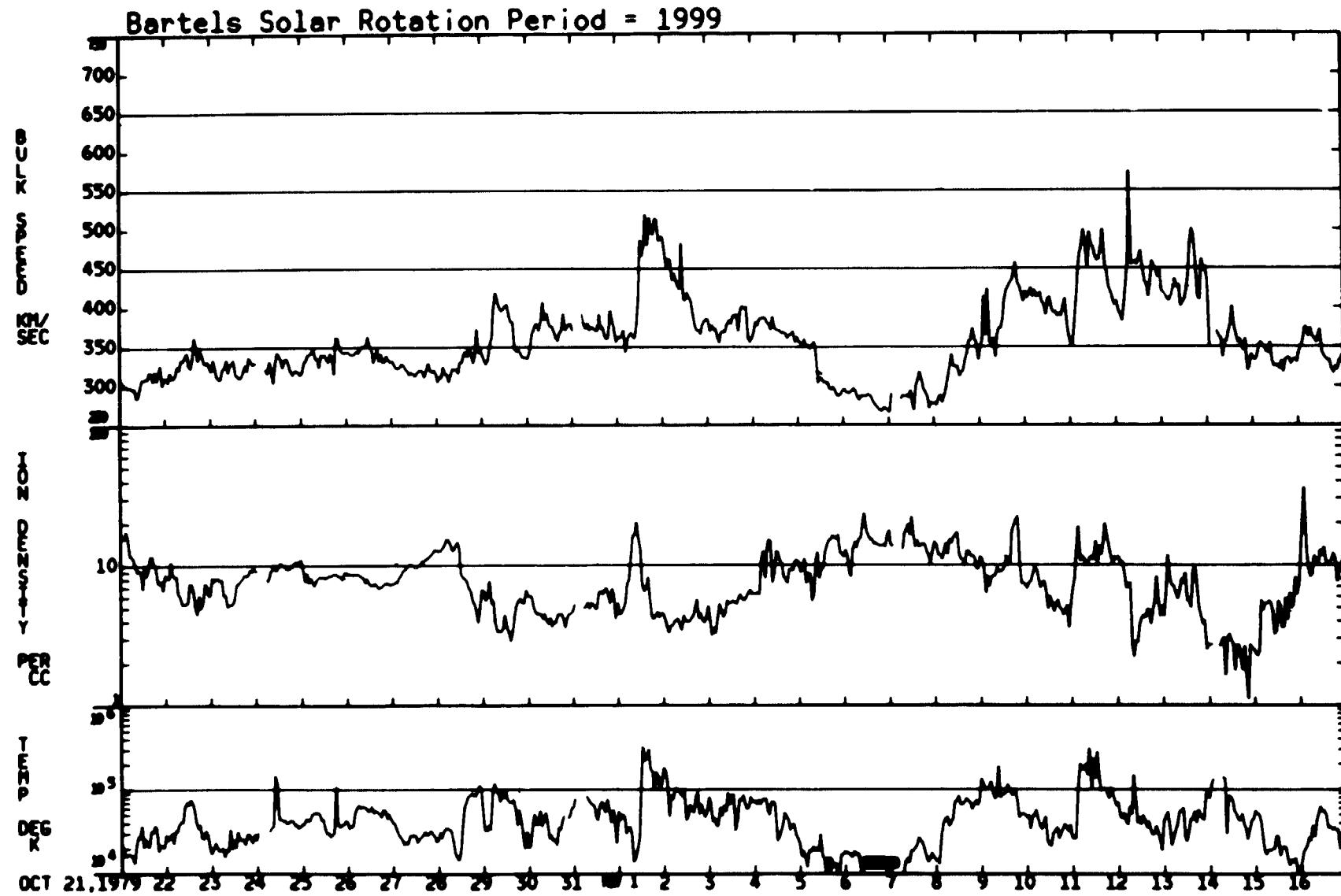


ORIGINAL PAGE IS  
OF POOR QUALITY

09/24/79 - 10/20/79



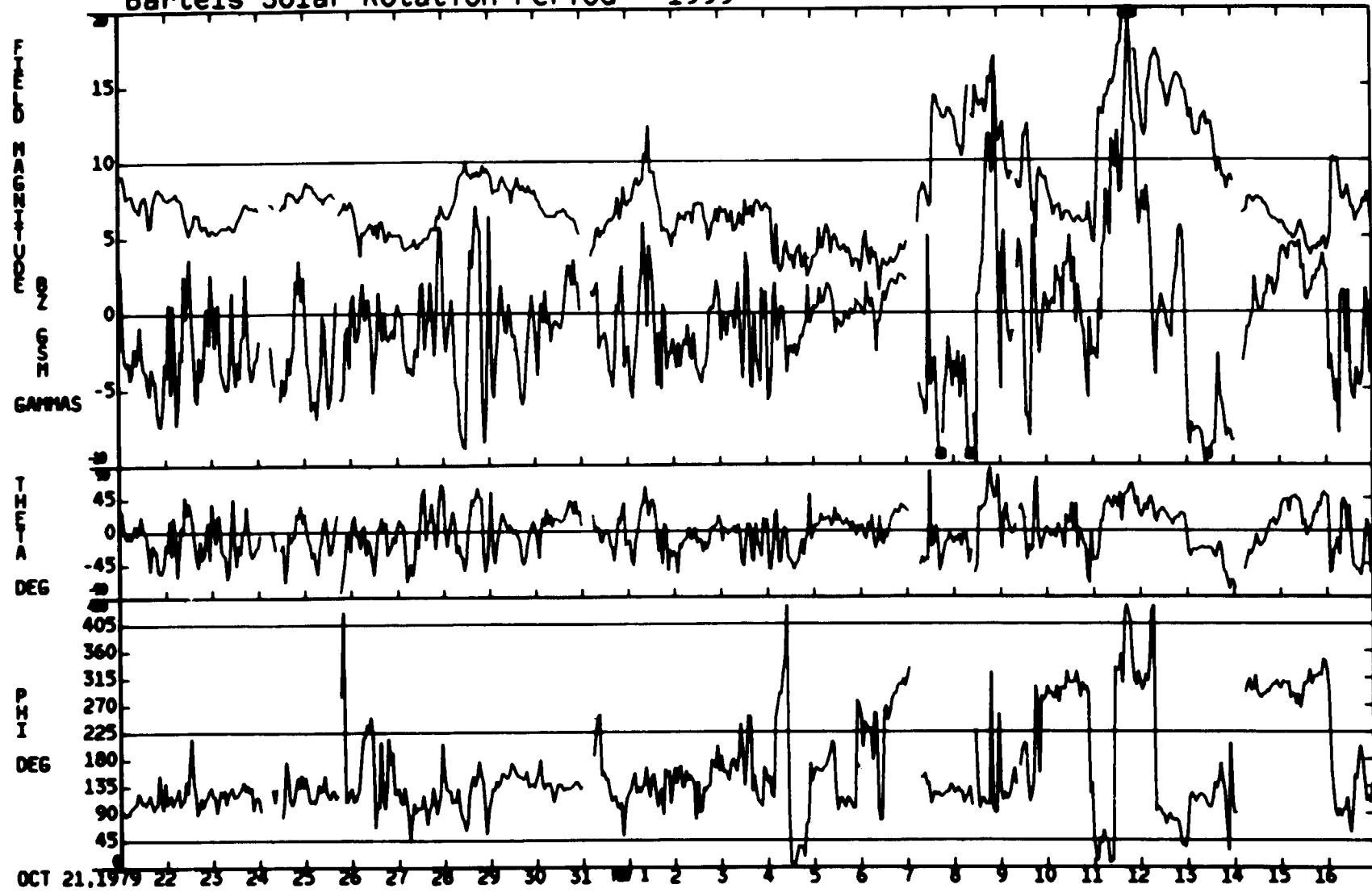
10/21/79 – 11/16/79



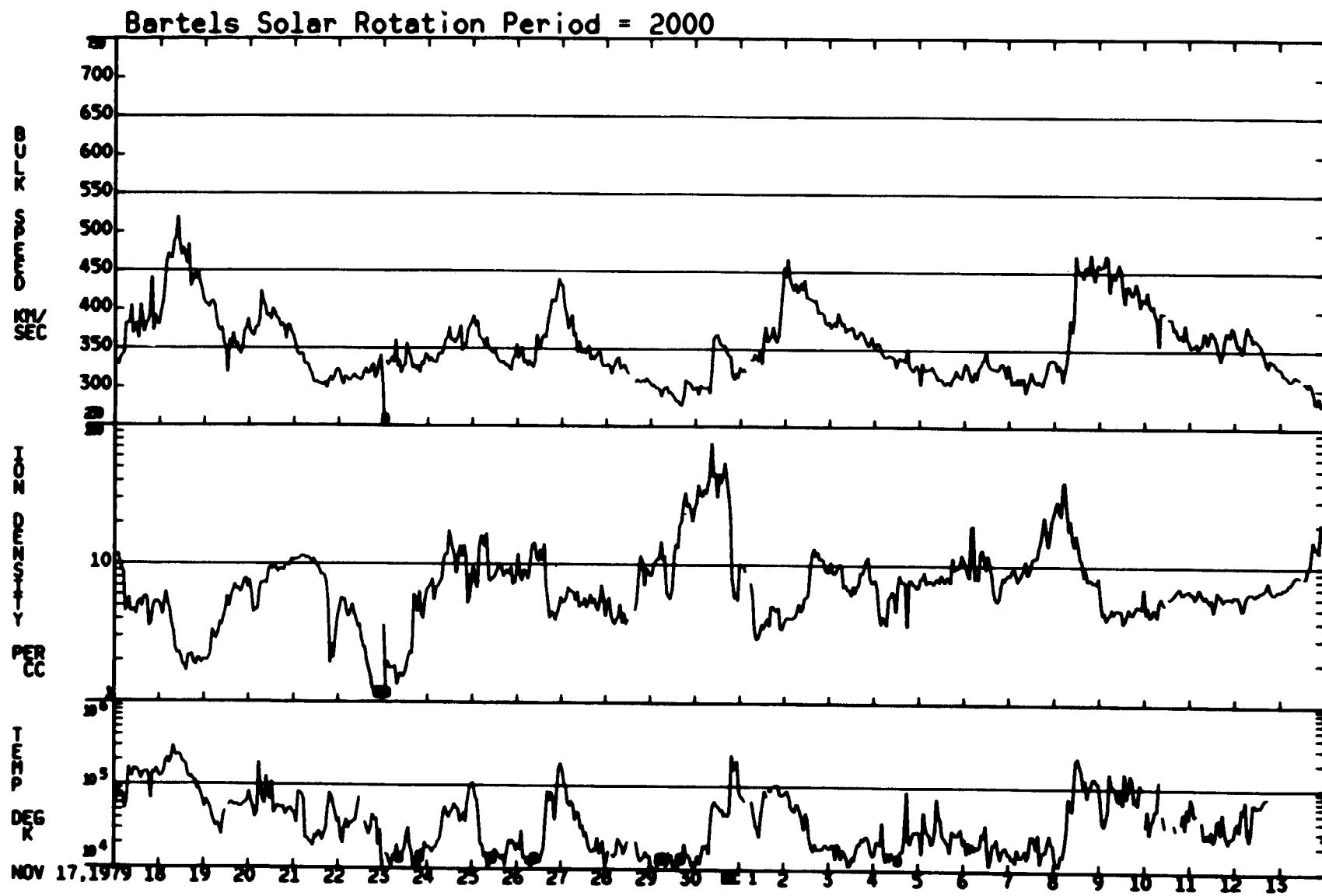
ORIGINAL PAGE IS  
OF POOR QUALITY

10/21/79 – 11/16/79

Bartels Solar Rotation Period = 1999

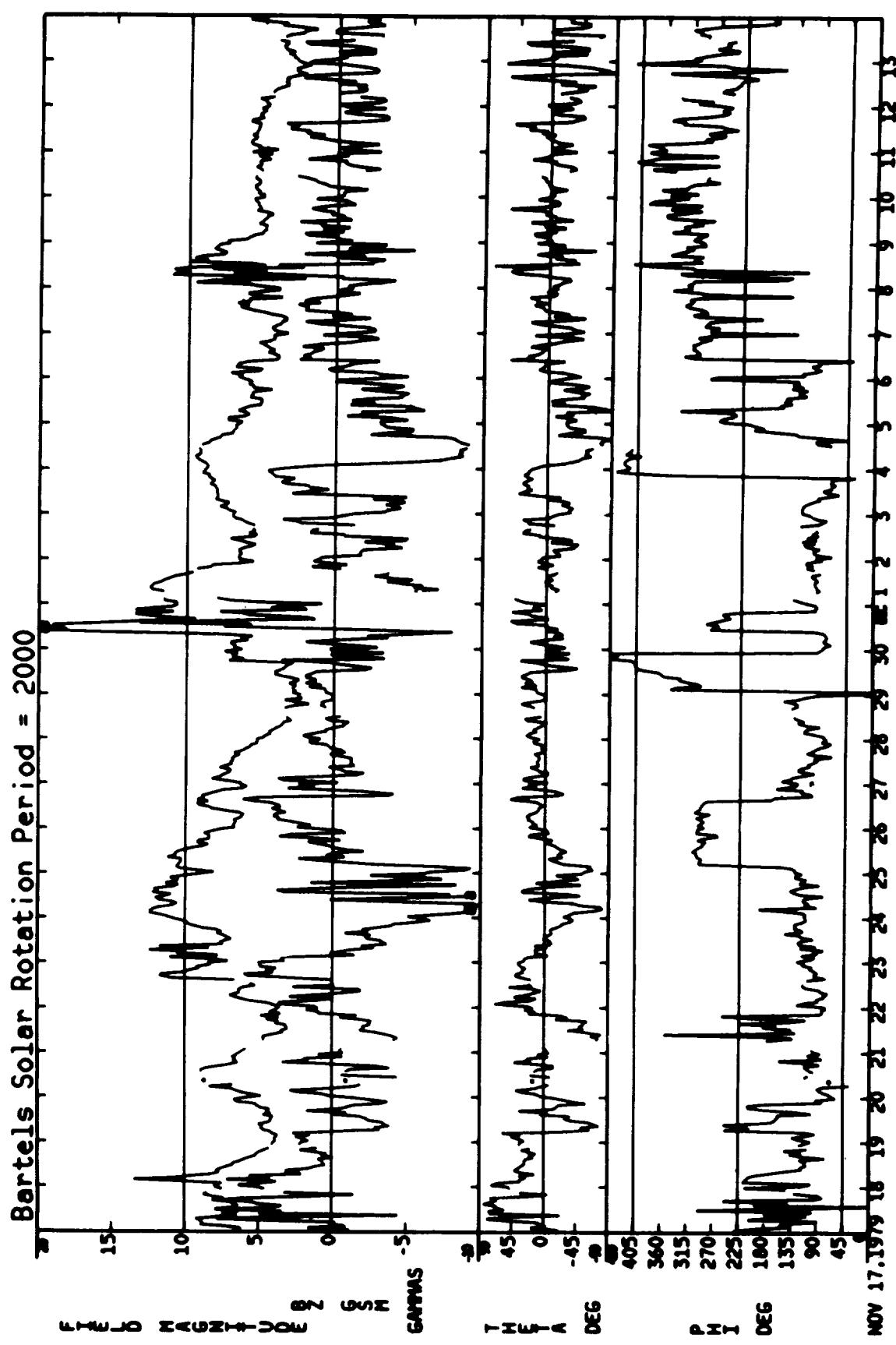


11/17/79 – 12/13/79



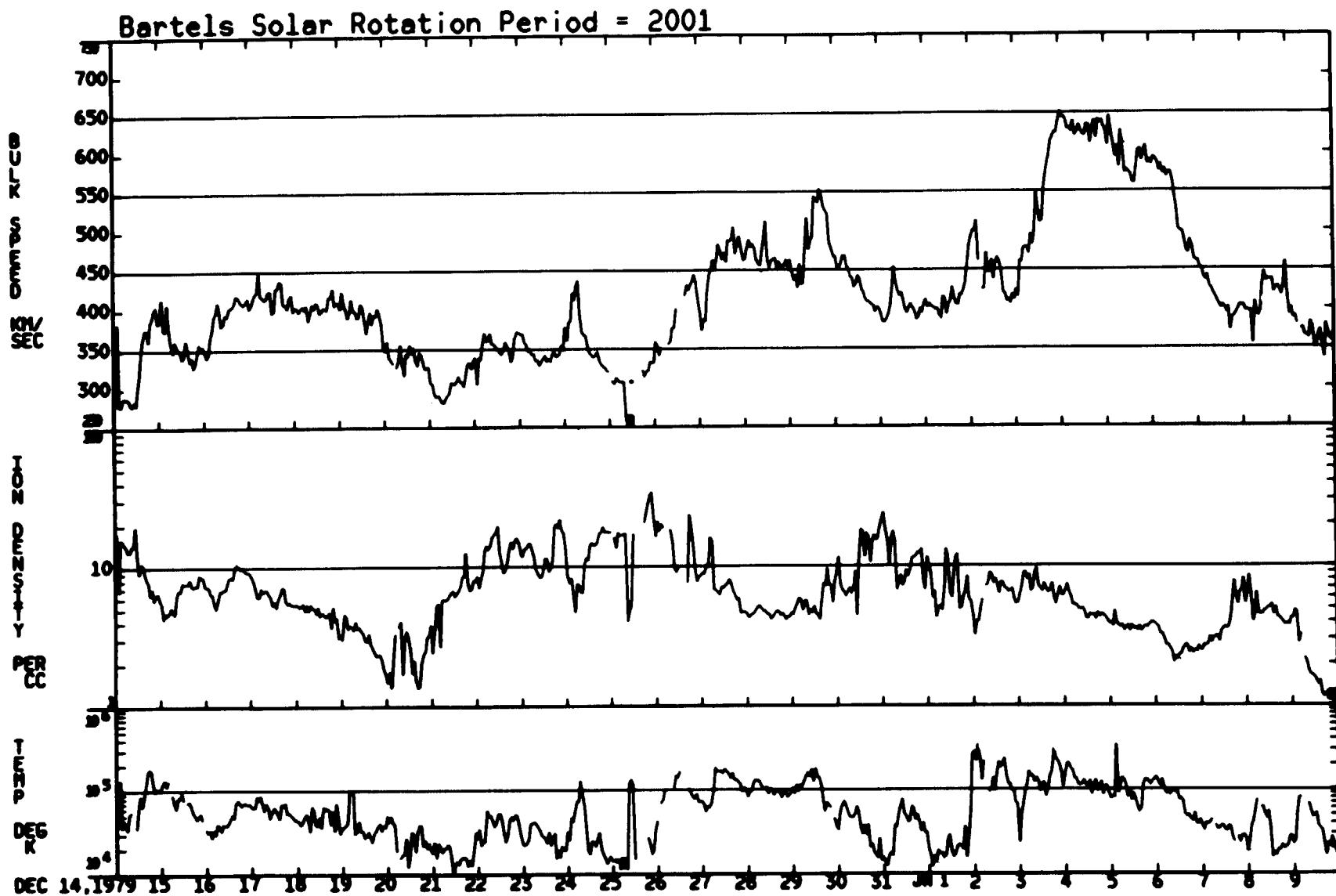
ORIGINAL PAGE IS  
OF POOR QUALITY

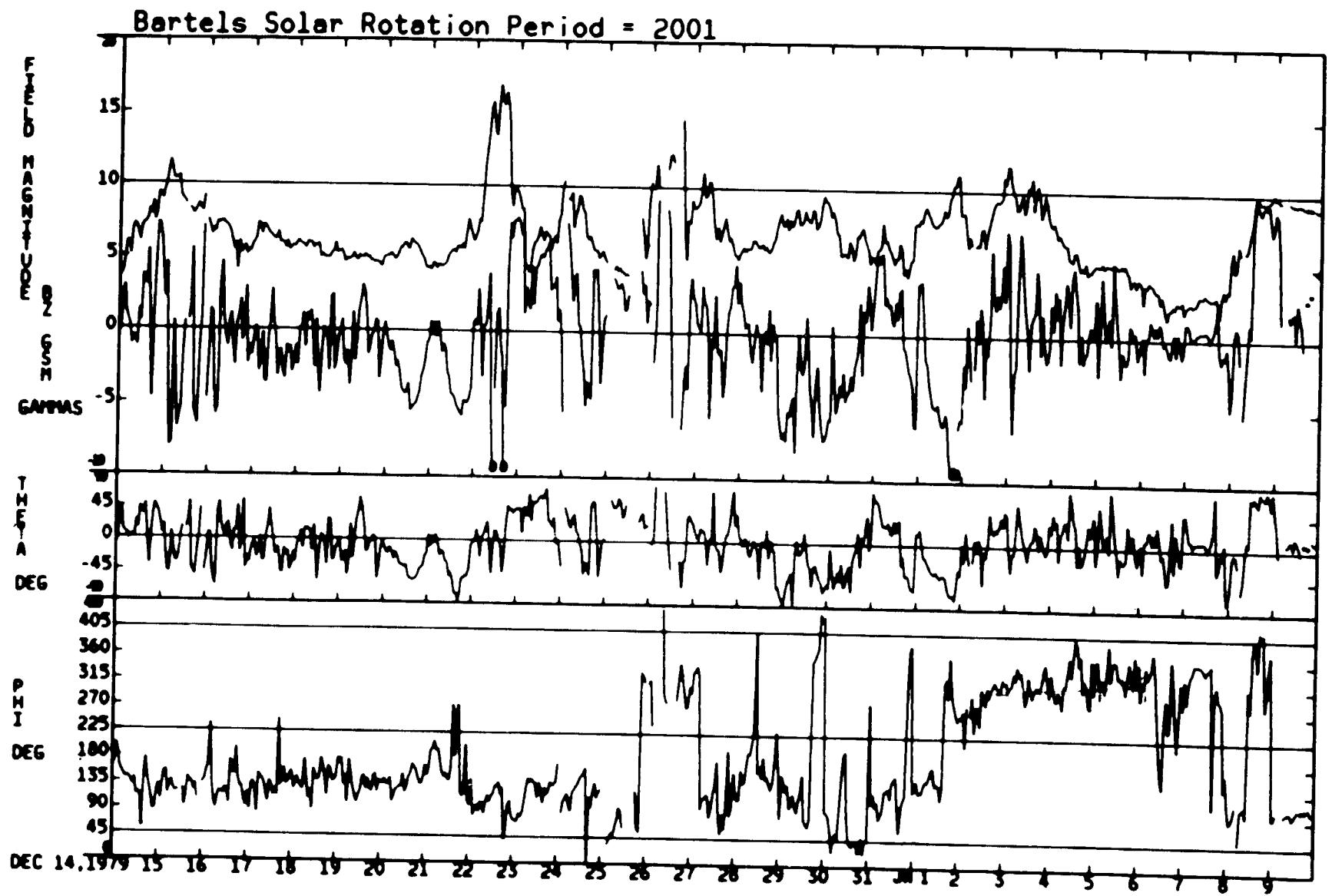
11/17/79 — 12/13/79



ORIGINAL PAGE IS  
OF POOR QUALITY

12/14/79 – 01/09/80

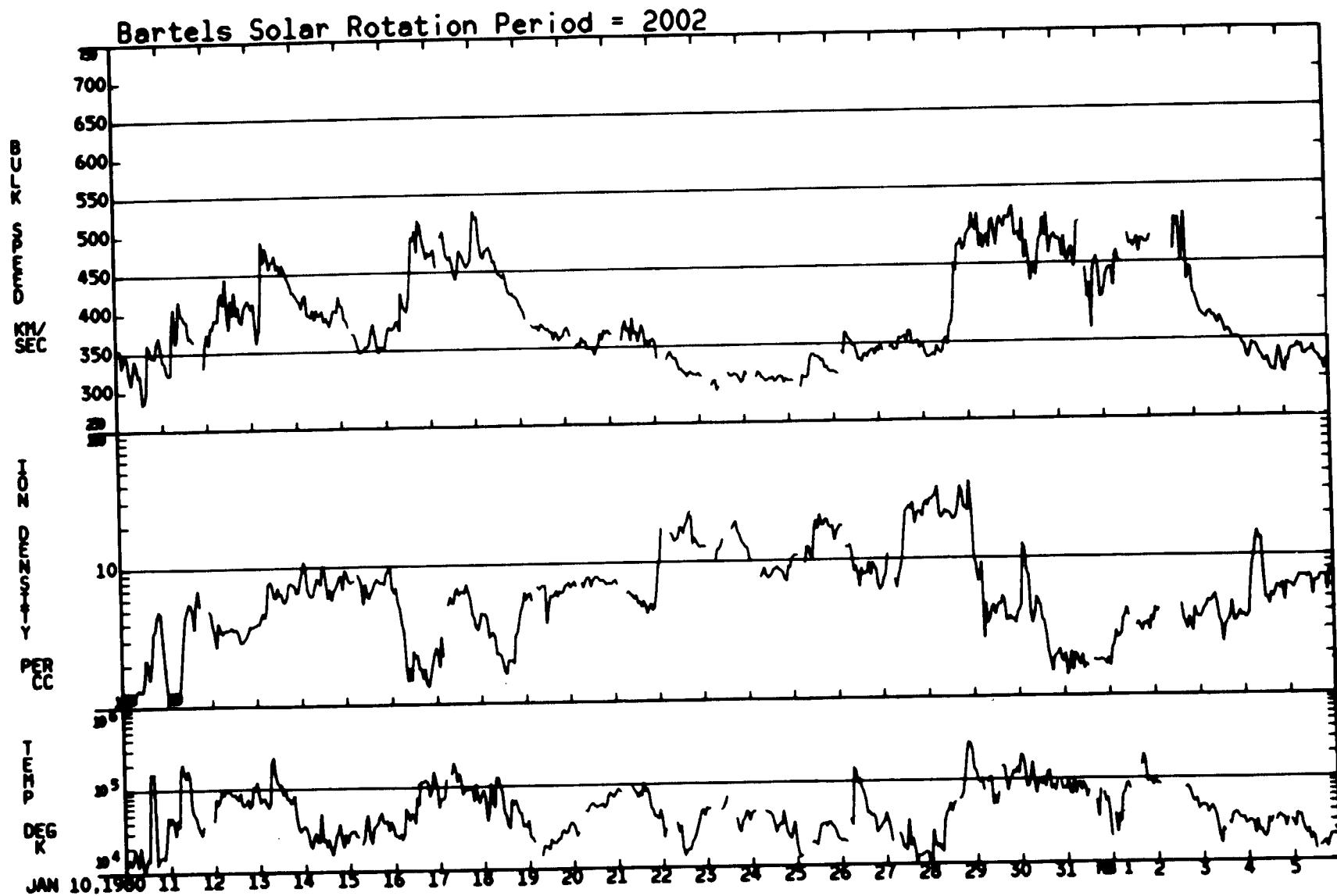




ORIGINAL PAGE IS  
OF POOR QUALITY

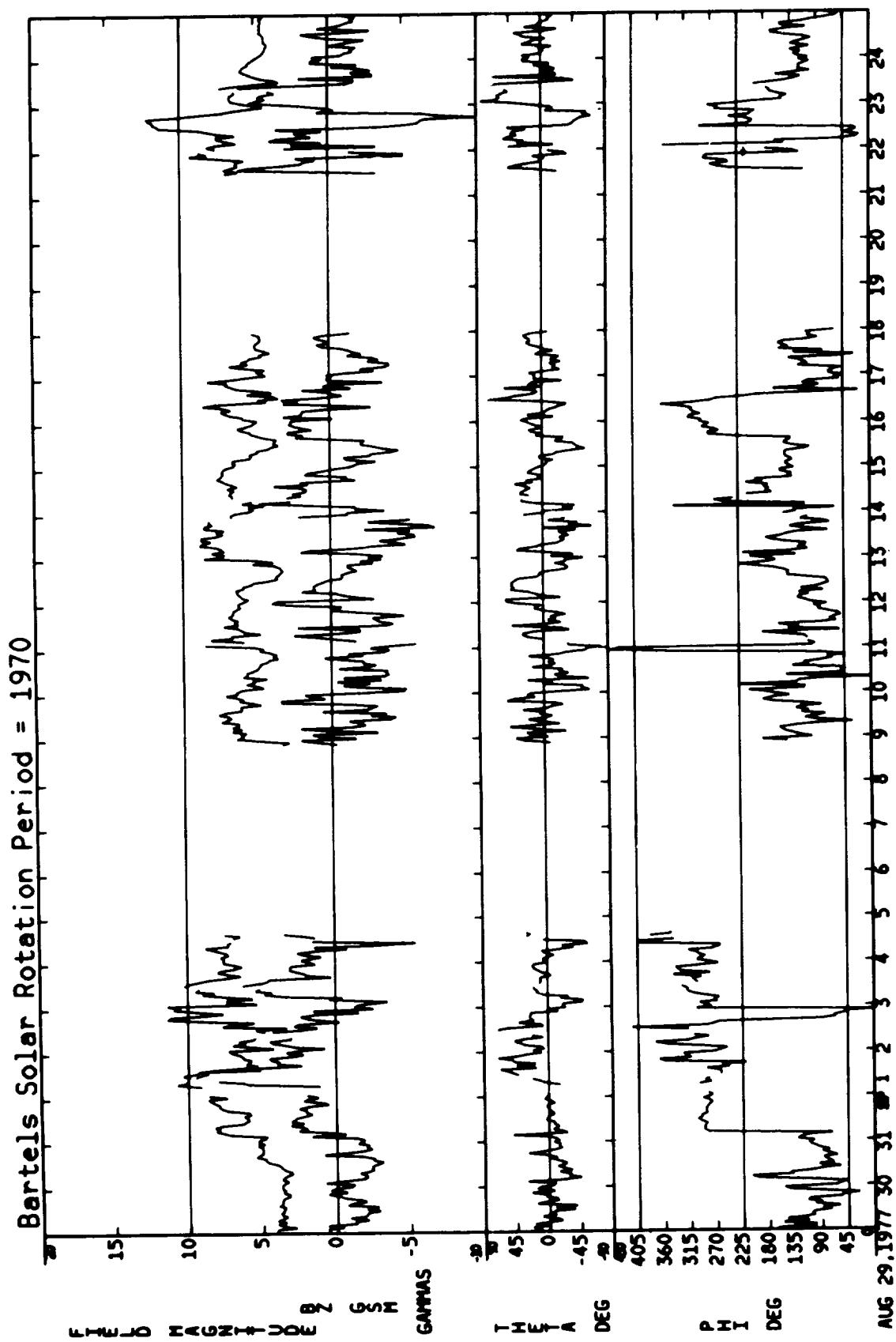
12/14/79 – 01/09/80

01/10/80 – 02/05/80

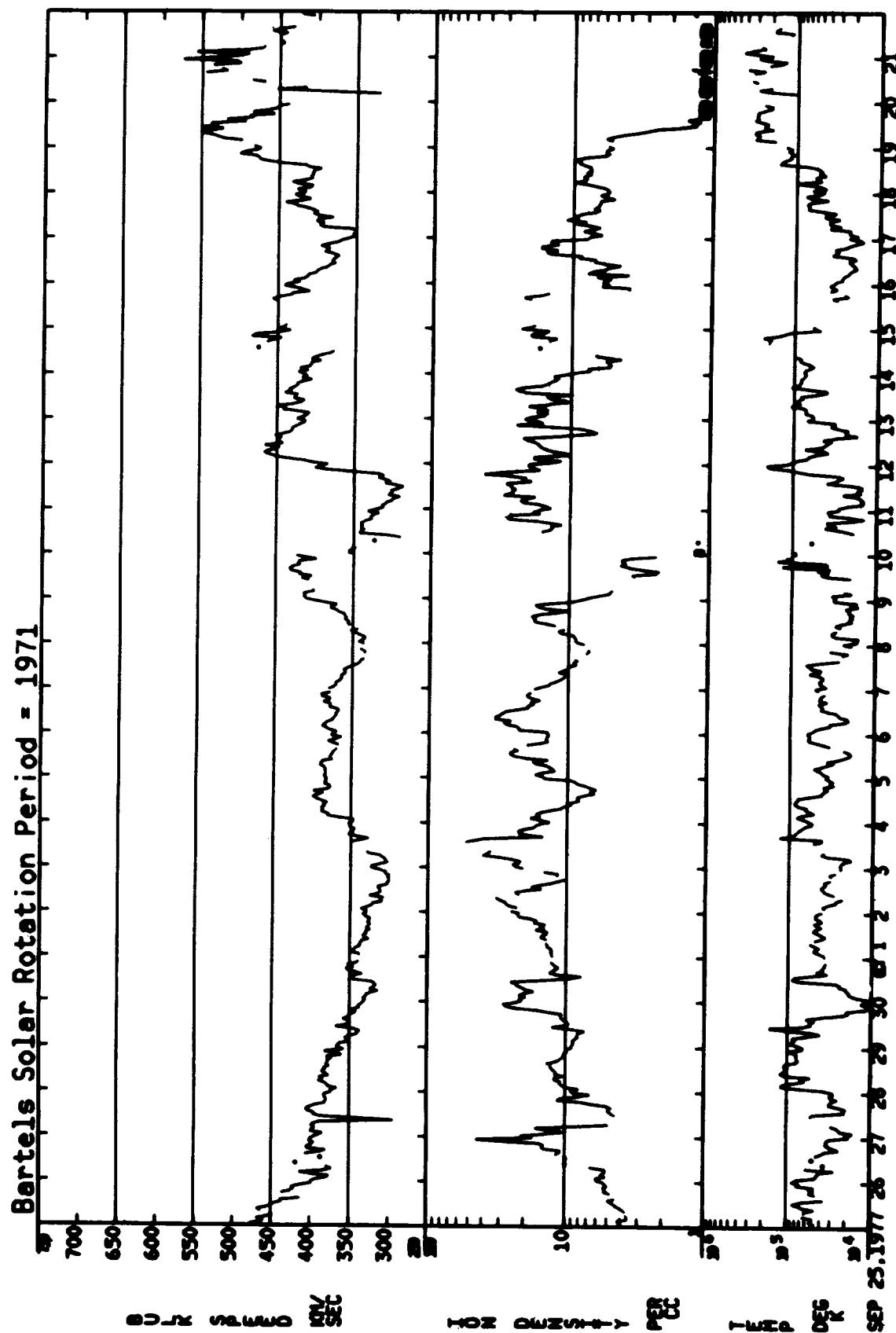


ORIGINAL PAGE IS  
OF POOR QUALITY

08/30/77 – 09/24/77



09/25/77 - 10/21/77

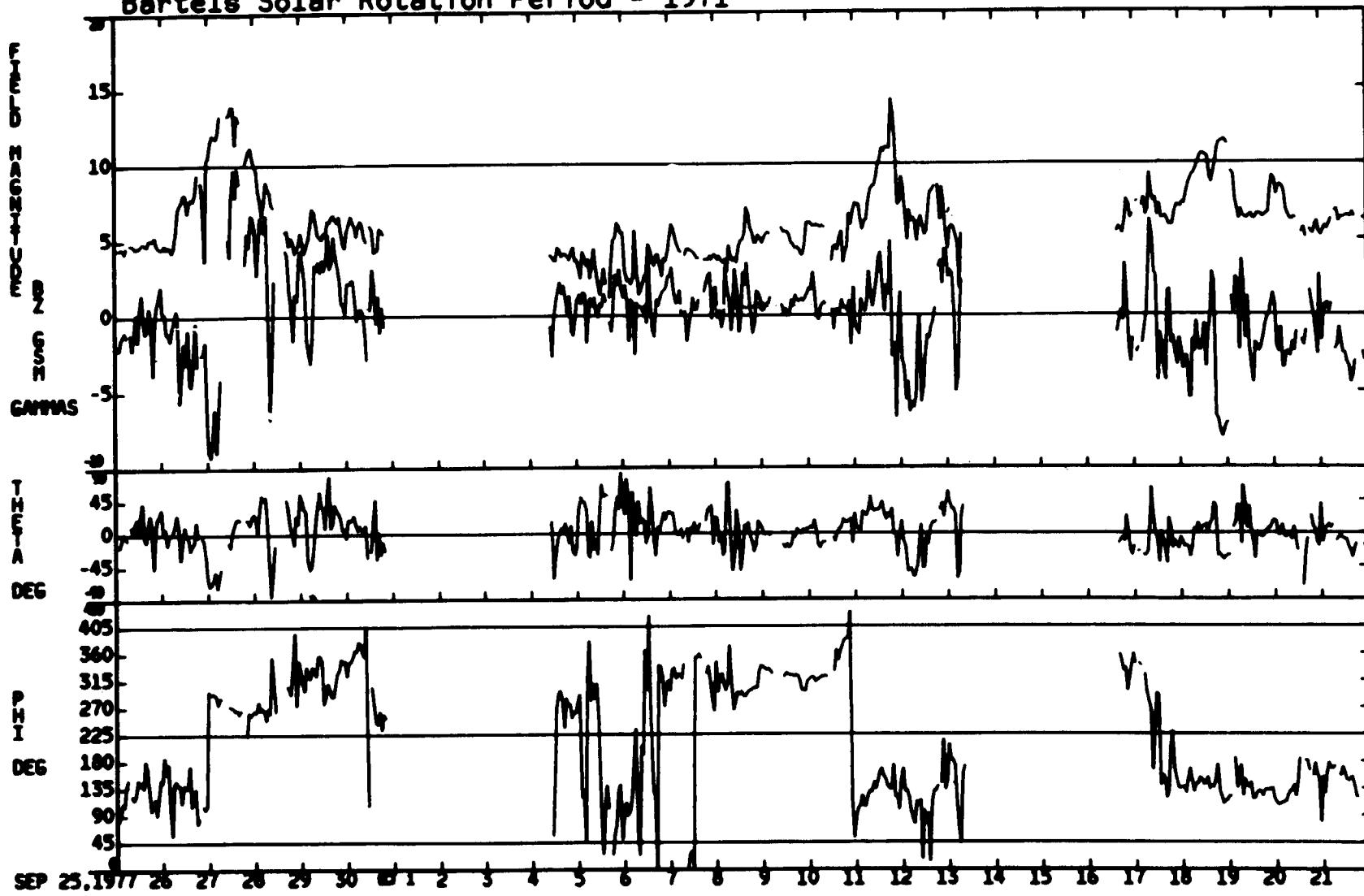


ORIGINAL PAGE IS  
OF POOR QUALITY

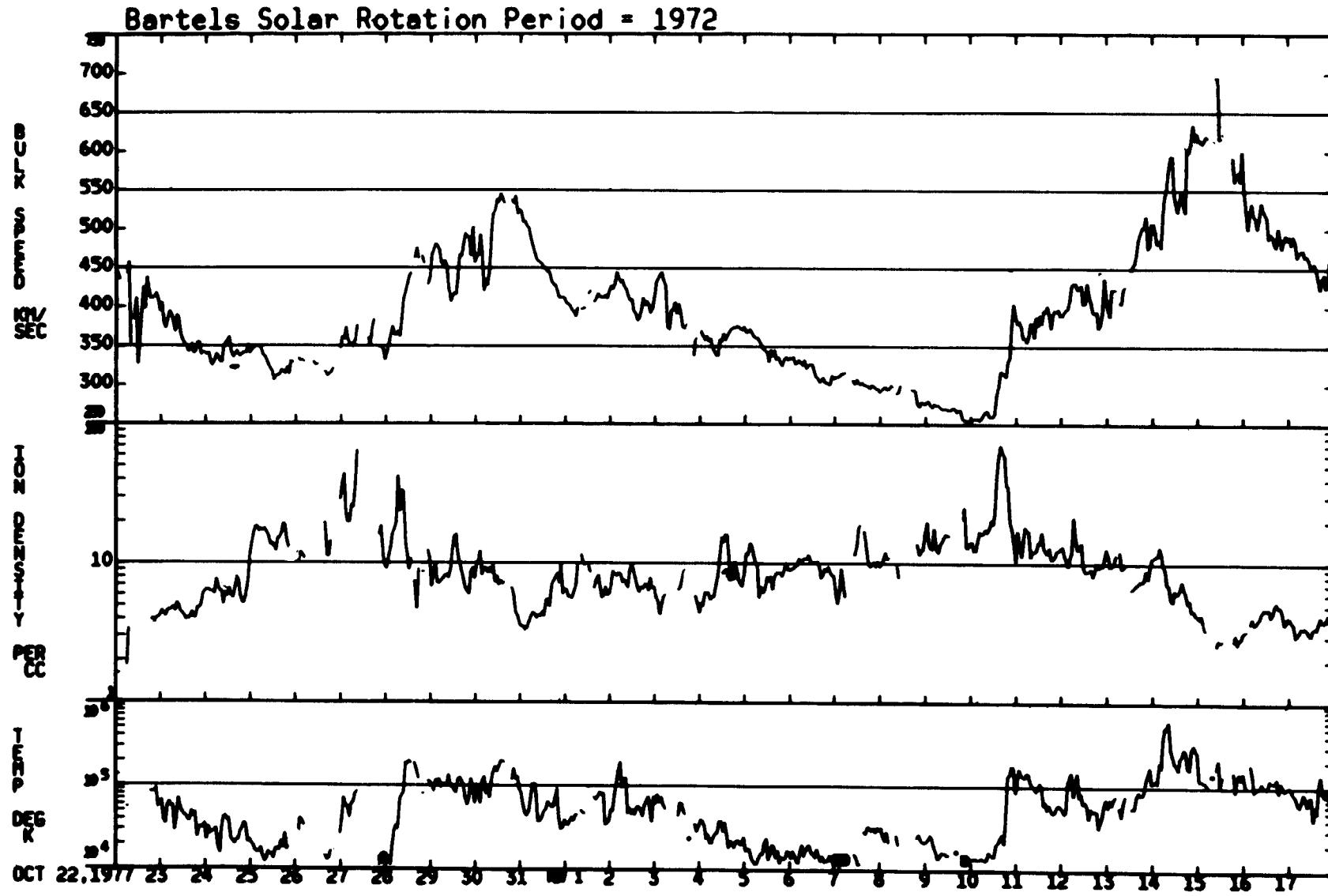
ORIGINAL PAGE IS  
OF POOR QUALITY

09/25/77 – 10/21/77

Bartels Solar Rotation Period = 1971

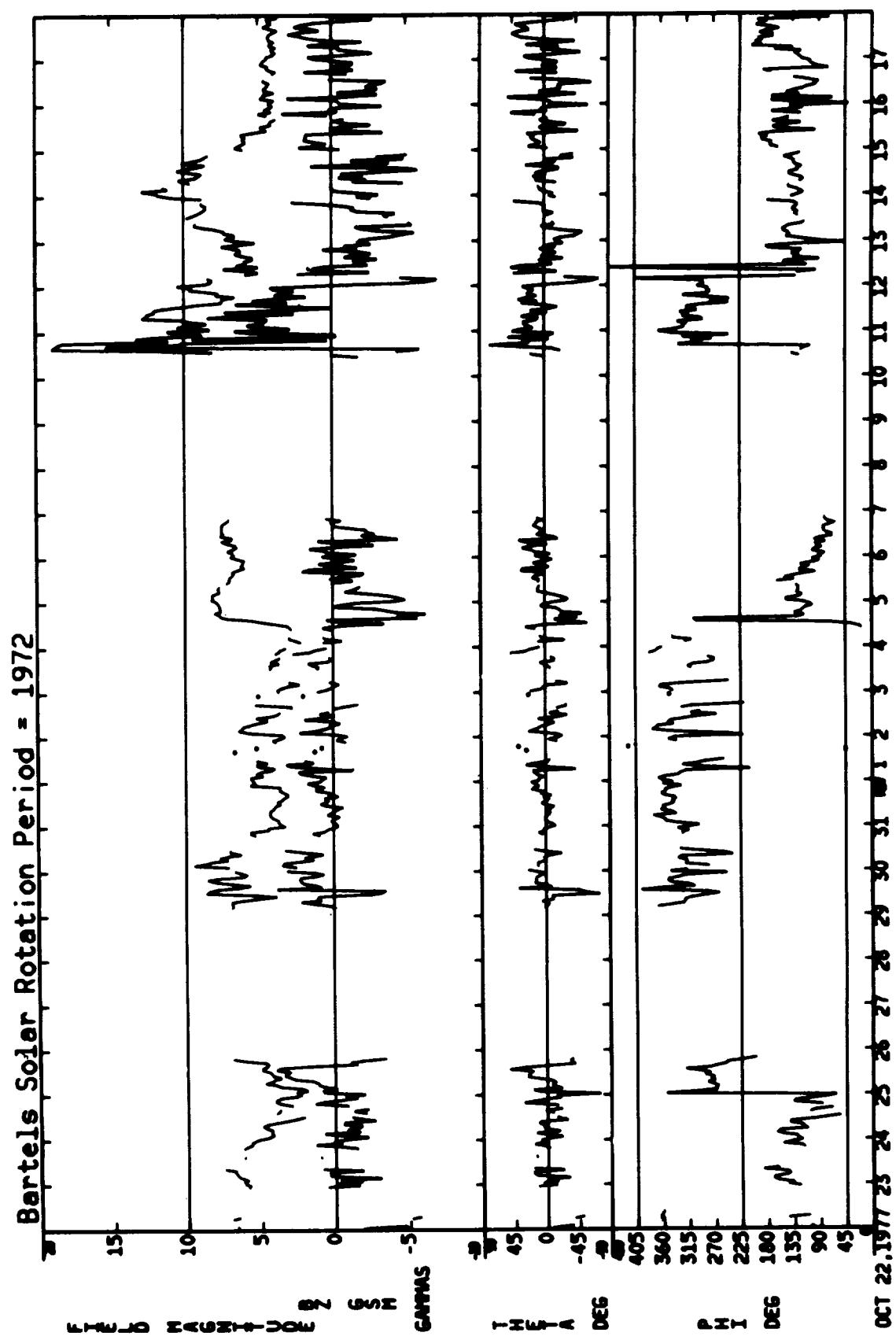


10/22/77 - 11/17/77

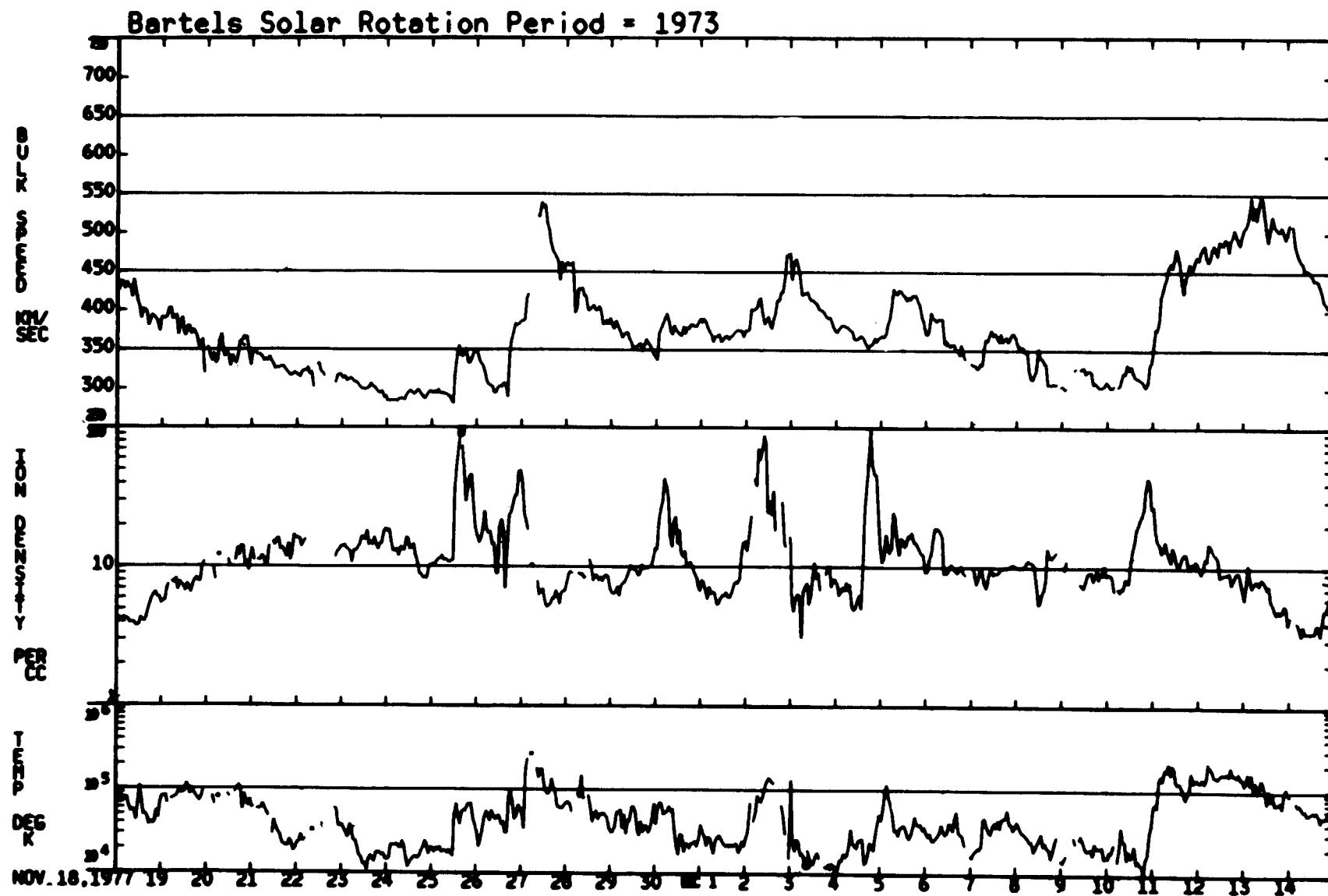


ORIGINAL PAGE IS  
OF POOR QUALITY

10/22/77 - 11/17/77

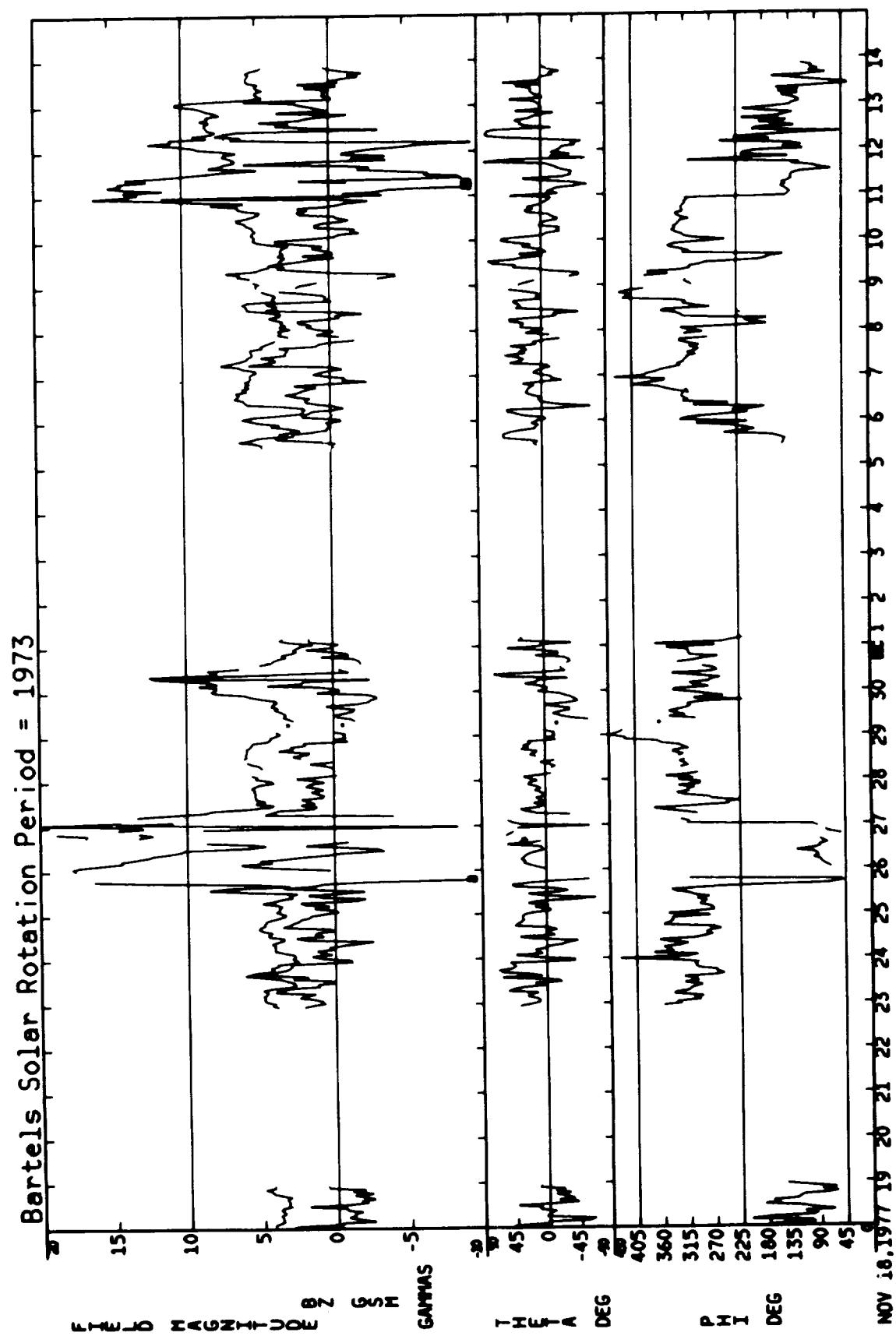


11/18/77 - 12/14/77

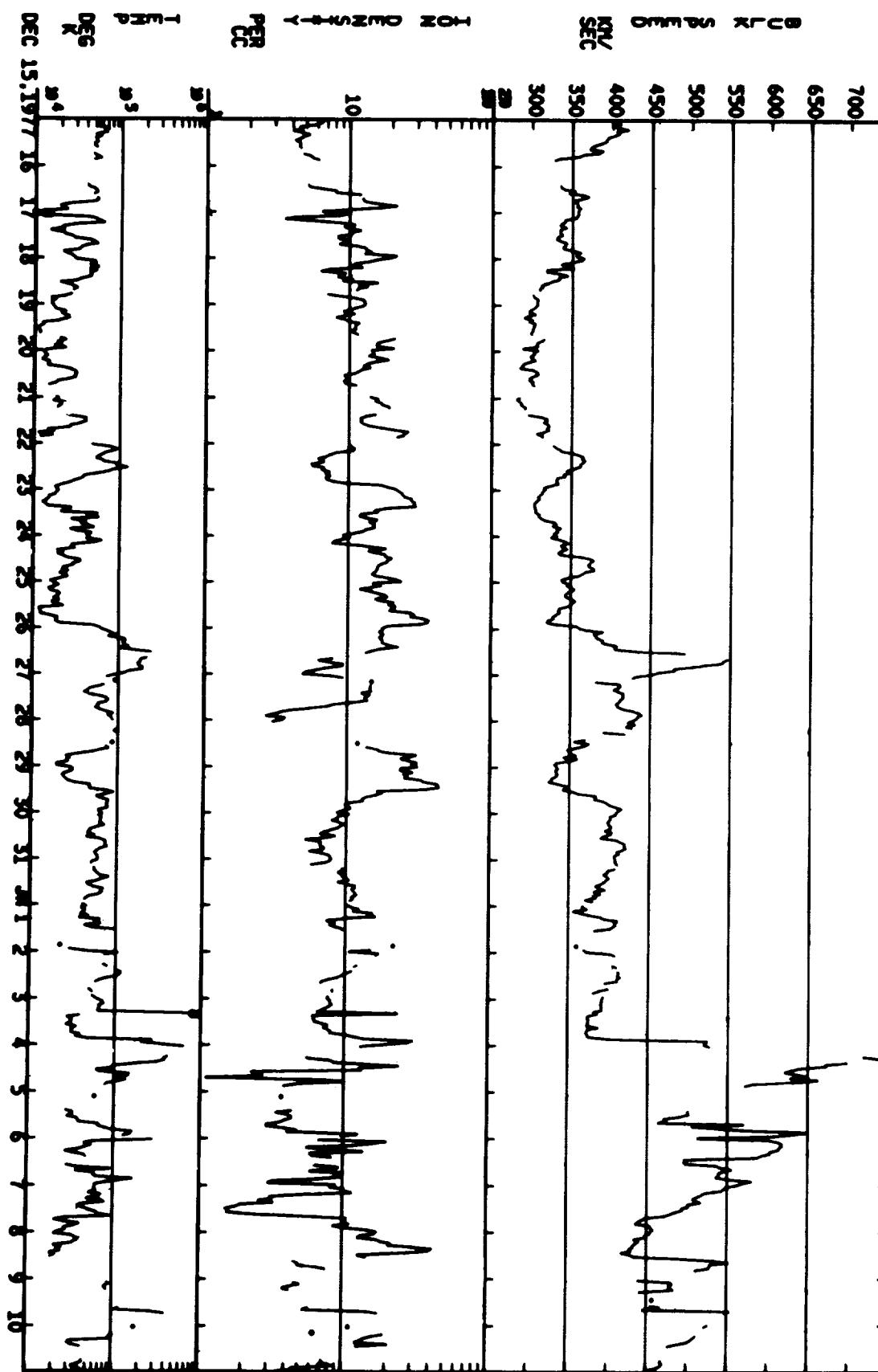


ORIGINAL PAGE IS  
OF POOR QUALITY

11/18/77 - 12/14/77



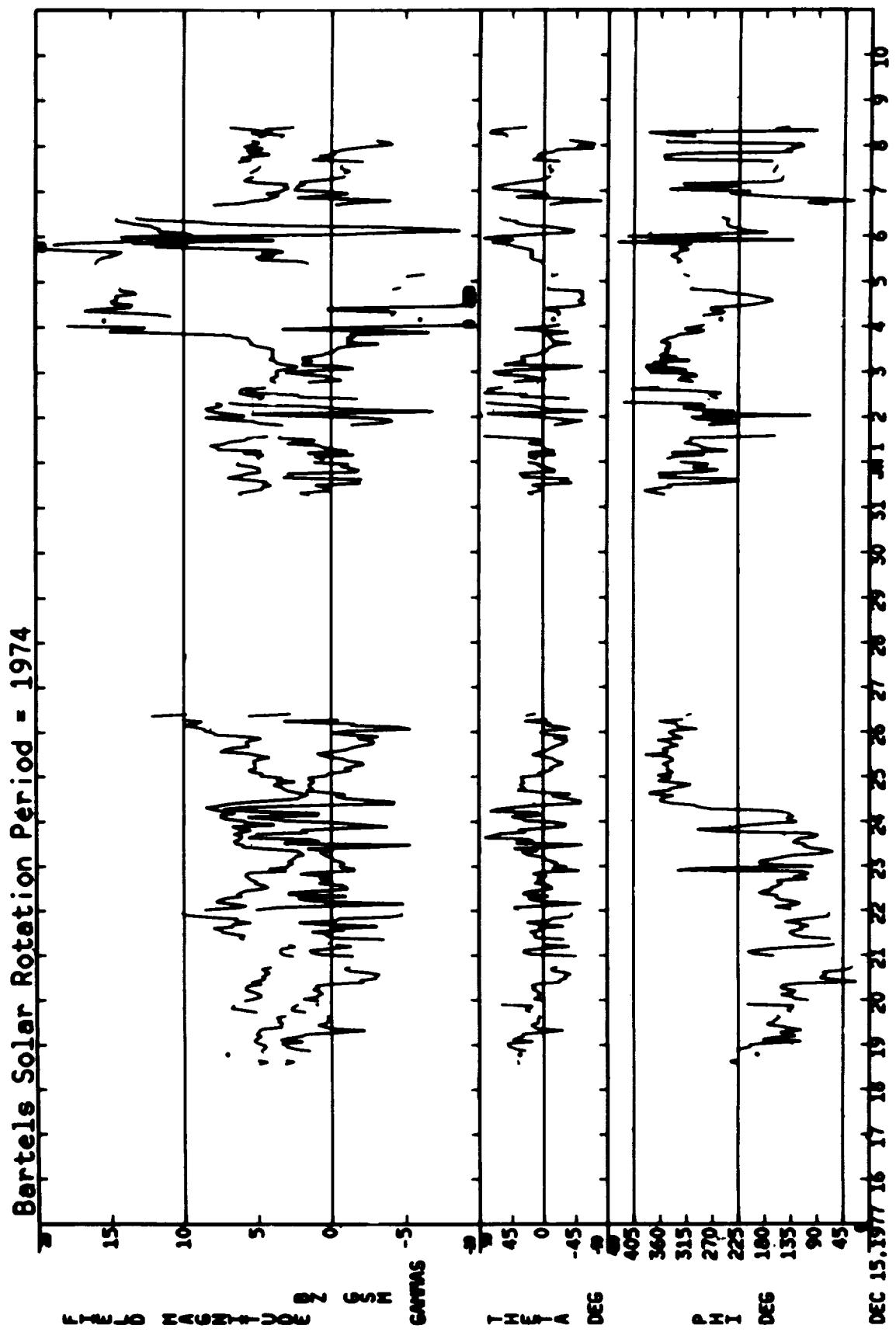
Bartels Solar Rotation Period = 1974



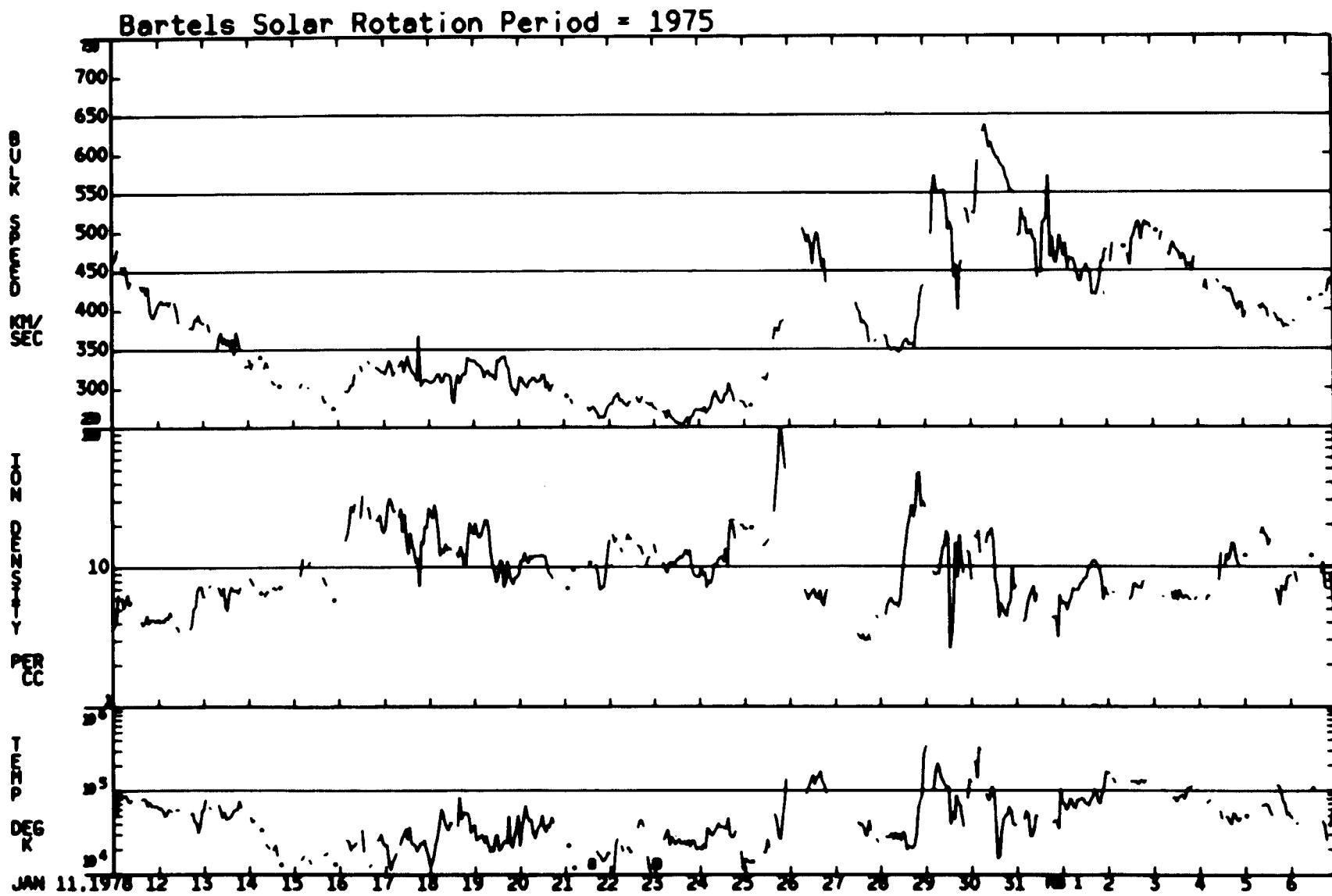
12/15/77 - 01/10/78

ORIGINAL PAGE IS  
OF POOR QUALITY

12/15/77 — 01/10/78

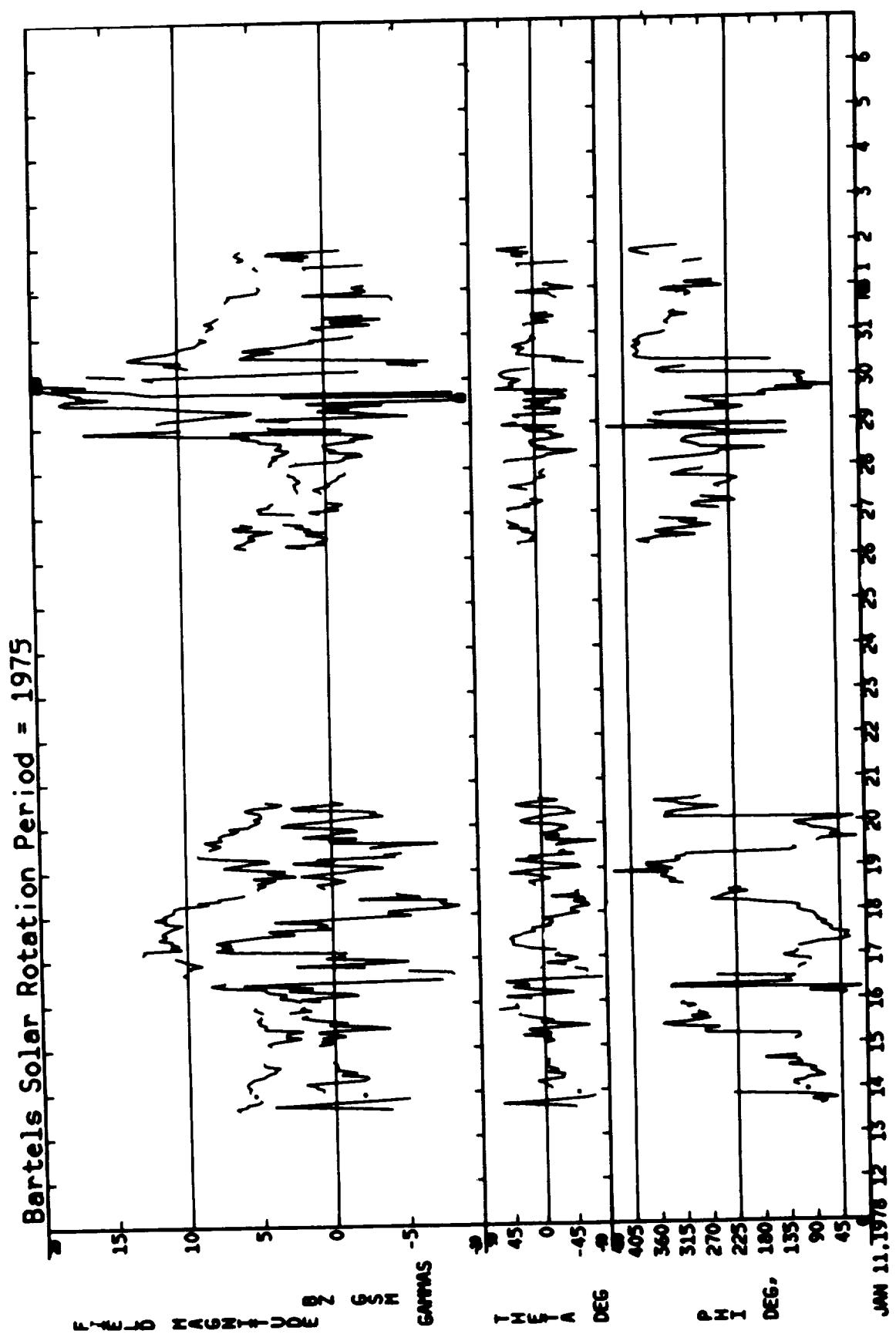


01/11/78 – 02/06/78

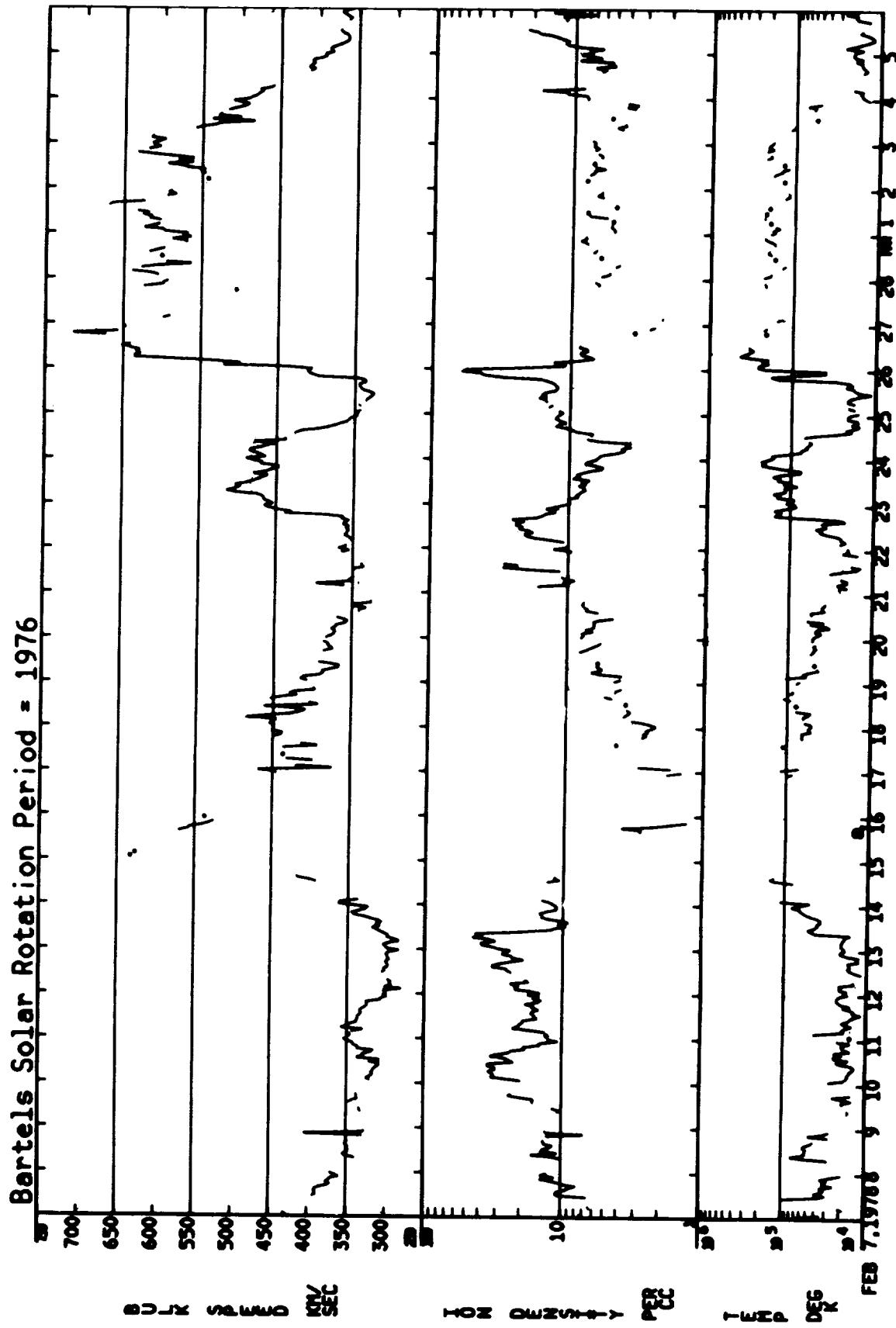


ORIGINAL PAGE IS  
OF POOR QUALITY

01/11/78 – 02/06/78

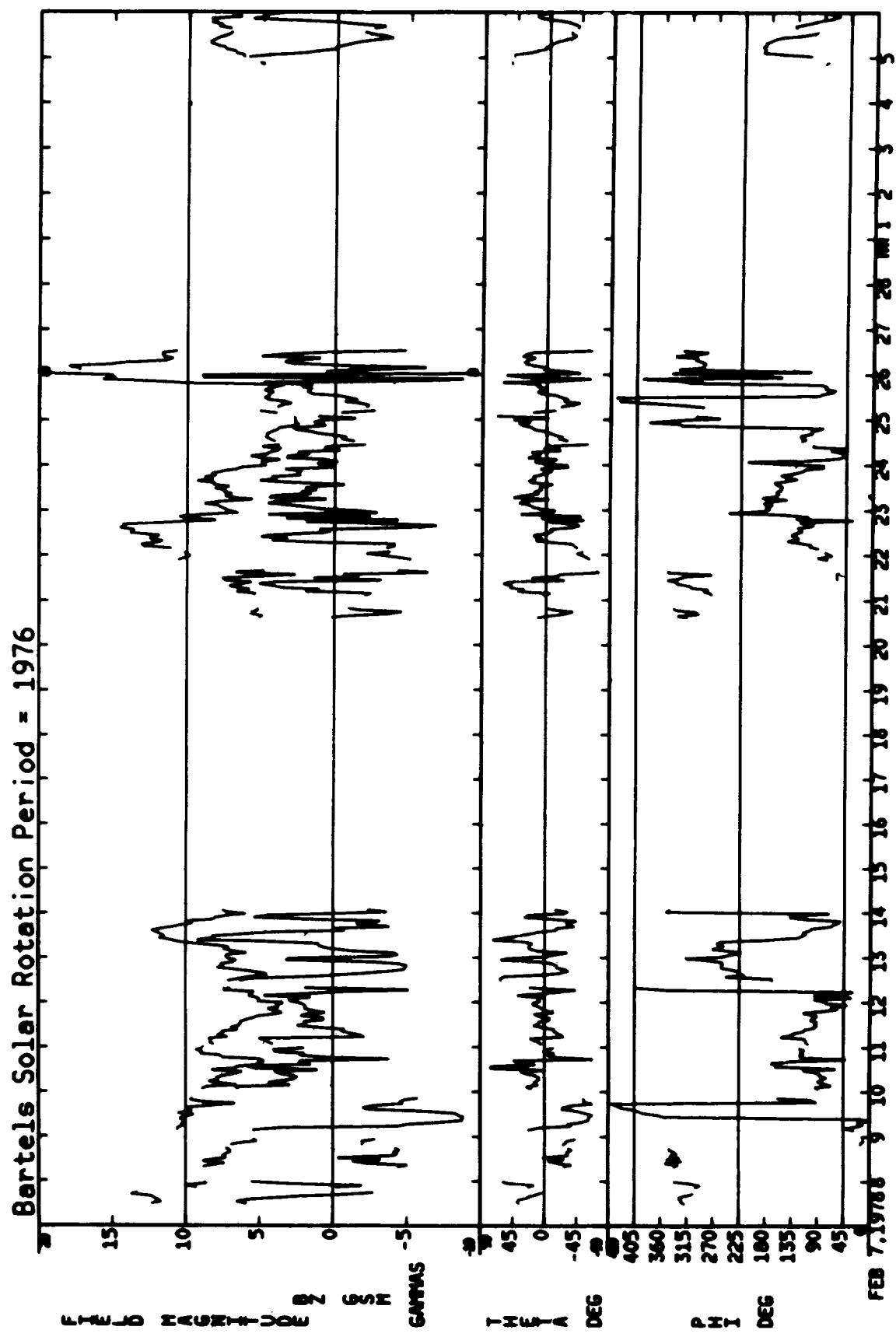


02/07/78 – 03/05/78

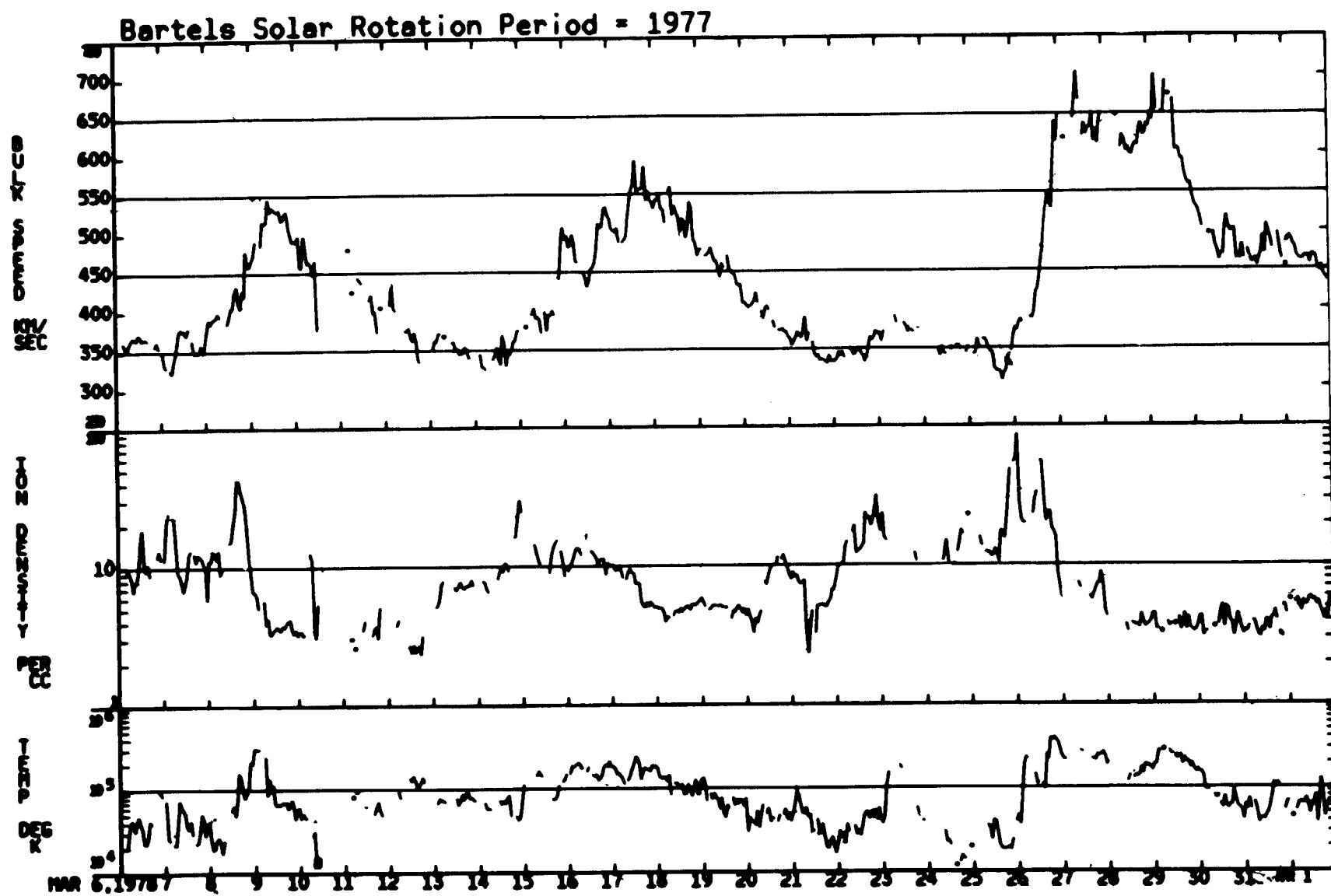


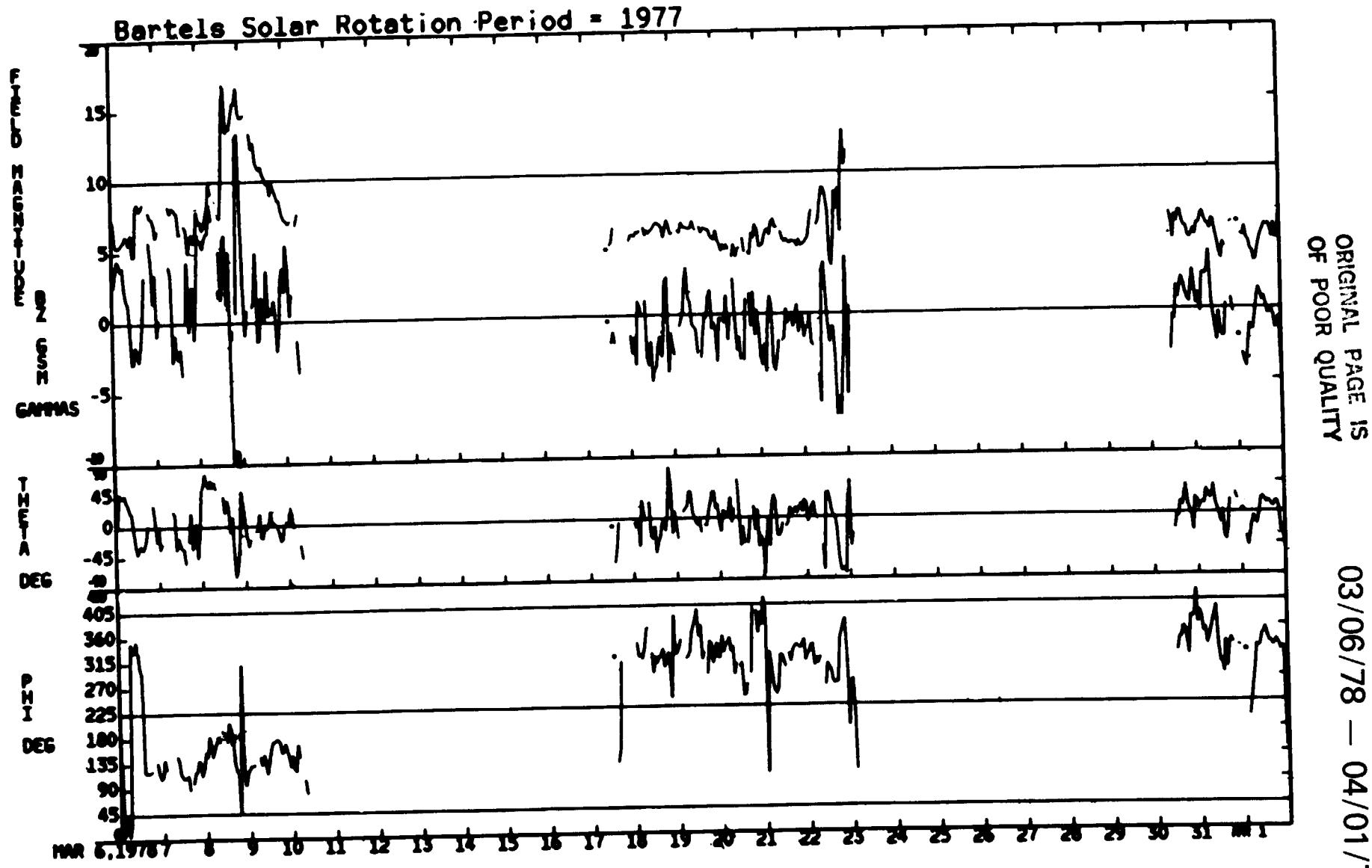
ORIGINAL PAGE IS  
OF POOR QUALITY

02/07/78 — 03/05/78

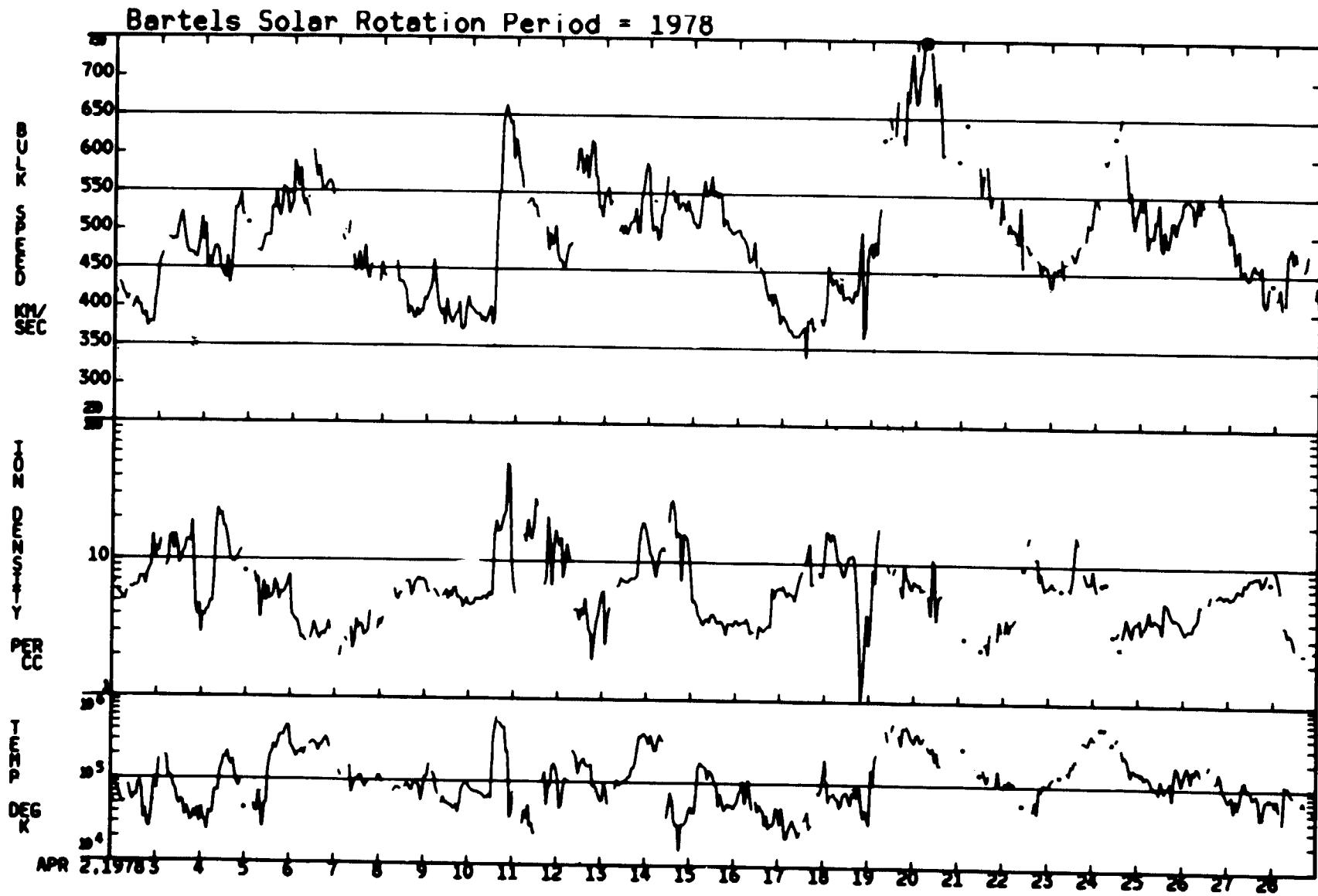


03/06/78 – 04/01/78



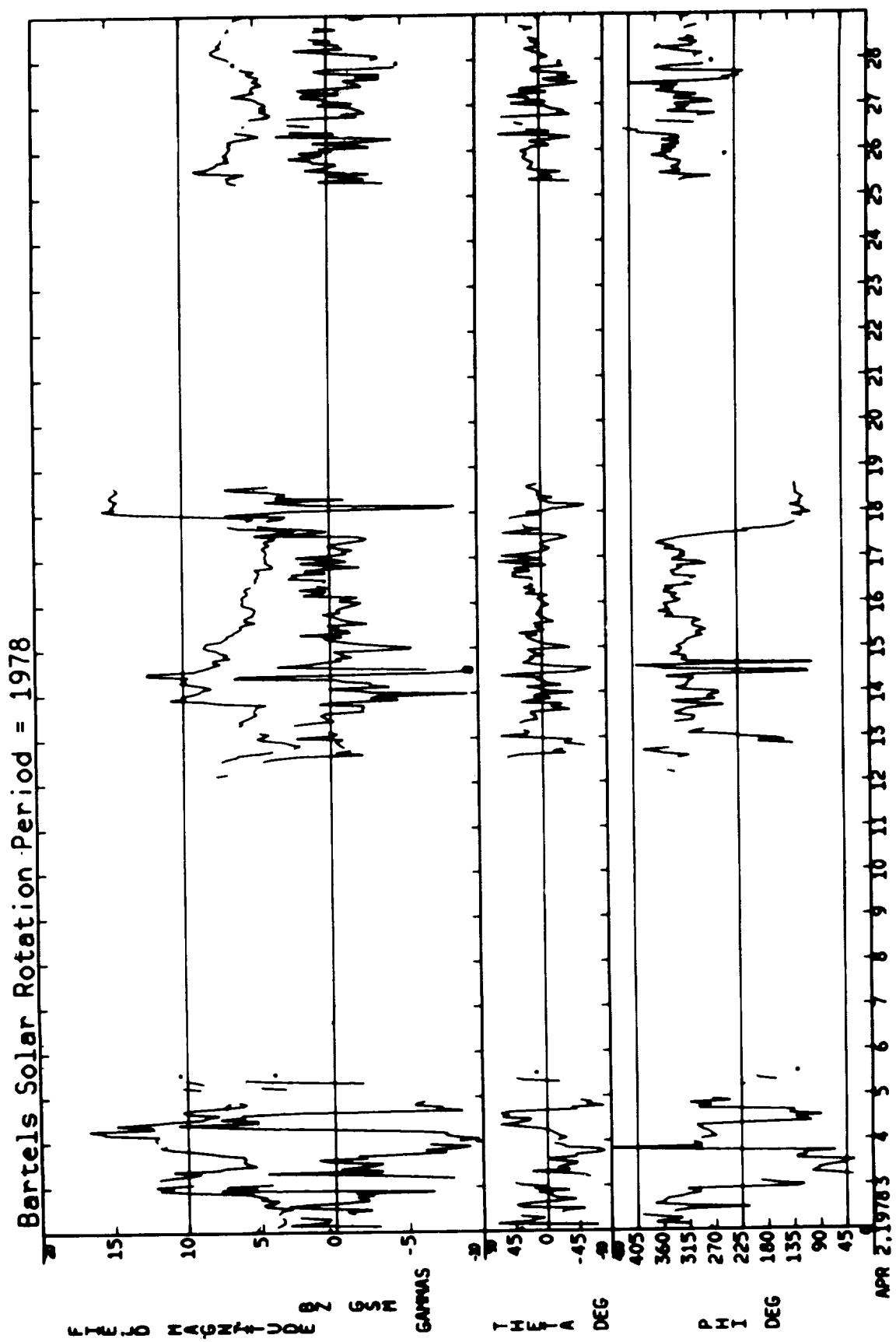


04/02/78 – 04/28/78

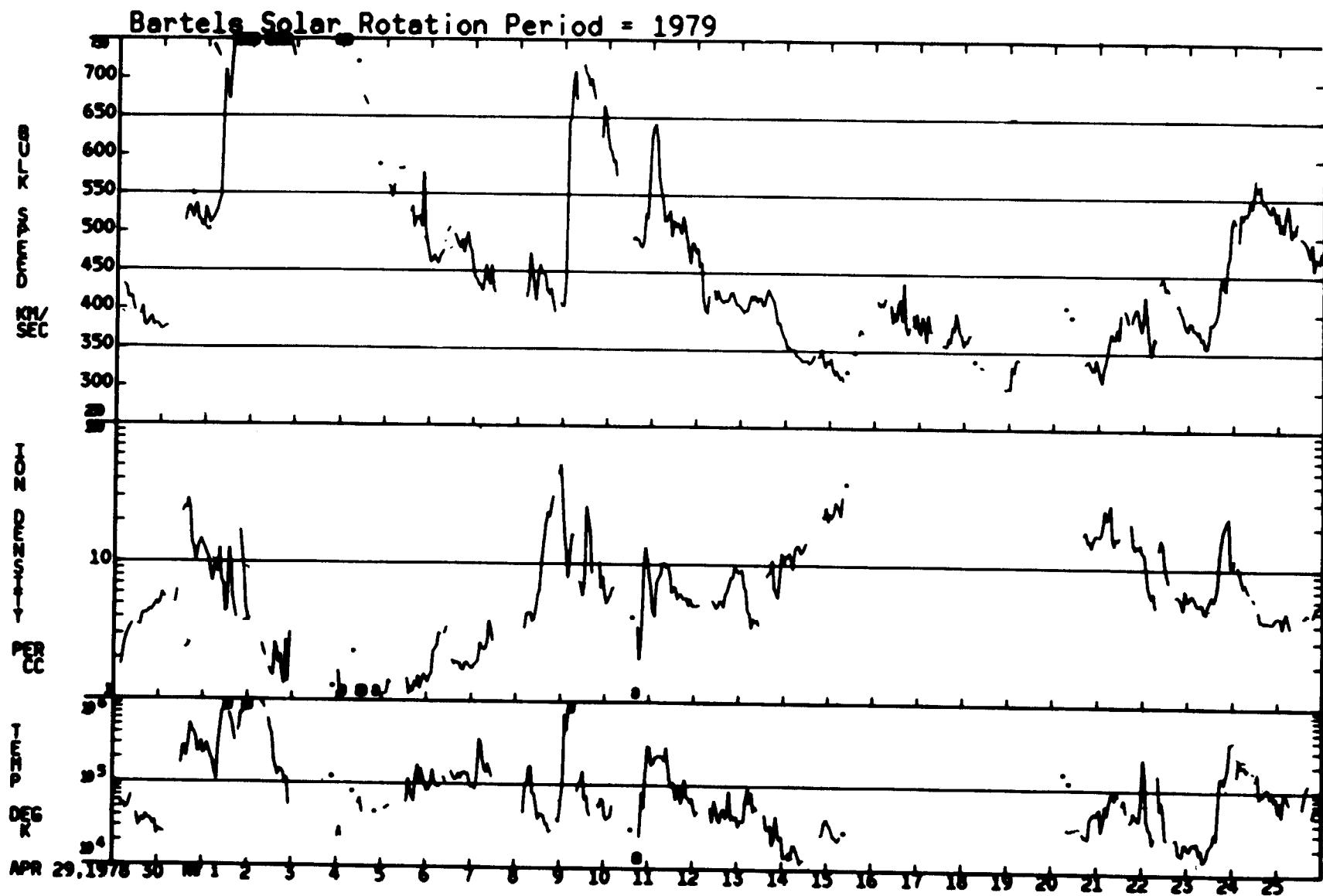


ORIGINAL PAGE IS  
OF POOR QUALITY

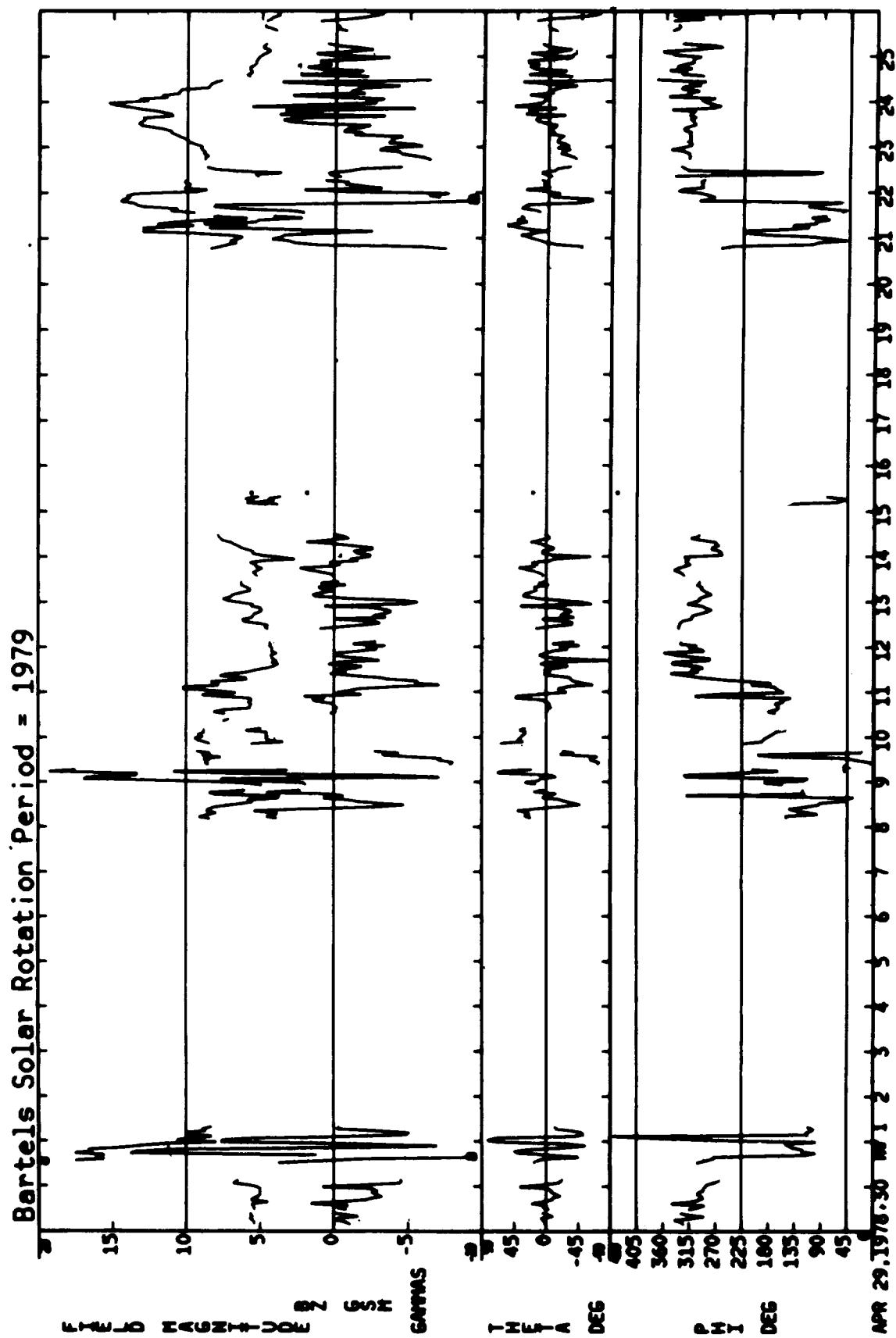
04/02/78 — 04/28/78



04/29/78 – 05/25/78

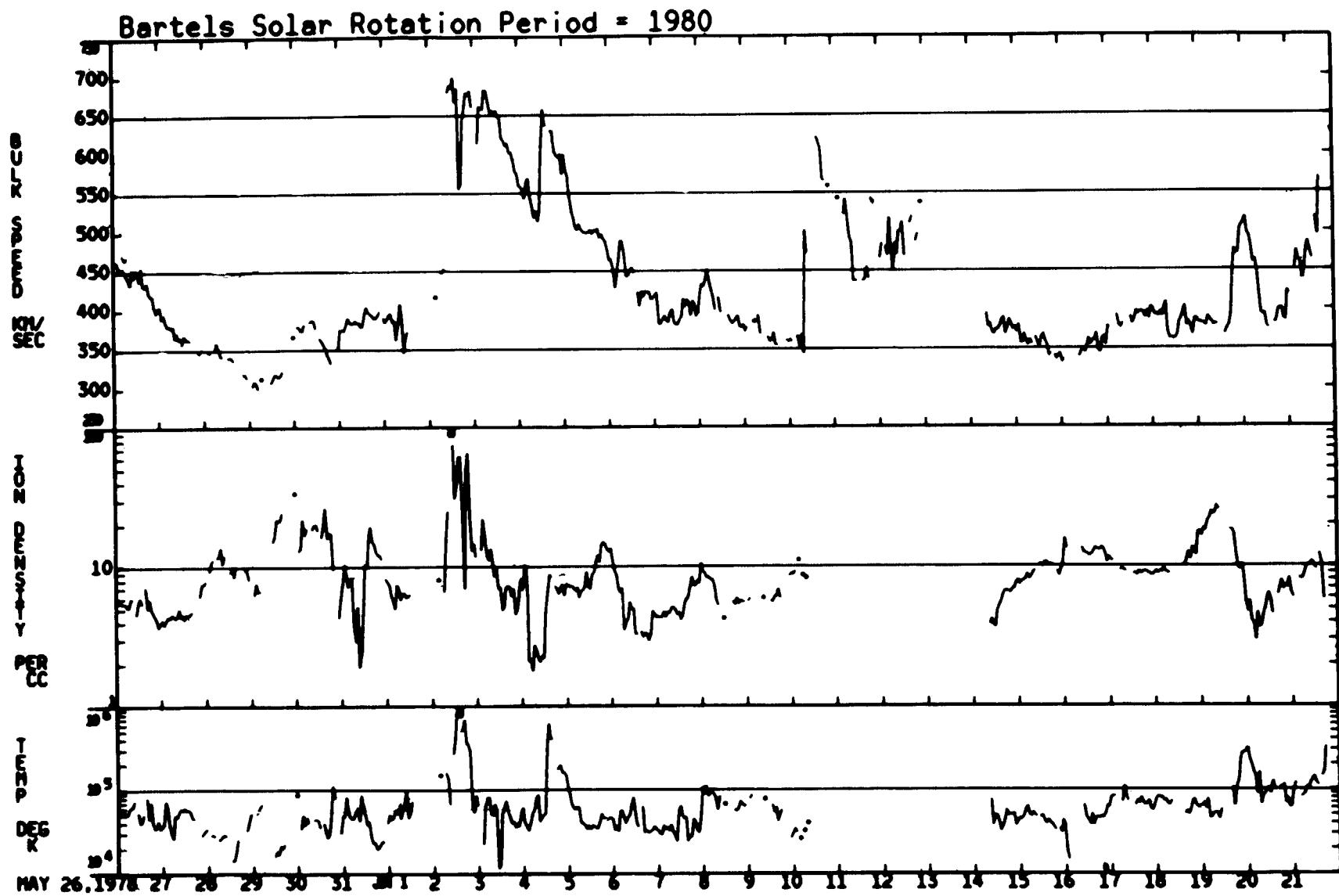


04/29/78 — 05/25/78



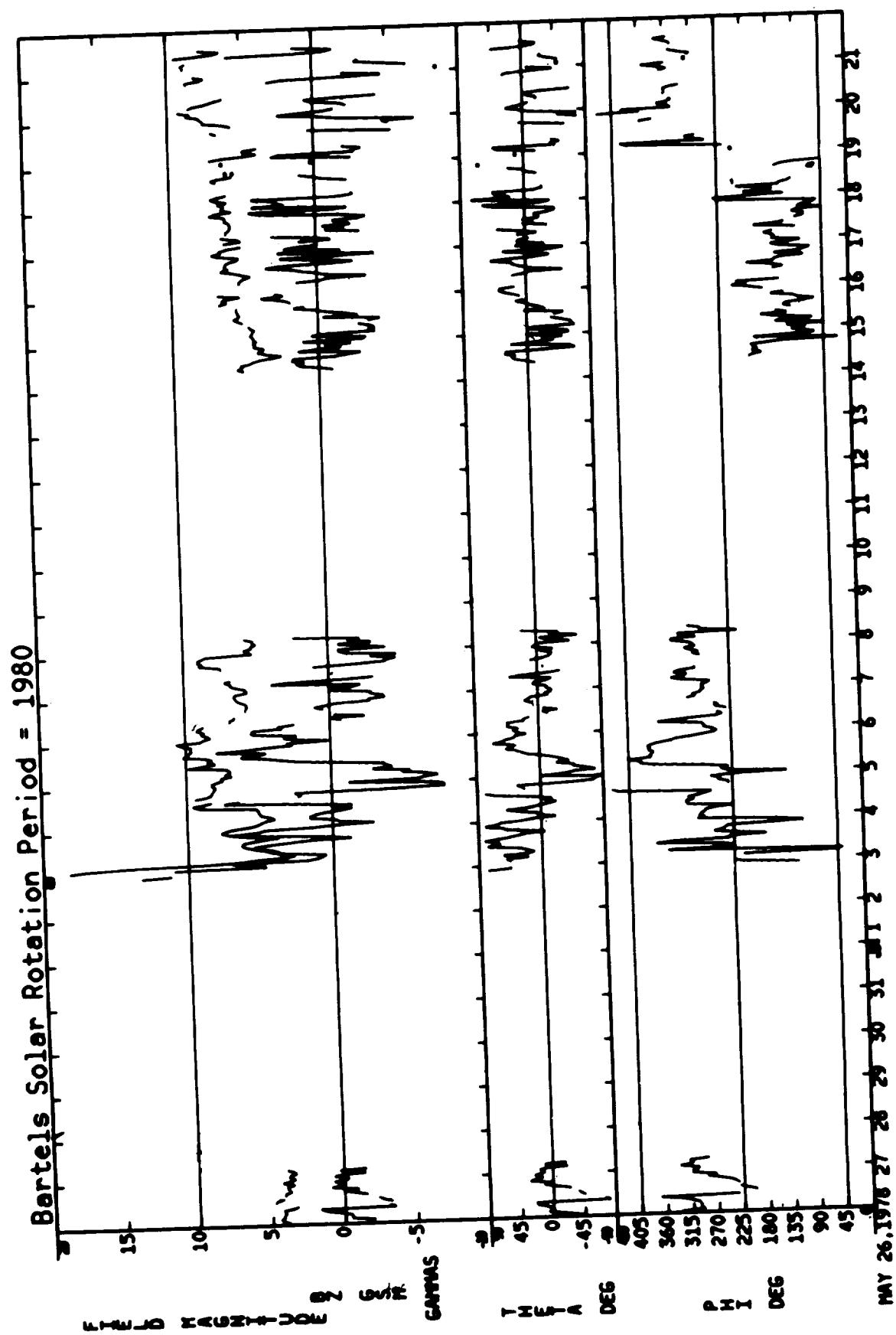
ORIGINAL PAGE IS  
OF POOR QUALITY

05/26/78 – 06/21/78

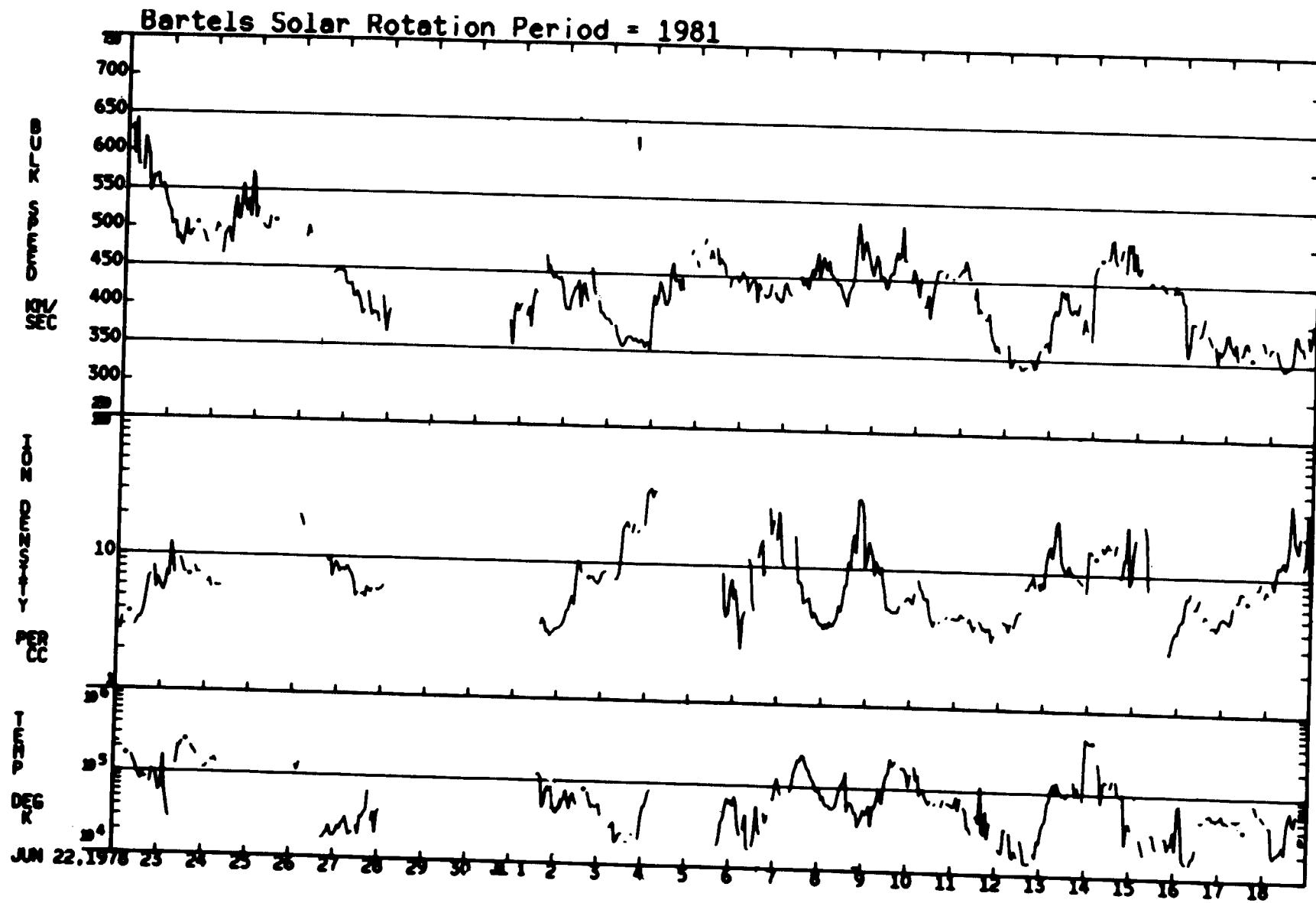


ORIGINAL PAGE IS  
OF POOR QUALITY

05/26/78 – 06/21/78



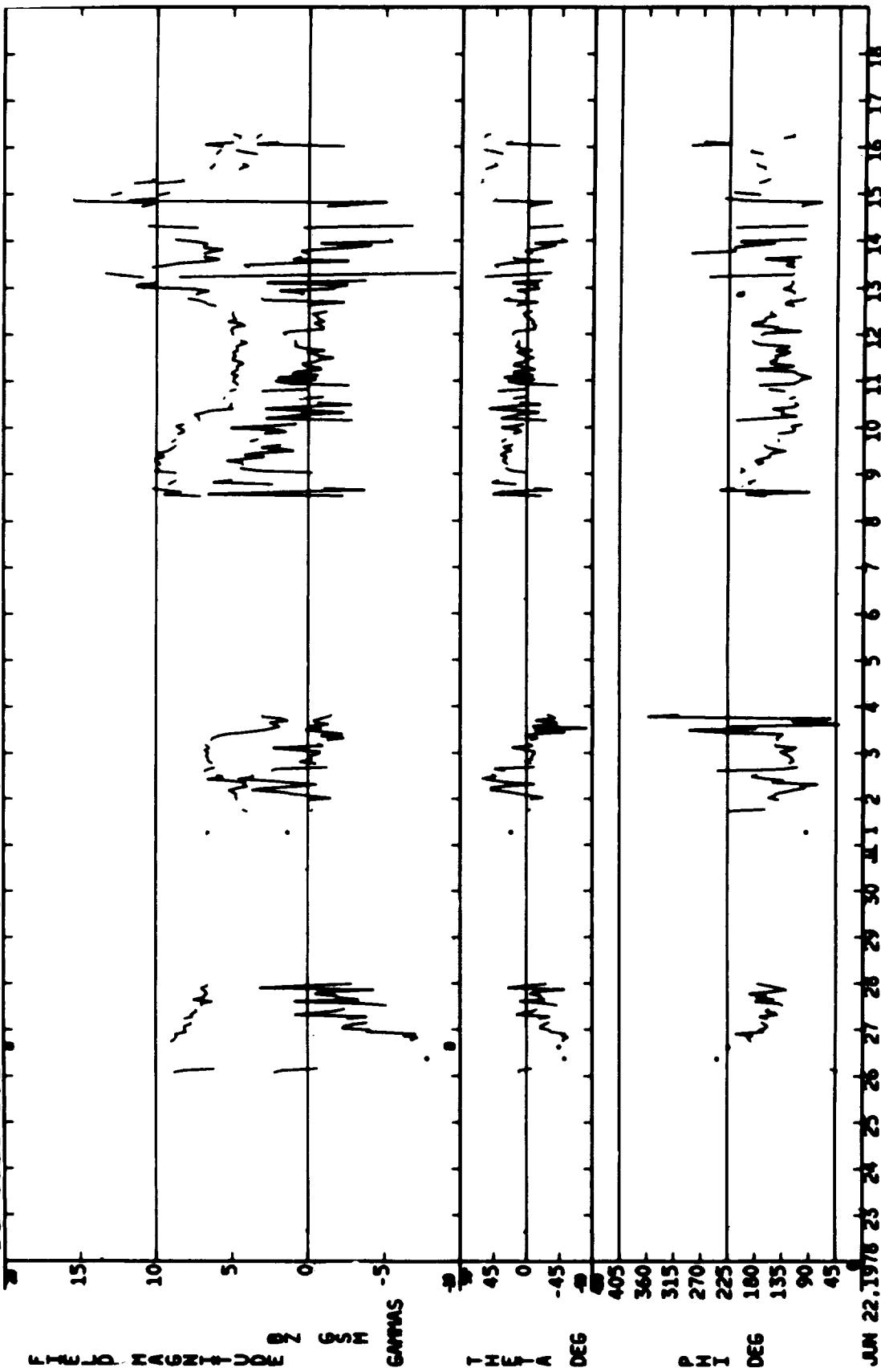
06/22/78 – 07/18/78



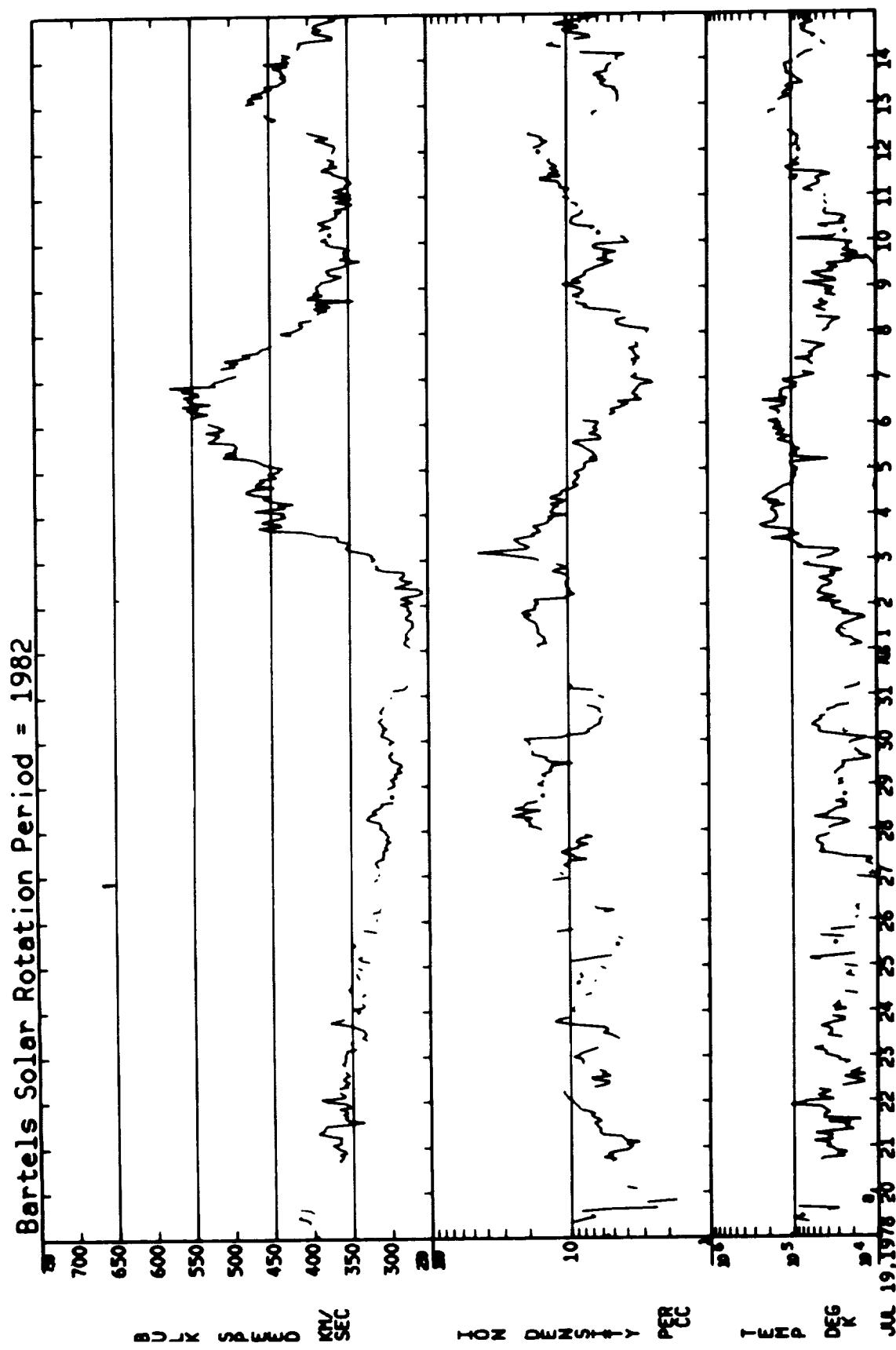
ORIGINAL PAGE IS  
OF POOR QUALITY

06/22/78 – 07/18/78

Bartels Solar Rotation Period = 1981

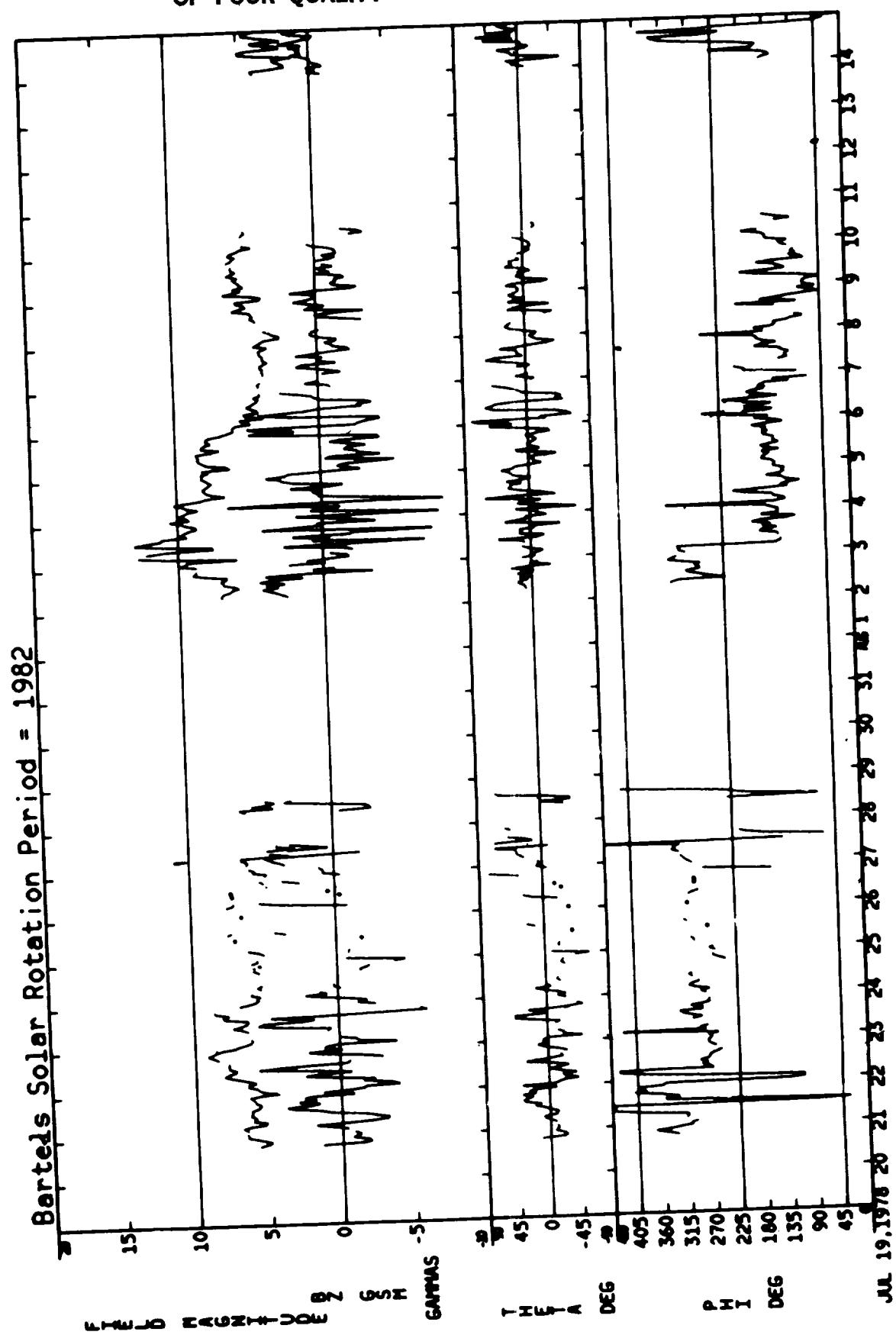


07/19/78 — 08/14/78

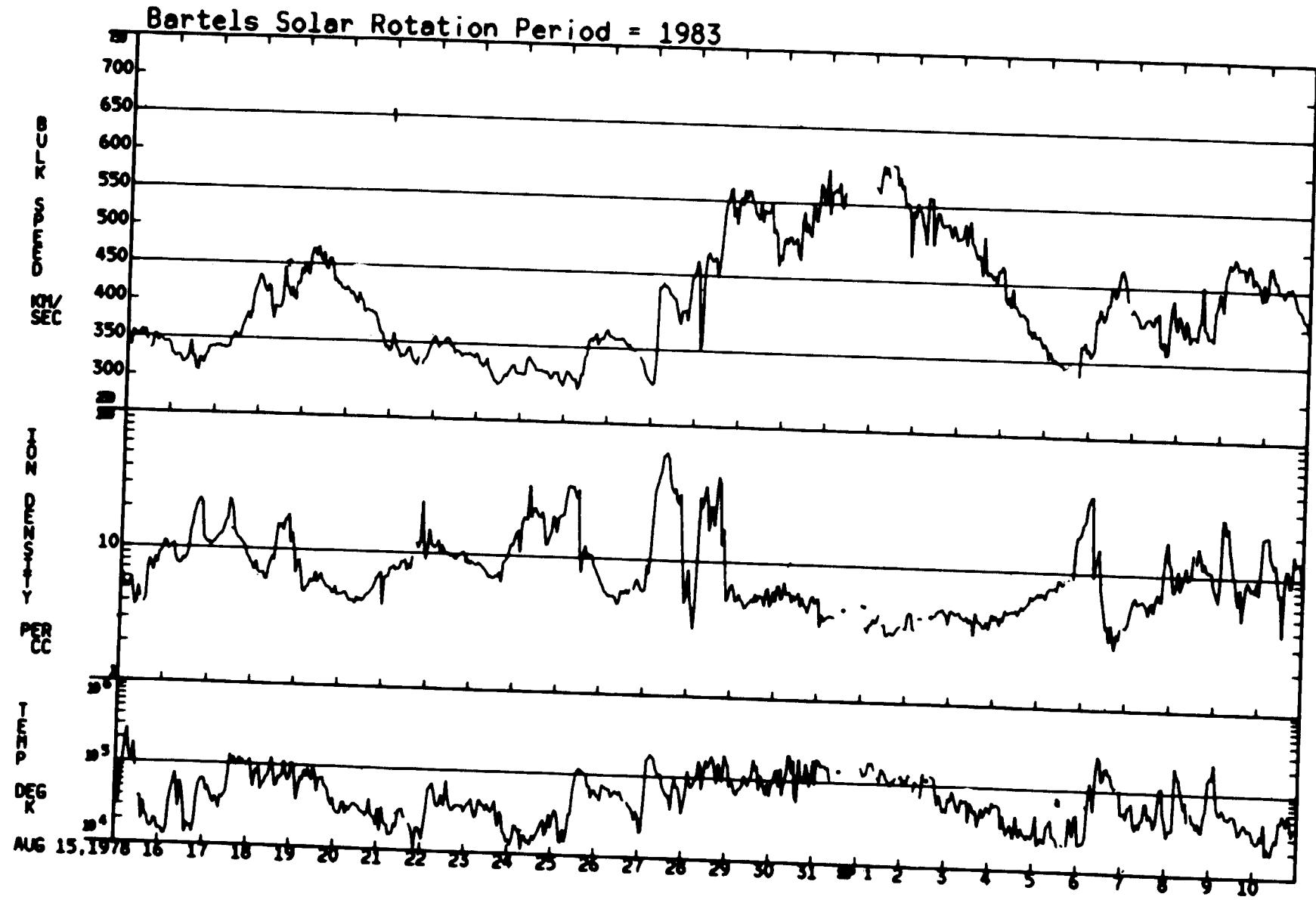


ORIGINAL PAGE IS  
OF POOR QUALITY

07/19/78 — 08/14/78

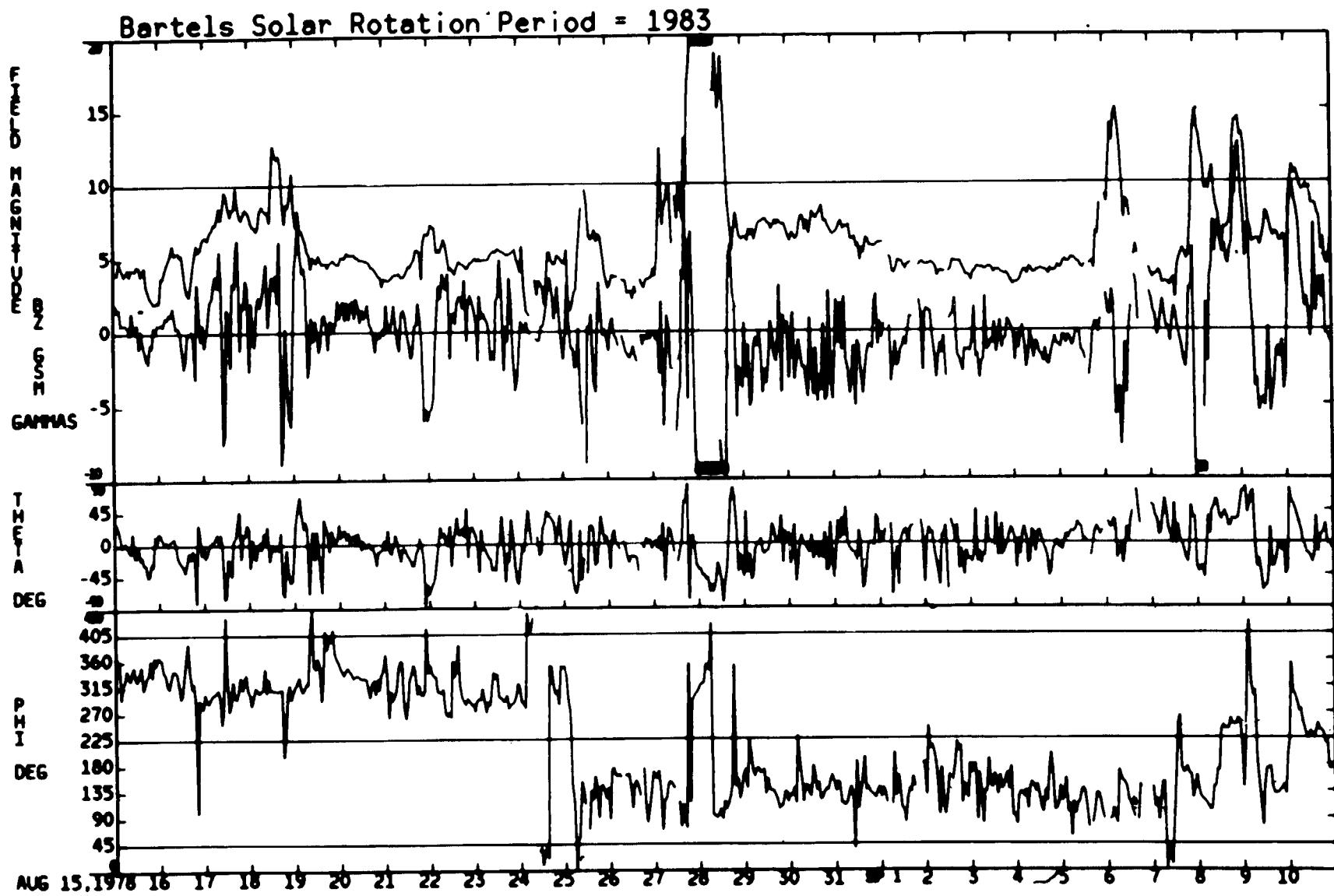


08/15/78 - 09/10/78

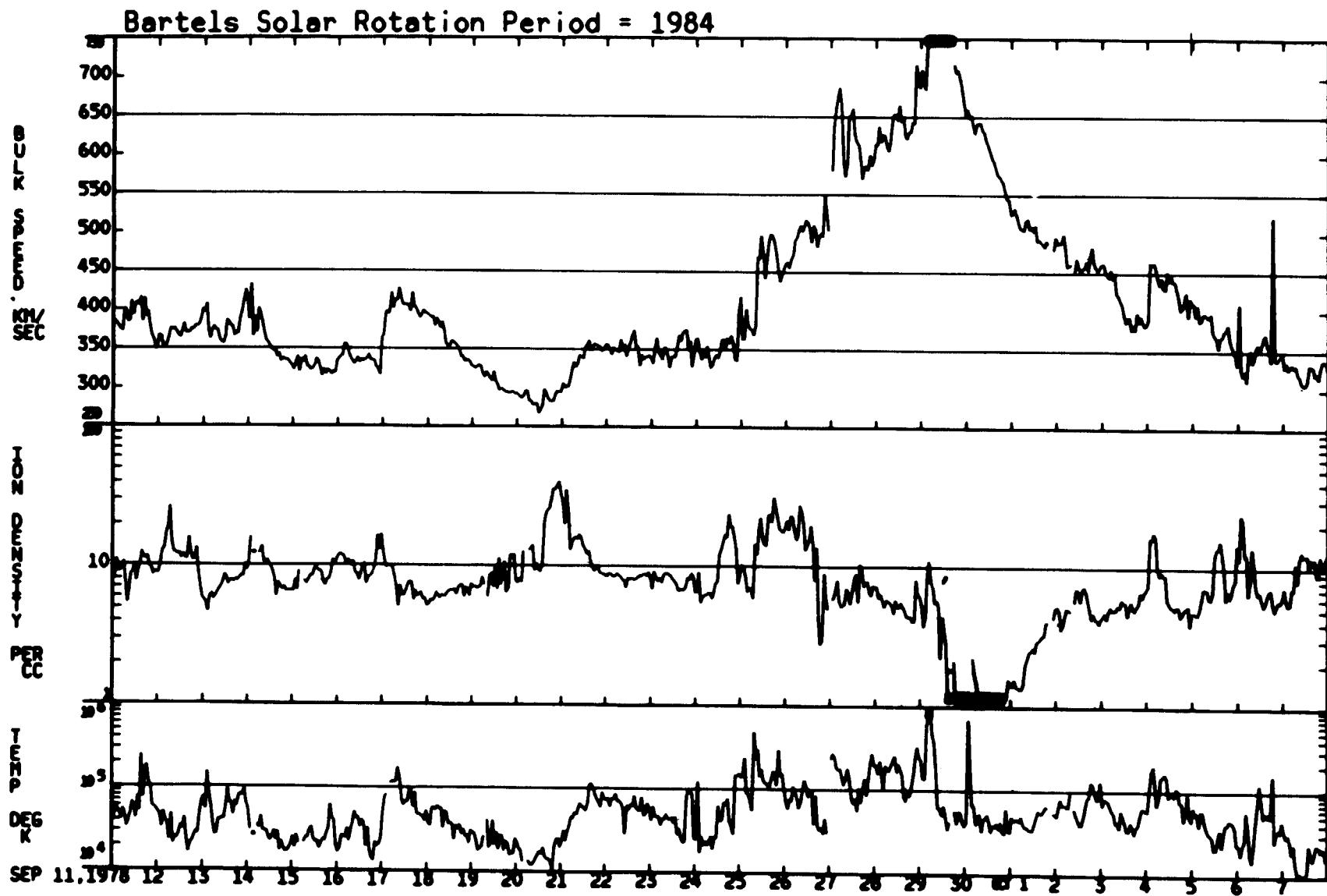


ORIGINAL PAGE IS  
OF POOR QUALITY

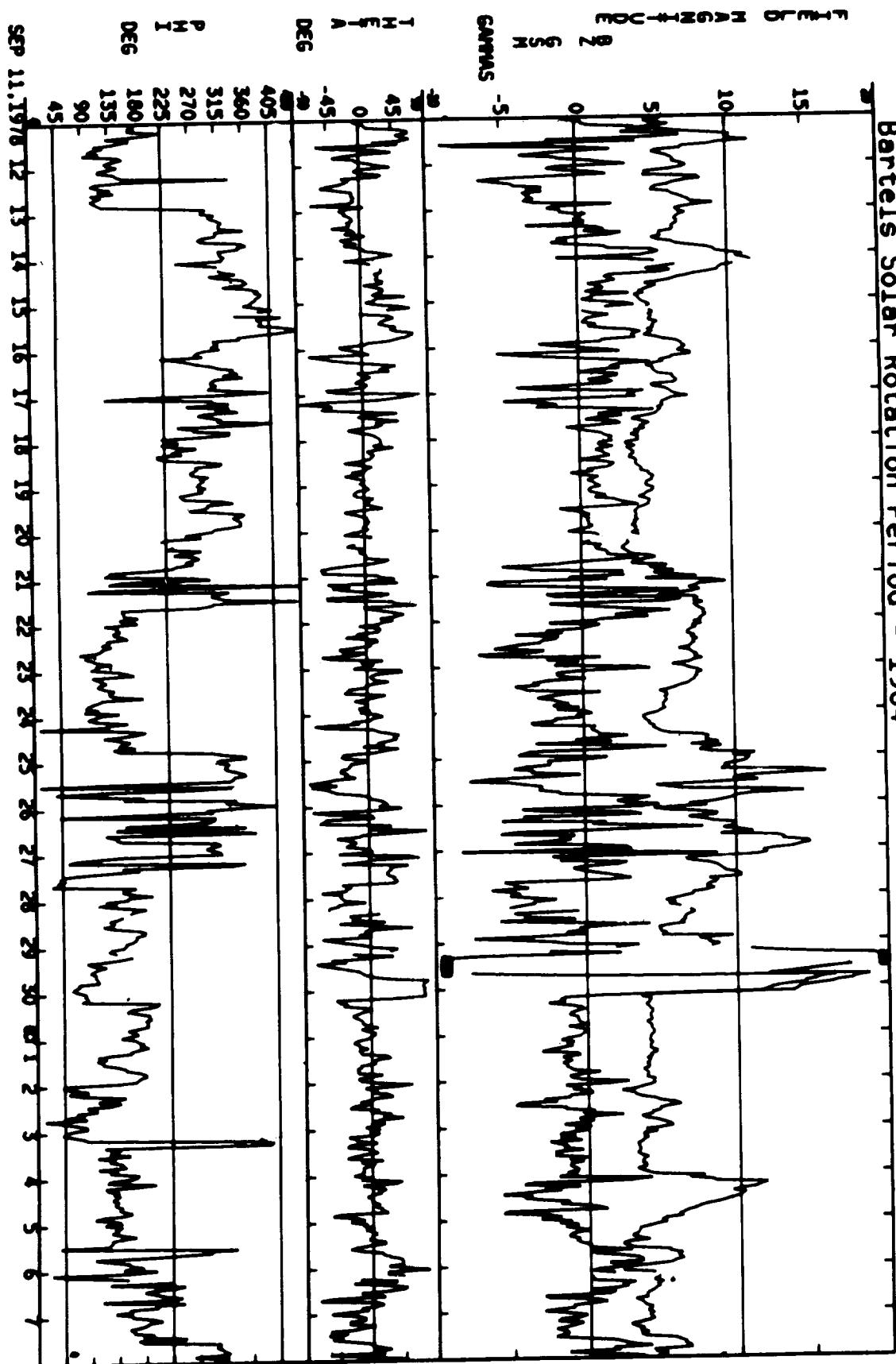
08/15/78 – 09/10/78



09/11/78 - 10/07/78



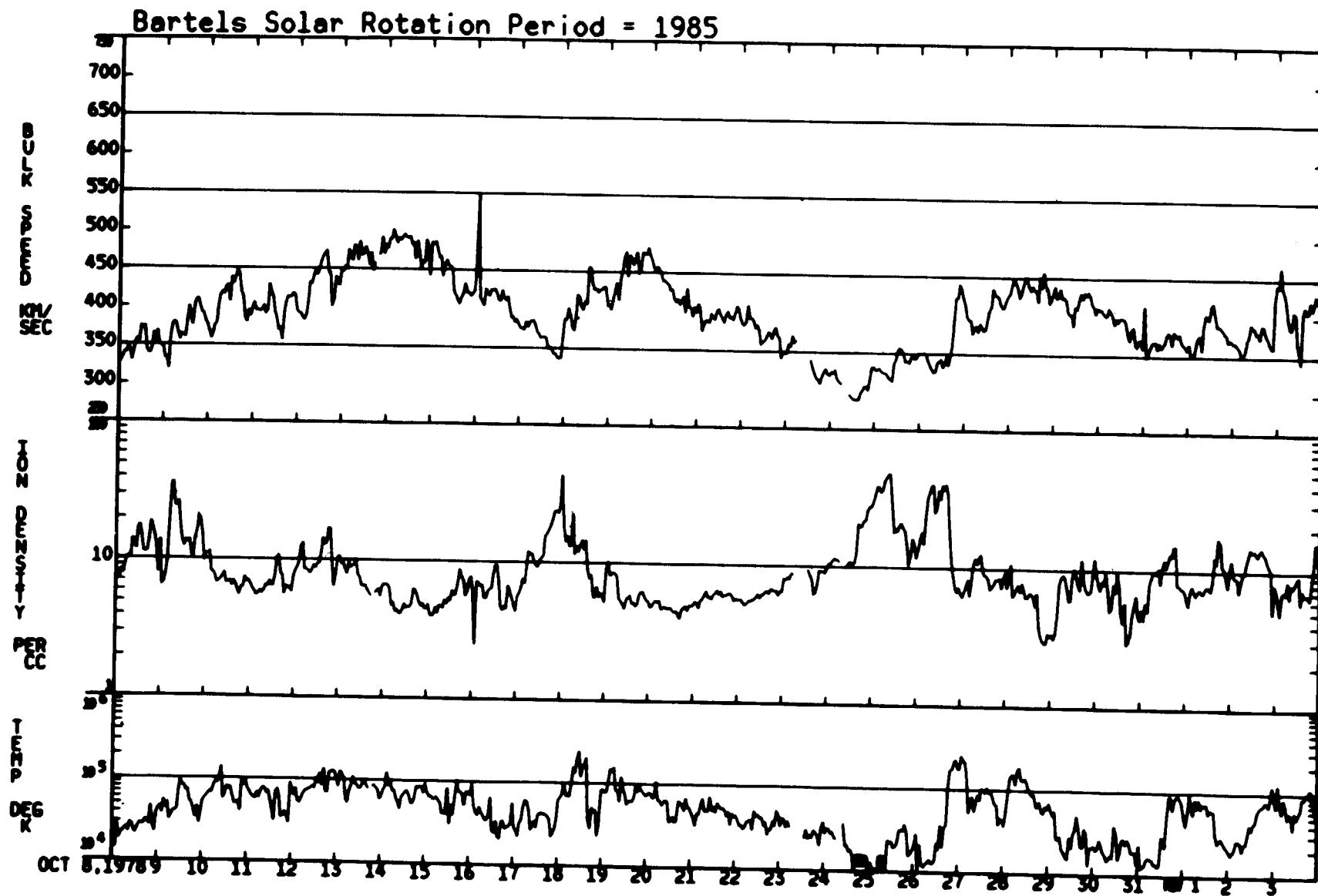
Bartels Solar Rotation Period = 1984



09/11/78 - 10/07/78

ORIGINAL PAGE IS  
OF POOR QUALITY

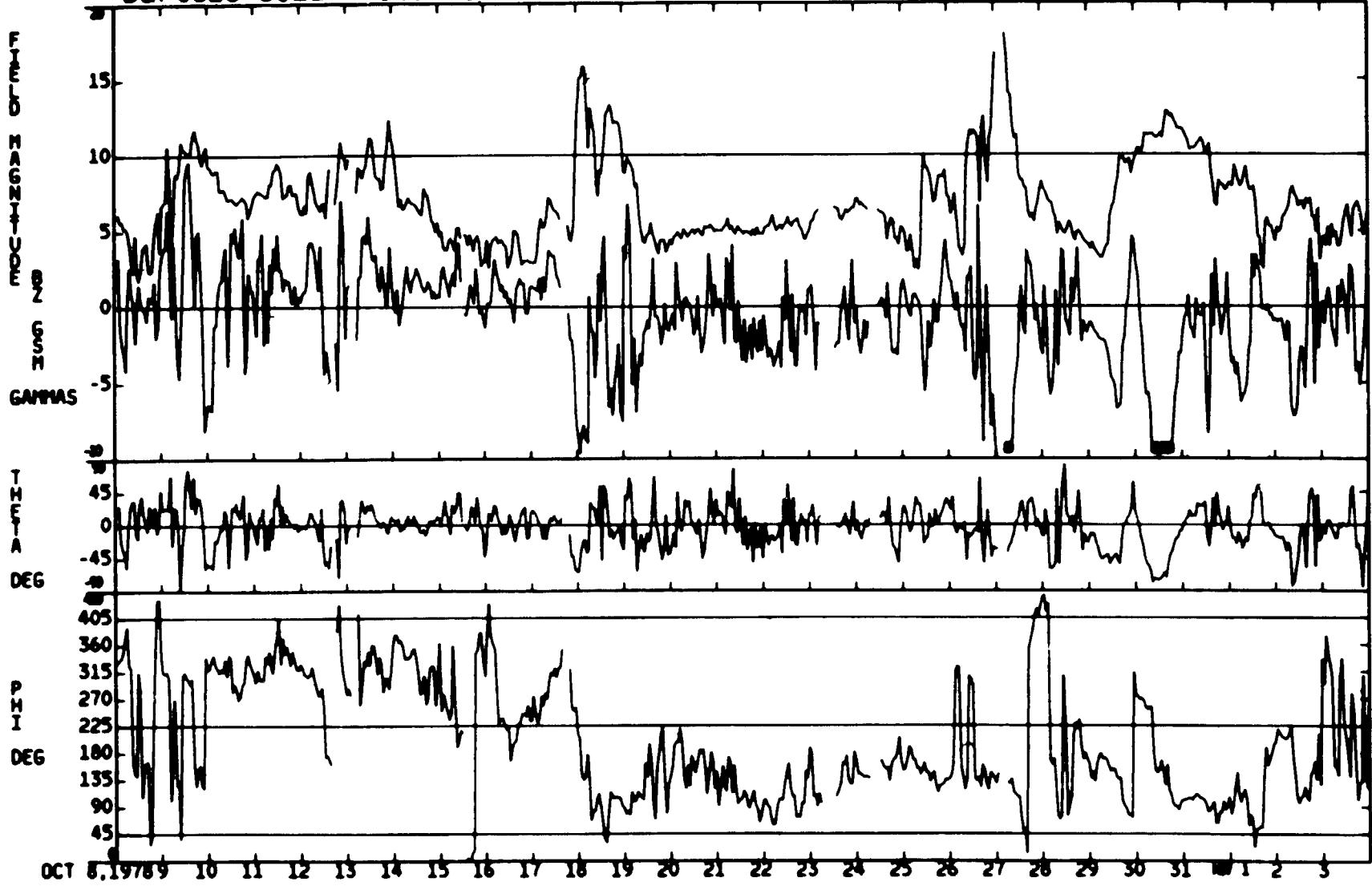
10/08/78 – 11/03/78



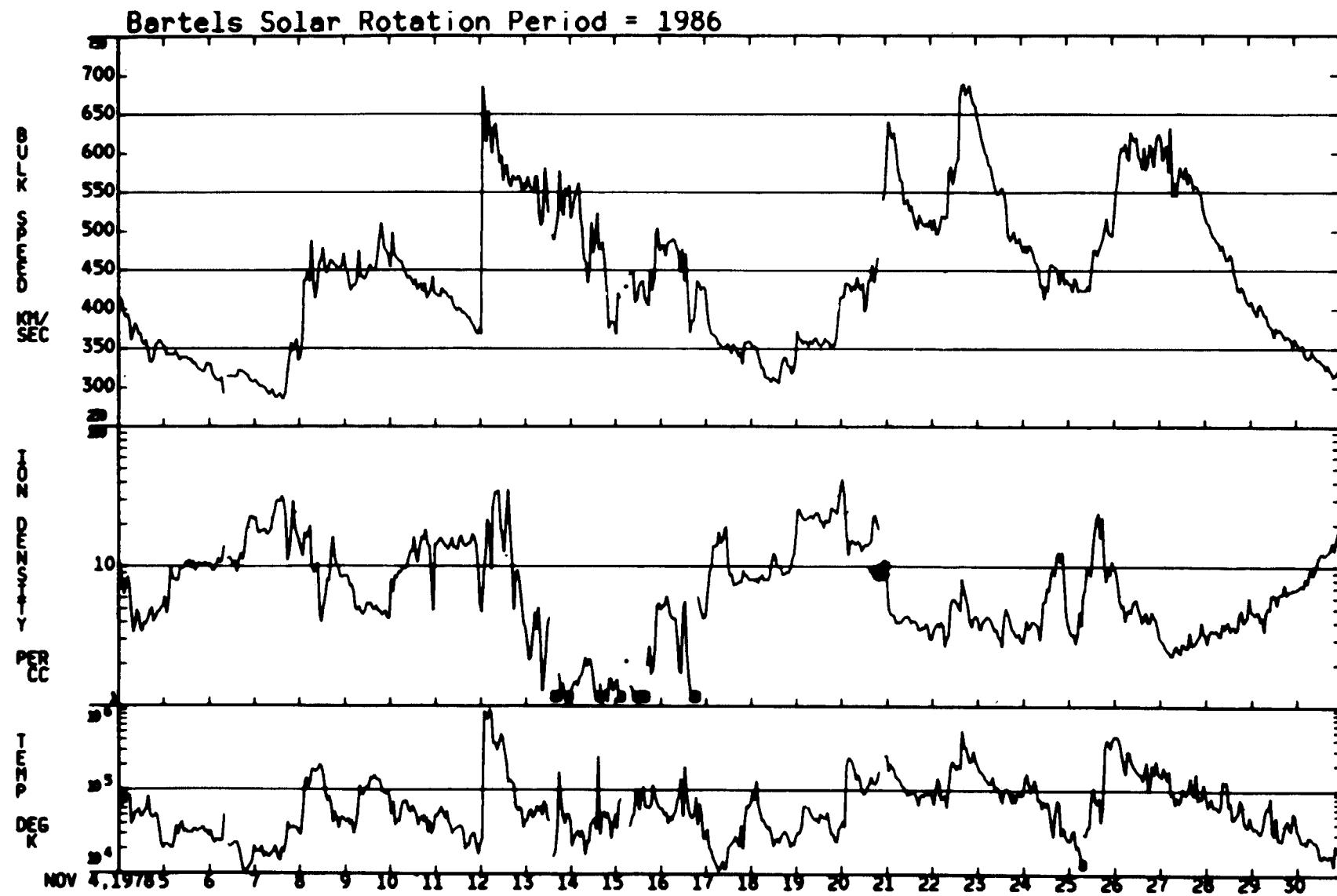
ORIGINAL PAGE IS  
OF POOR QUALITY

10/08/78 – 11/03/78

Bartels Solar Rotation Period = 1985

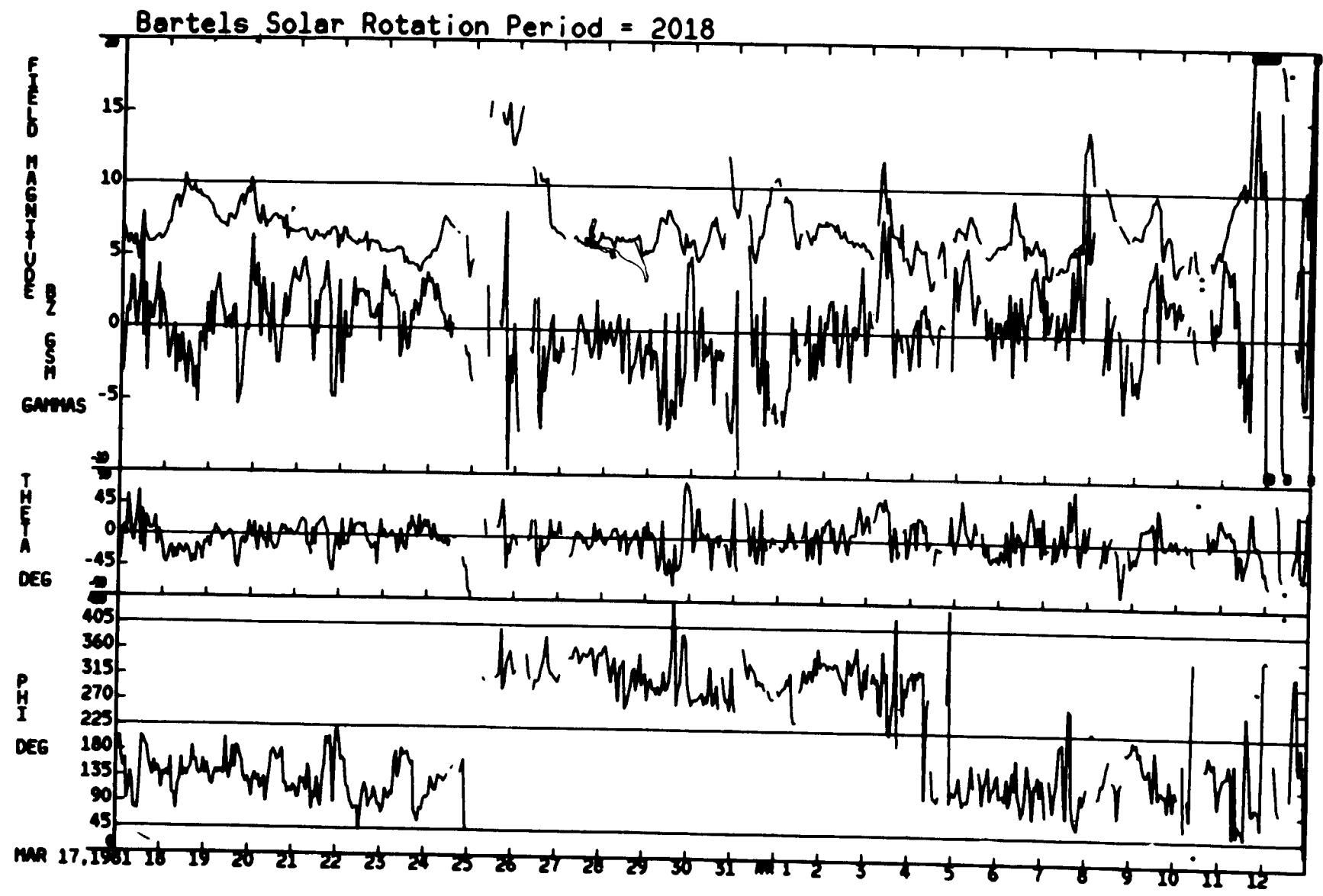


11/04/78 - 11/30/78

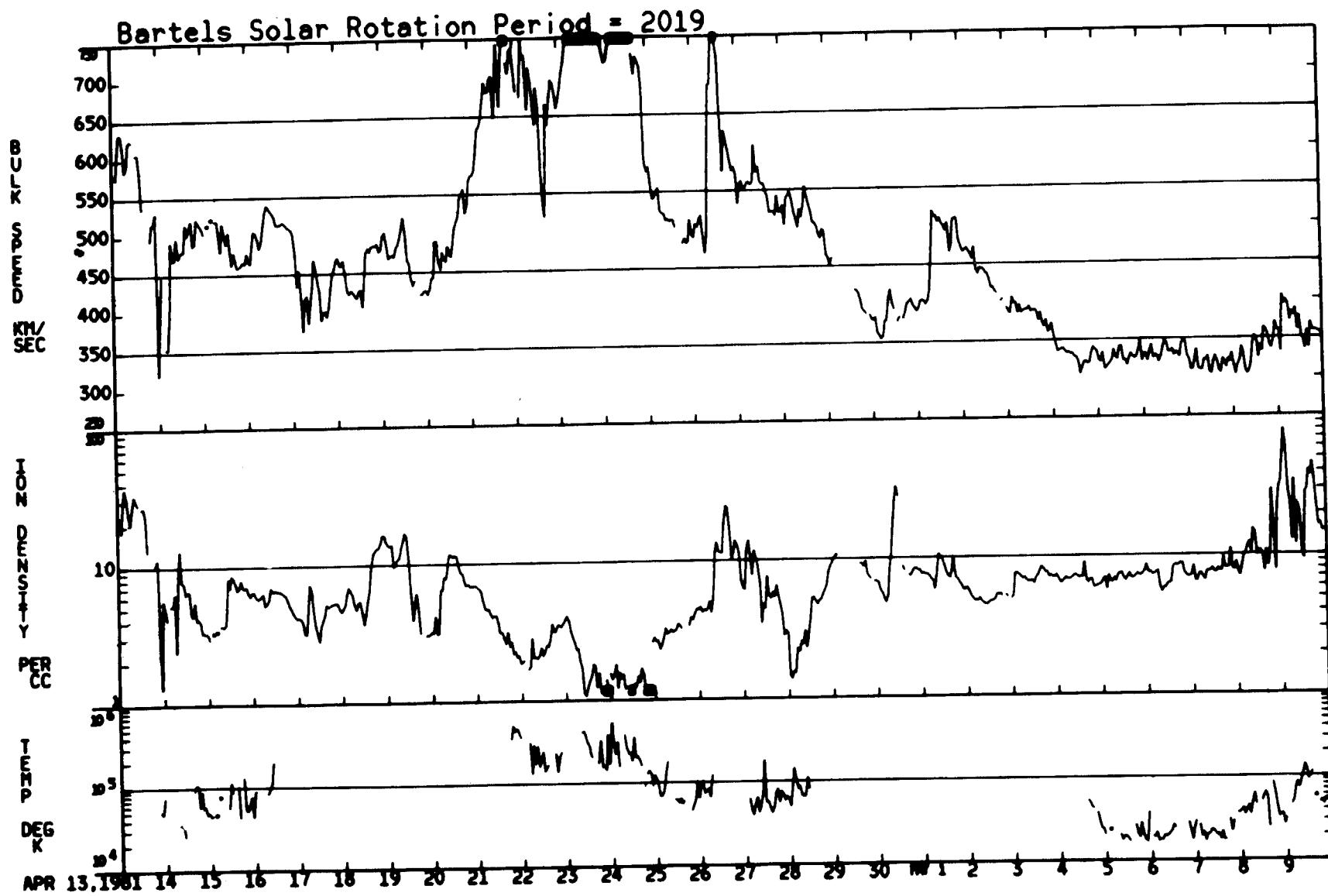


ORIGINAL PAGE IS  
OF POOR  
QUALITY

03/17/81 – 04/12/81



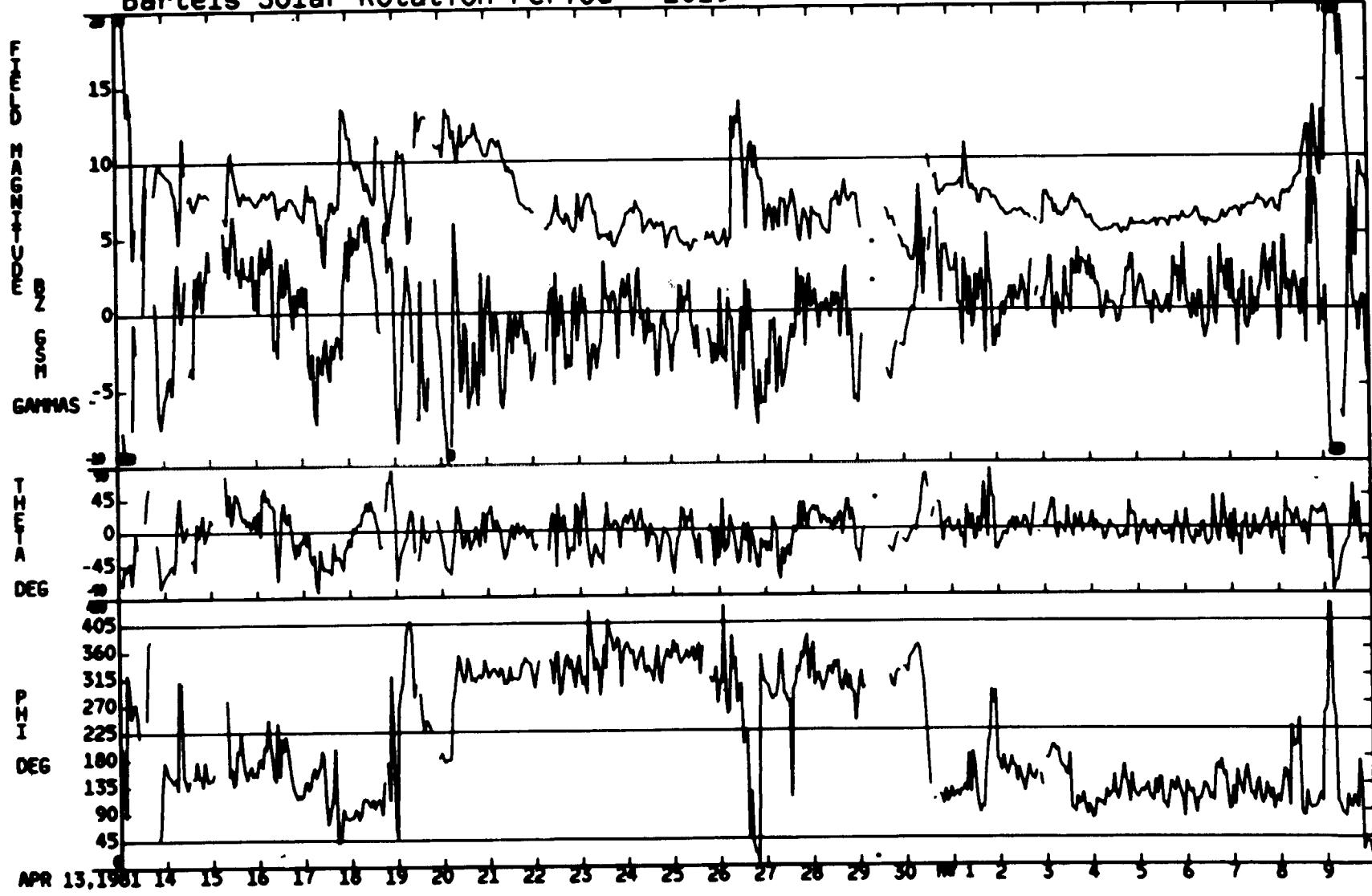
04/13/81 – 05/09/81



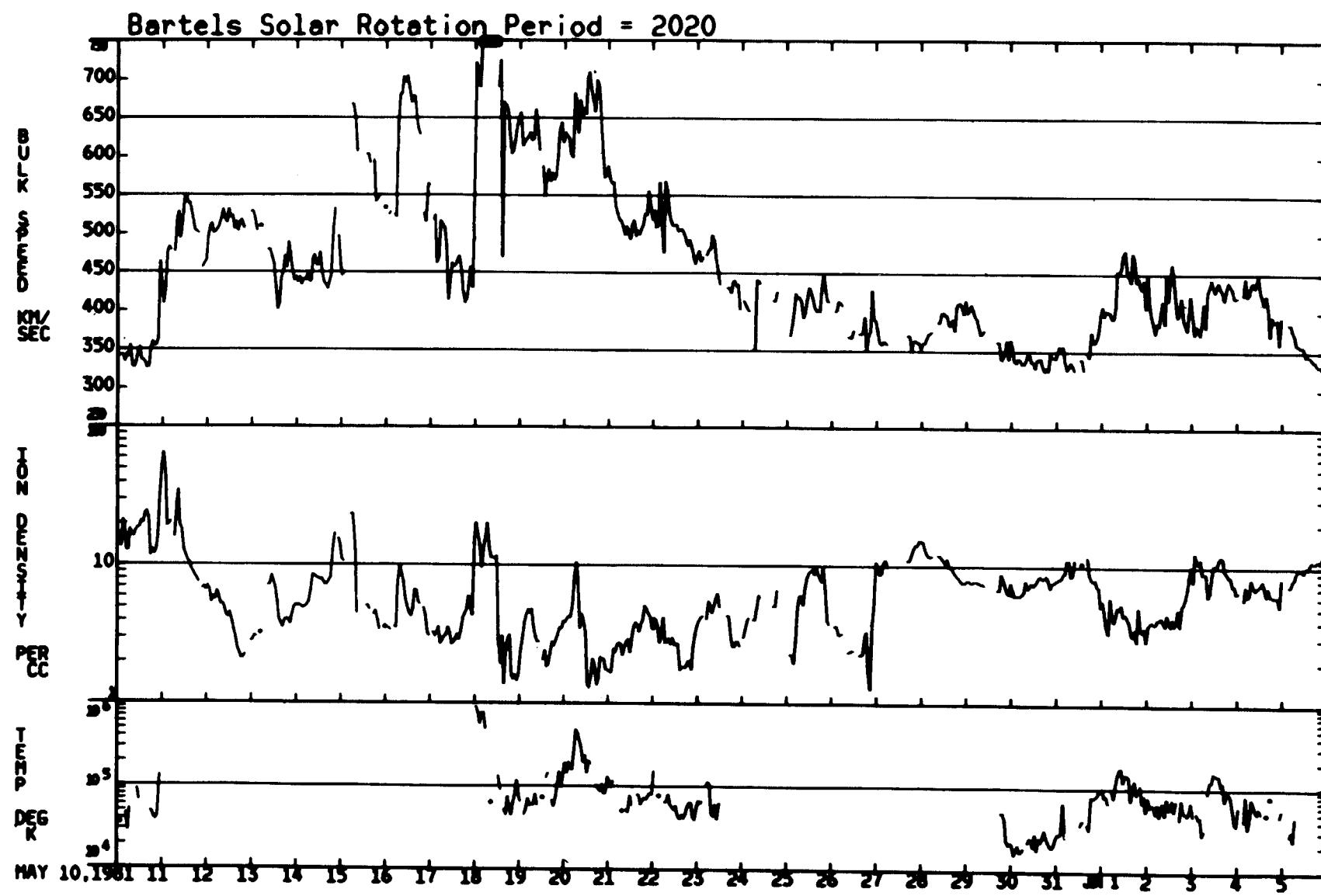
ORIGINAL PAGE IS  
OF POOR QUALITY

04/13/81 — 05/09/81

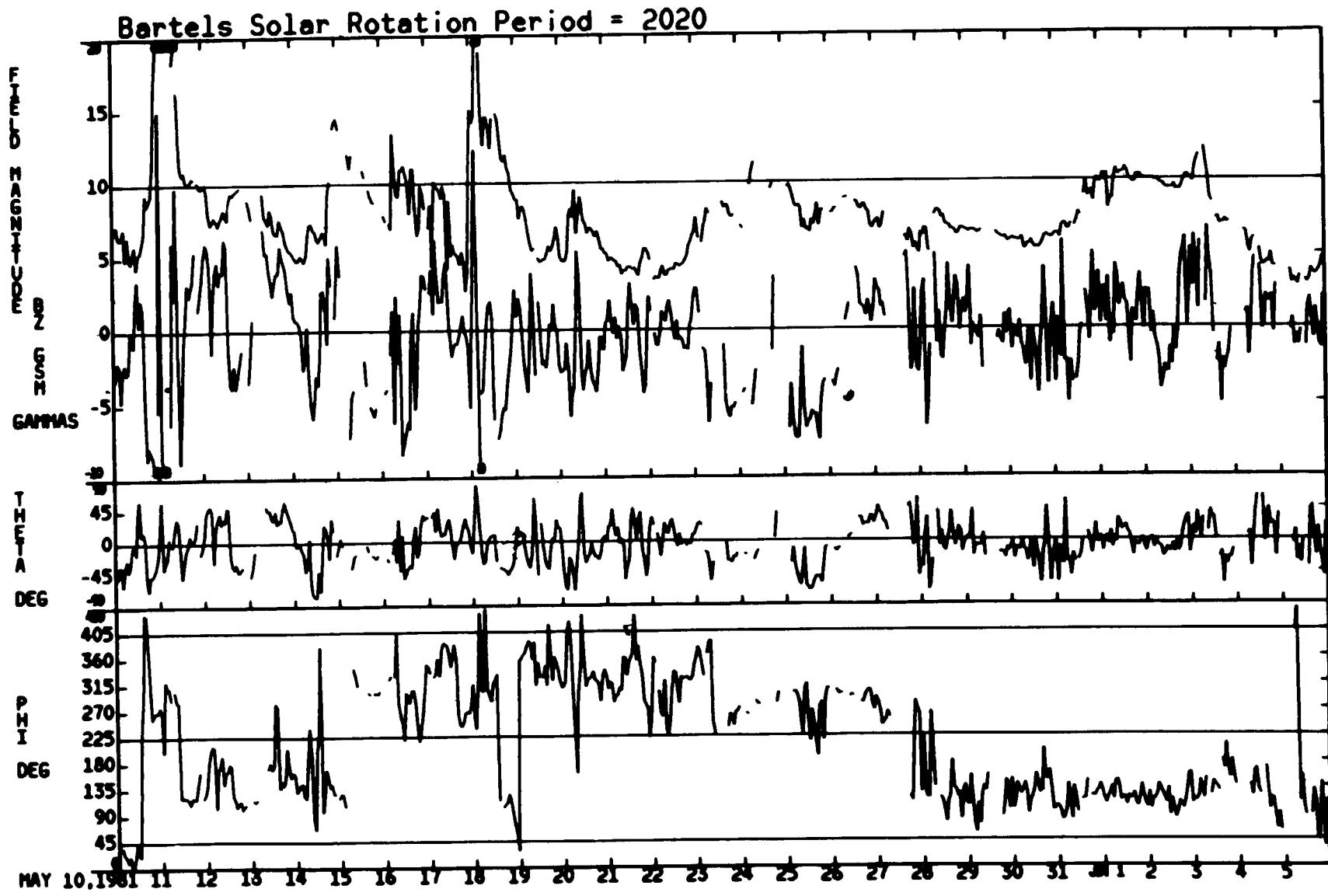
Bartels Solar Rotation Period = 2019



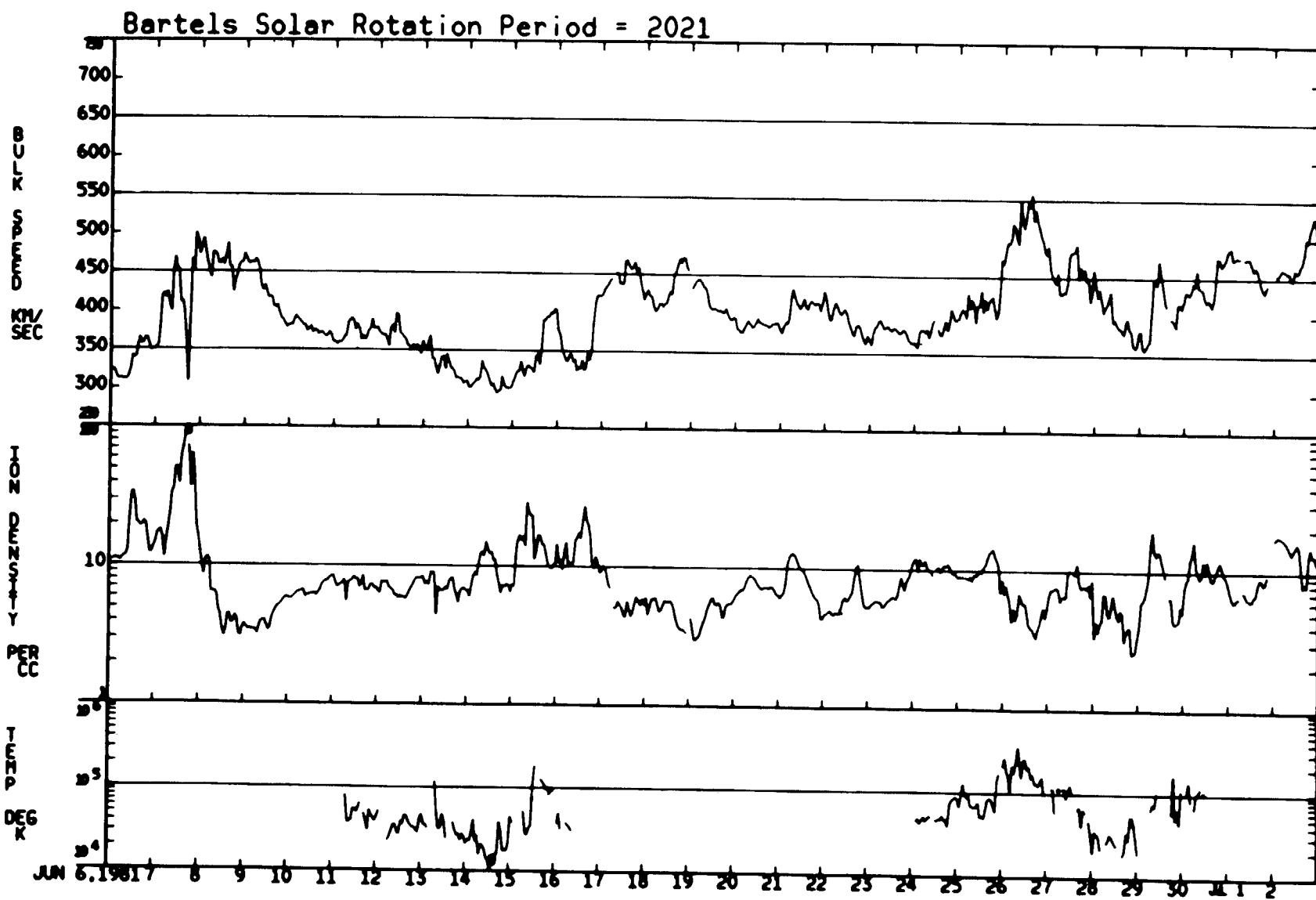
05/10/81 – 06/05/81



05/10/81 – 06/05/81  
ORIGINAL PAGE IS  
OF POOR QUALITY



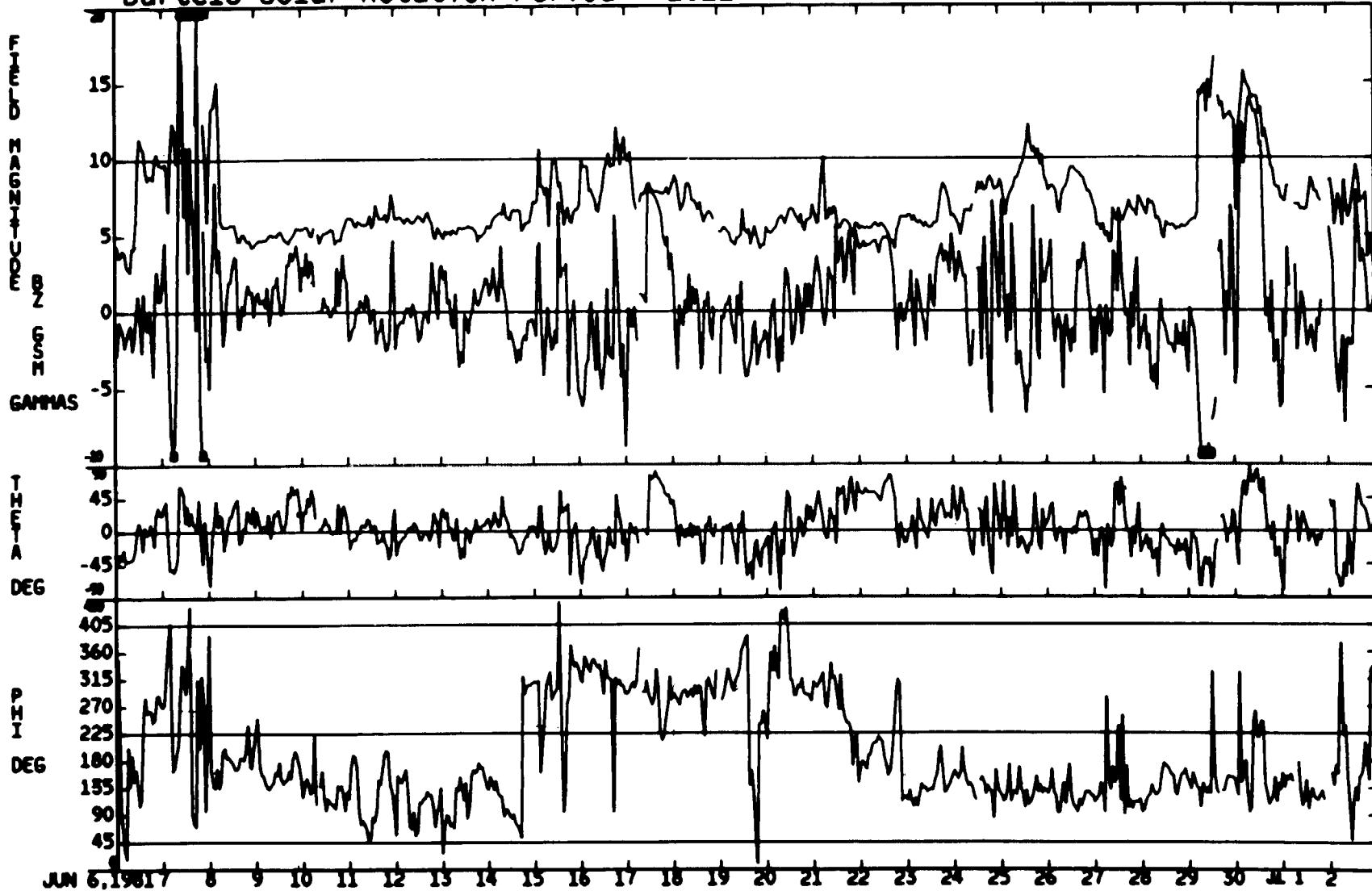
06/06/81 — 07/02/81



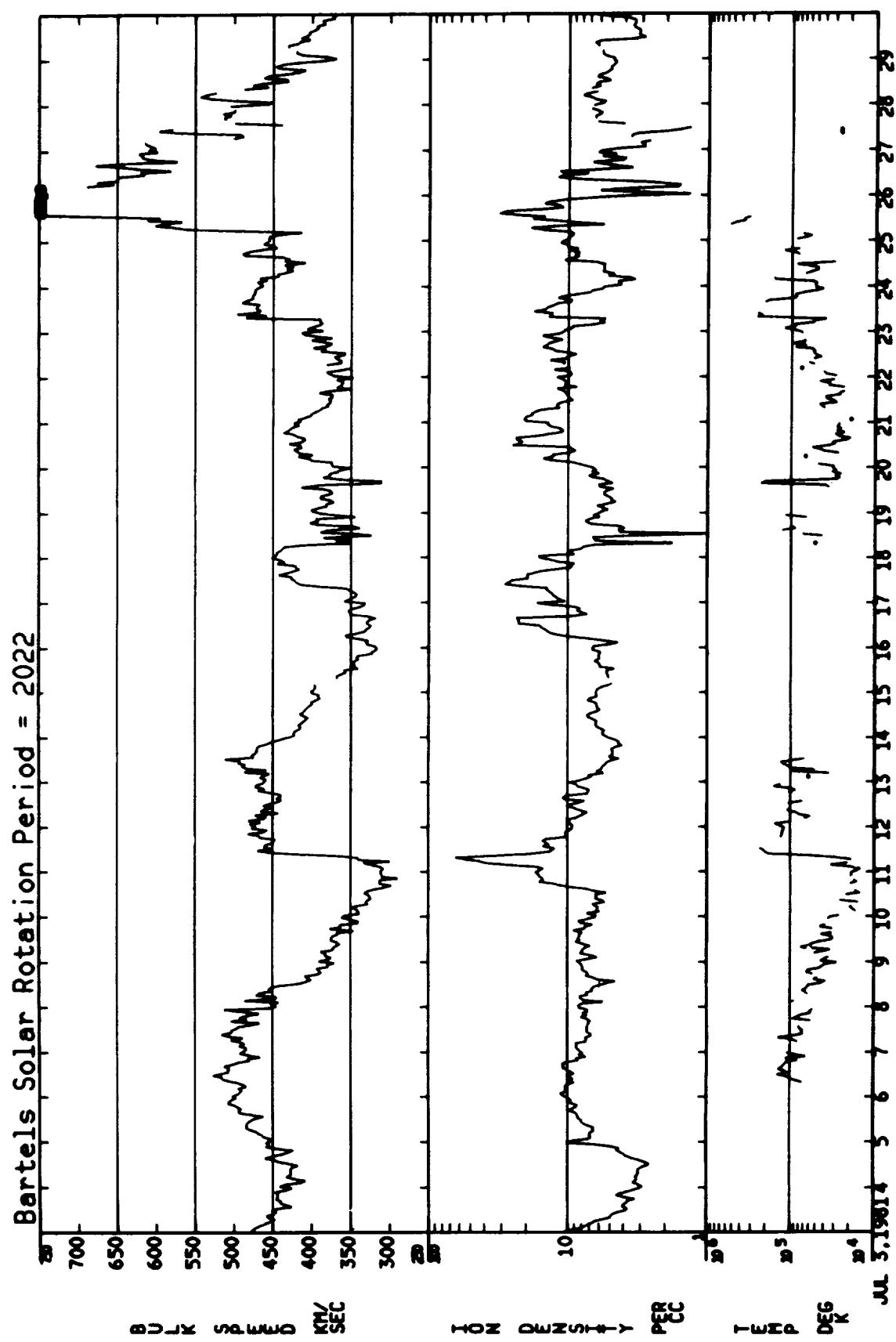
ORIGINAL PAGE IS  
OF POOR QUALITY

06/06/81 — 07/02/81

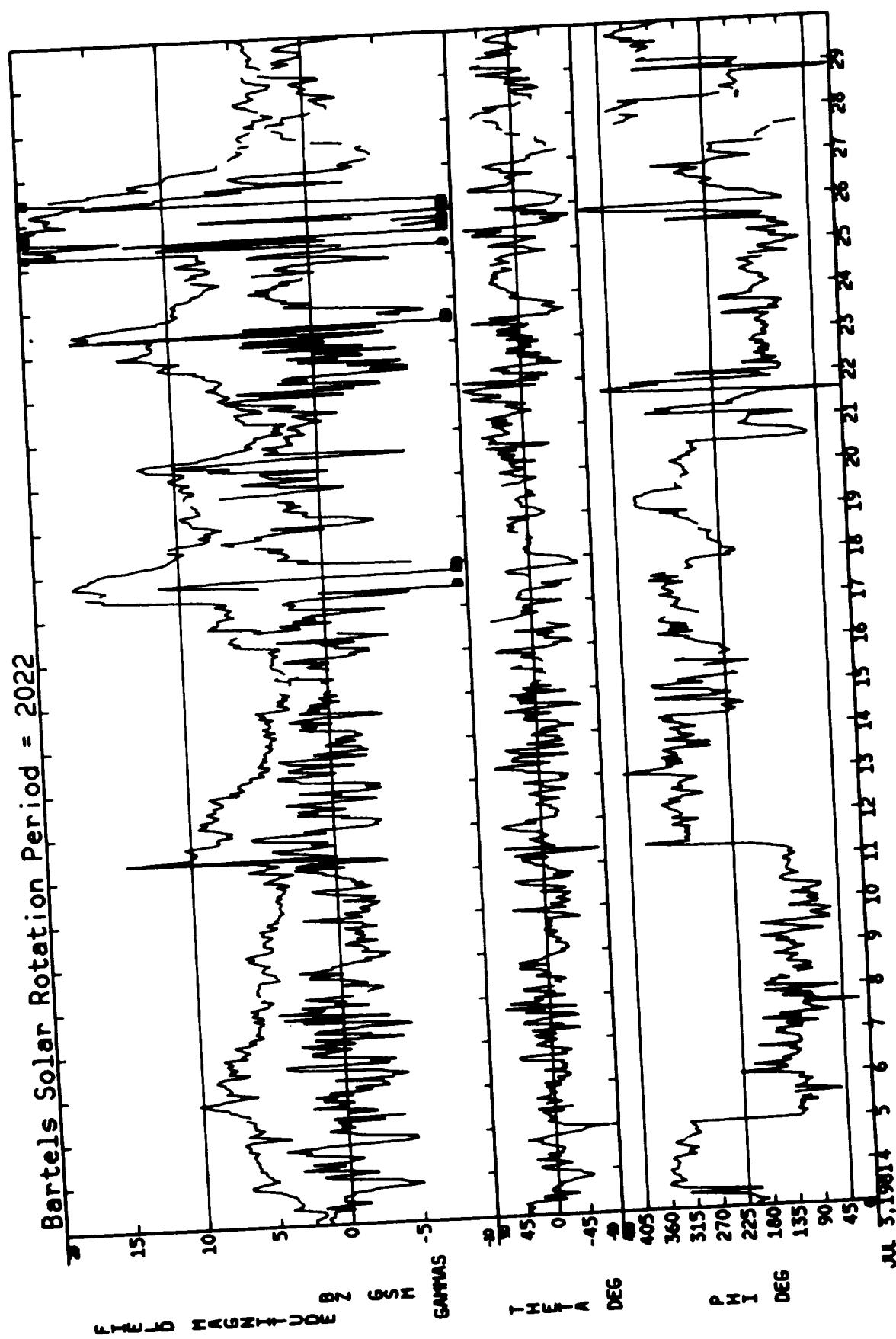
Bartels Solar Rotation Period = 2021



07/03/81 – 07/29/81

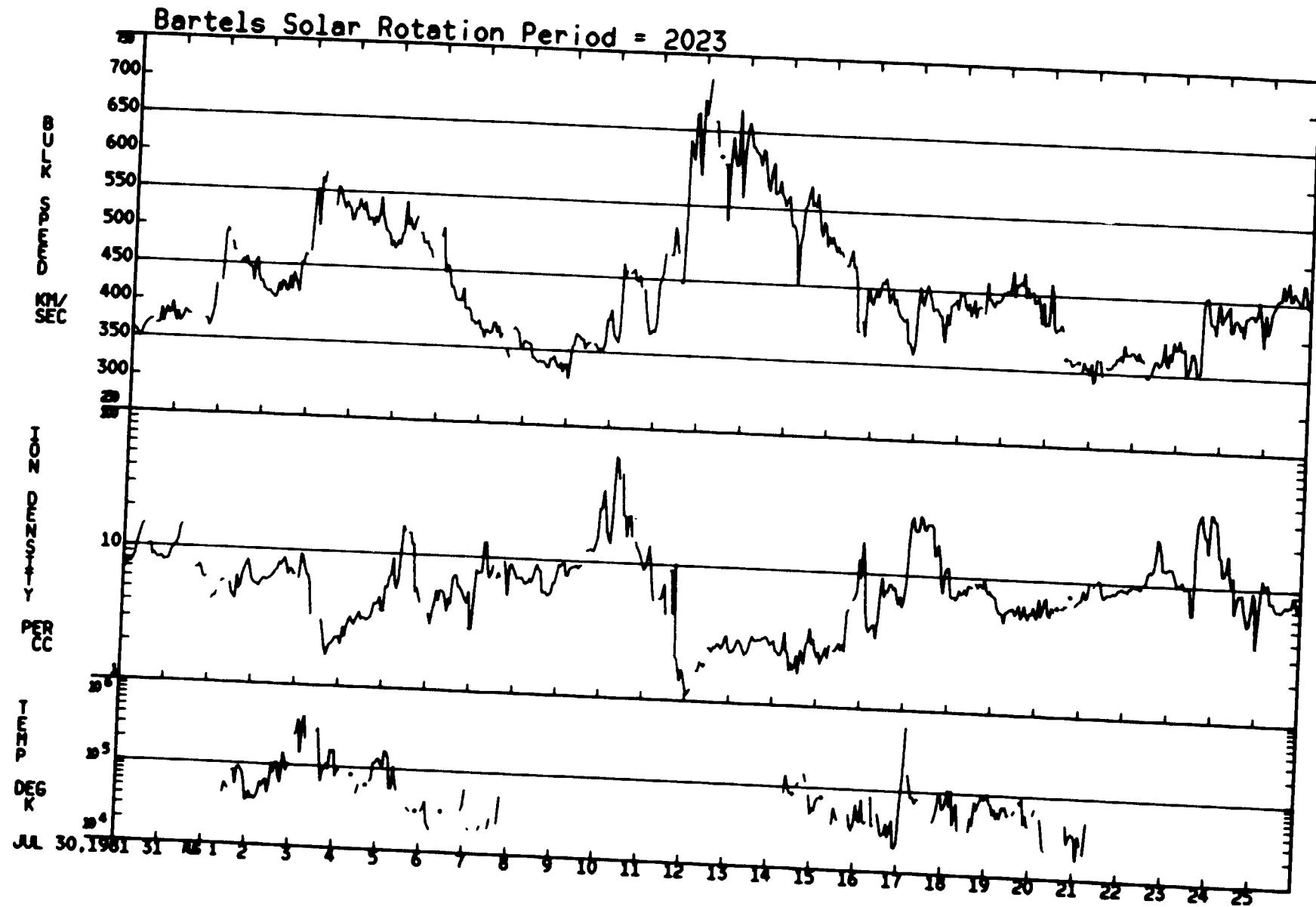


07/03/81 - 07/29/81



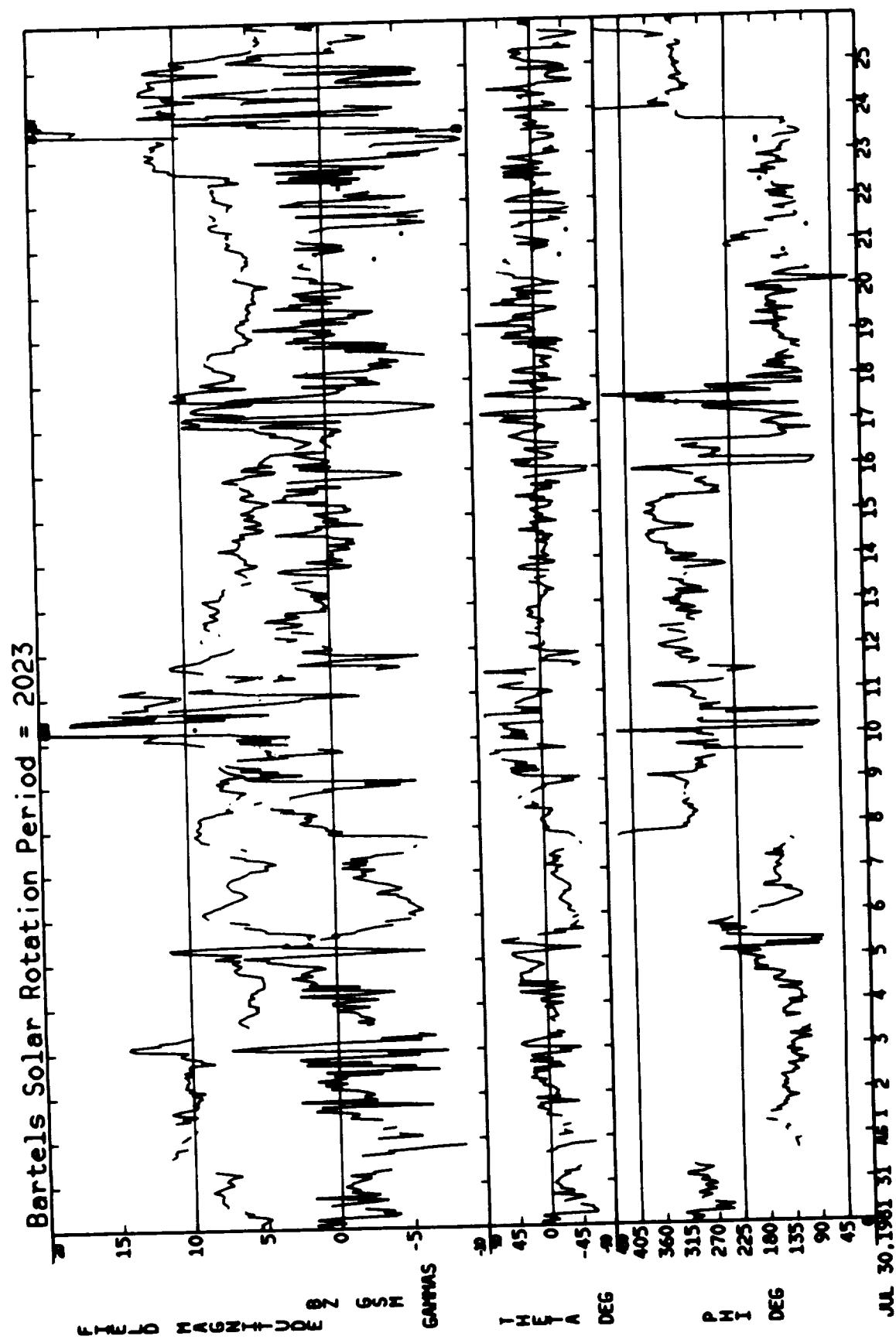
ORIGINAL PAGE IS  
OF POOR QUALITY

07/30/81 – 08/25/81

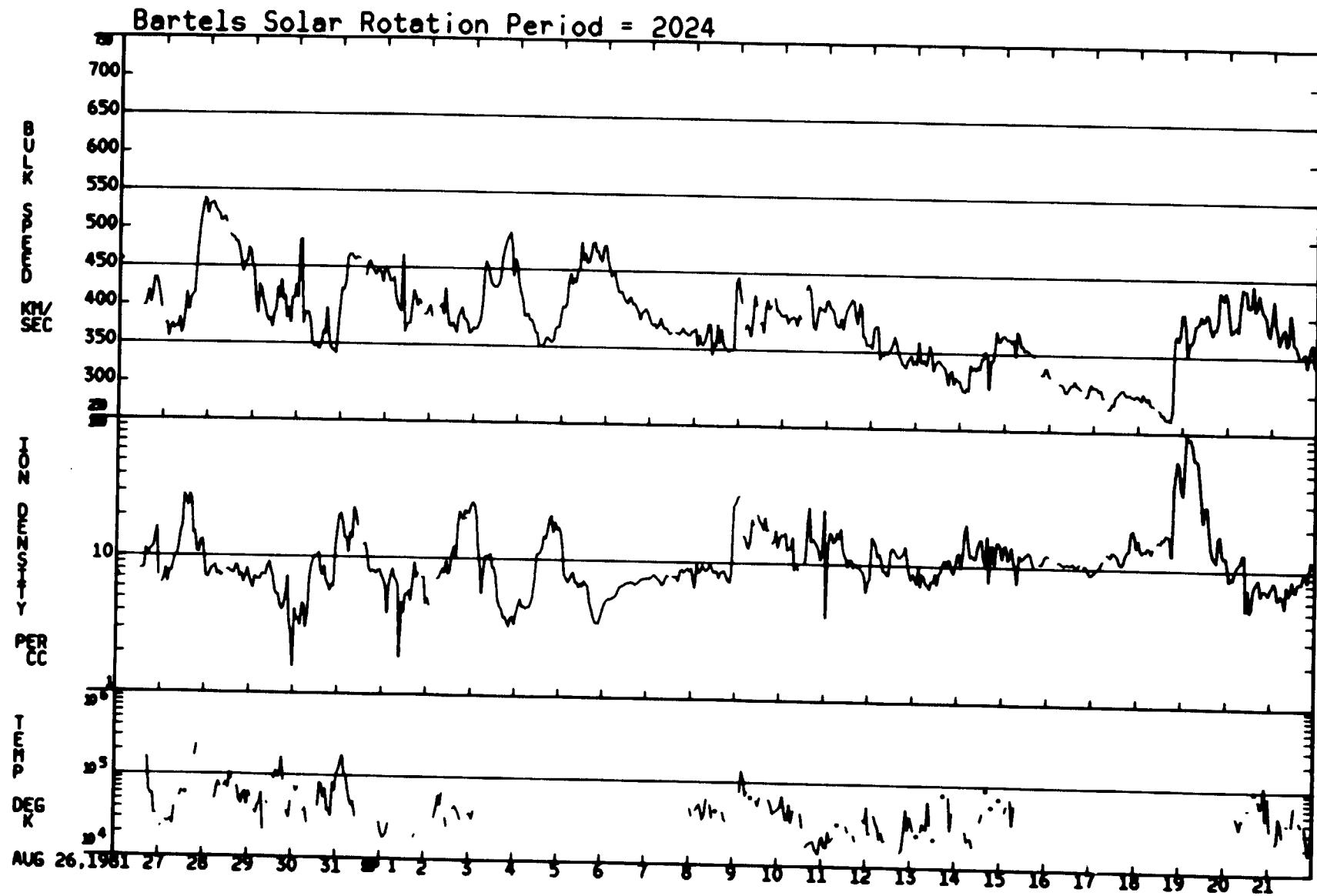


ORIGINAL PAGE IS  
OF POOR QUALITY

07/30/81 - 08/25/81

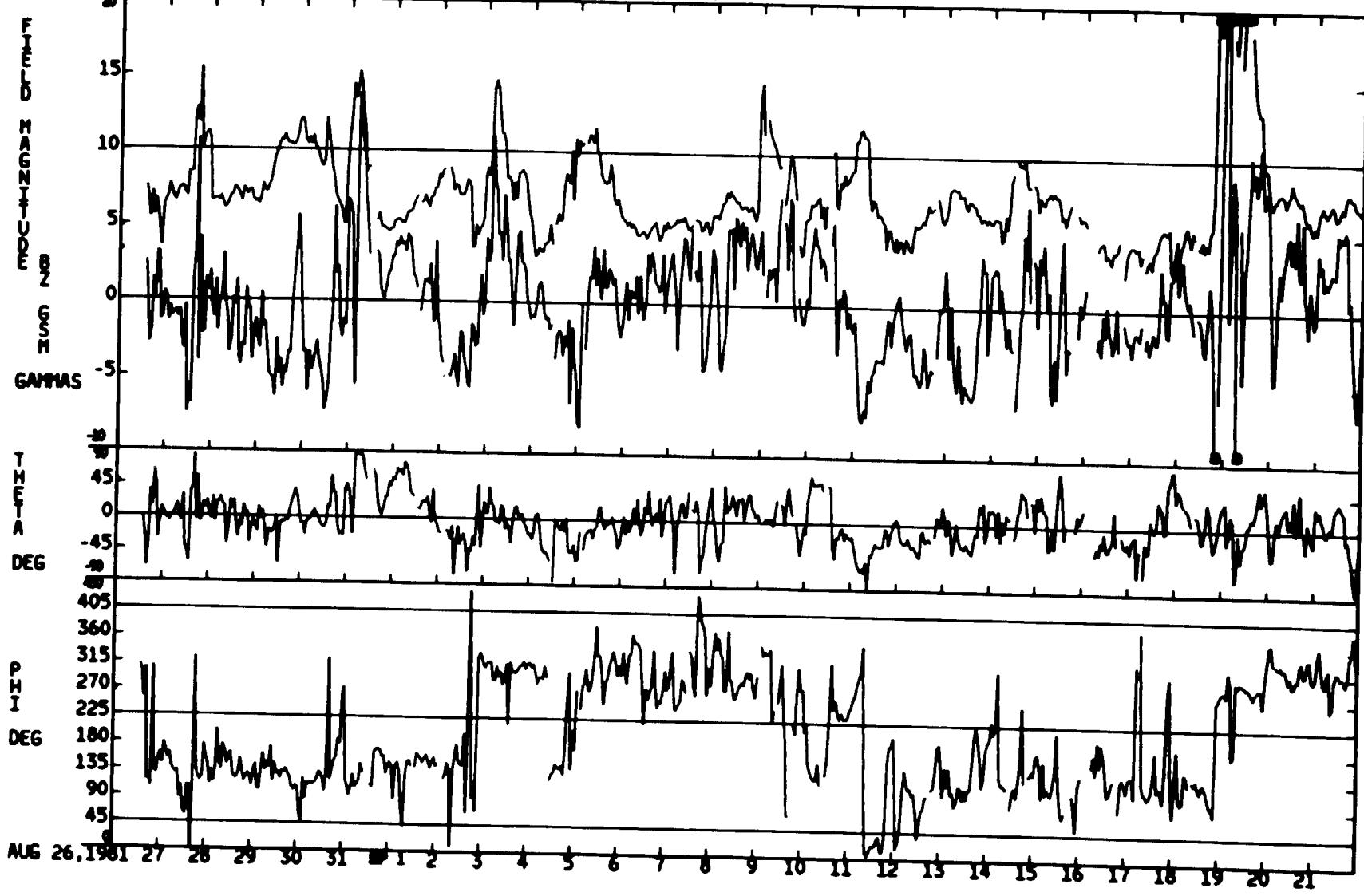


08/26/81 — 09/21/81

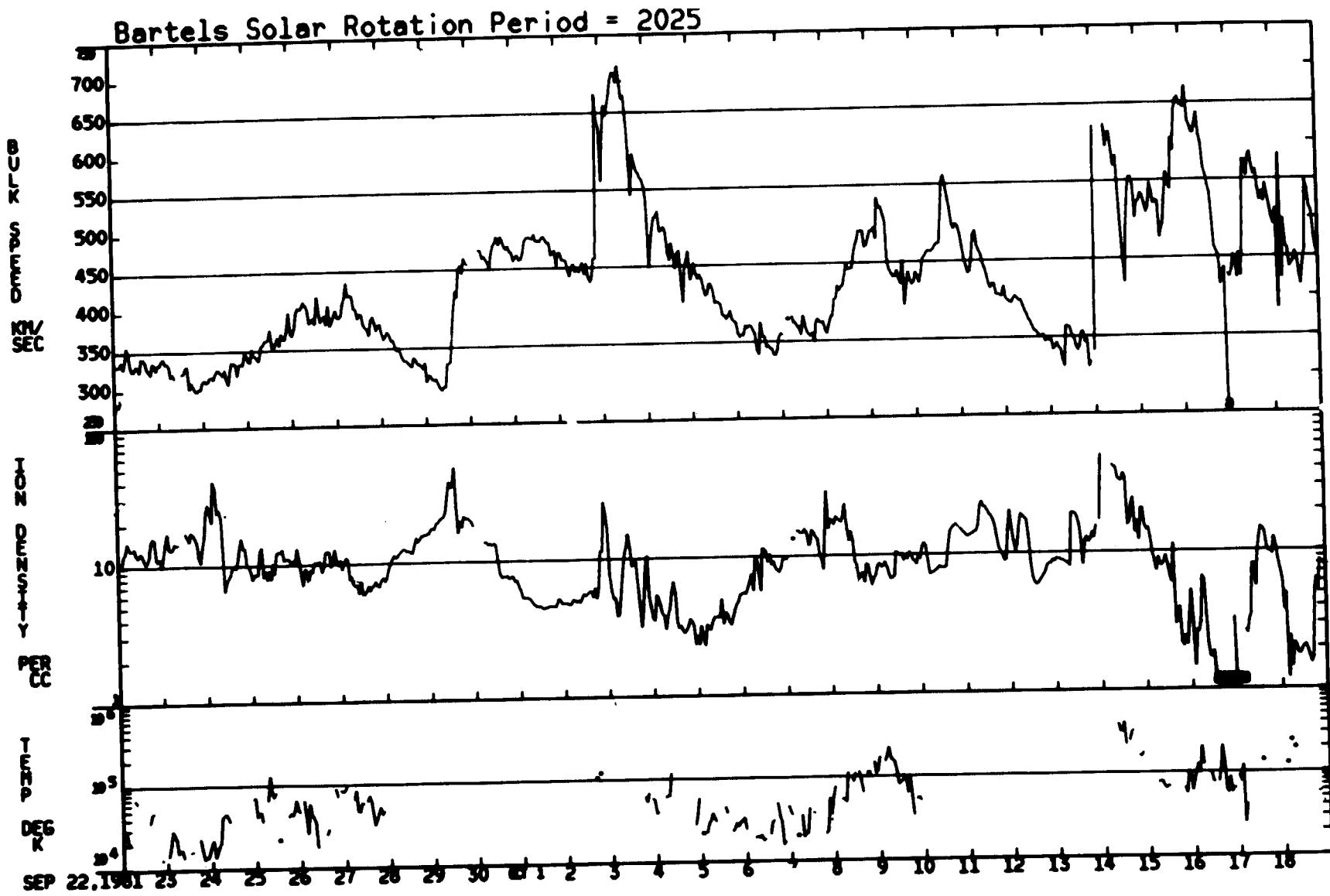


08/26/81 – 09/21/81

Bartels Solar Rotation Period = 2024

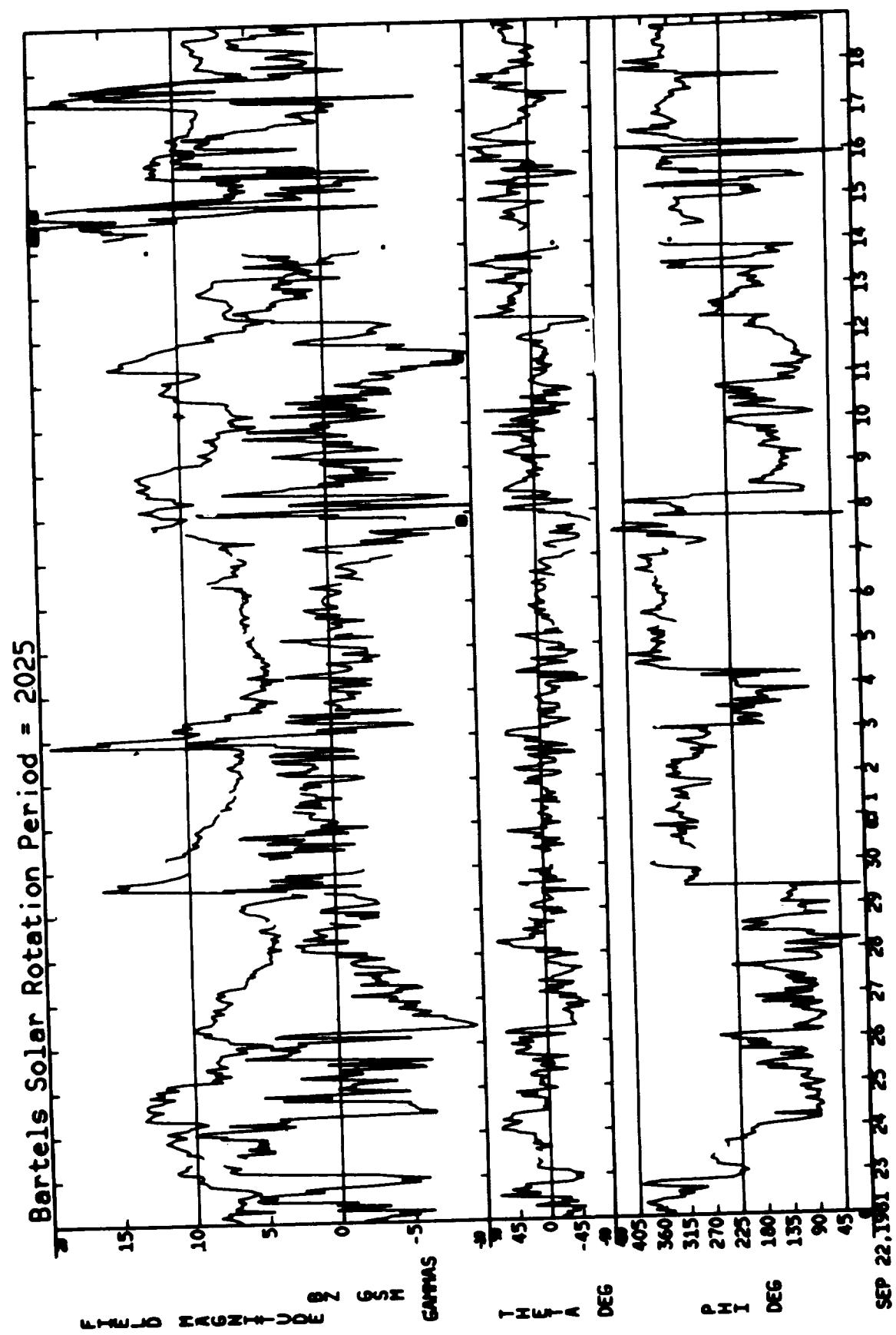


09/22/81 – 10/18/81

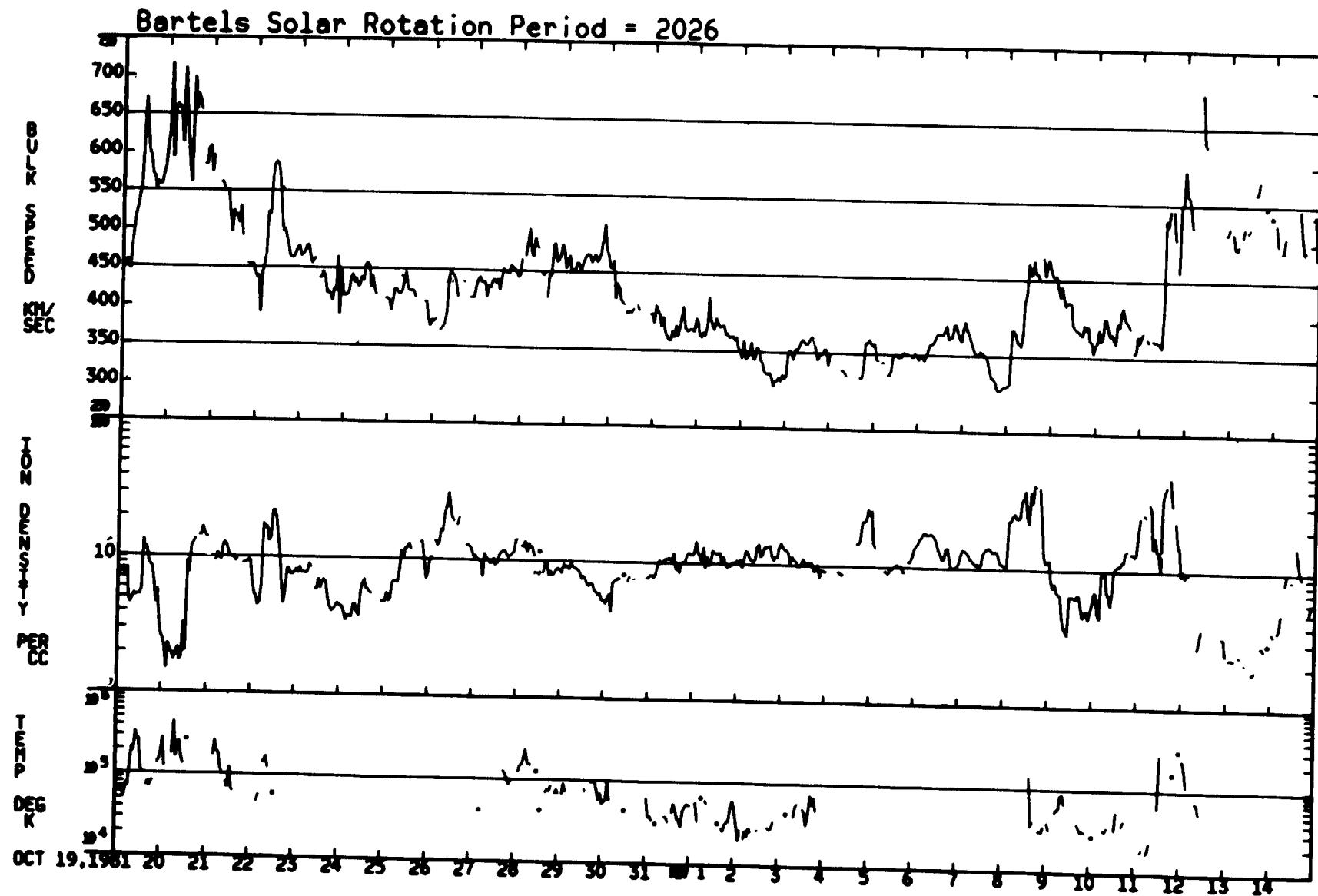


ORIGINAL PAGE IS  
OF POOR QUALITY

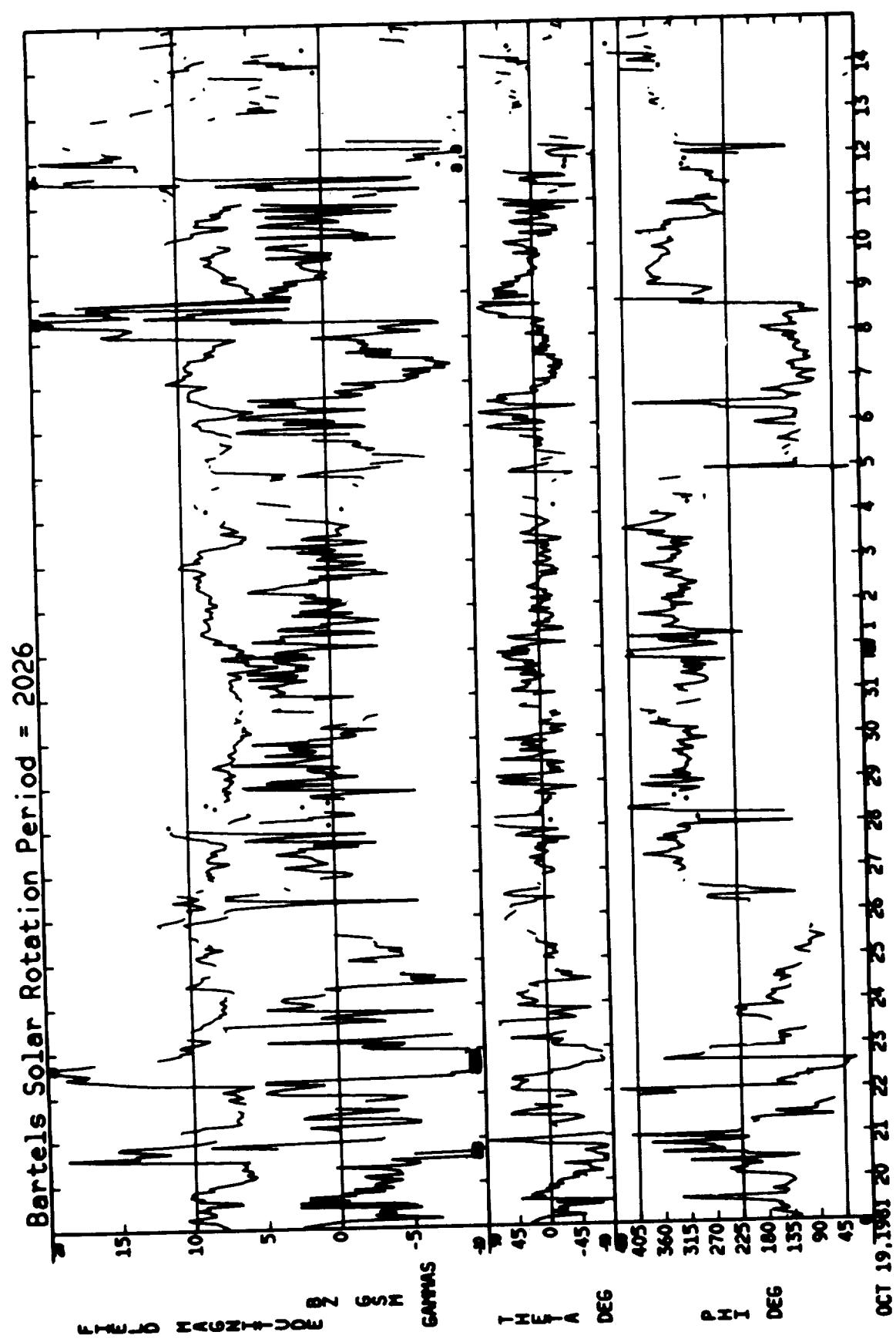
09/22/81 - 10/18/81



10/19/81 — 11/14/81

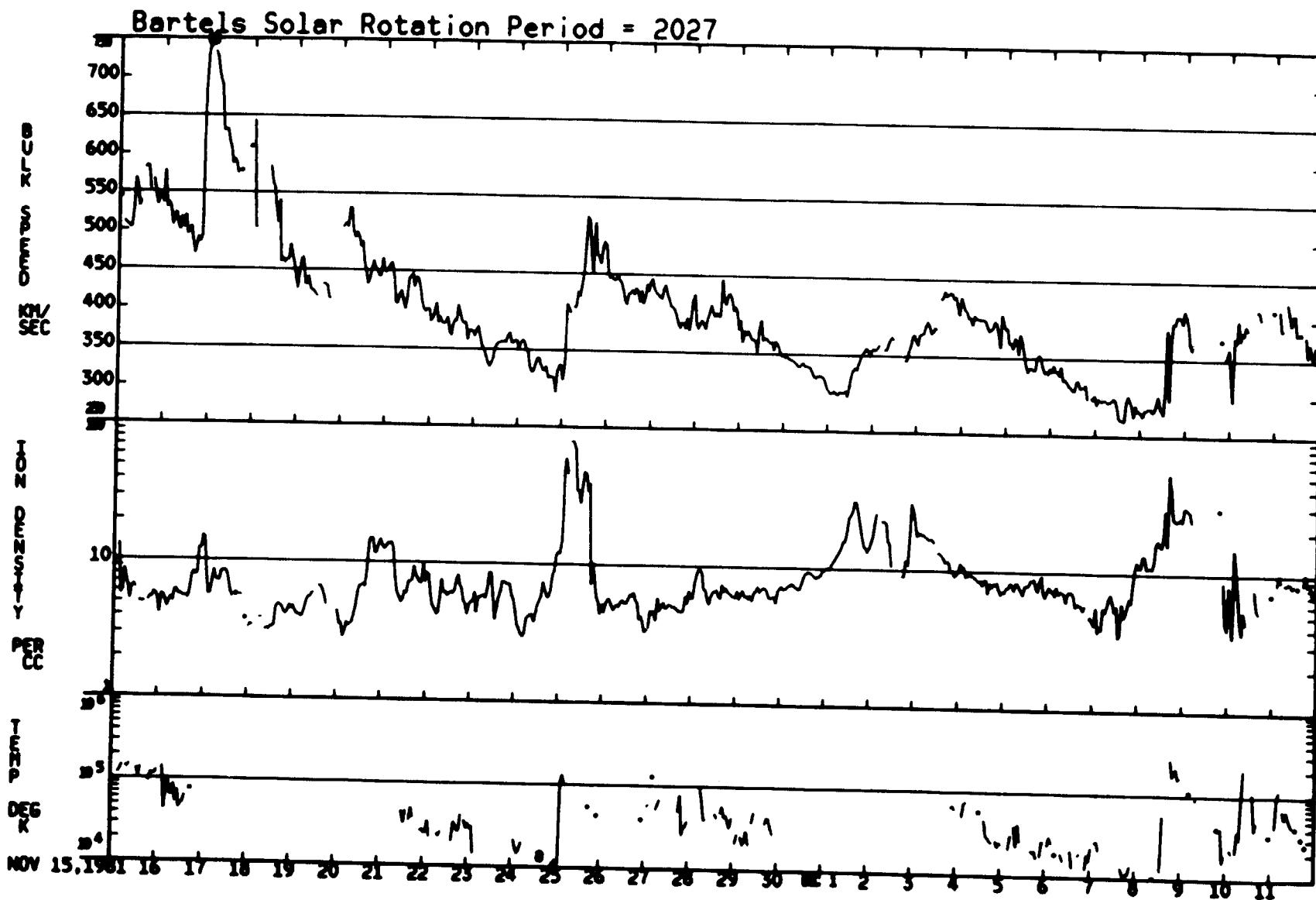


10/19/81 - 11/14/81



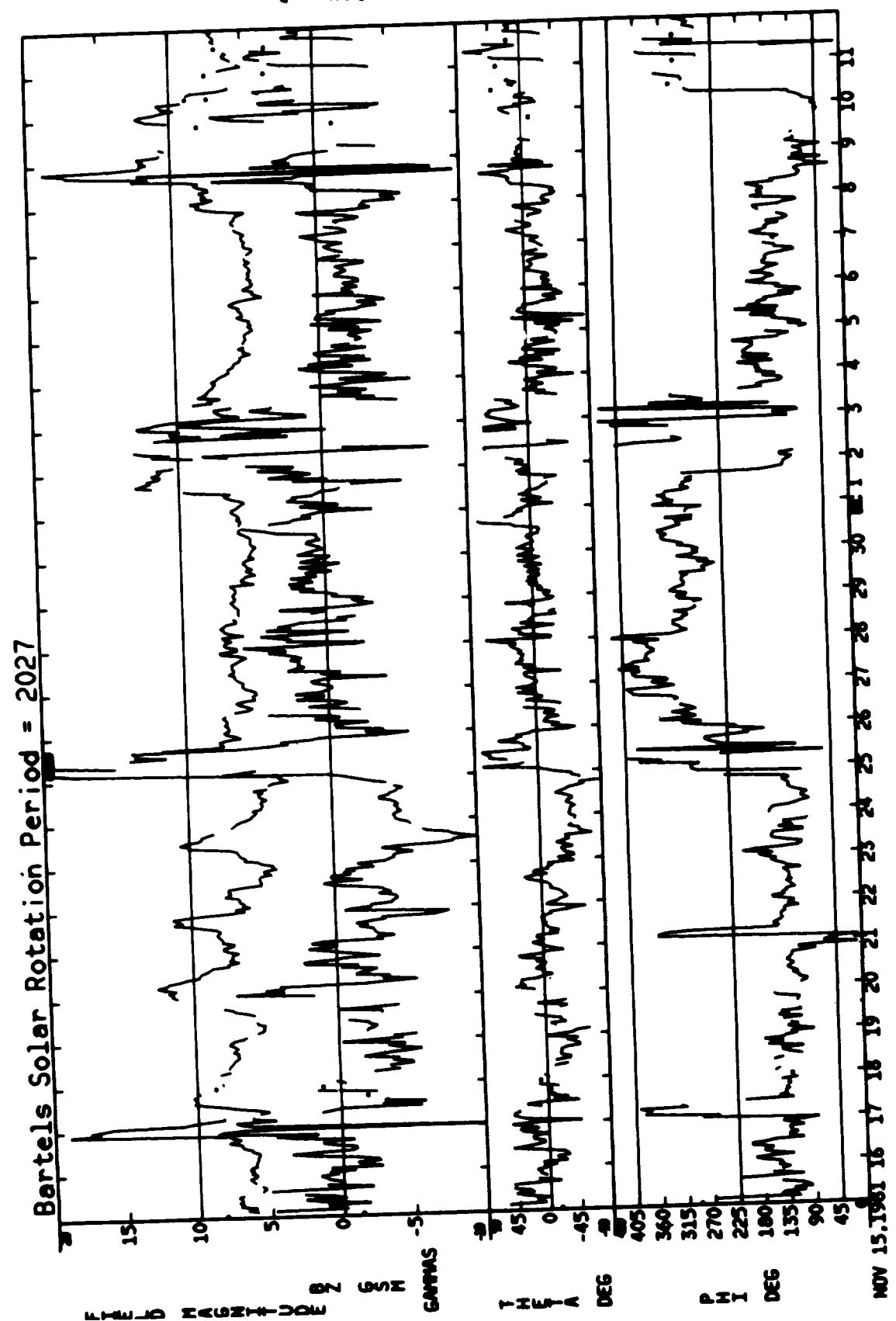
ORIGINAL PAGE IS  
OF POOR QUALITY

11/15/81 – 12/11/81

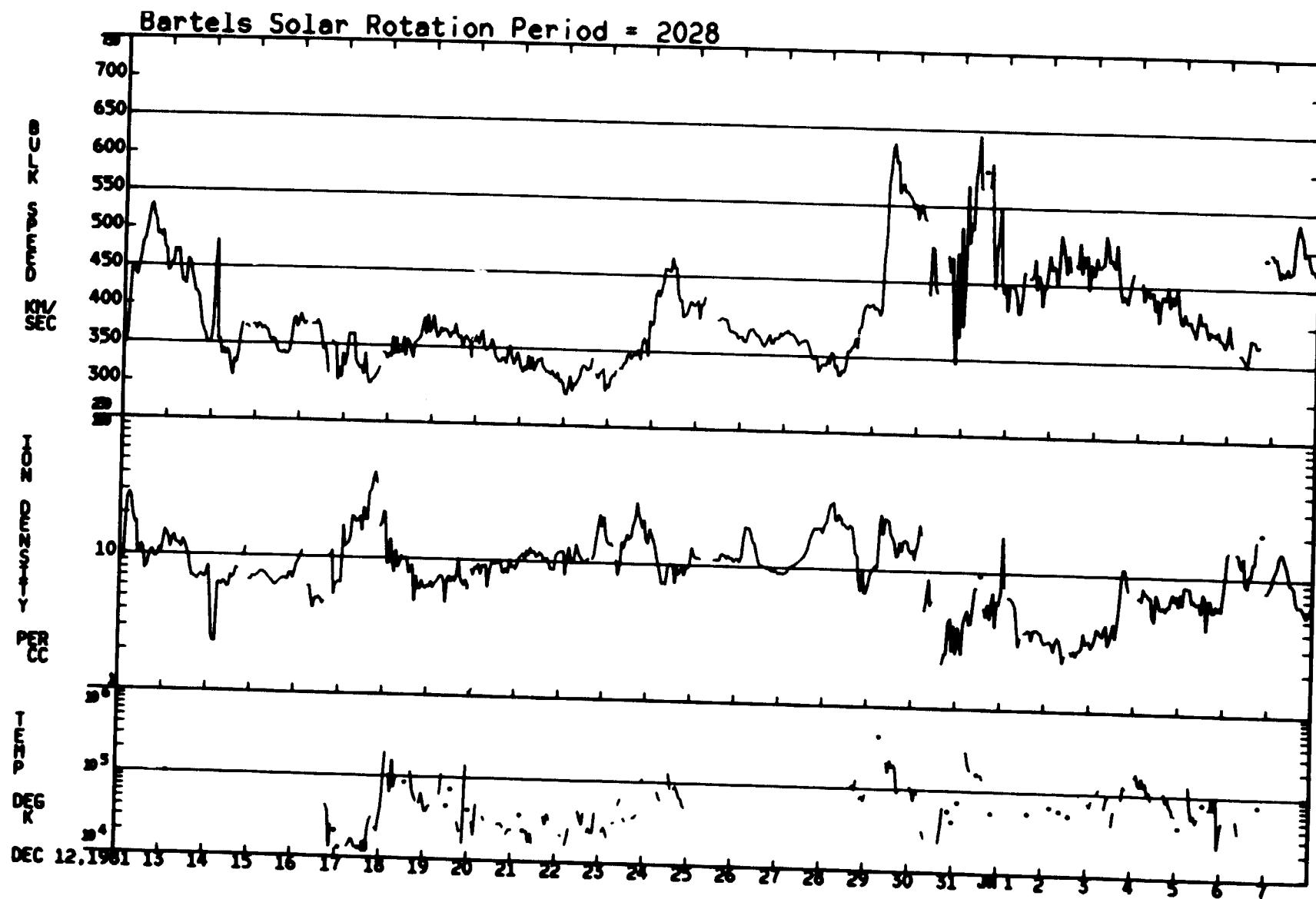


ORIGINAL PAGE IS  
OF POOR QUALITY

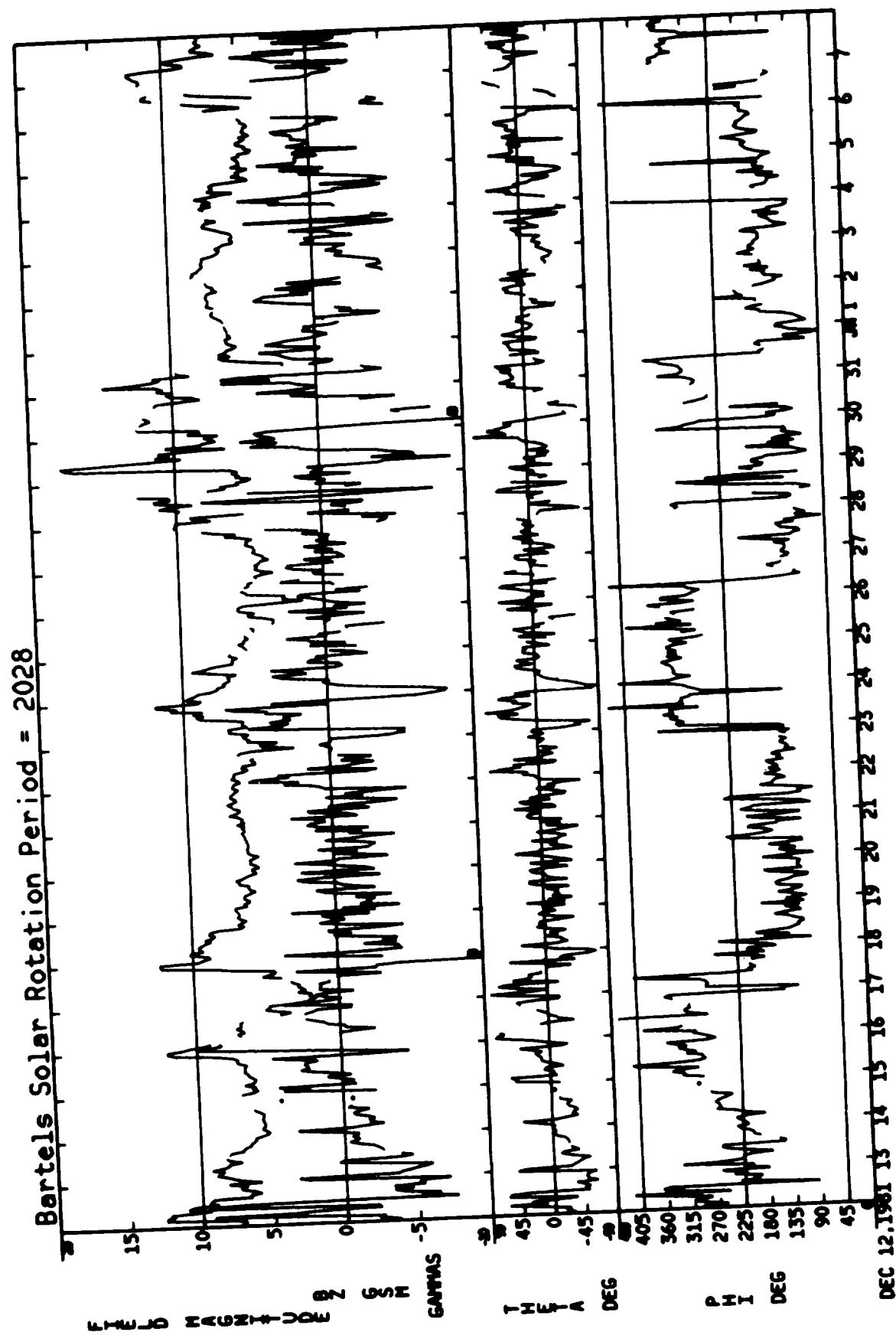
11/15/81 - 12/11/81



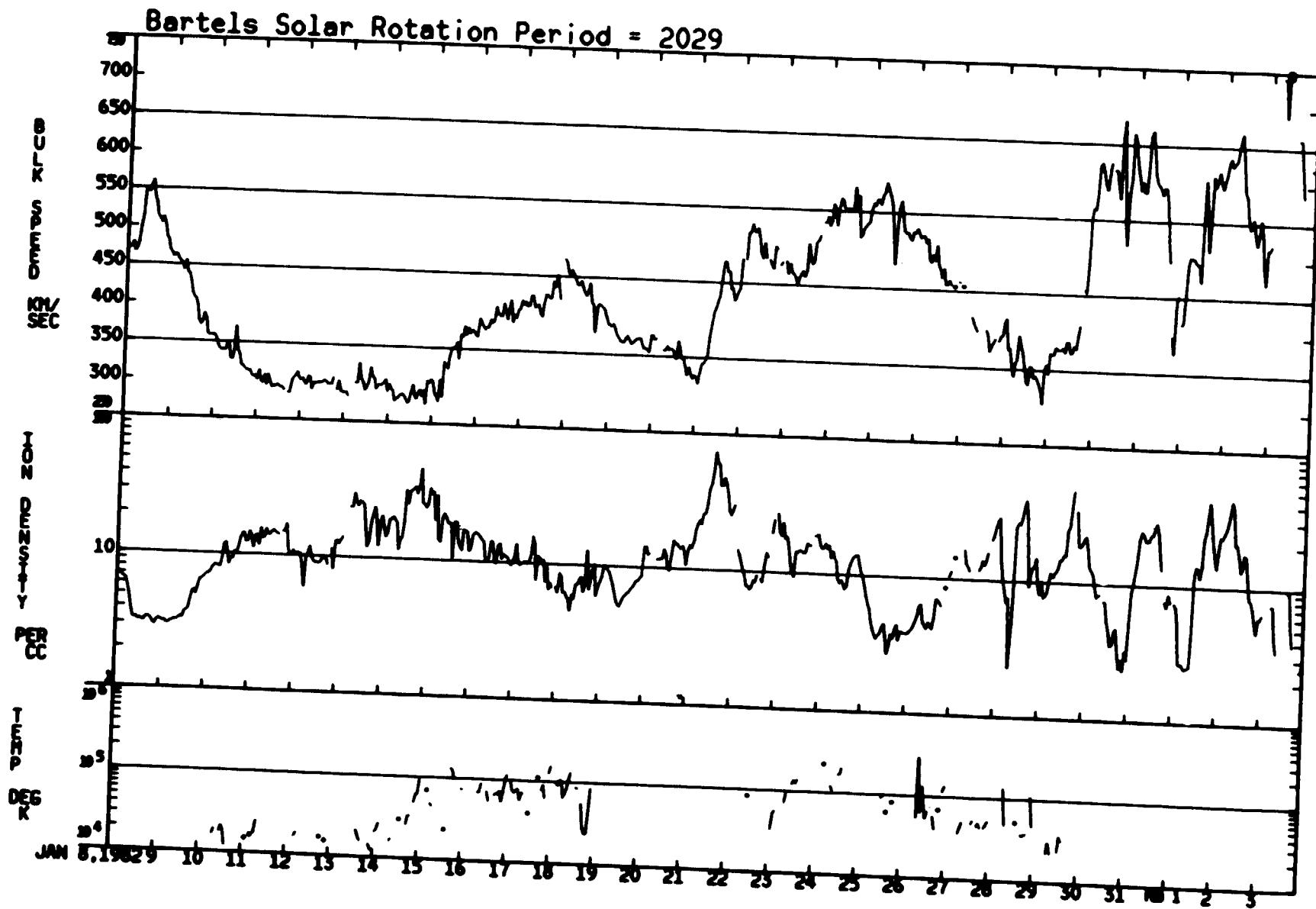
12/12/81 – 01/07/82



ORIGINAL PAGE IS  
OF POOR QUALITY 12/12/81 - 01/07/82

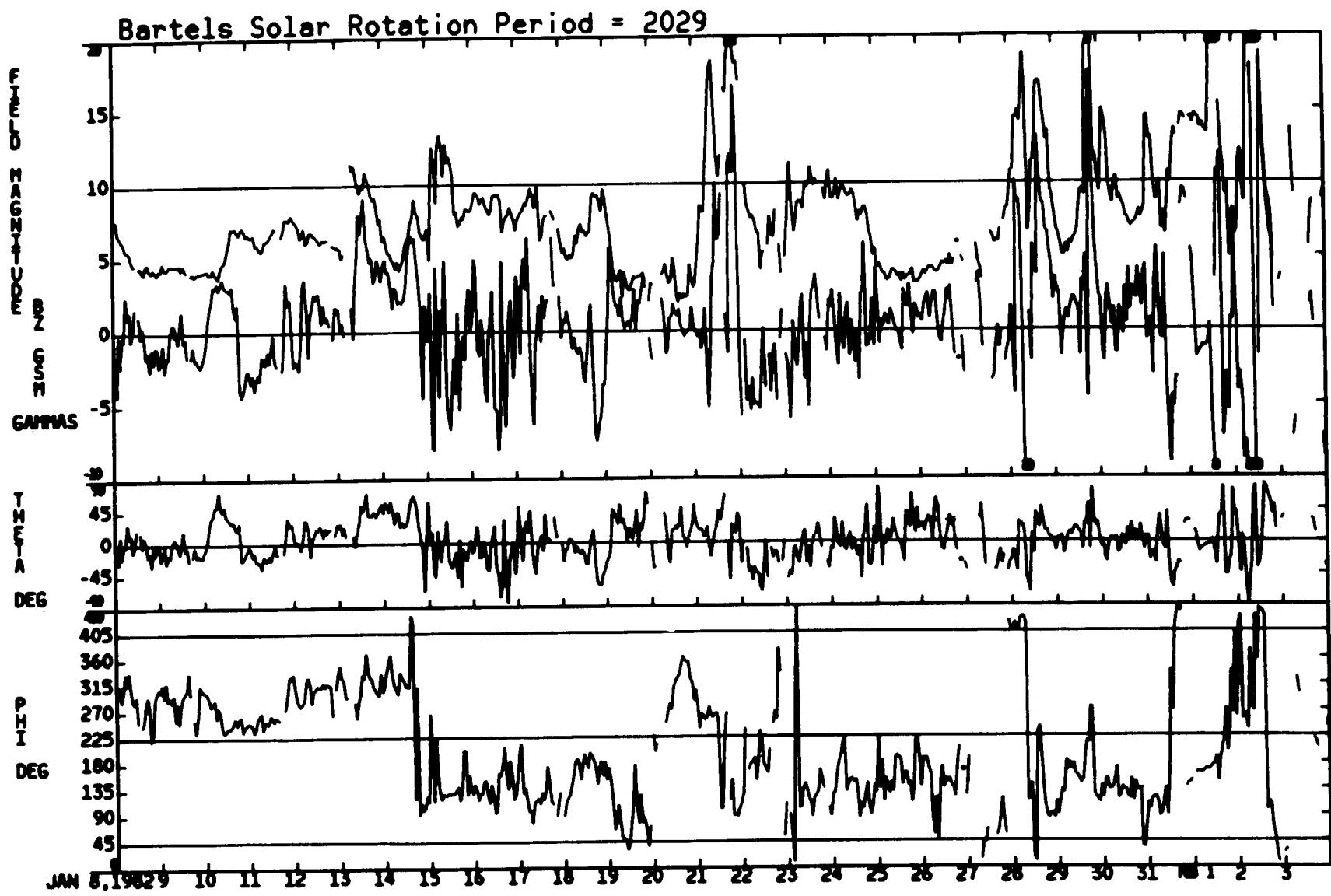


01/08/82 - 02/03/82

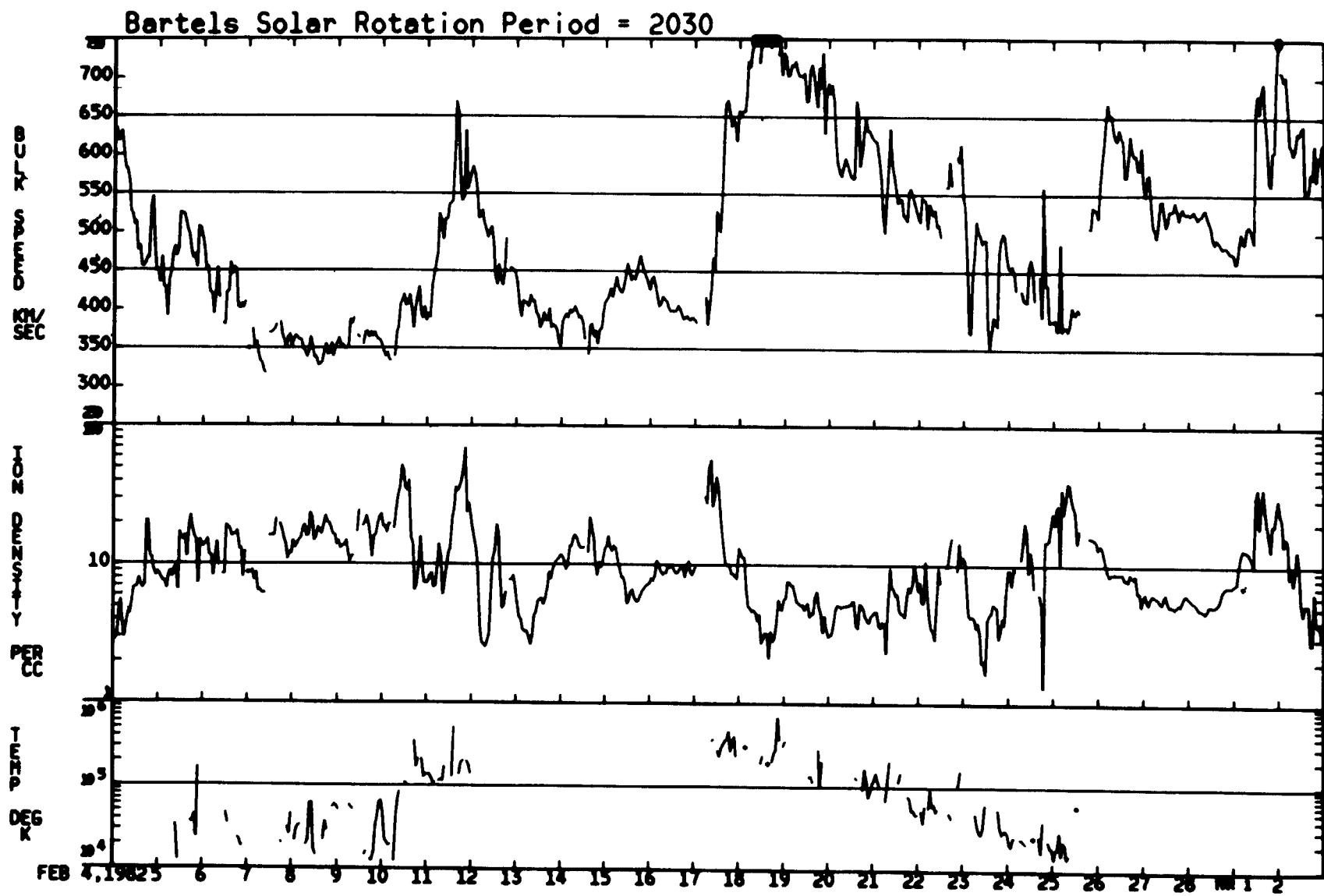


ORIGINAL PAGE IS  
OF POOR QUALITY

01/08/82 – 02/03/82

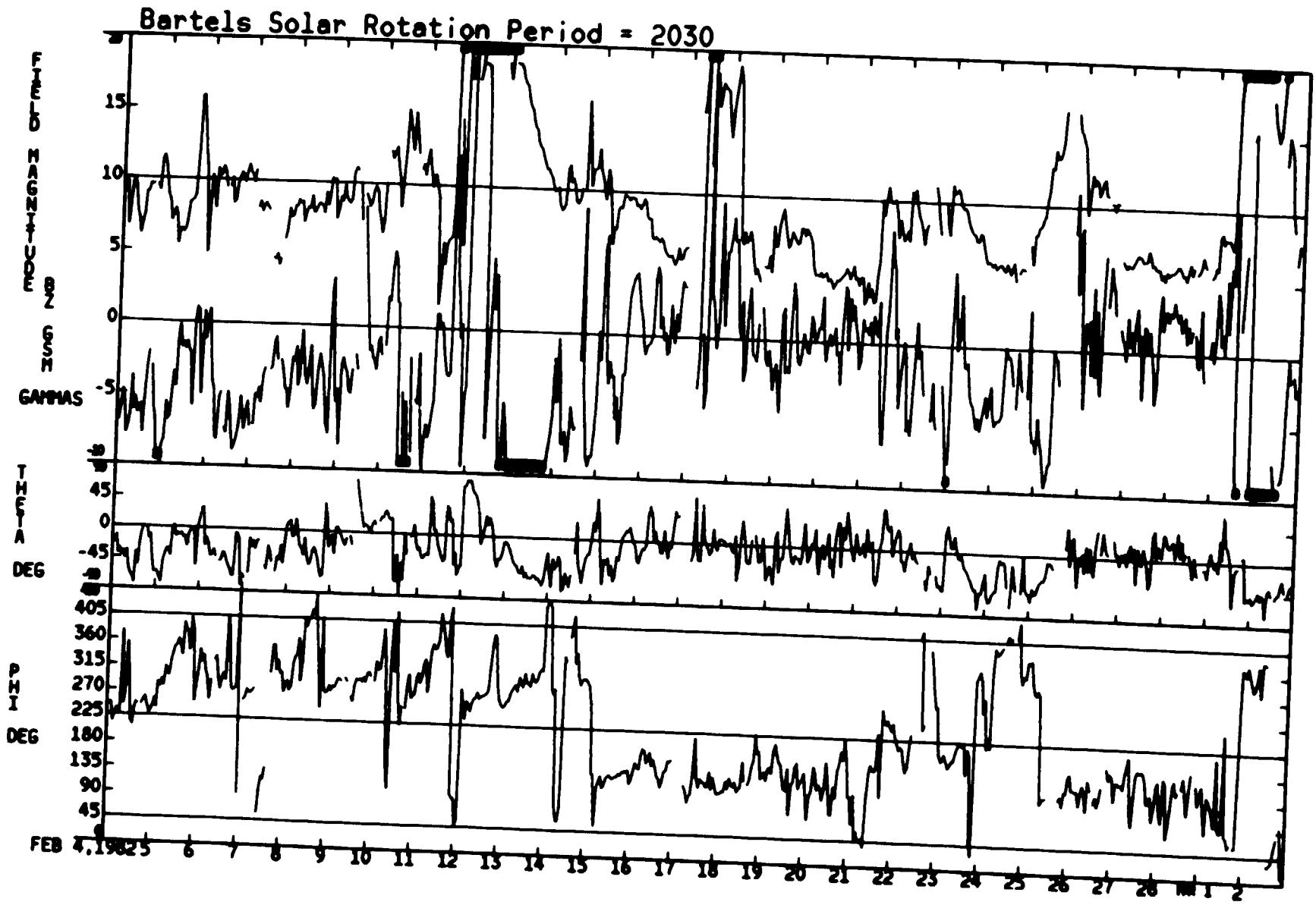


02/04/82 - 03/02/82

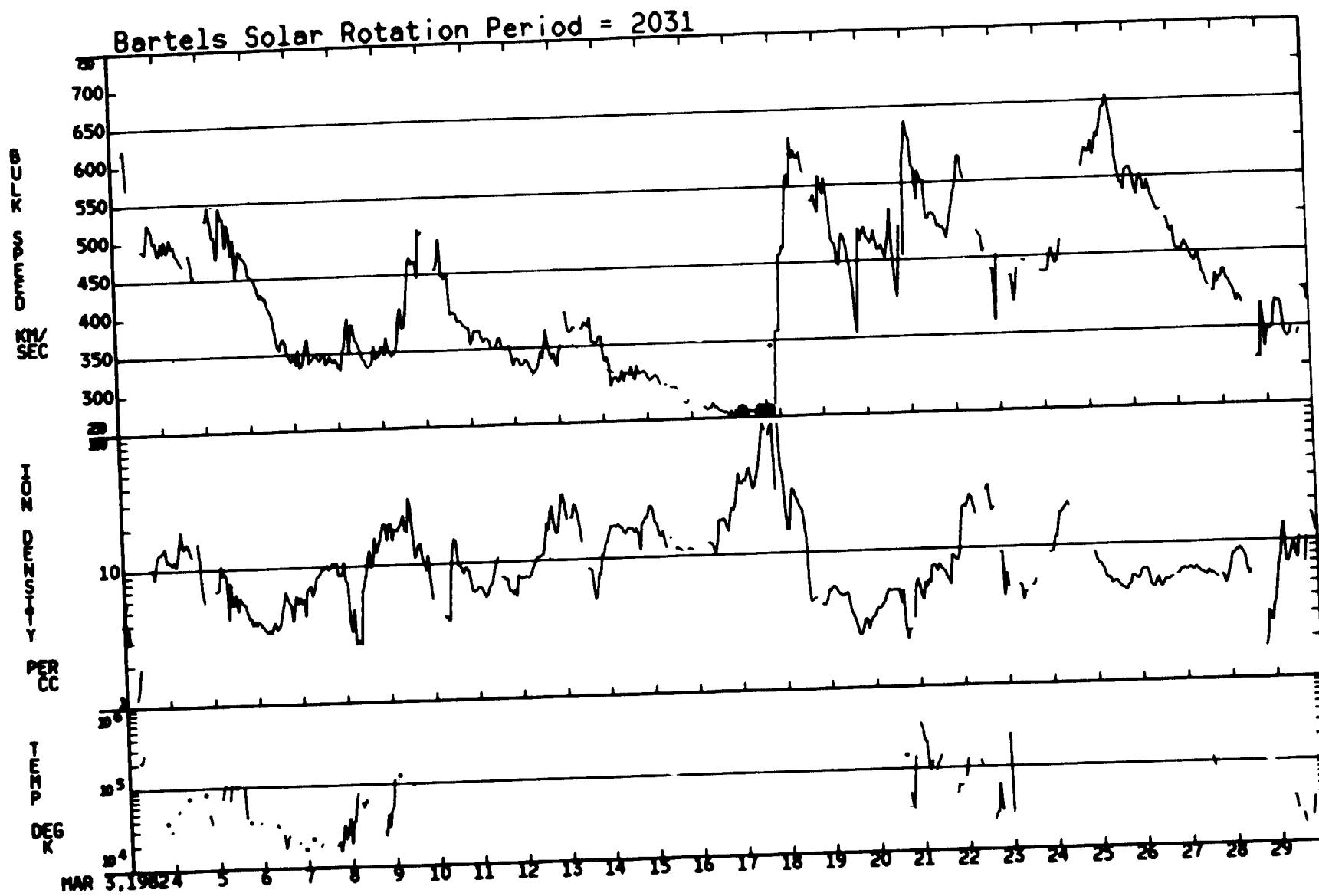


ORIGINAL PAGE IS  
OF POOR QUALITY

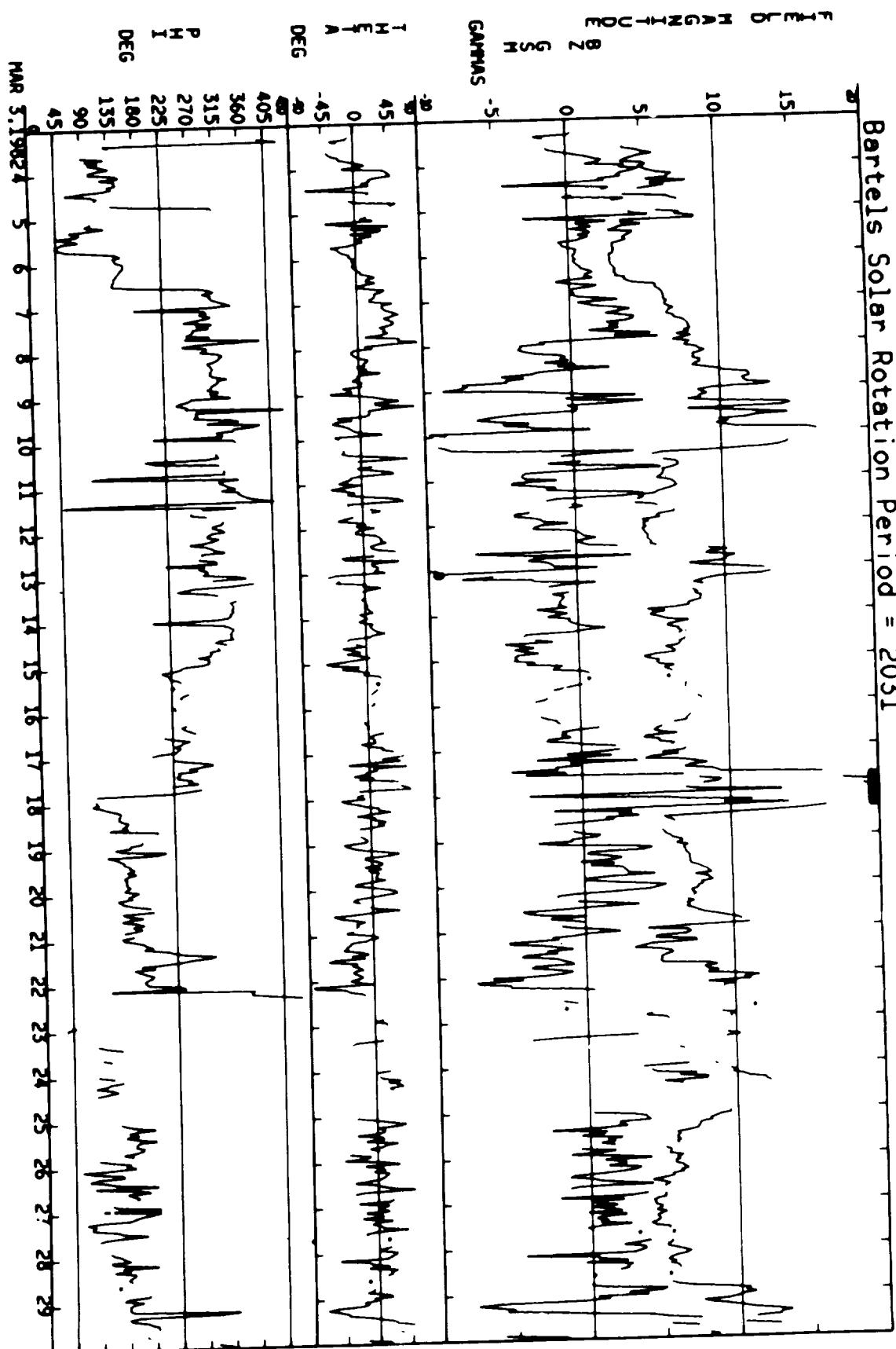
02/04/82 — 03/02/82



03/03/82 – 03/29/82



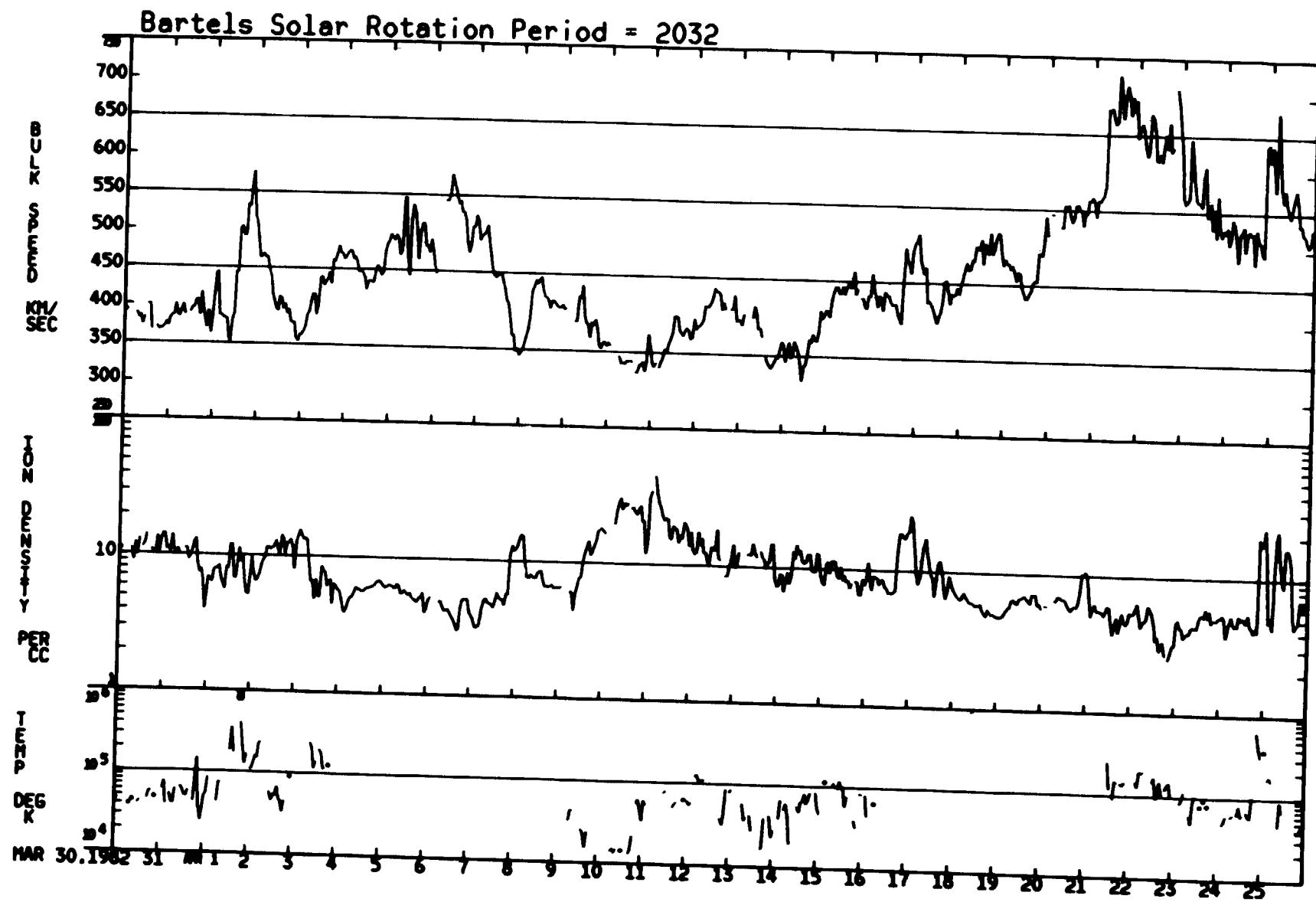
Bartels Solar Rotation Period = 2031



03/03/82 - 03/29/82

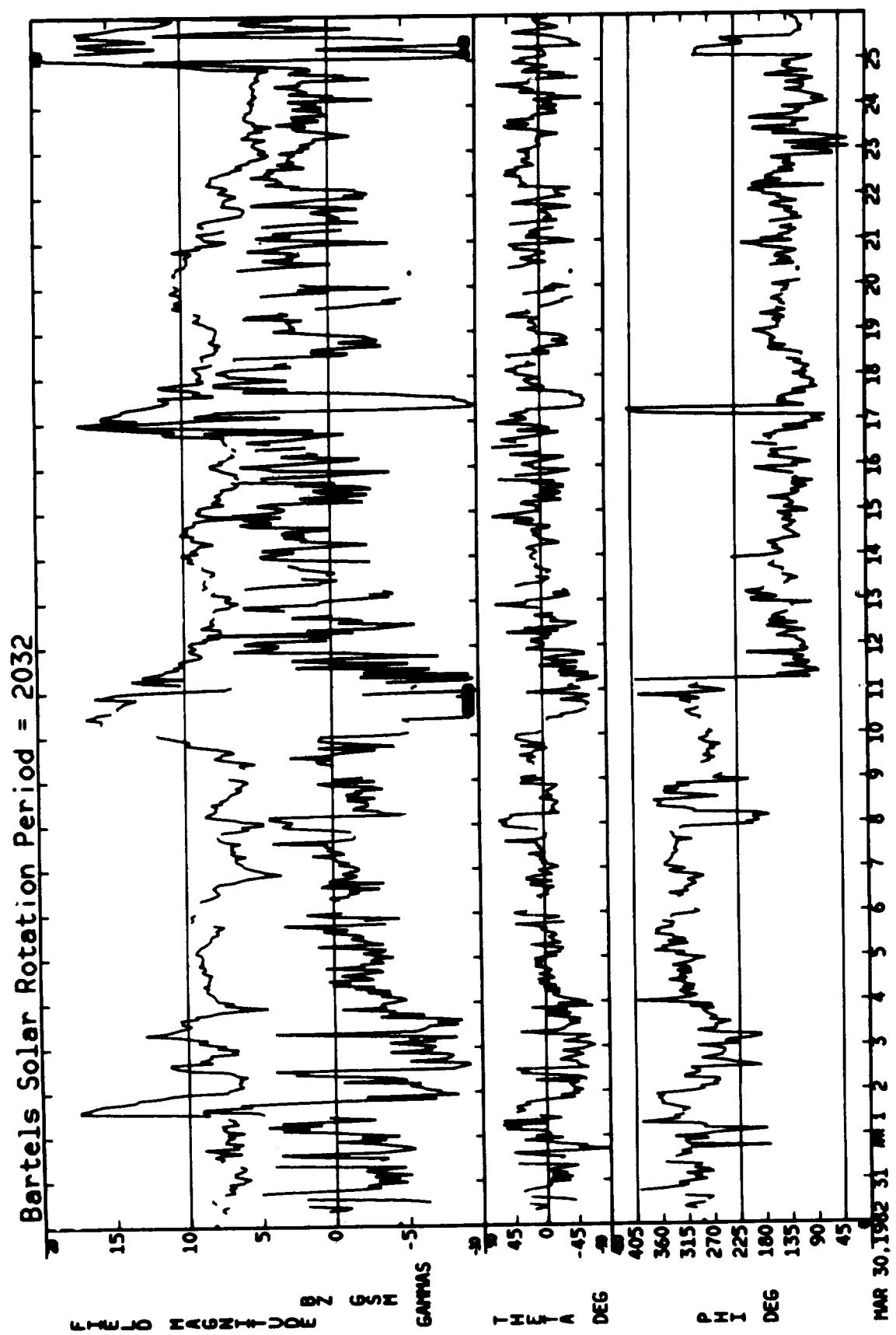
ORIGINAL PAGE IS  
OF POOR QUALITY

03/30/82 – 04/25/82

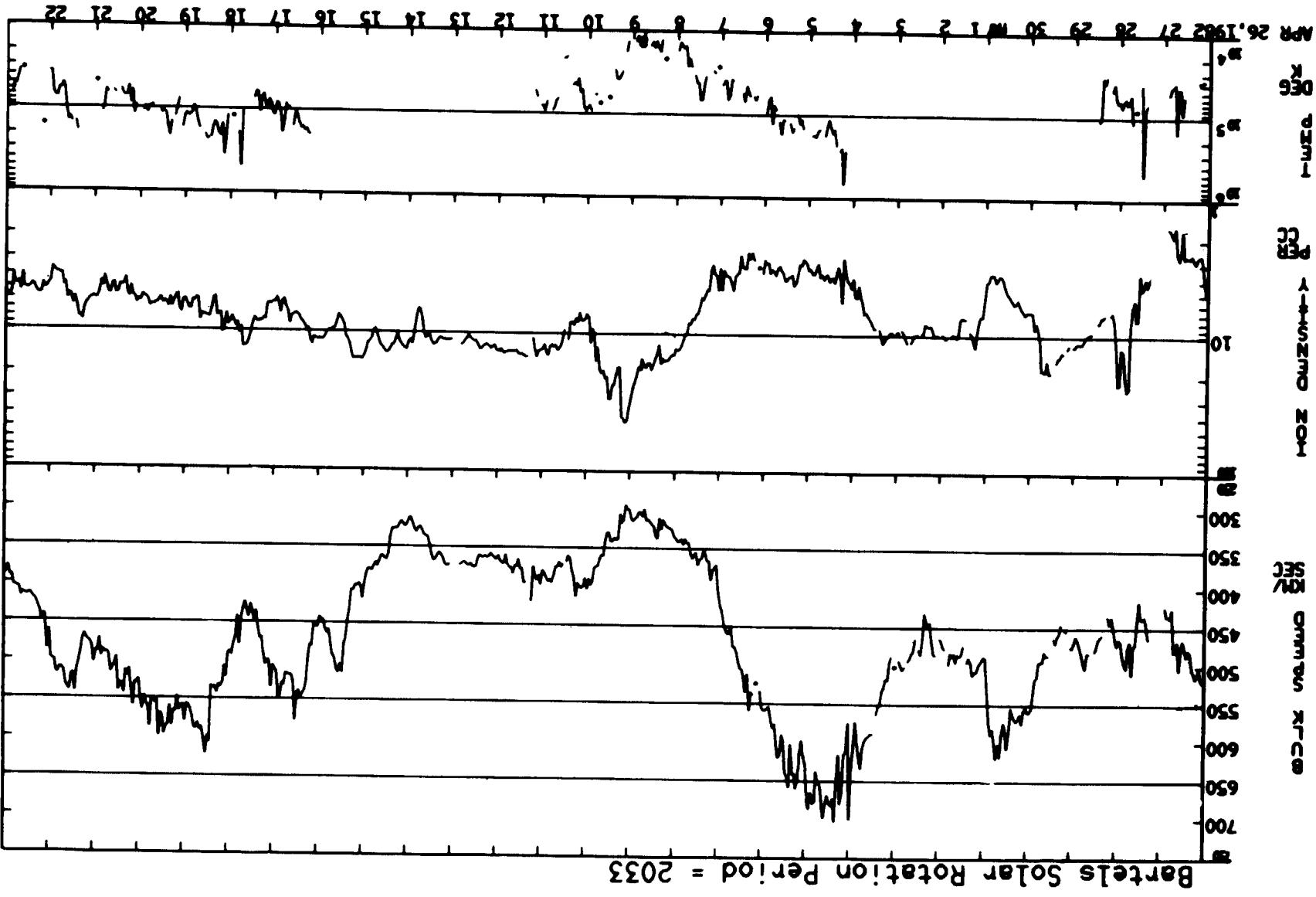


ORIGINAL PAGE IS  
OF POOR QUALITY

03/30/82 — 04/25/82



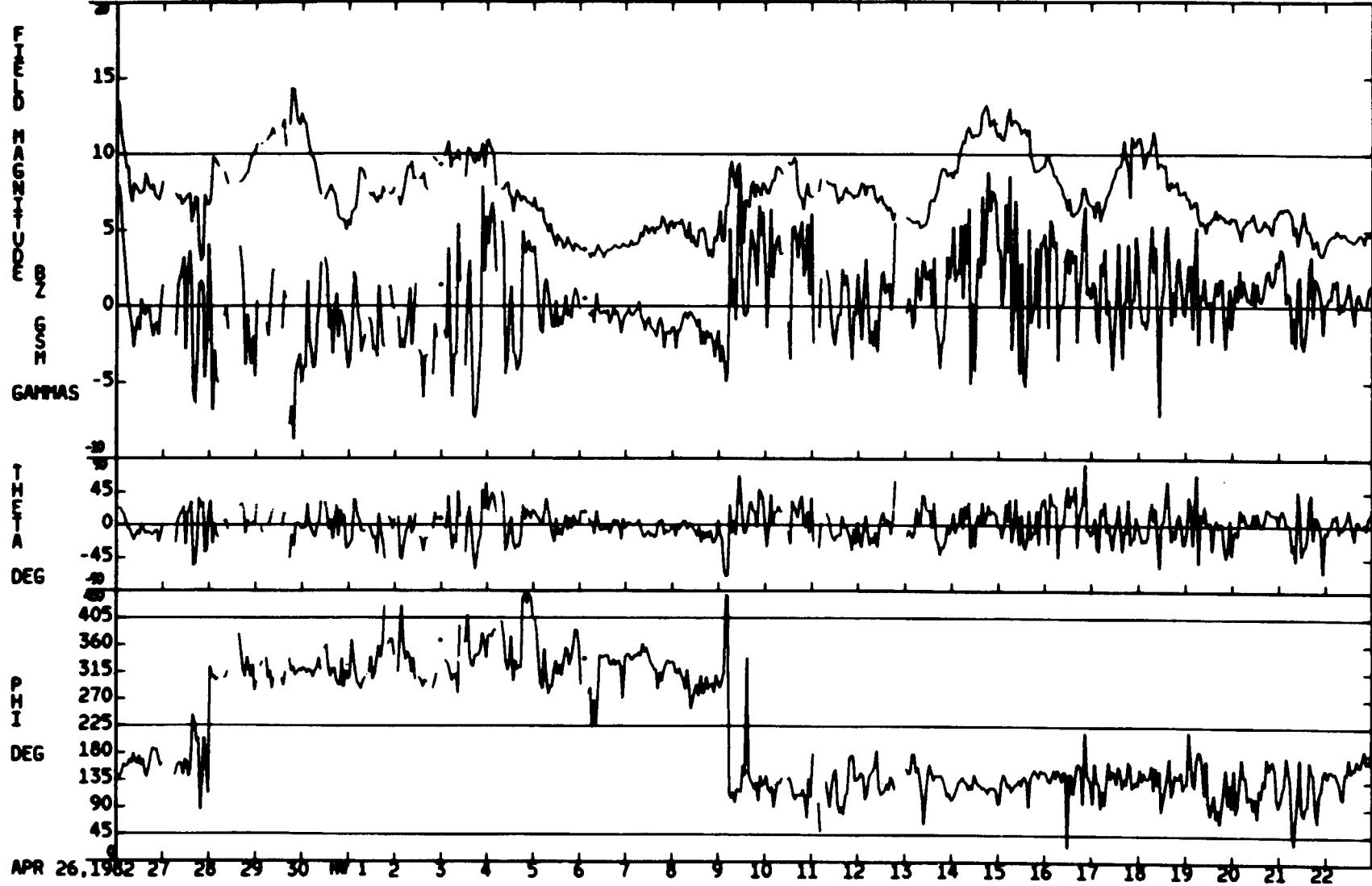
04/26/82 - 05/22/82



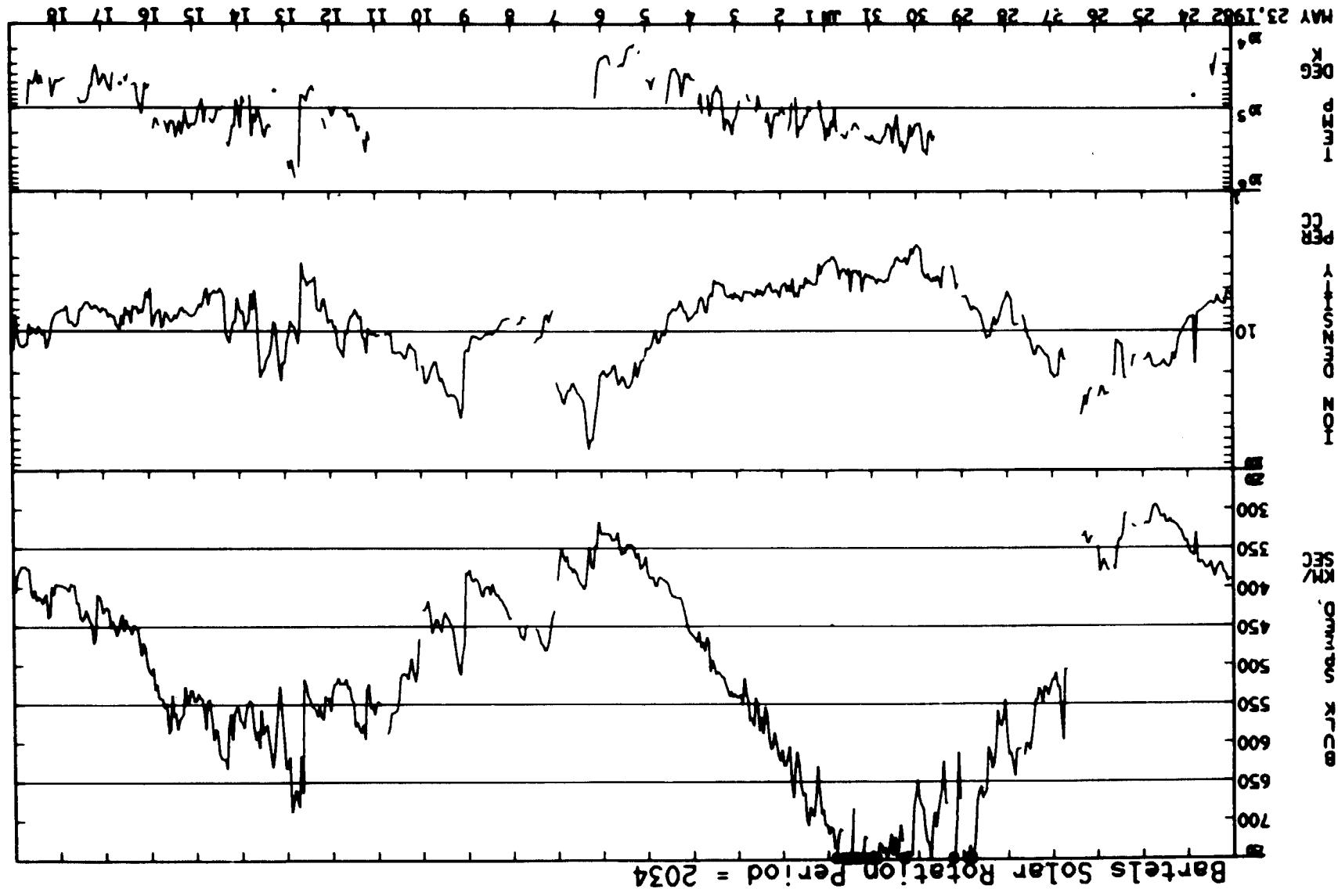
ORIGINAL PAGE IS  
OF POOR QUALITY

04/26/82 - 05/22/82

Bartels Solar Rotation Period = 2033



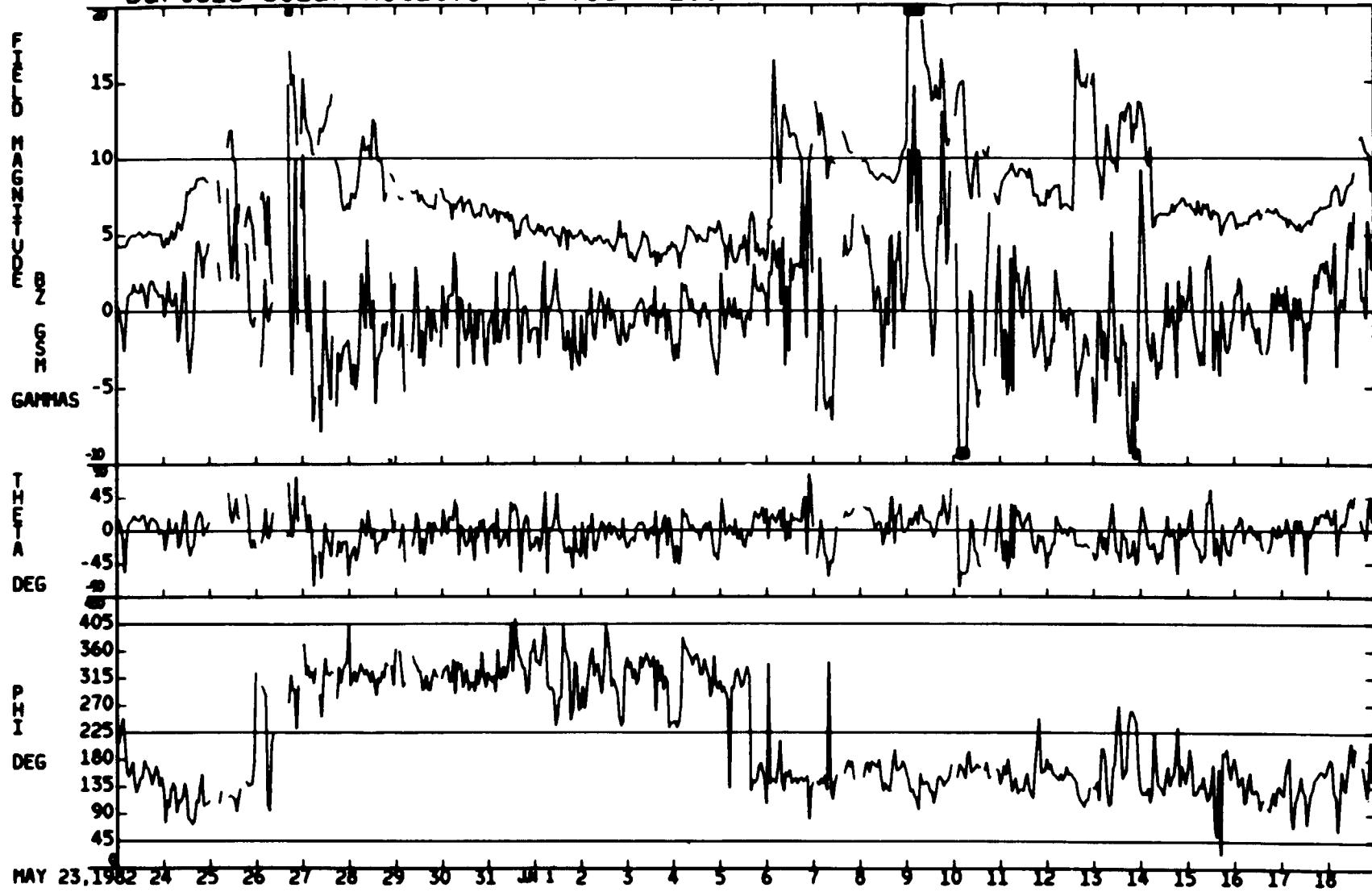
05/23/82 - 06/18/82



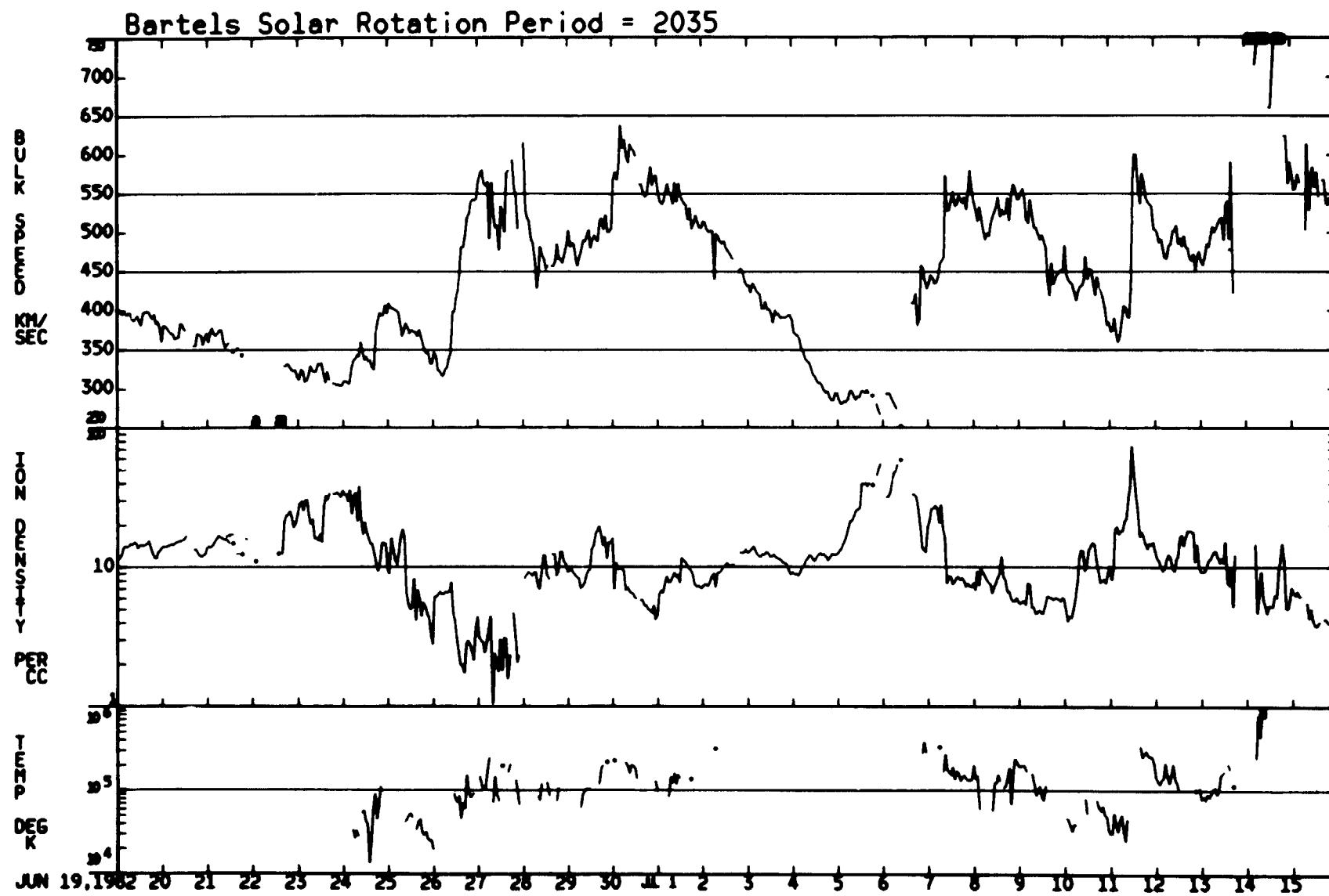
ORIGINAL PAGE IS  
OF POOR  
QUALITY

05/23/82 – 06/18/82

Bartels Solar Rotation Period = 2034

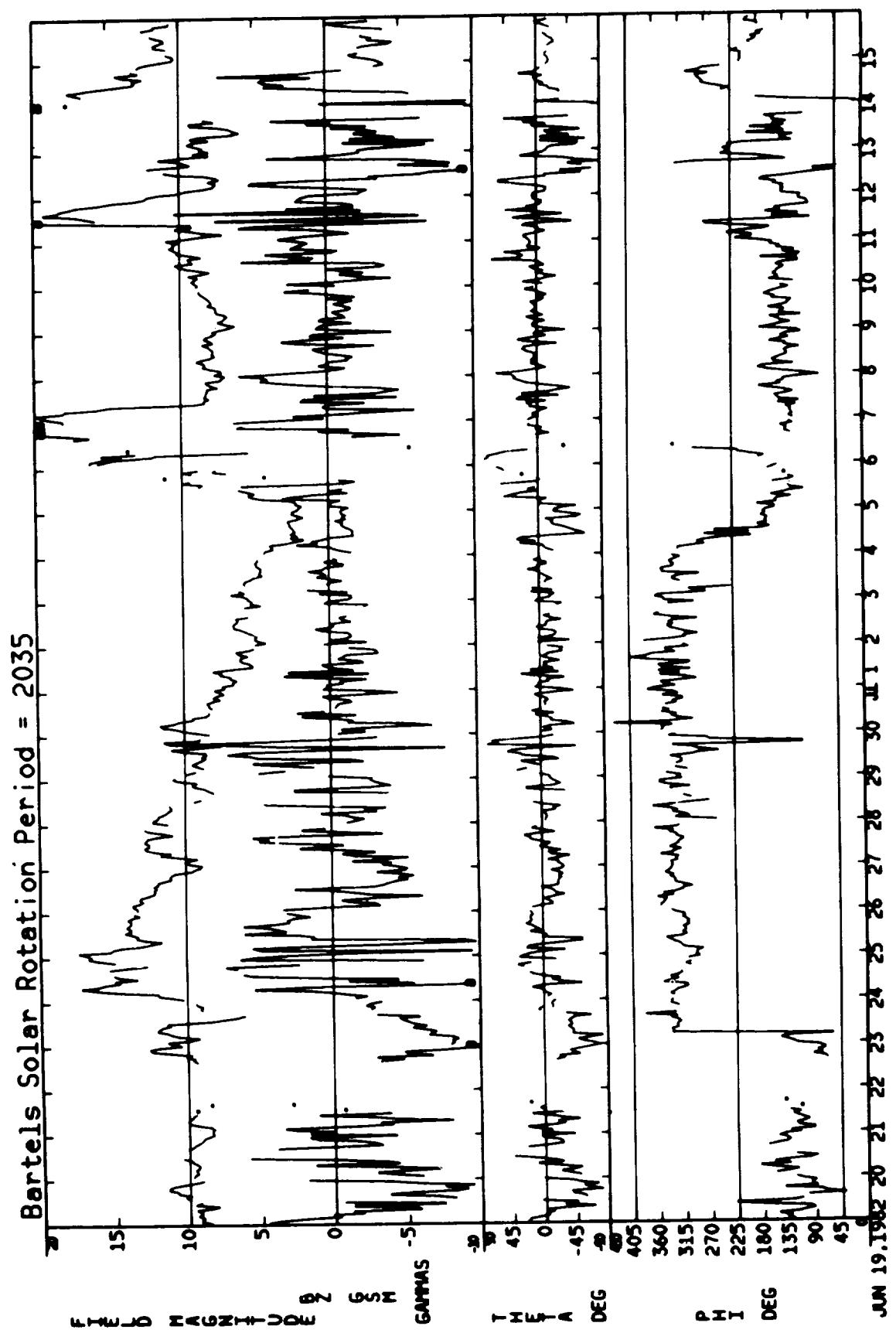


06/19/82 – 07/15/82

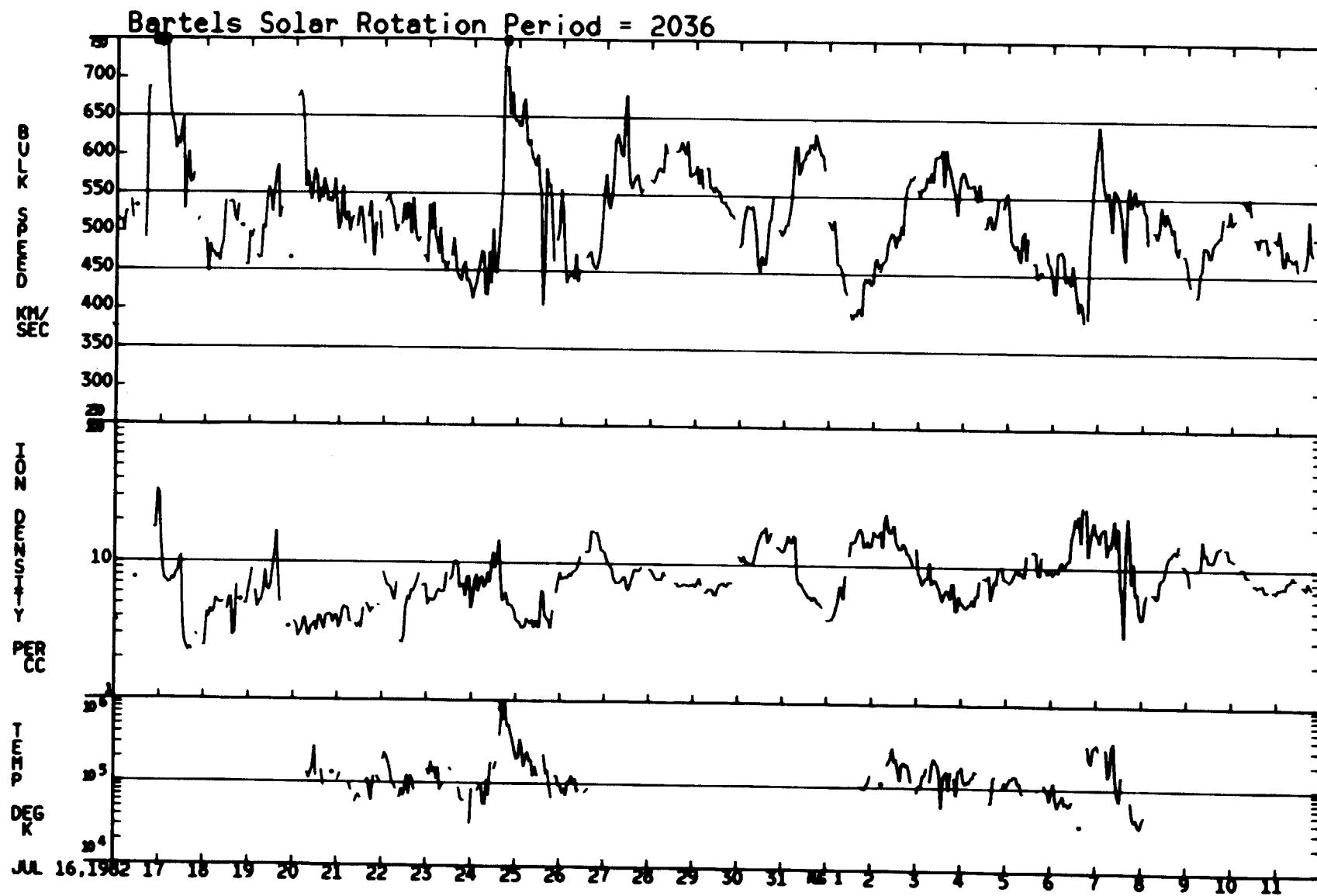


ORIGINAL PAGE IS  
OF POOR QUALITY

06/19/82 - 07/15/82

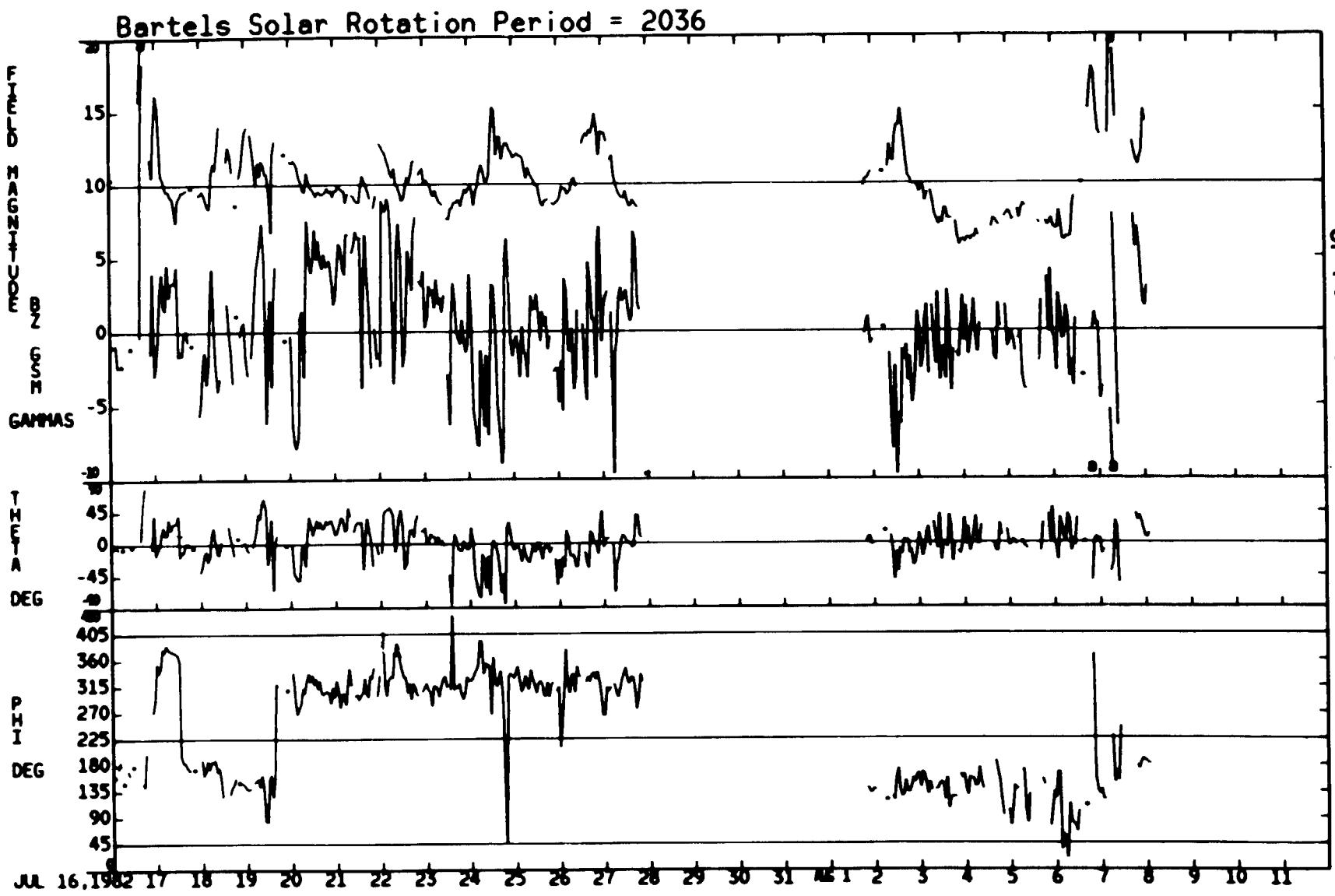


07/16/82 — 08/11/82

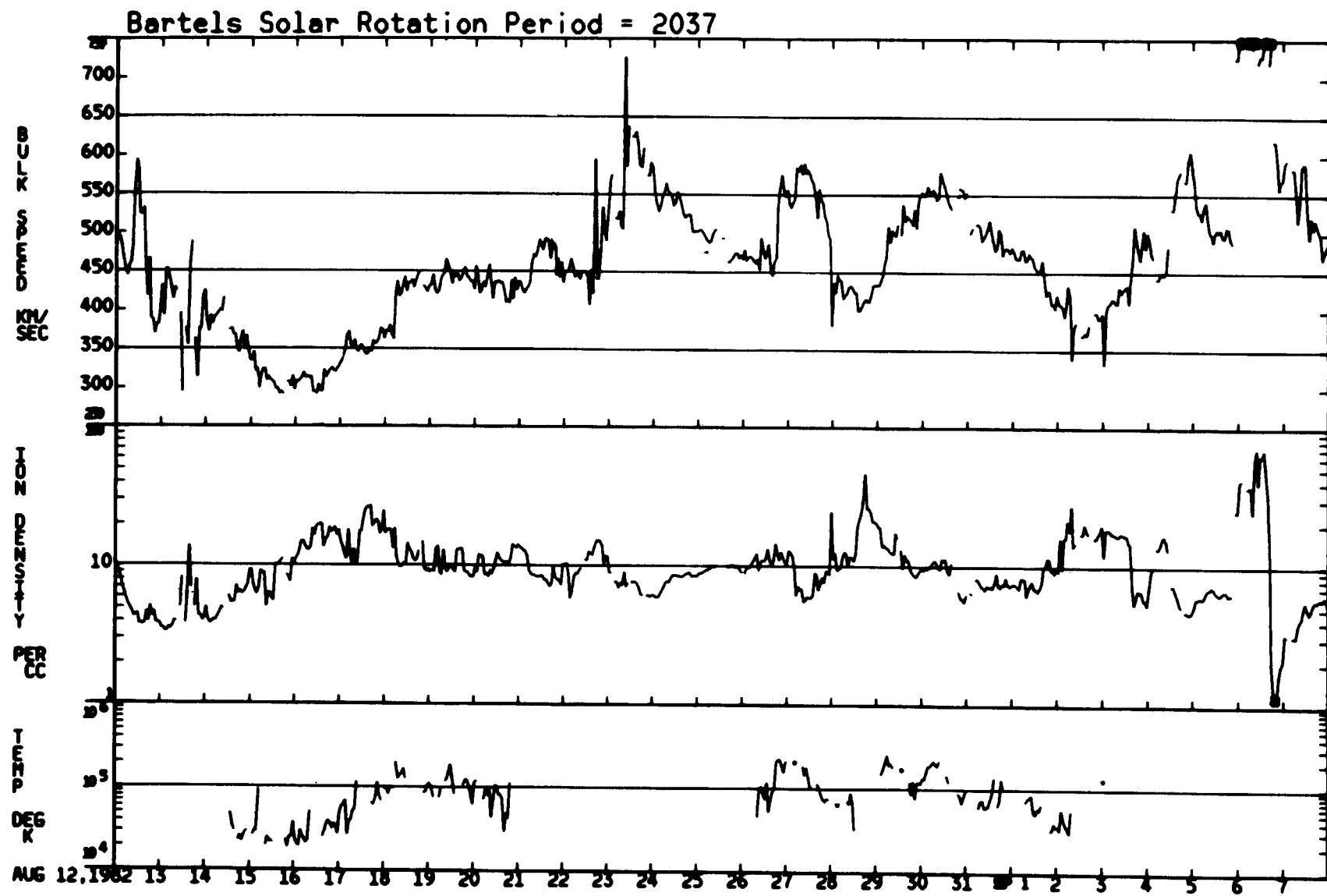


07/16/82 - 08/11/82

ORIGINAL PAGE IS  
OF POOR  
QUALITY

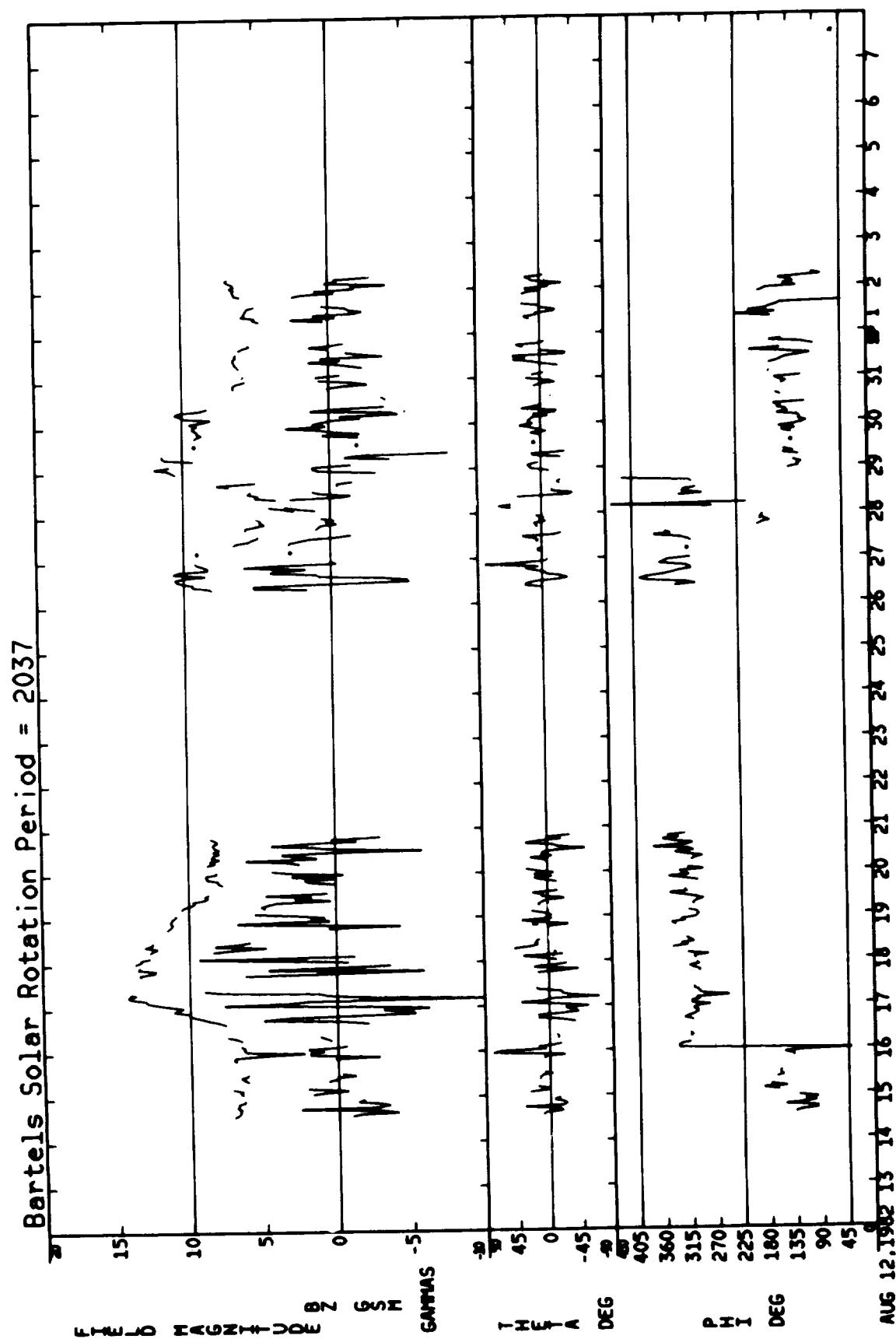


08/12/82 – 09/07/82

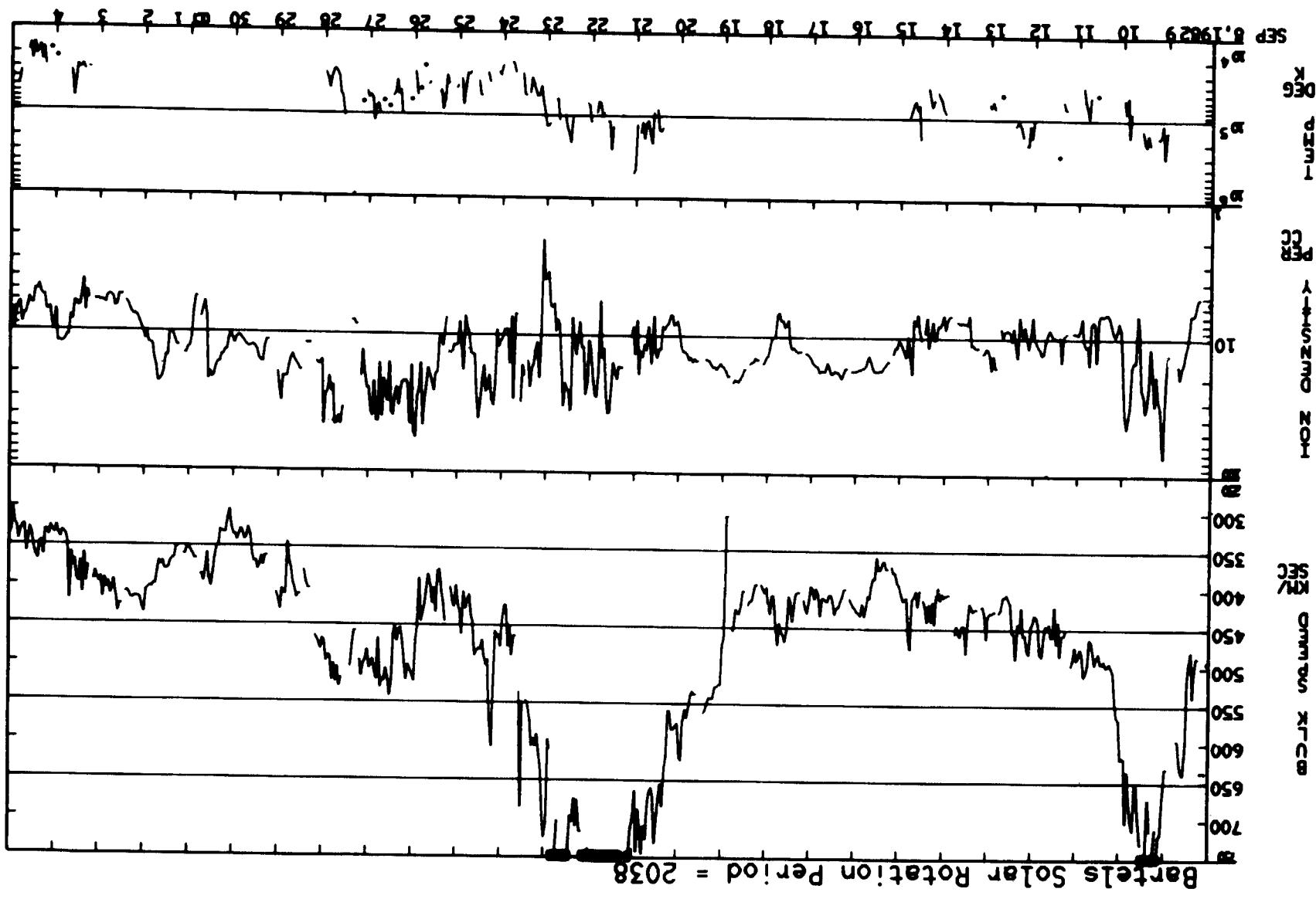


ORIGINAL PAGE IS  
OF POOR QUALITY

08/12/82 — 09/07/82

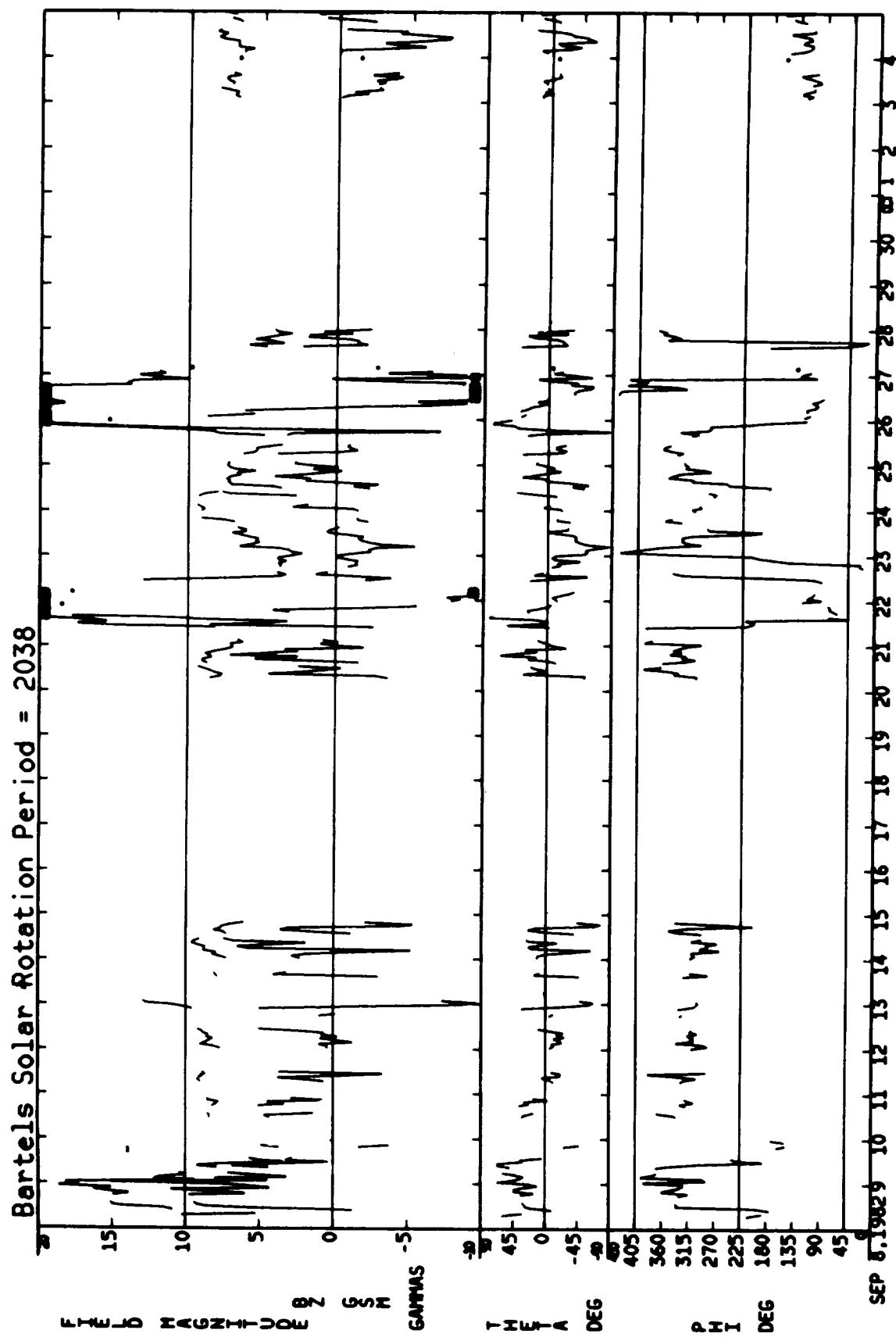


09/08/82 - 10/04/82

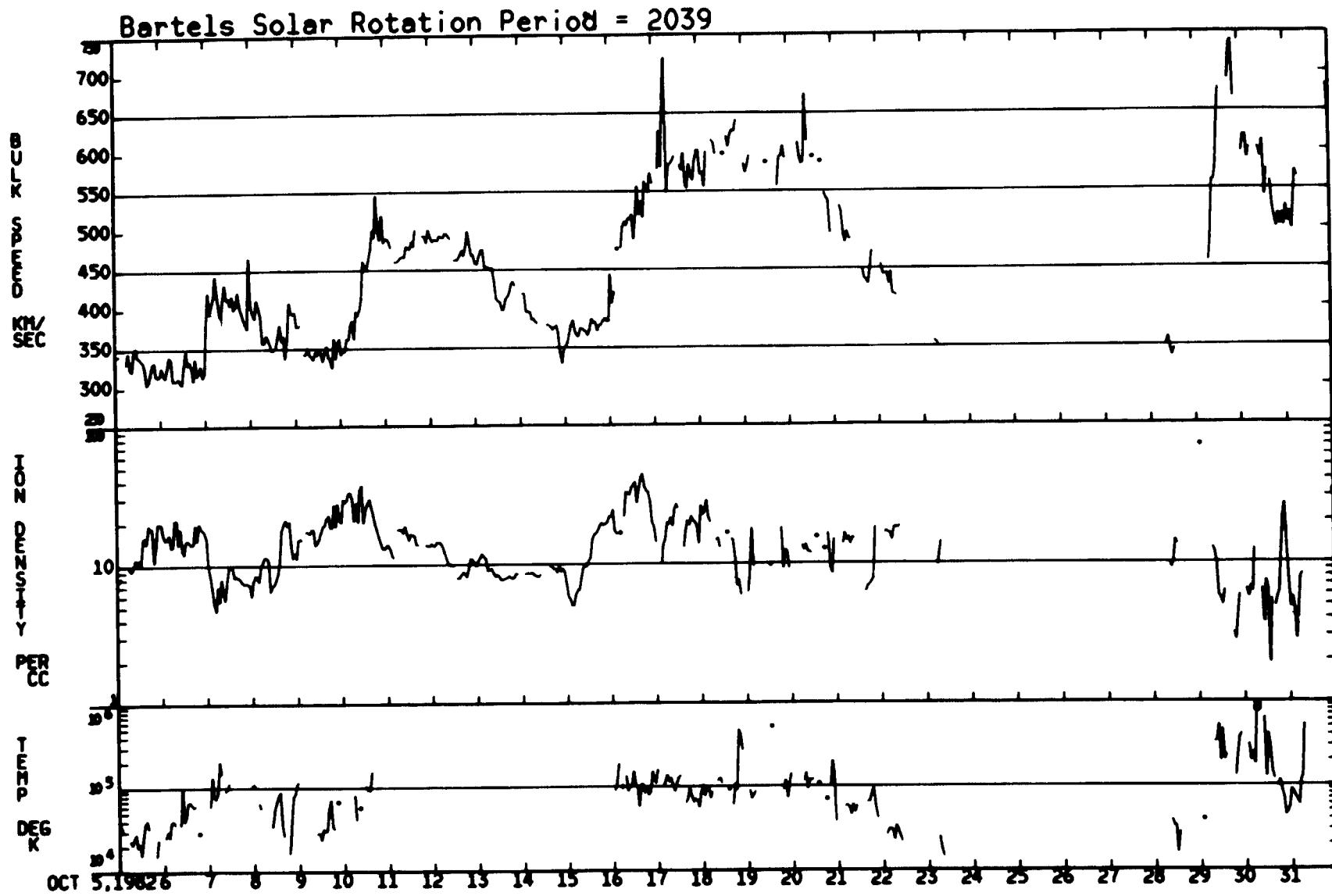


ORIGINAL PAGE IS  
OF POOR QUALITY

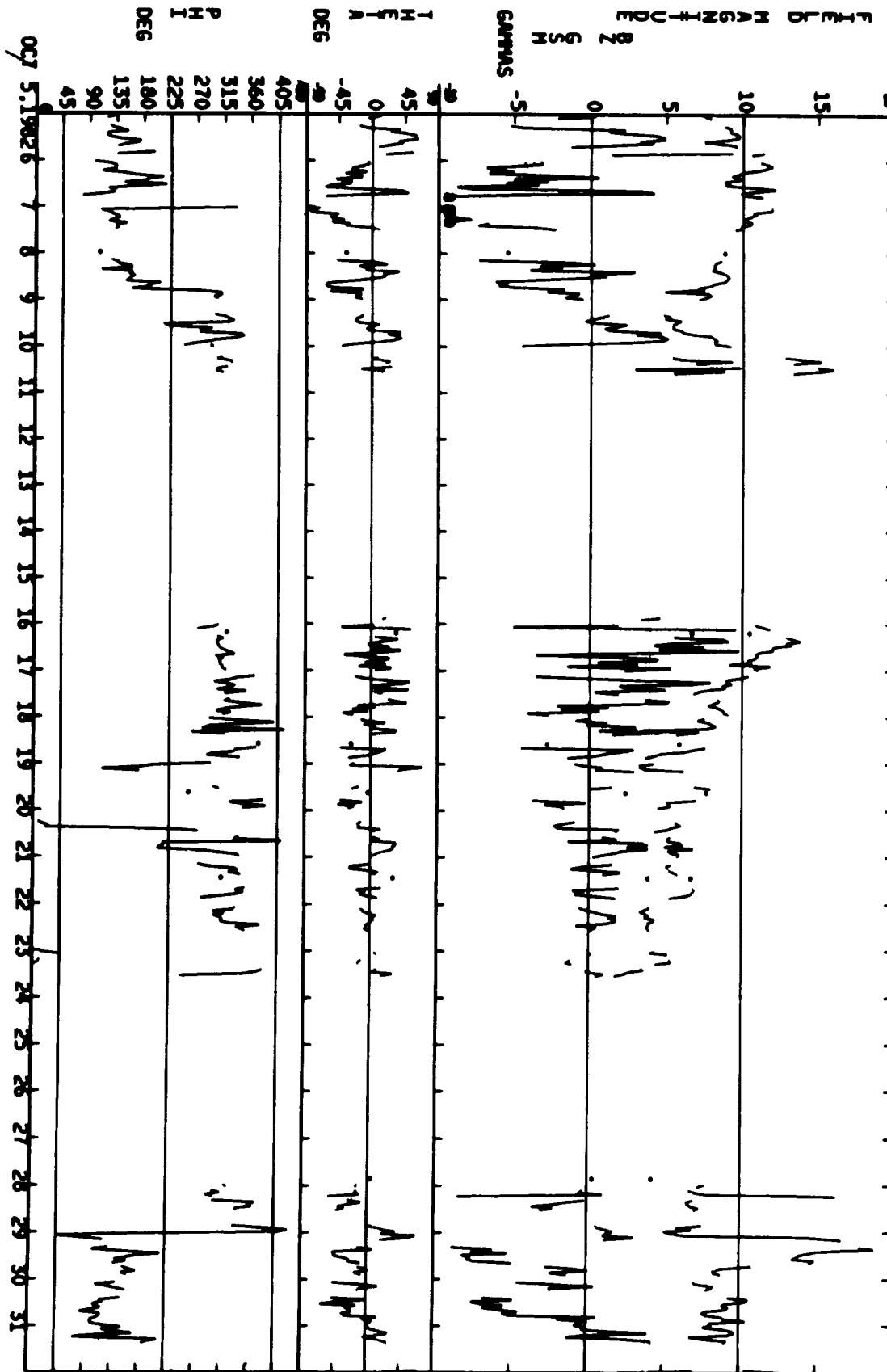
09/08/82 — 10/04/82



10/05/82 — 10/31/82



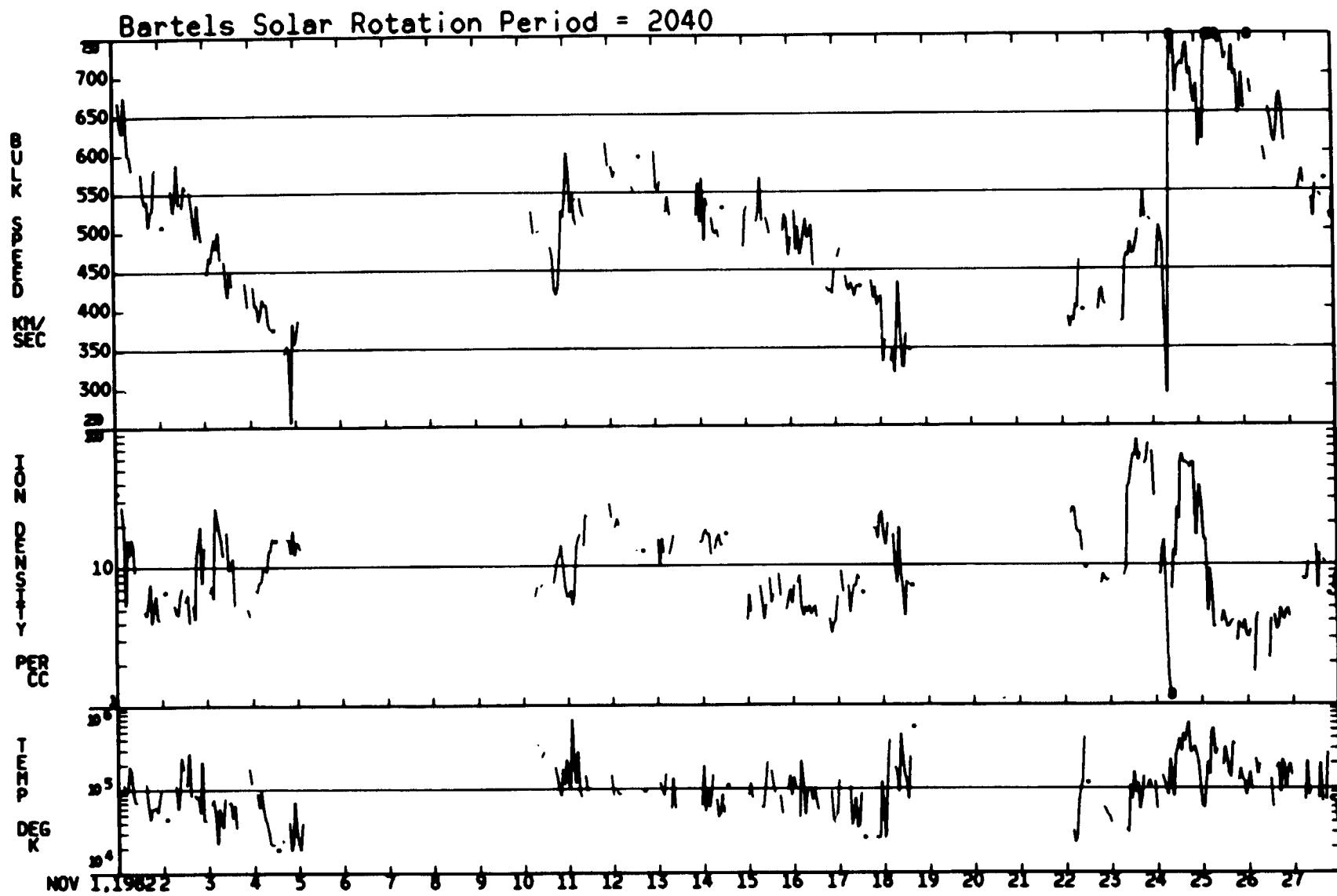
Bartels Solar Rotation Period = 2039



ORIGINAL PAGE IS  
OF POOR QUALITY

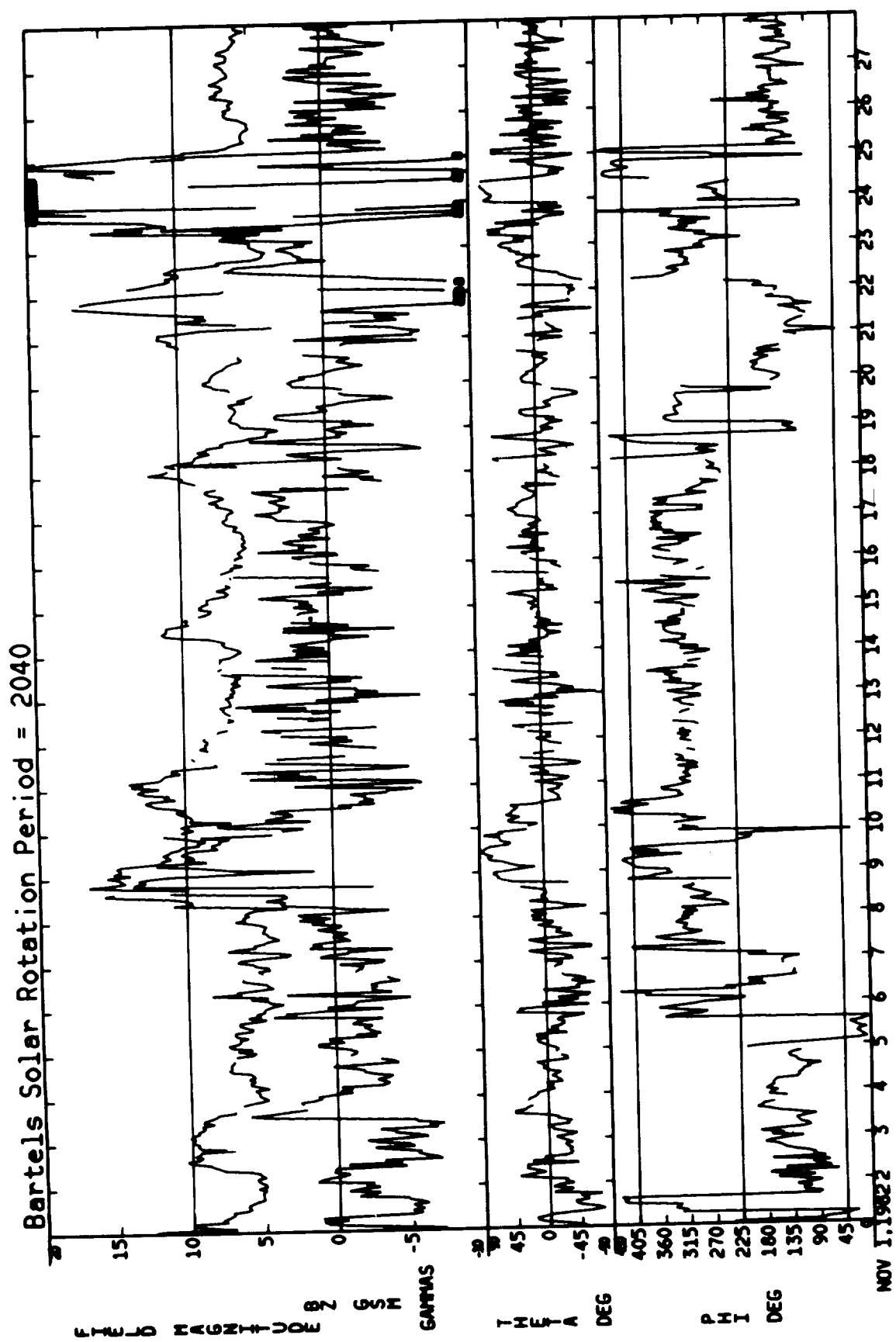
10/05/82 - 10/31/82

11/01/82 - 11/27/82

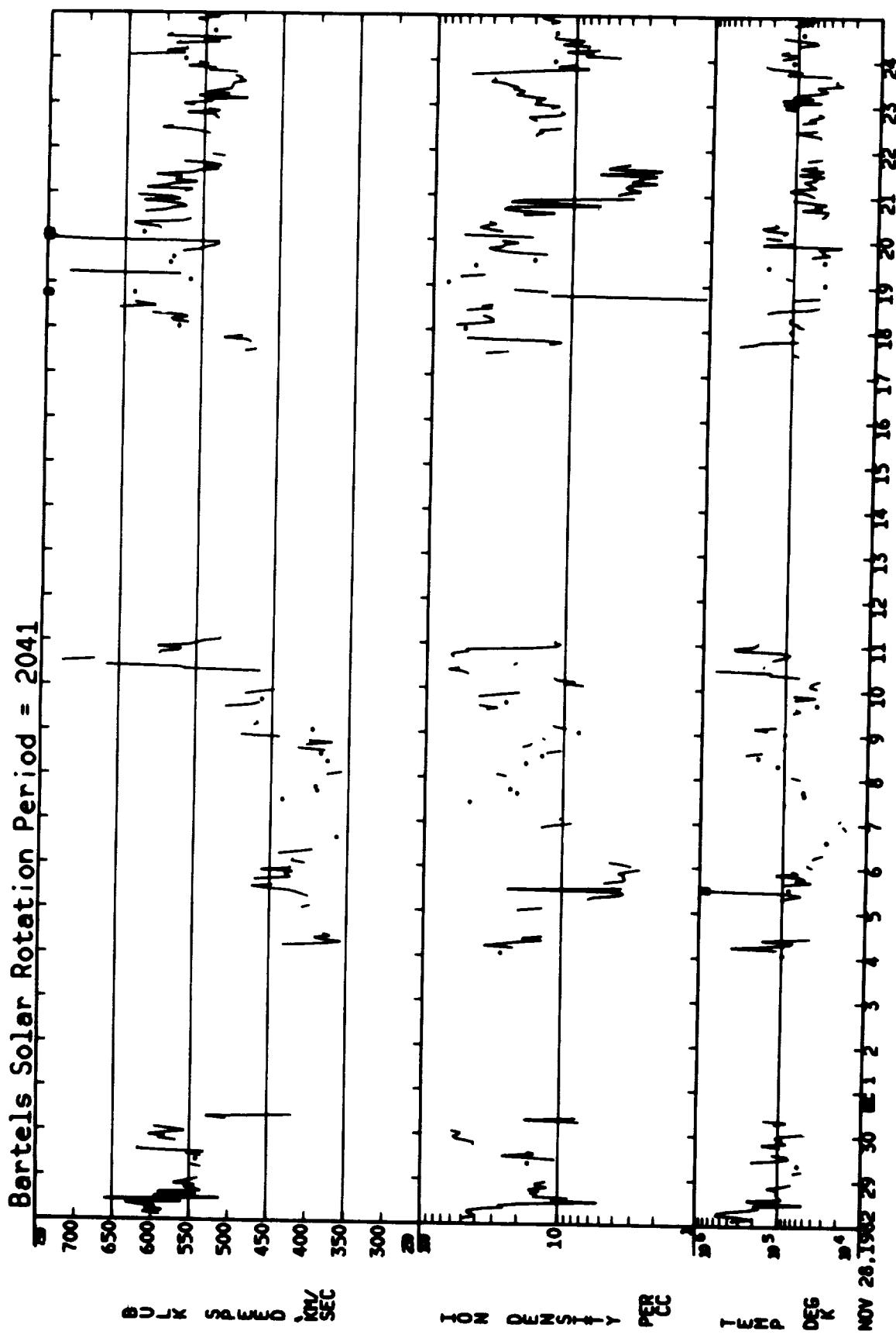


ORIGINAL PAGE IS  
OF POOR QUALITY

11/01/82 - 11/27/82

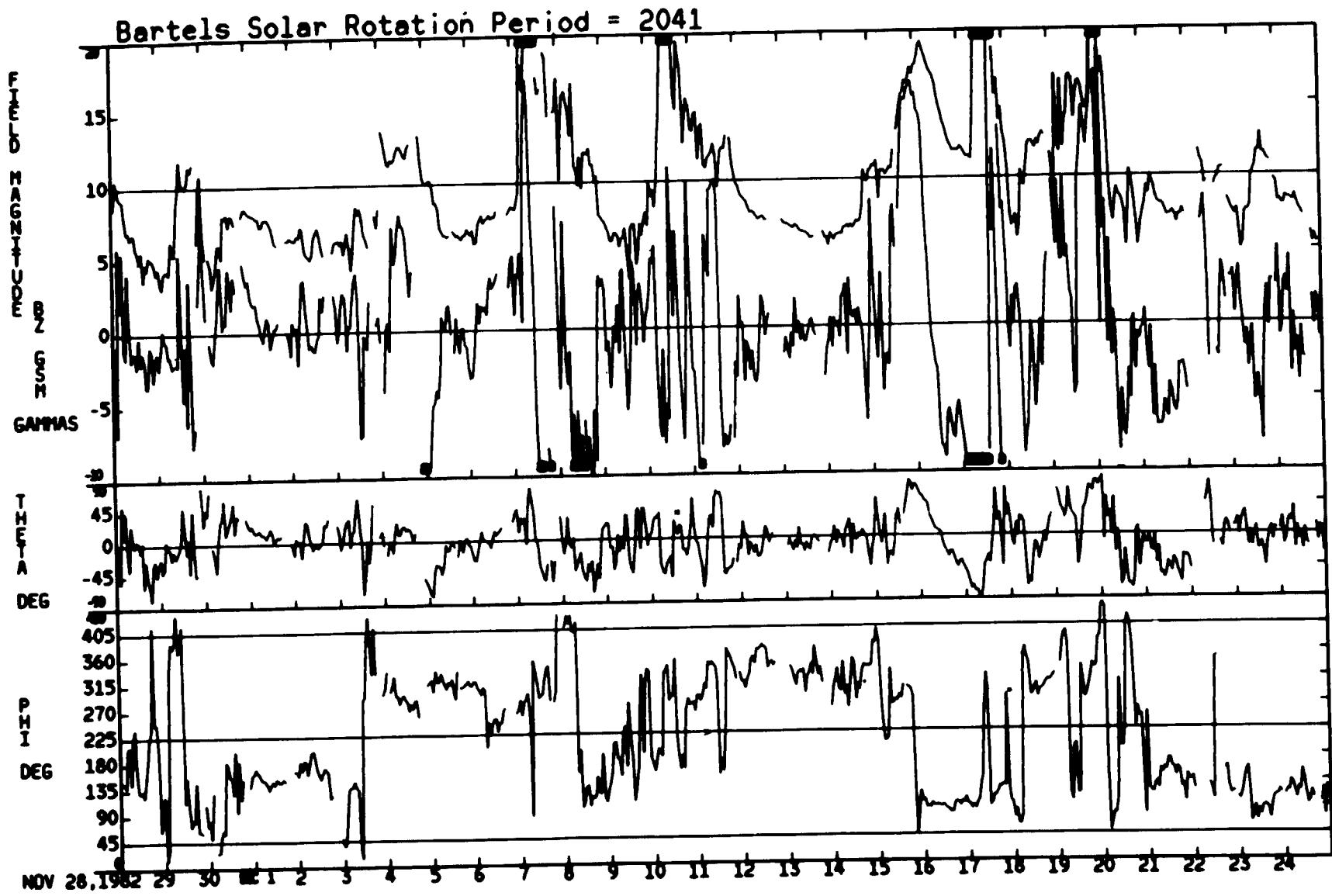


11/28/82 — 12/24/82

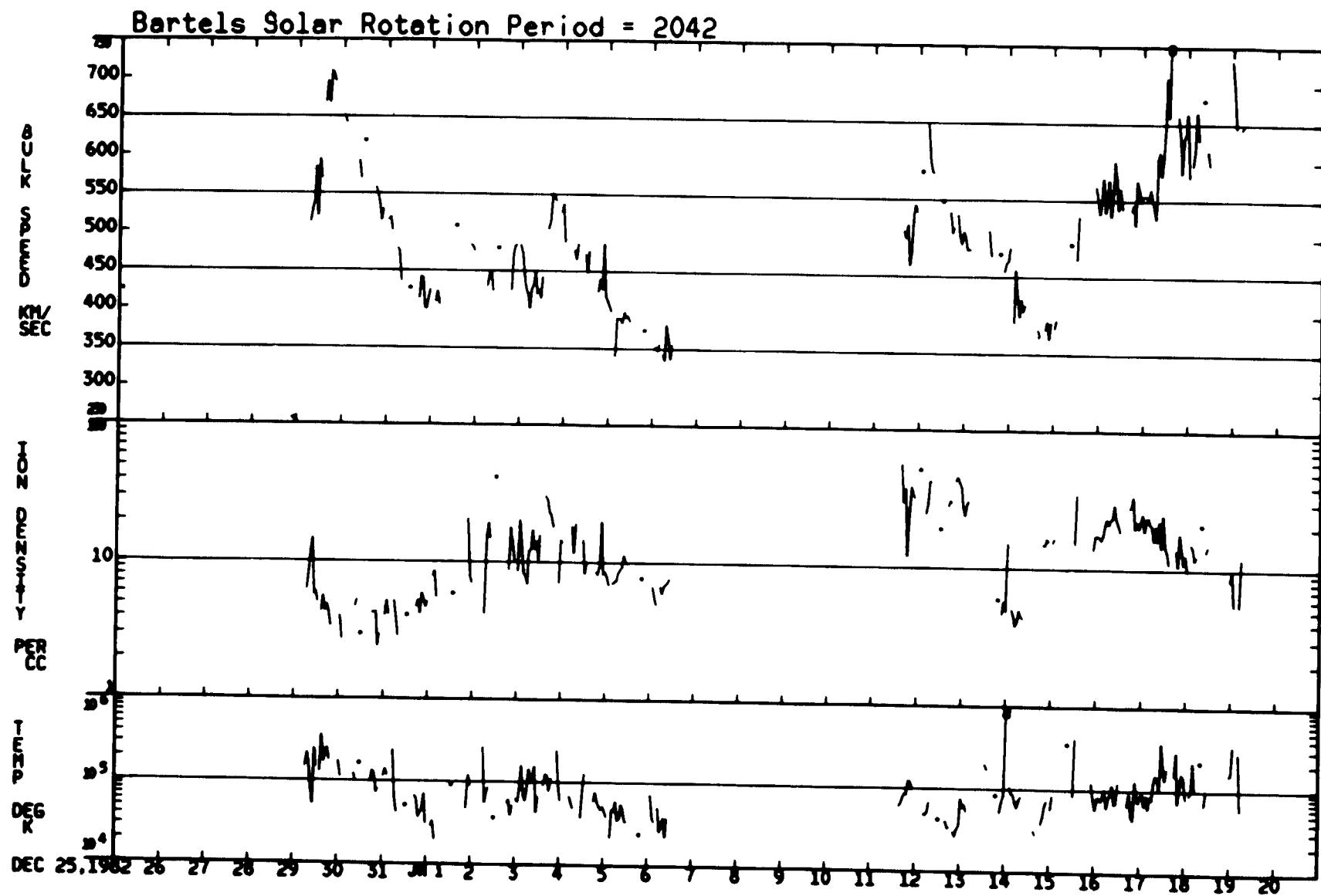


ORIGINAL PAGE IS  
OF POOR QUALITY

11/28/82 - 12/24/82

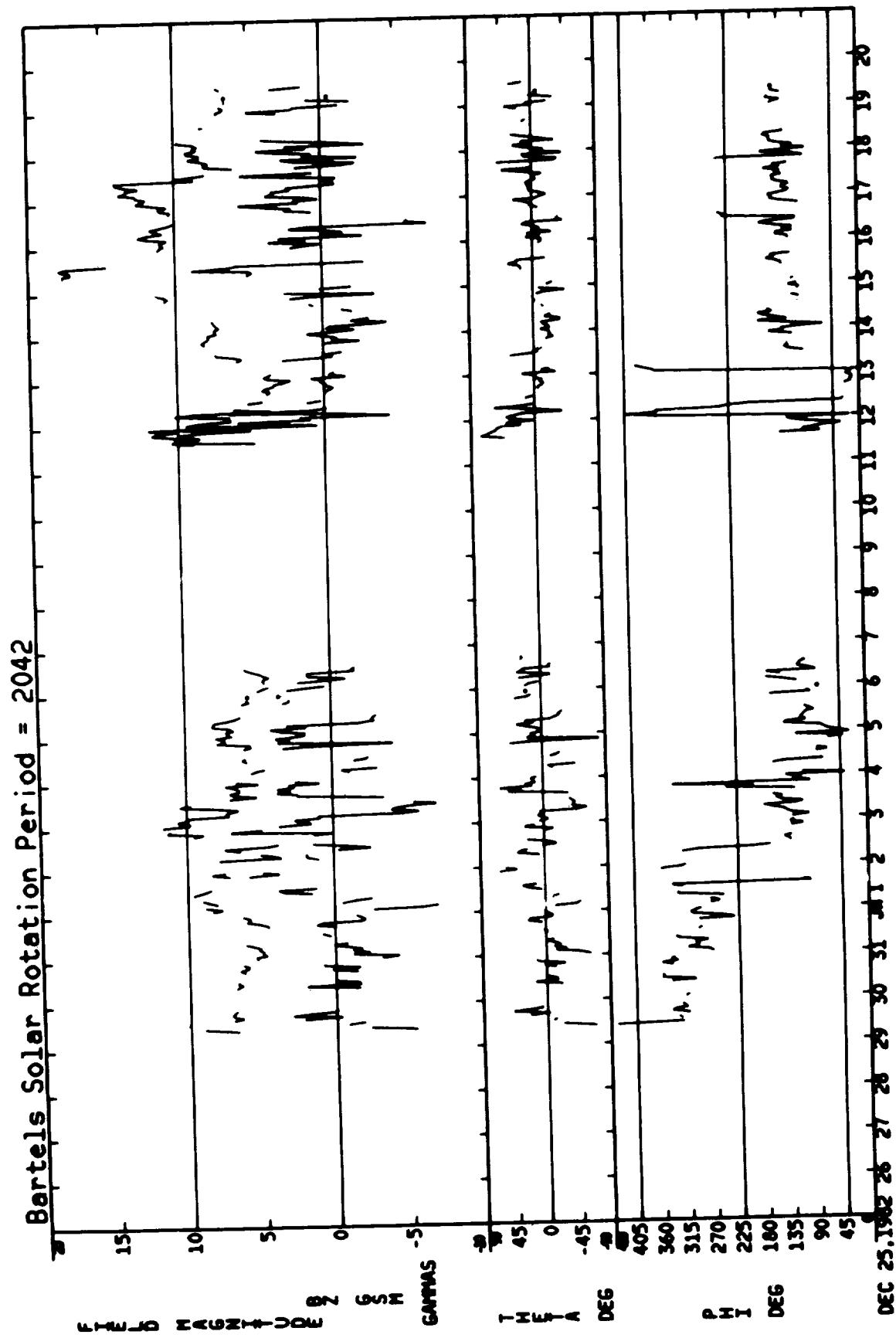


12/25/82 – 01/20/83

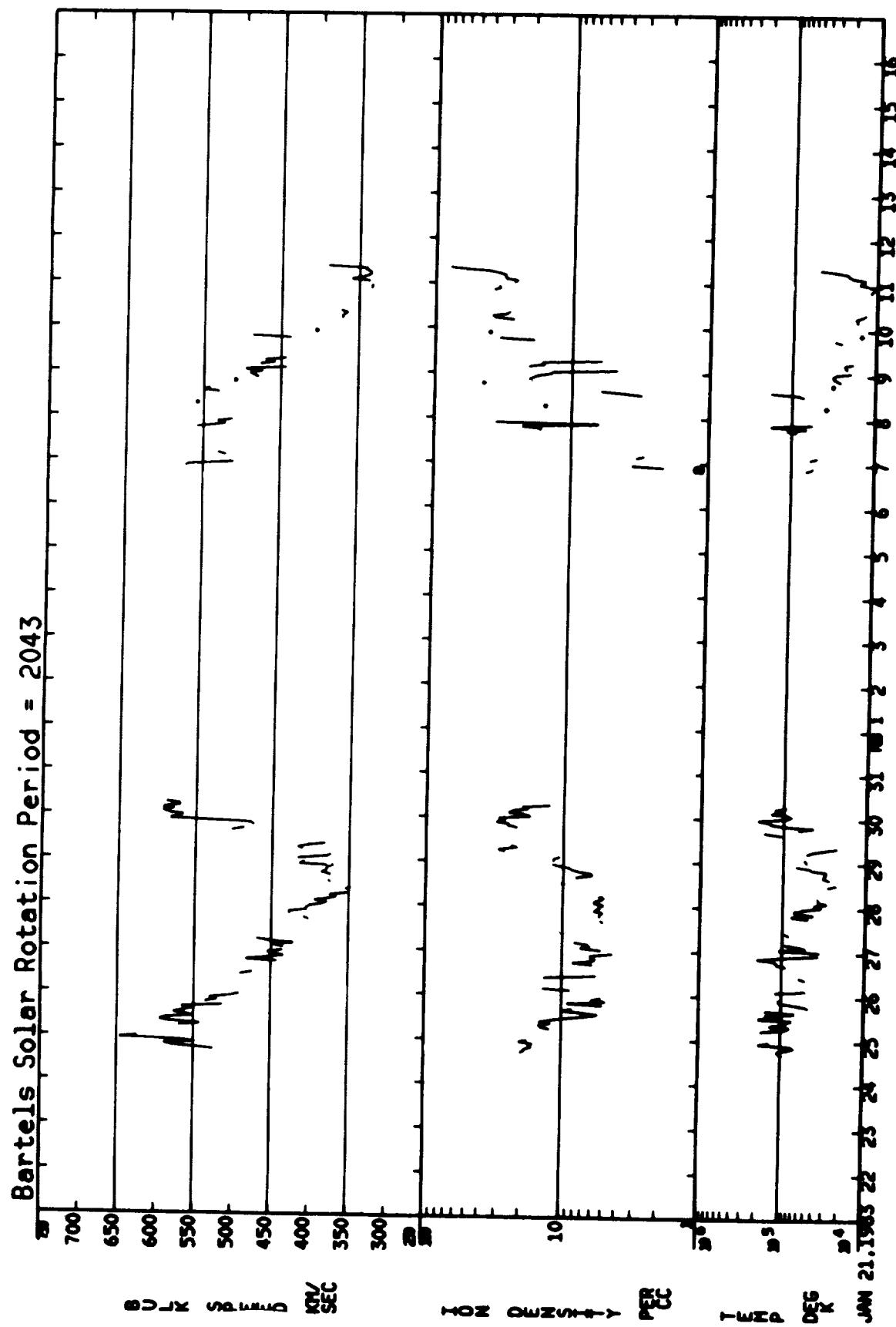


ORIGINAL PAGE IS  
OF POOR QUALITY

12/25/82 - 01/20/83



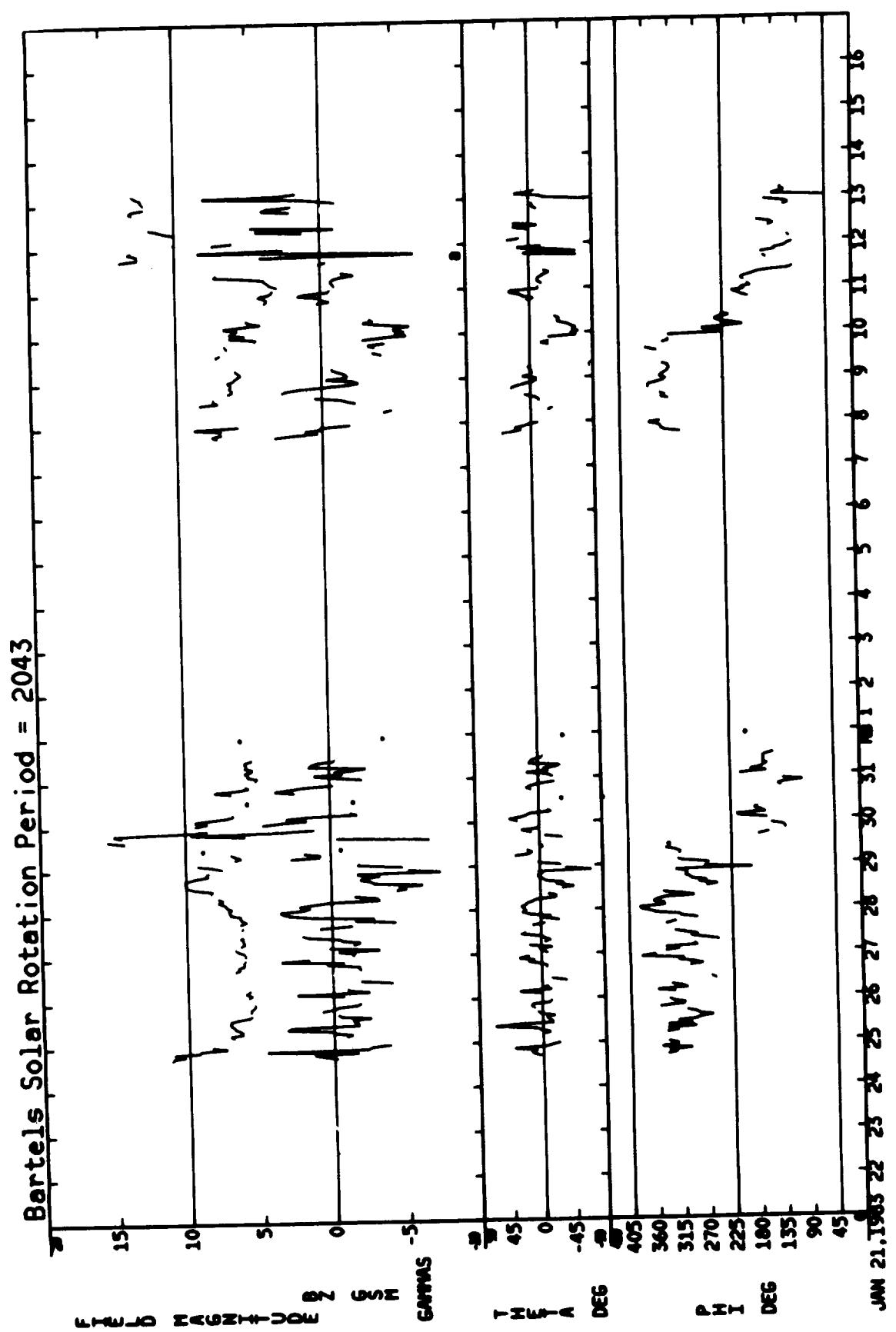
01/21/83 – 02/16/83



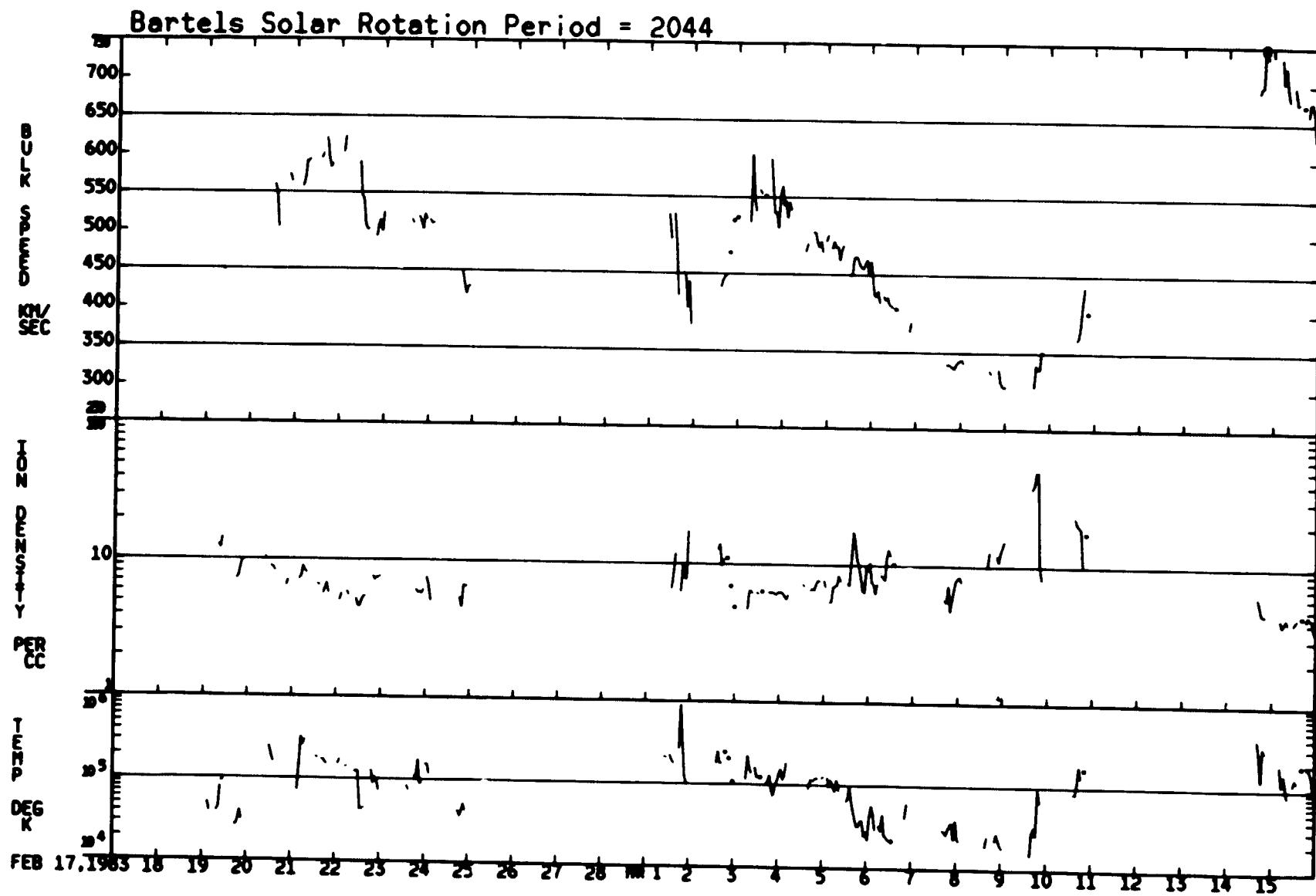
ORIGINAL PAGE IS  
OF POOR QUALITY

ORIGINAL PAGE IS  
OF POOR QUALITY

01/21/83 - 02/16/83

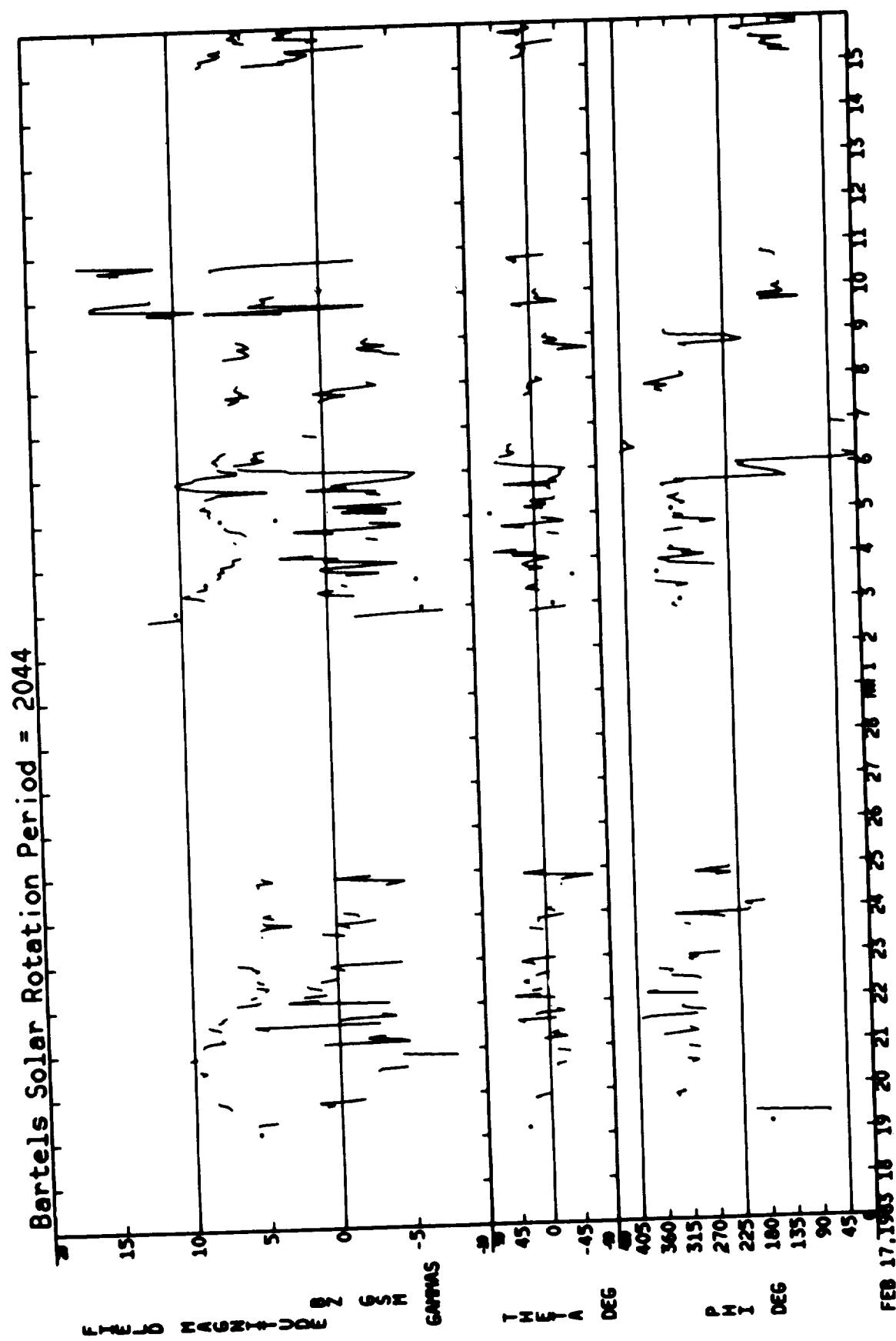


02/17/83 – 03/15/83

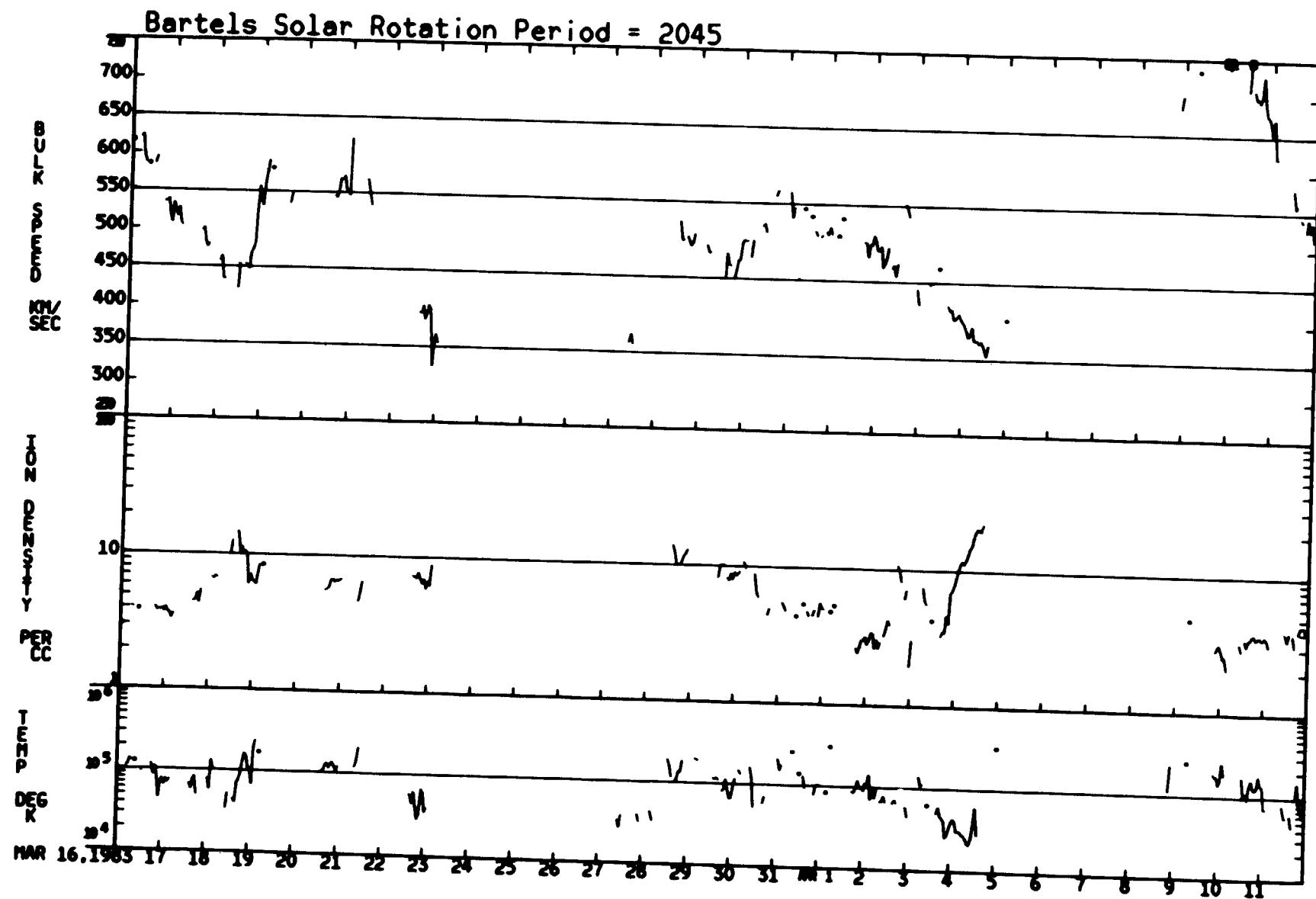


ORIGINAL PAGE IS  
OF POOR QUALITY

02/17/83 — 03/15/83

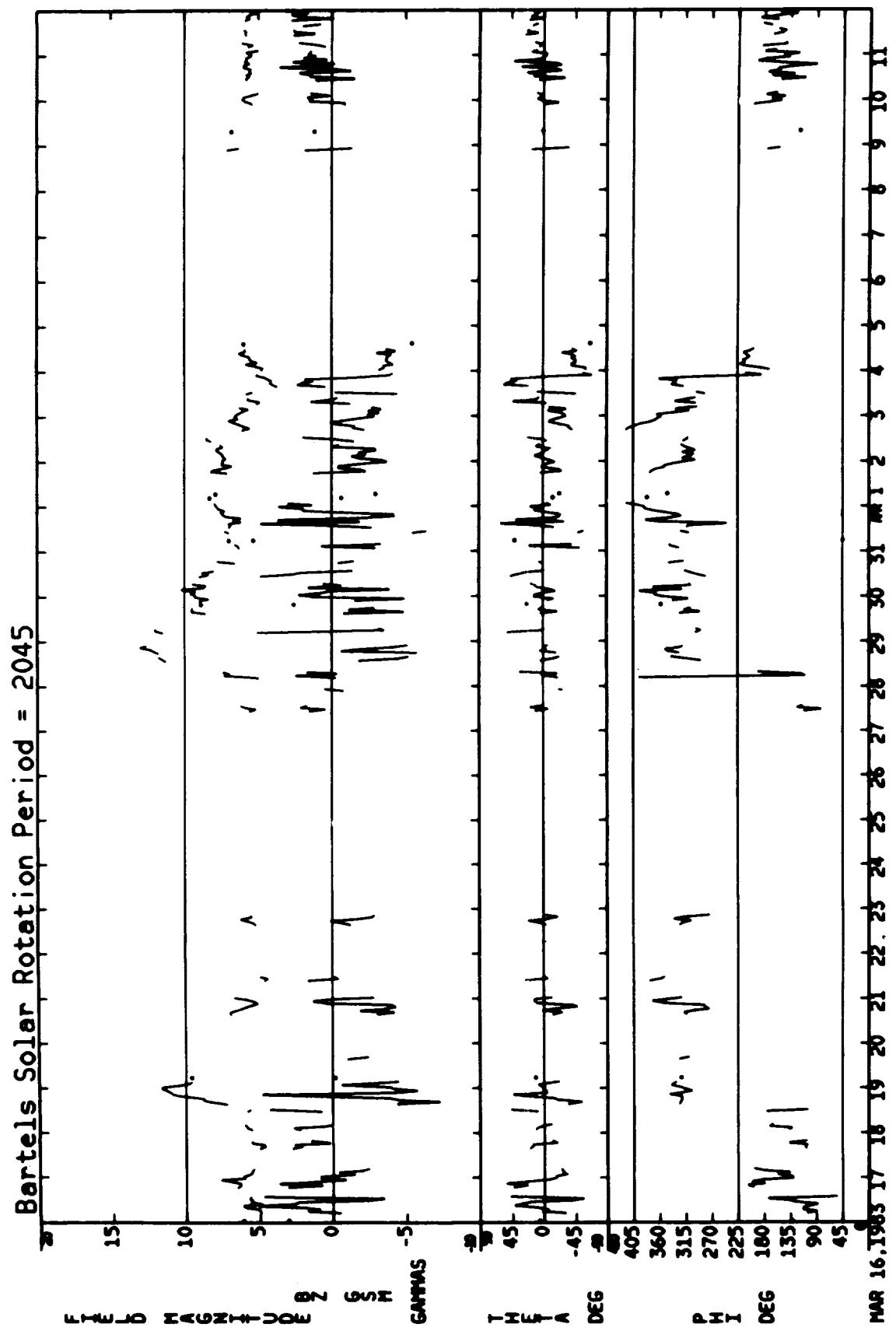


03/16/83 – 04/11/83

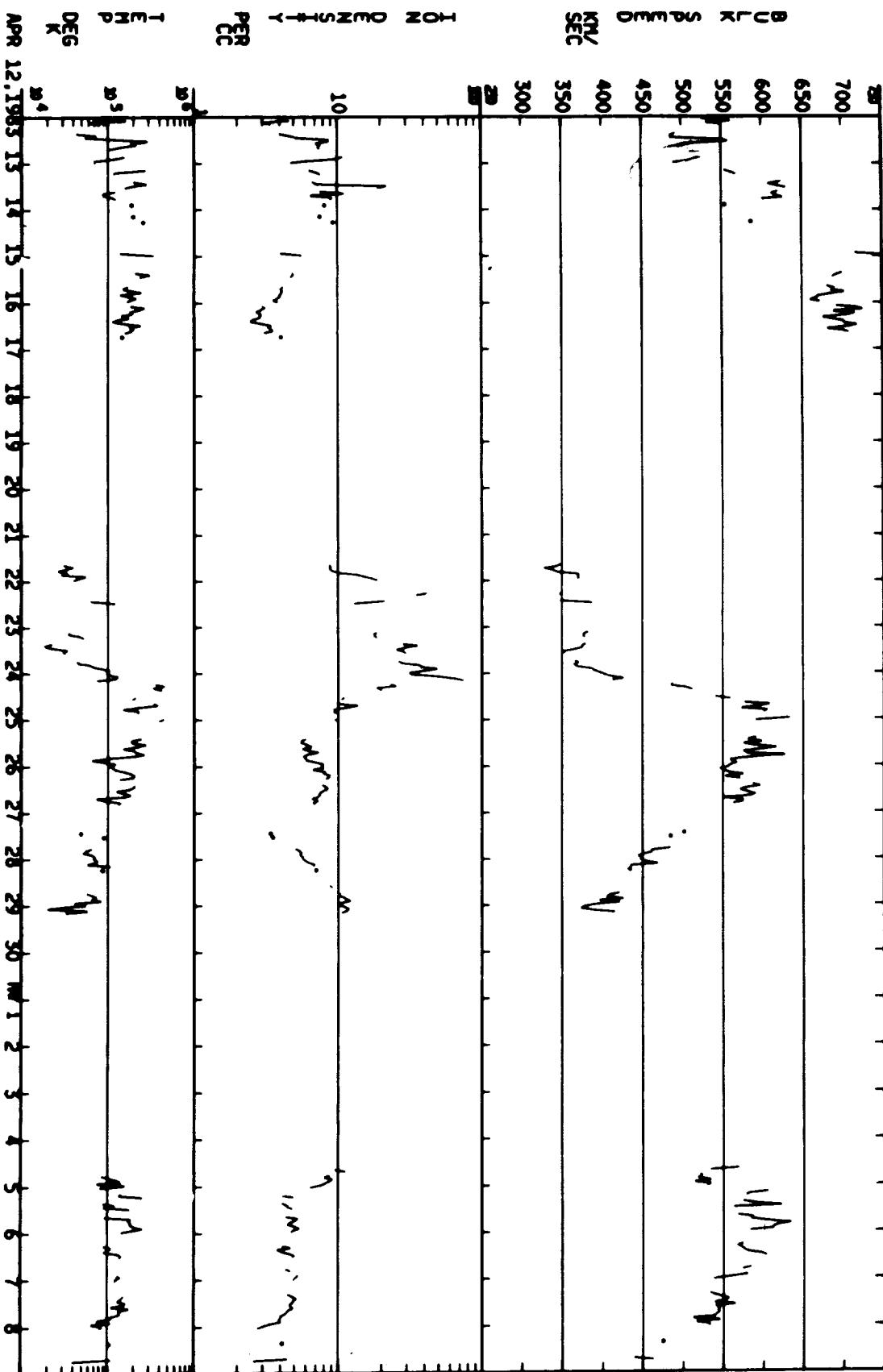


ORIGINAL PAGE IS  
OF POOR QUALITY

03/16/83 - 04/11/83



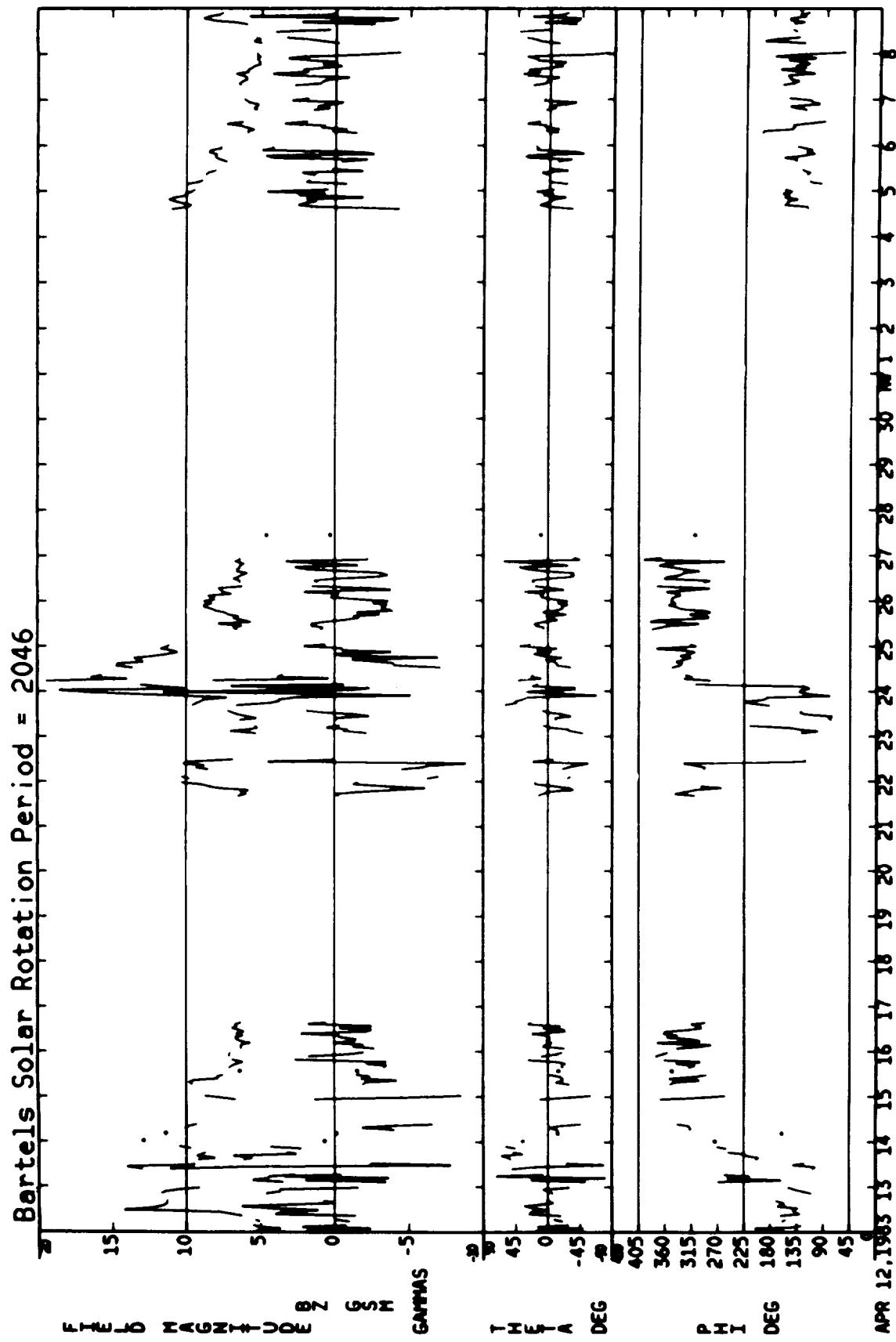
Bartels Solar Rotation Period = 2046



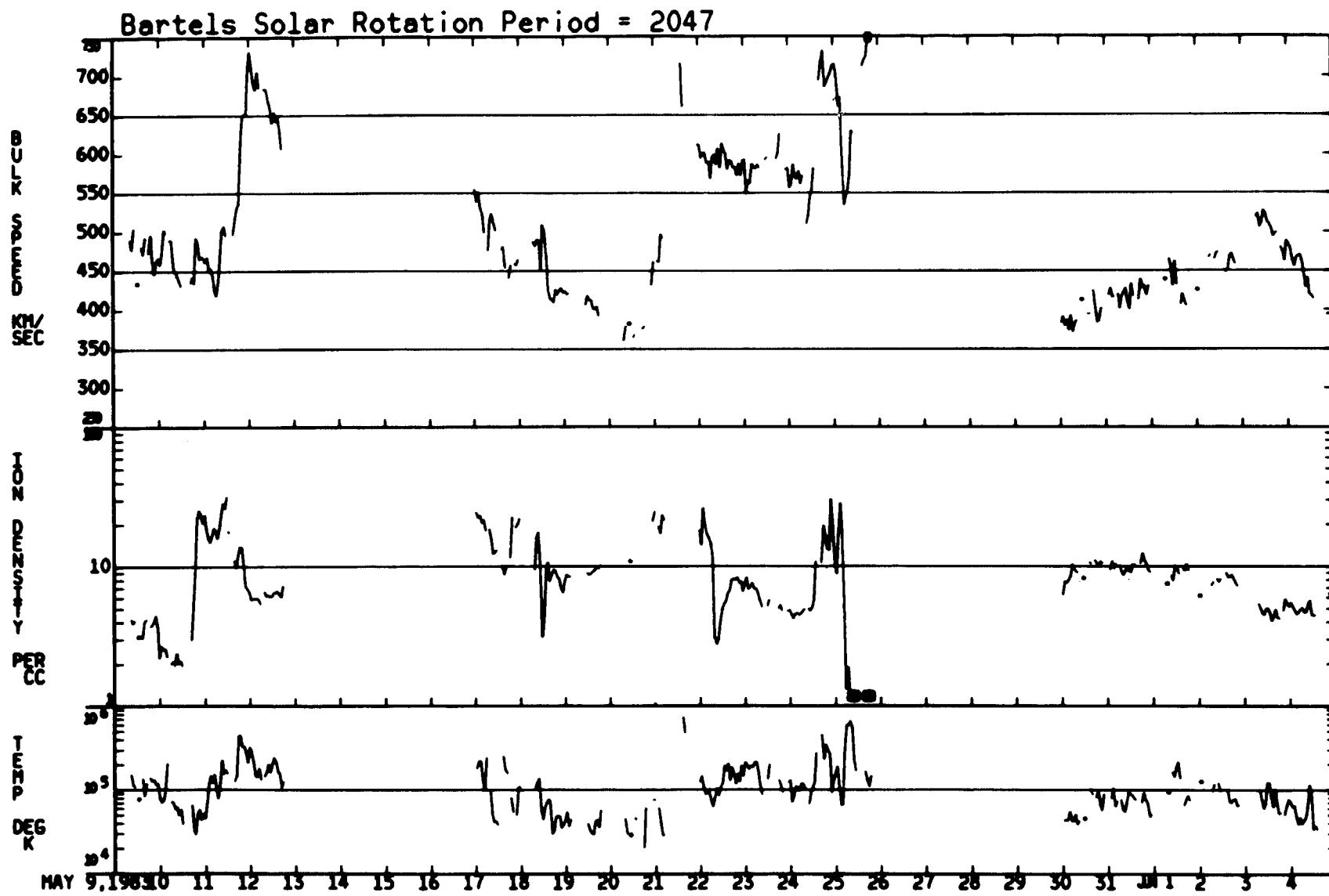
04/12/83 - 05/08/83

ORIGINAL PAGE IS  
OF POOR QUALITY

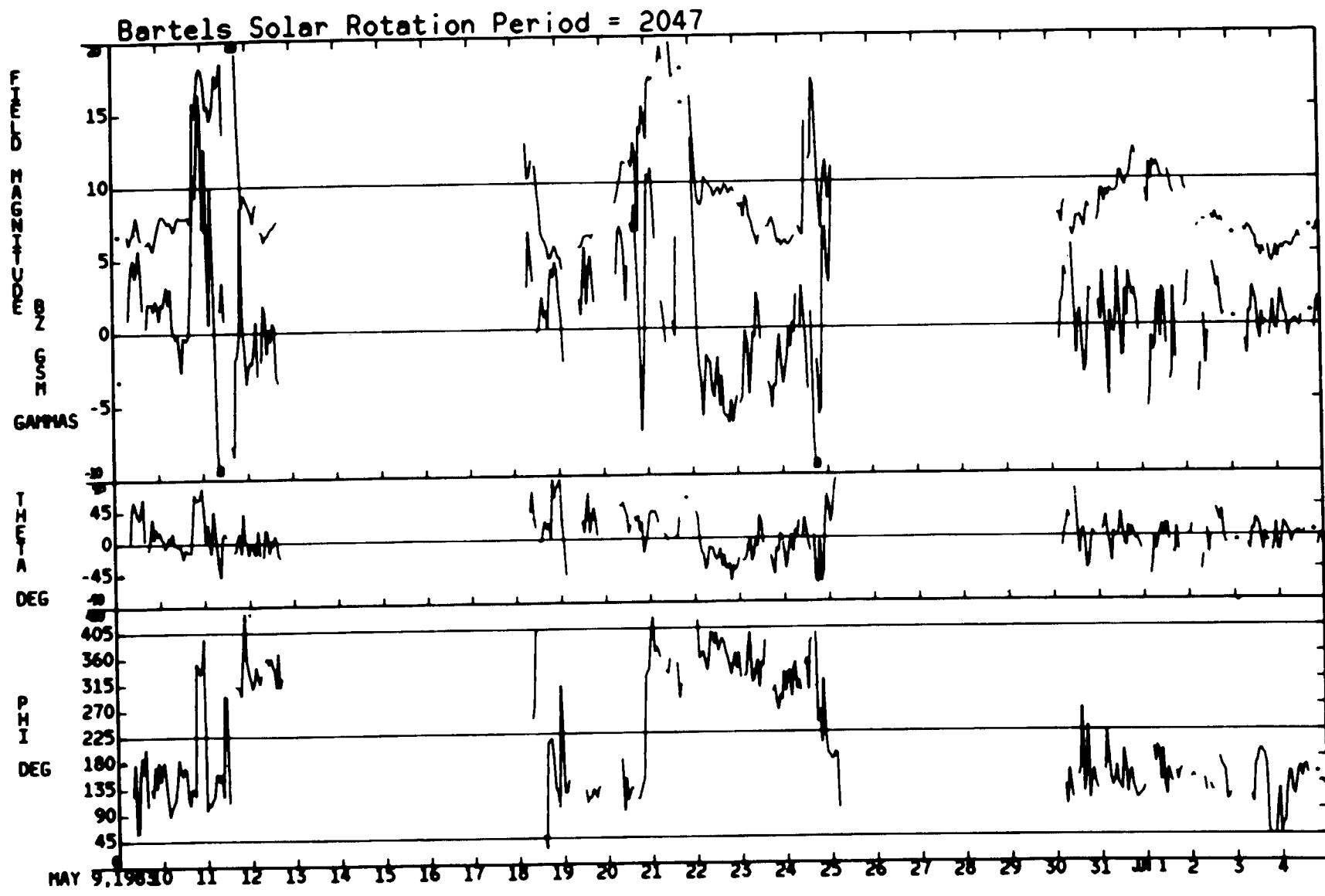
04/12/83 — 05/08/83



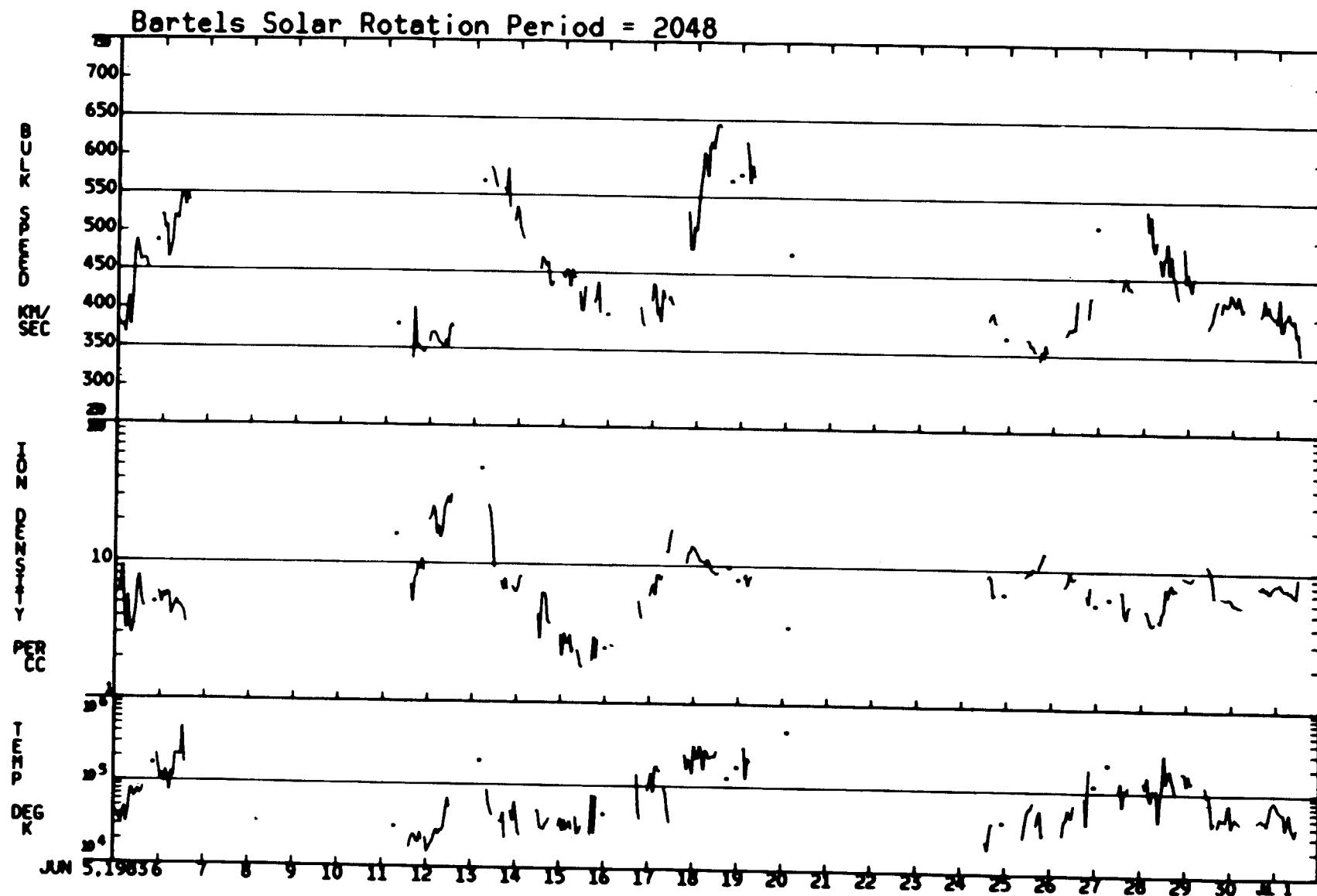
05/09/83 — 06/04/83



05/09/83 – 06/04/83  
ORIGINAL PAGE IS  
OF POOR QUALITY

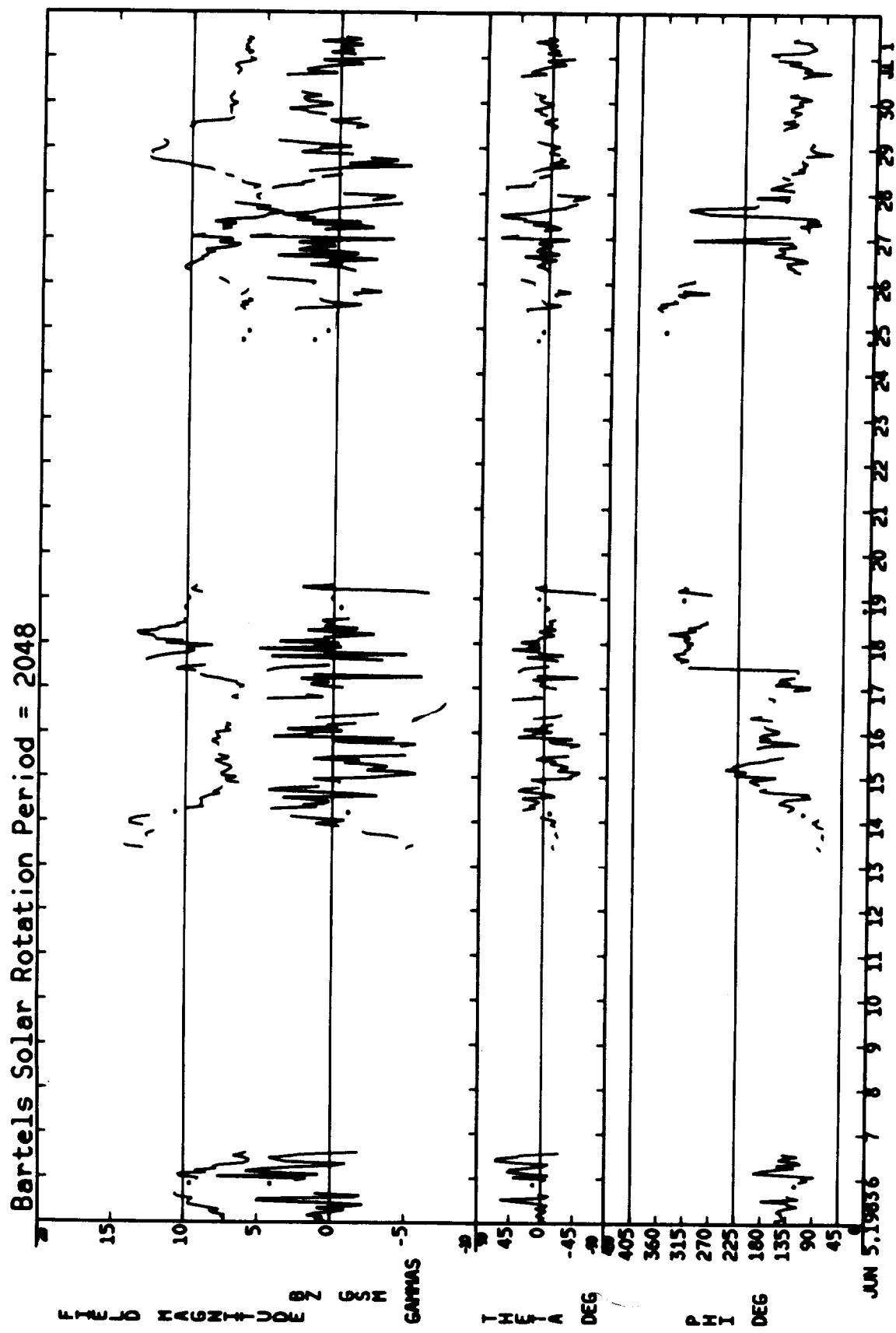


06/05/83 — 07/01/83

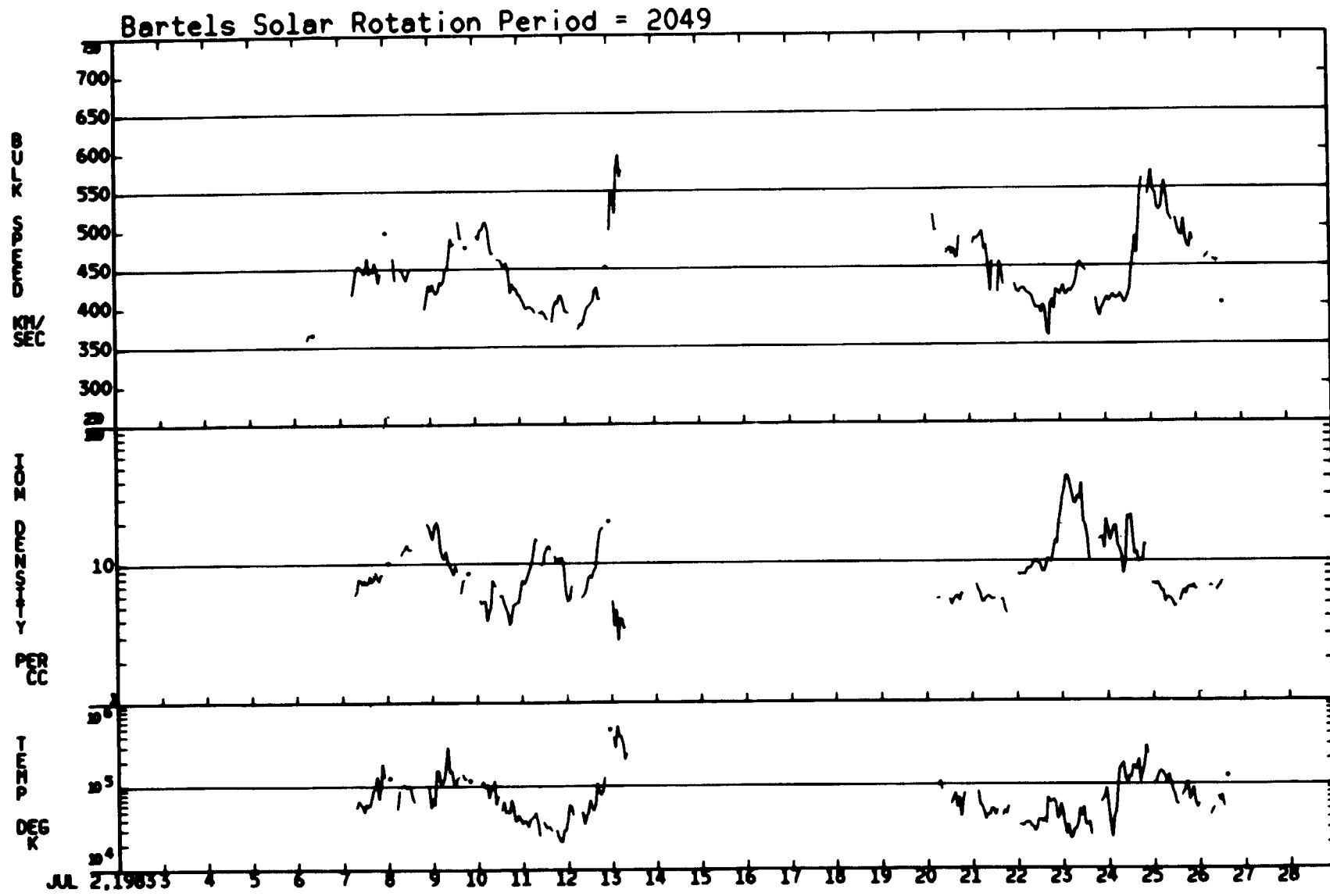


ORIGINAL PAGE IS  
OF POOR QUALITY

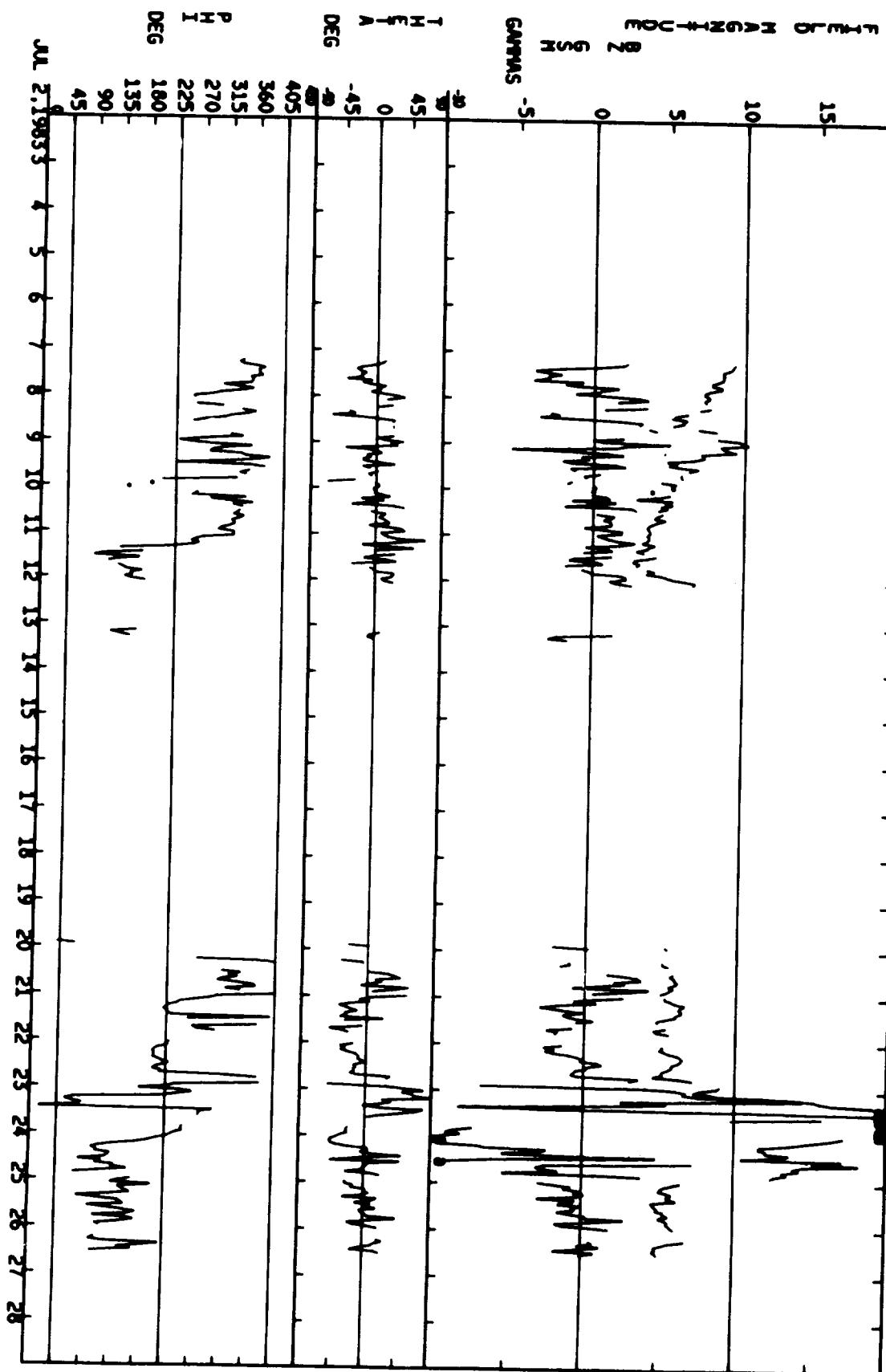
06/05/83 – 07/01/83



07/02/83 — 07/28/83

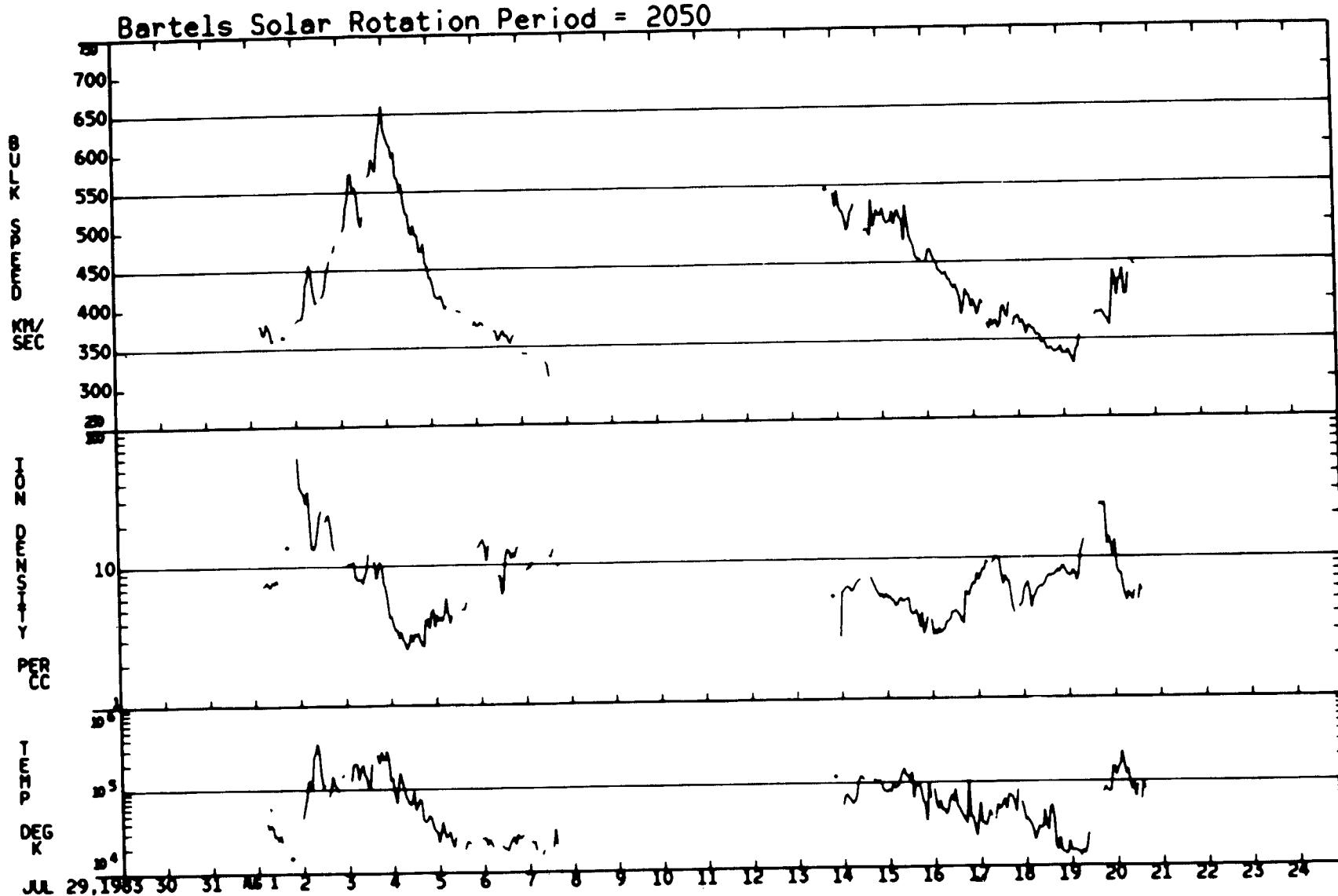


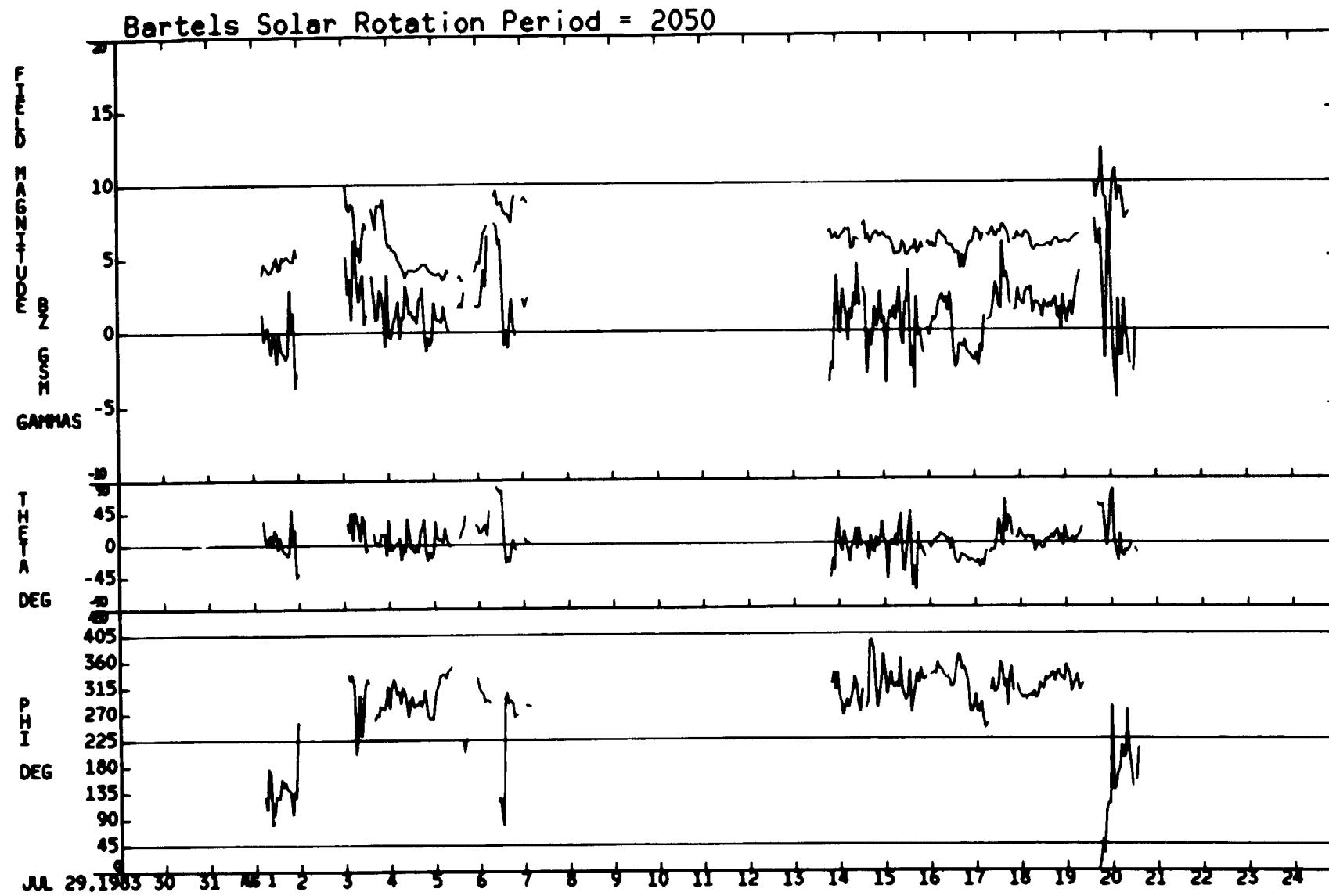
Bartels Solar Rotation Period = 2049



07/02/83 - 07/28/83

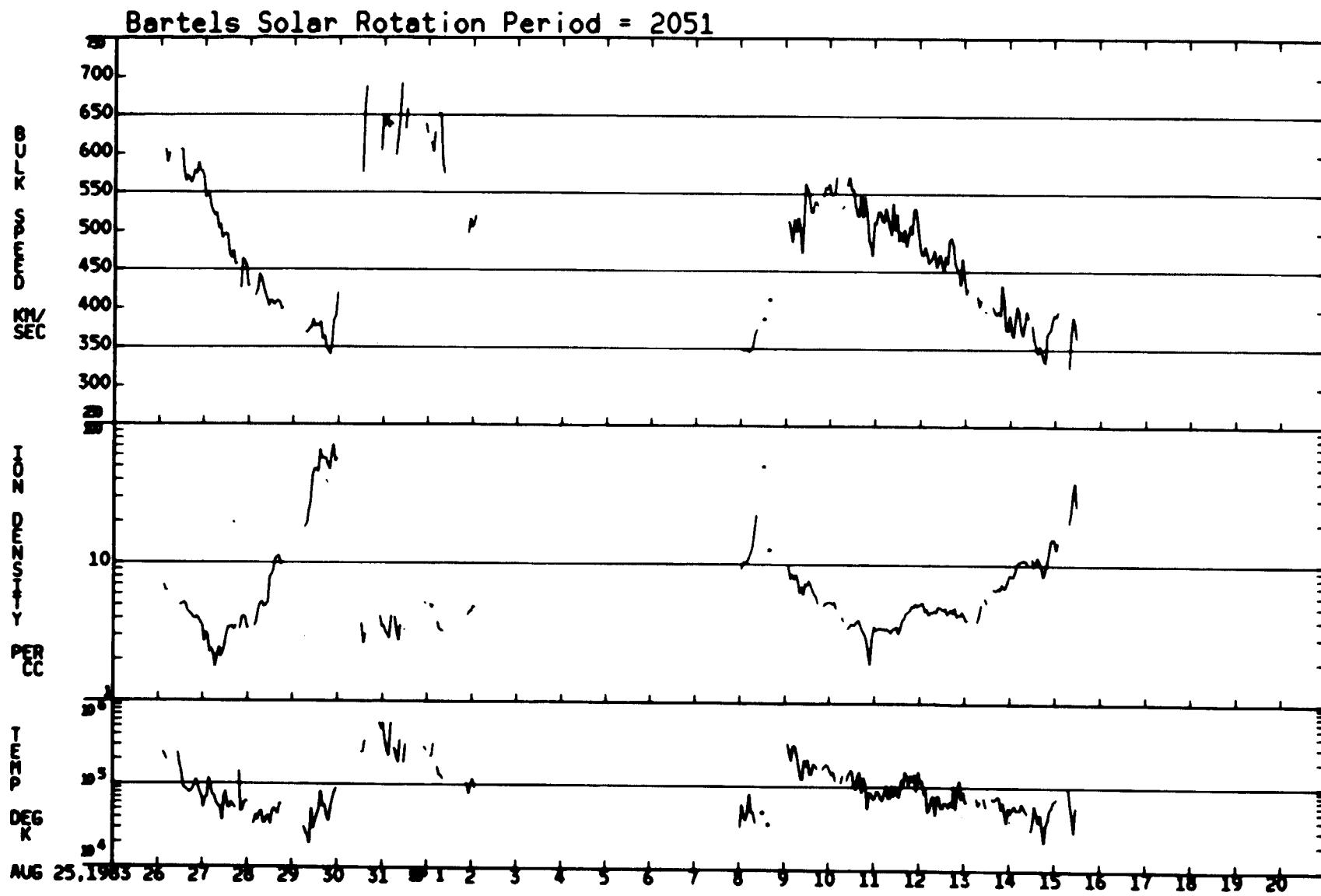
07/29/83 - 08/24/83



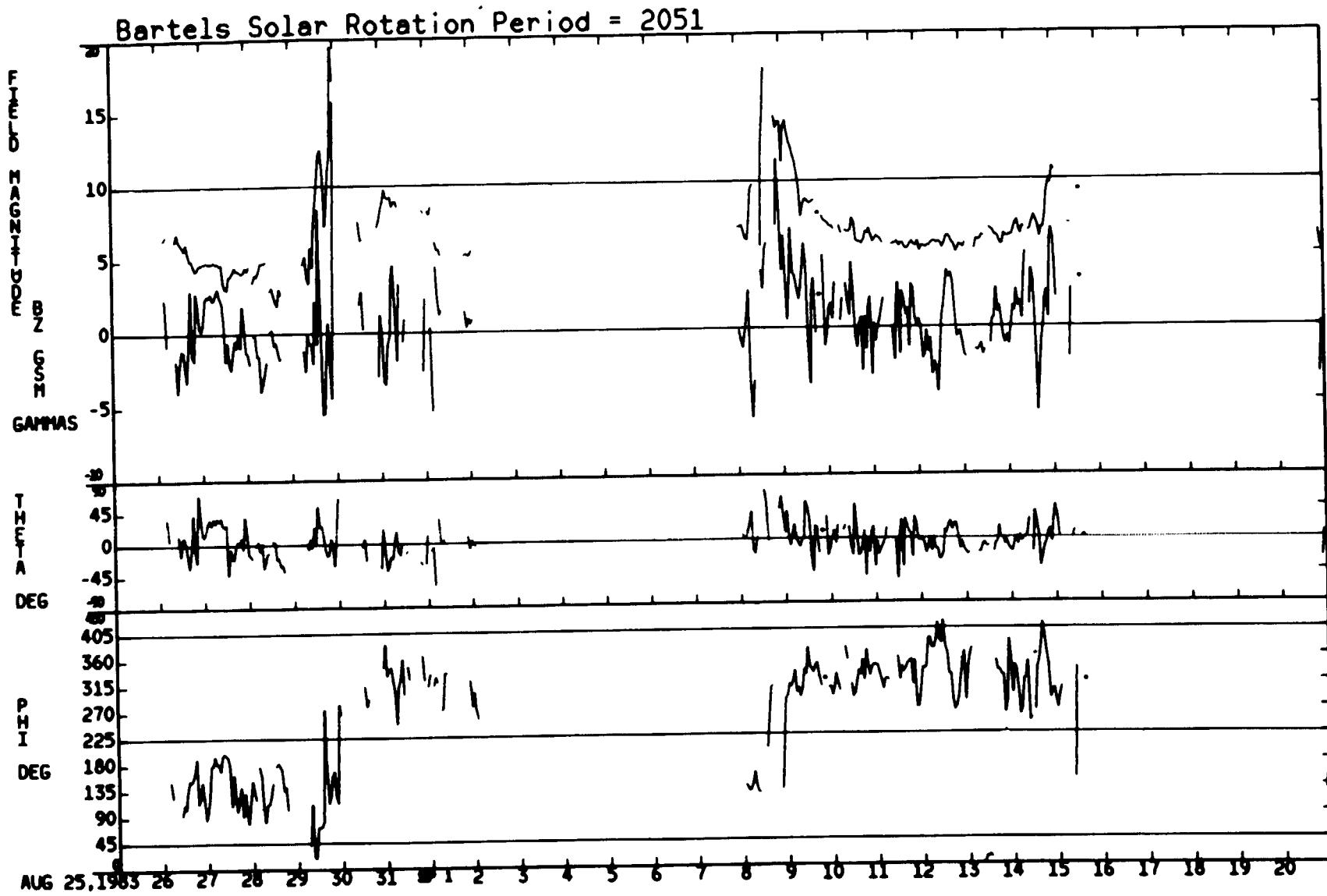


07/29/83 – 08/24/83

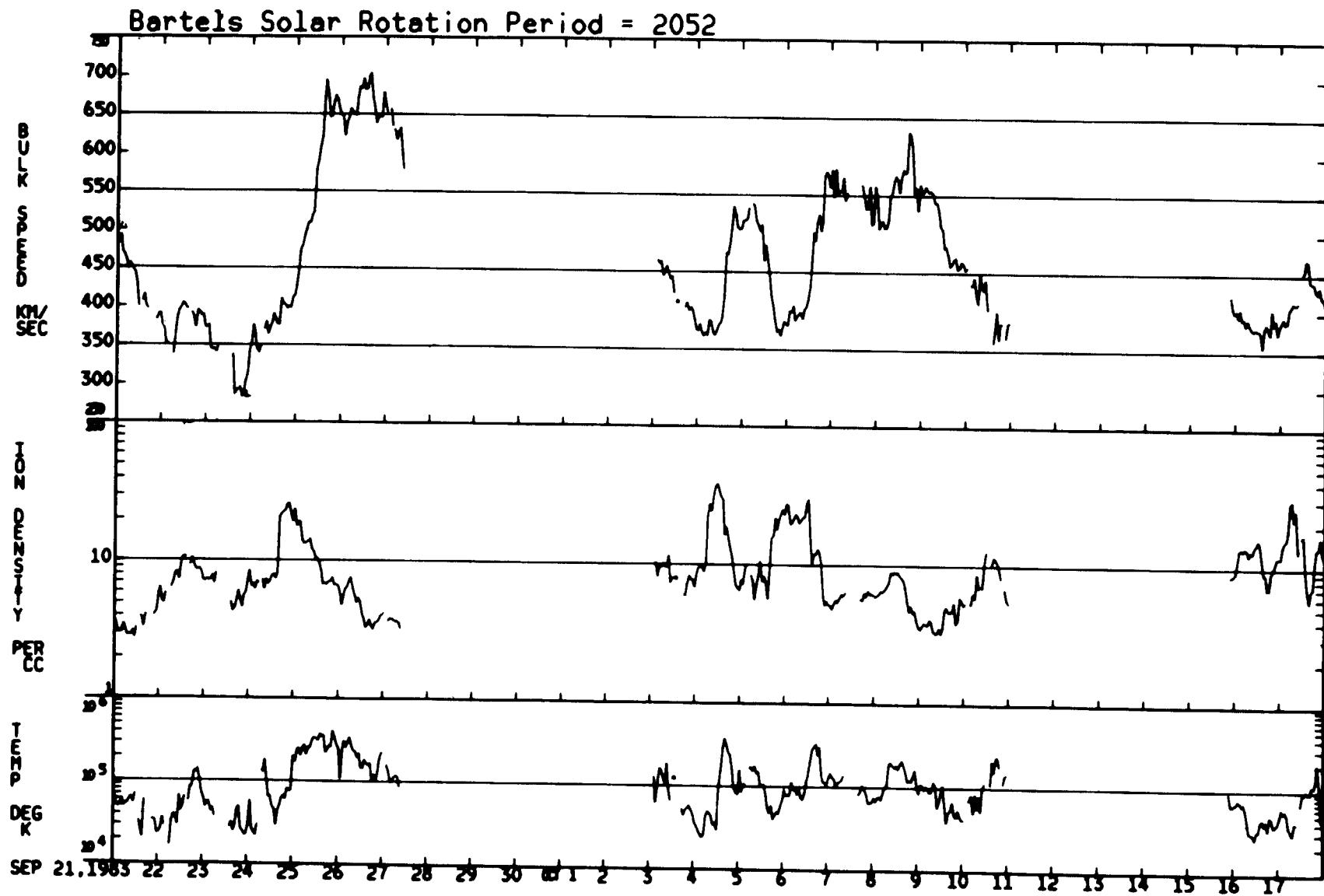
08/25/83 – 09/20/83



08/25/83 – 09/20/83  
ORIGINAL PAGE IS  
OF POOR QUALITY

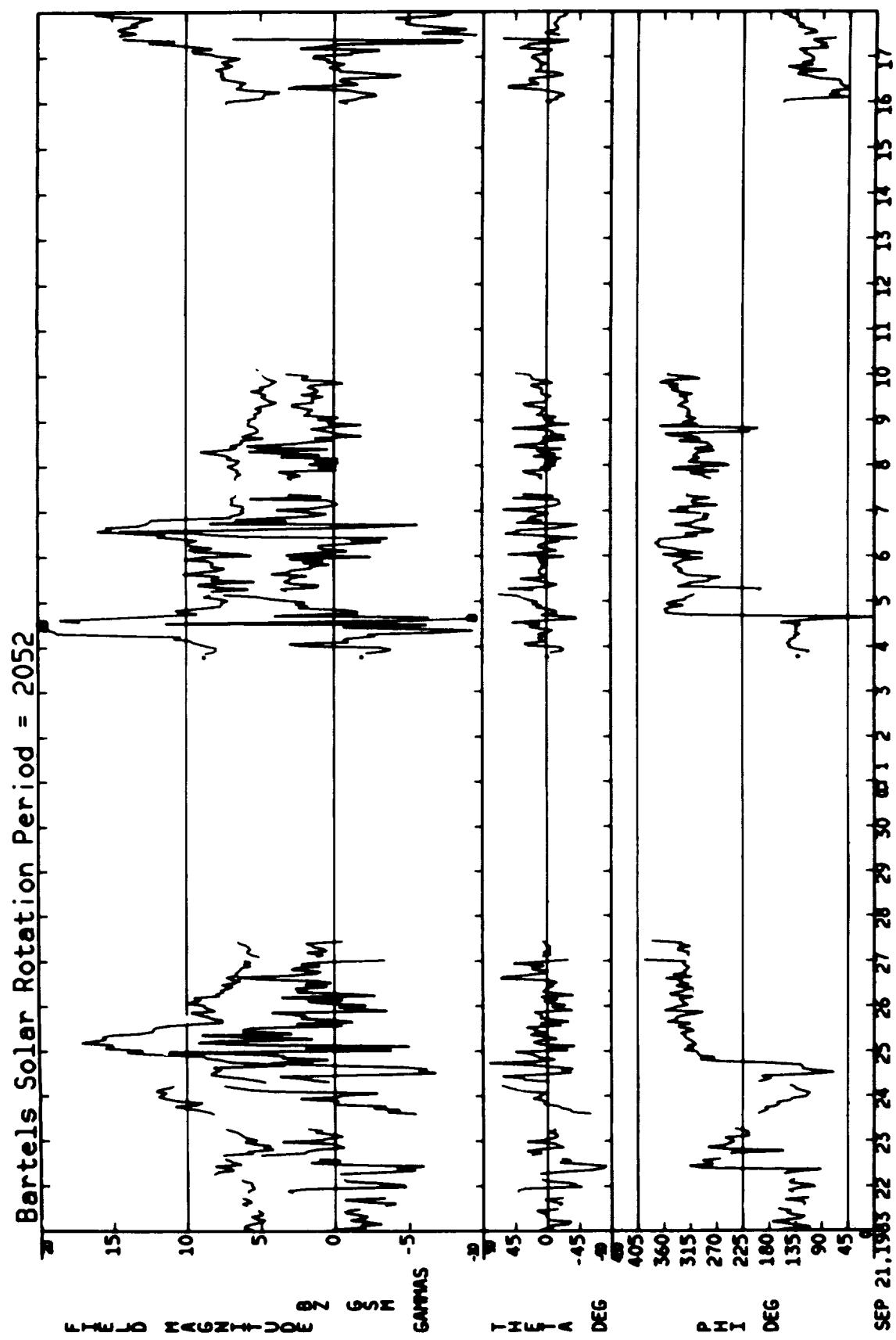


09/21/83 — 10/17/83

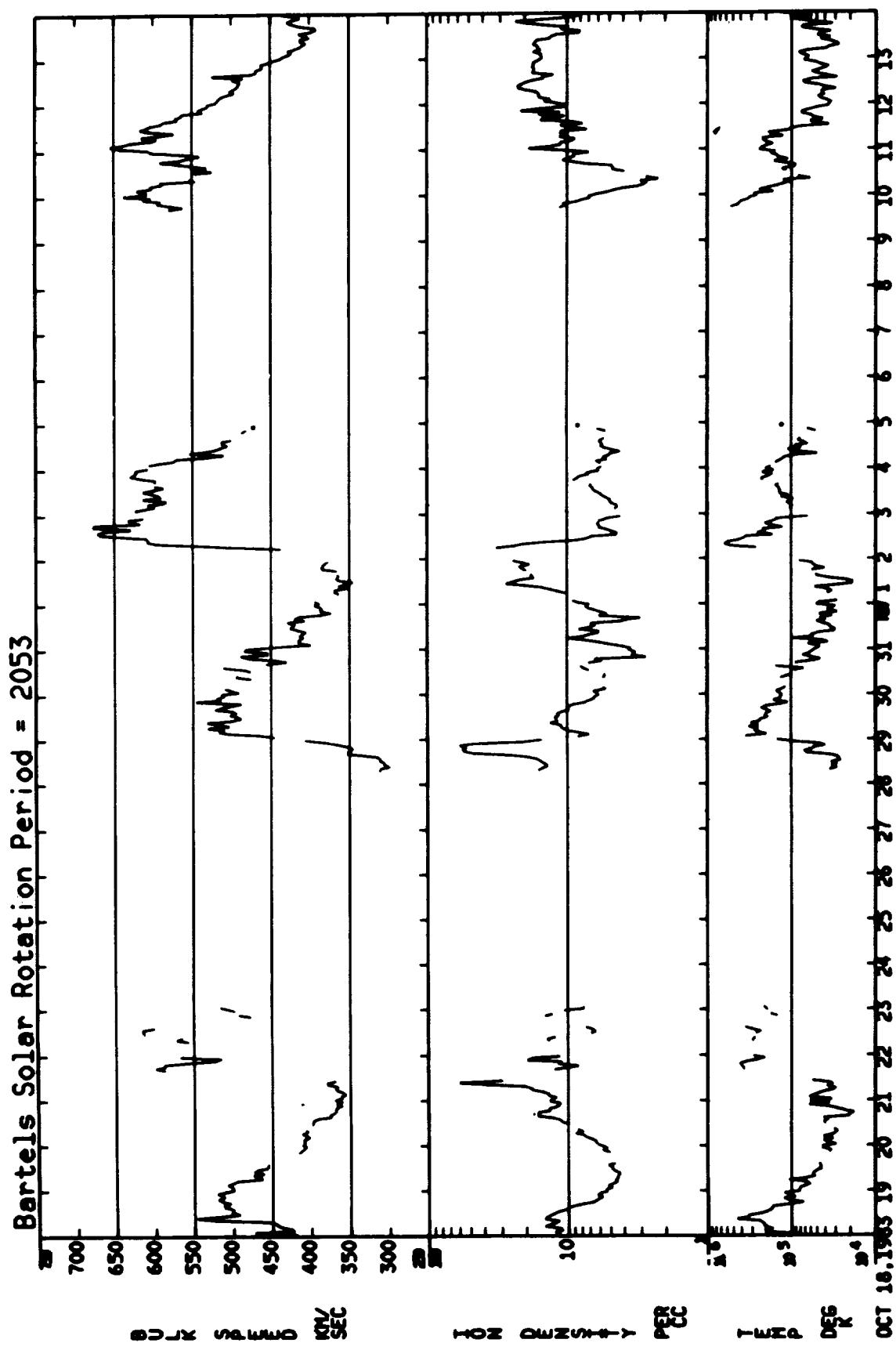


ORIGINAL PAGE IS  
OF POOR QUALITY

09/21/83 — 10/17/83

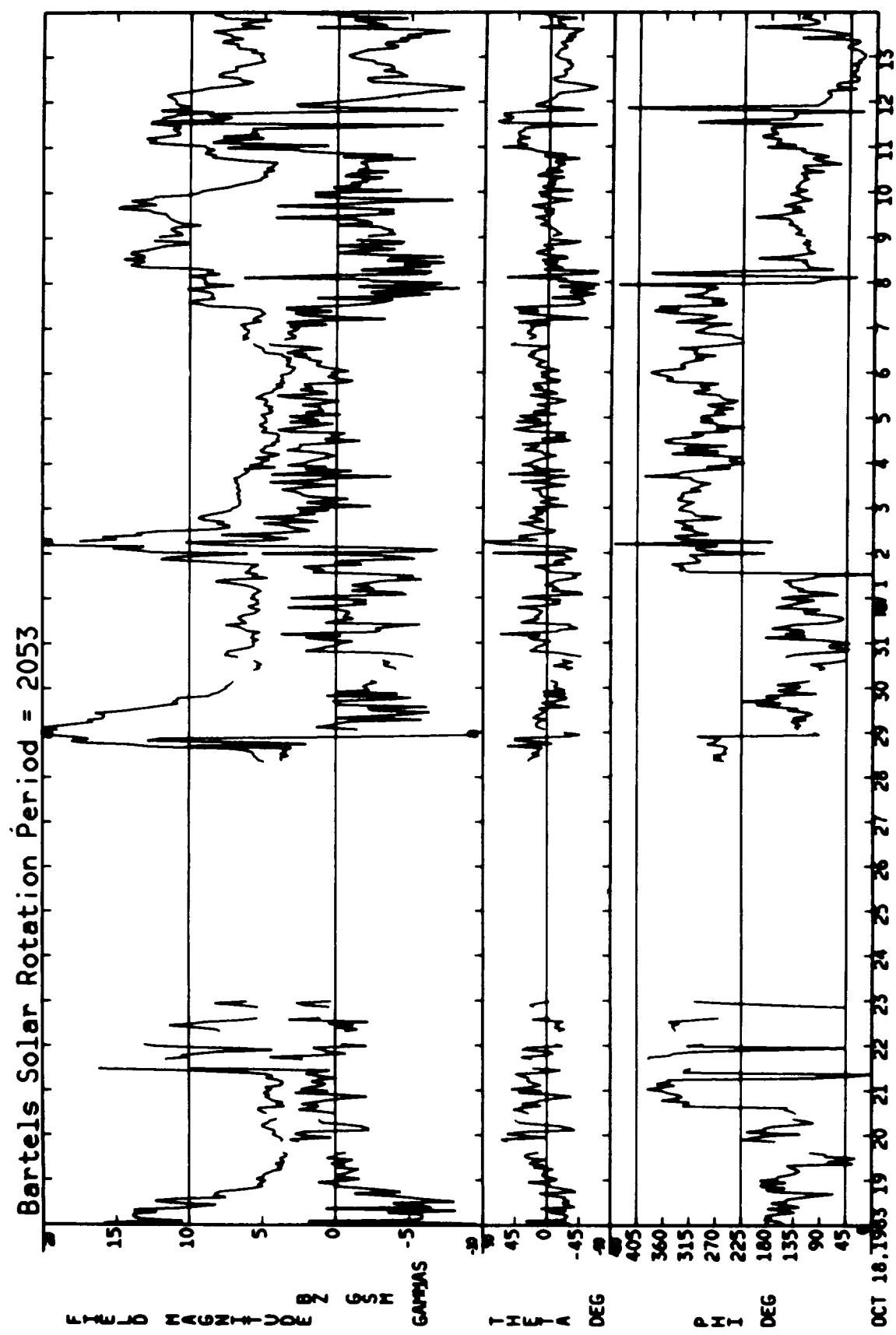


10/18/83 — 11/13/83

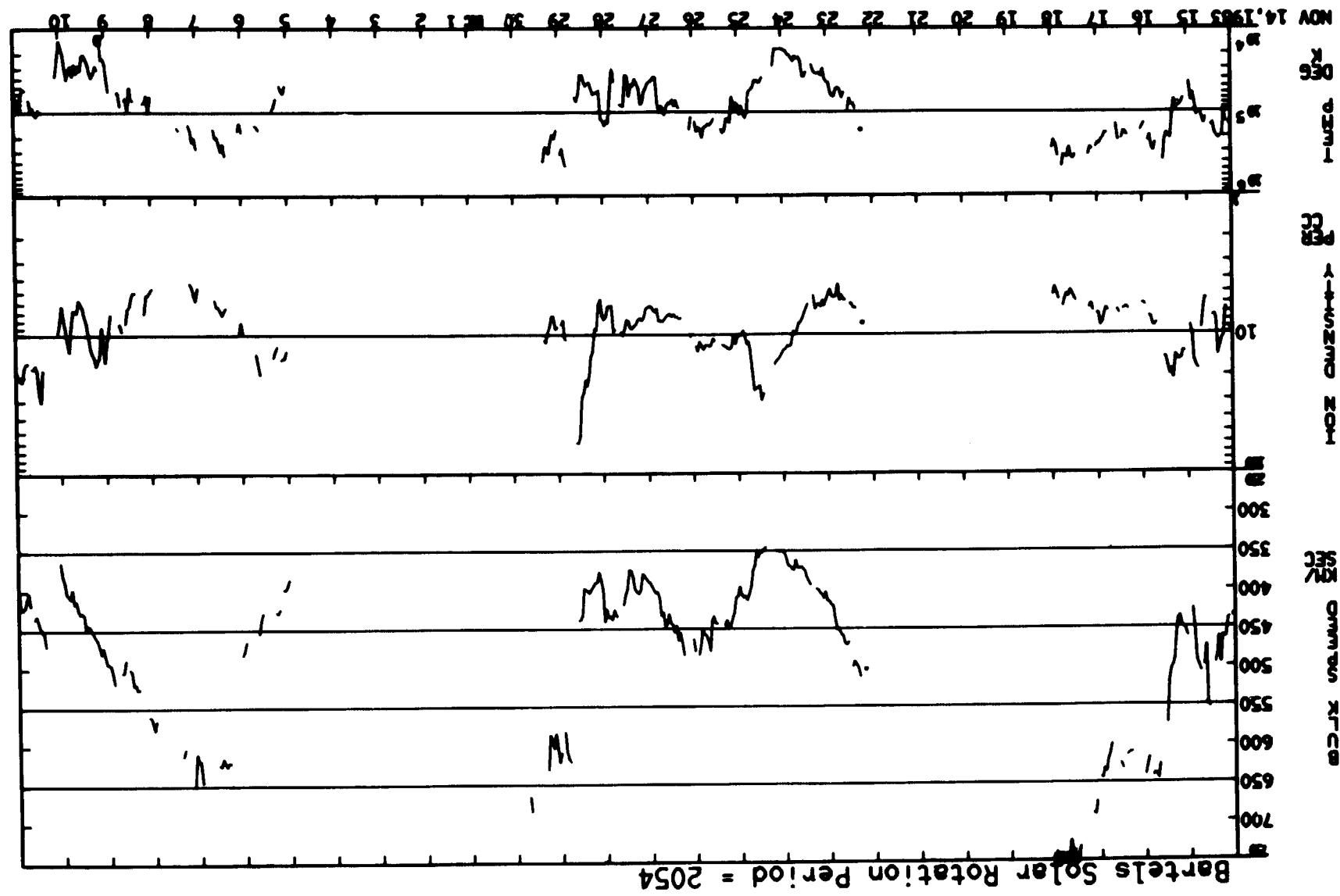


ORIGINAL PAGE IS  
OF POOR QUALITY

10/18/83 — 11/13/83



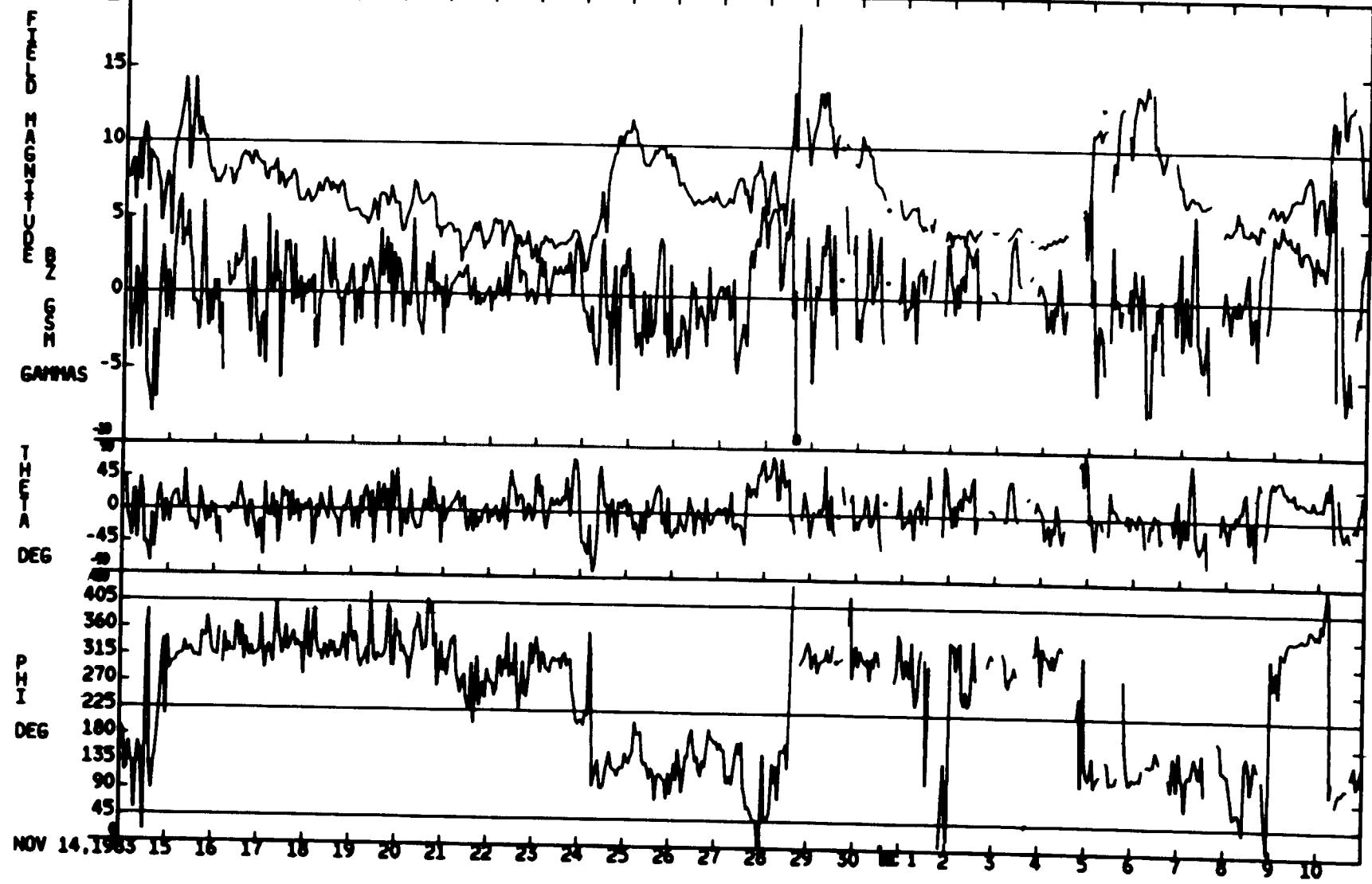
11/14/83 - 12/10/83



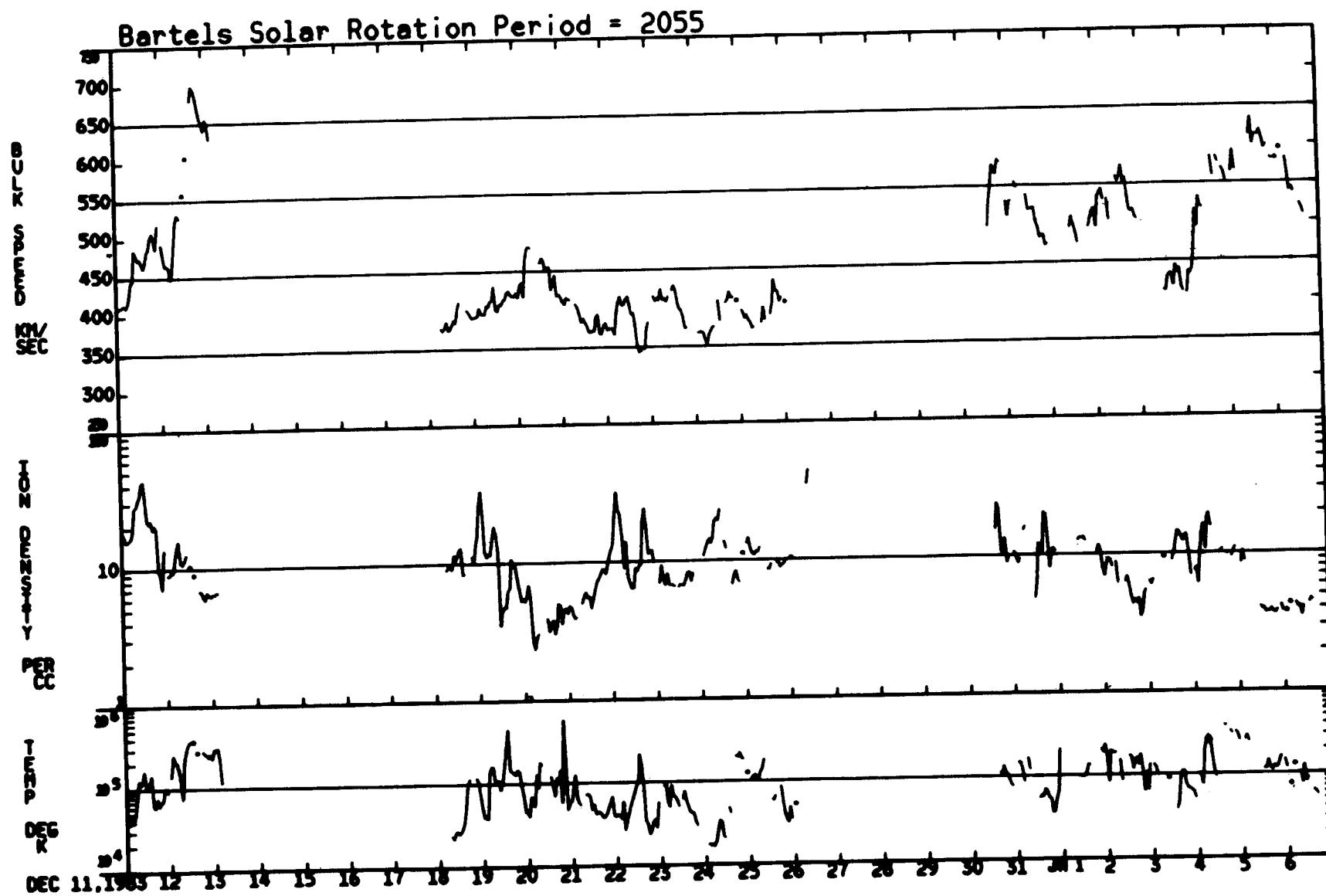
ORIGINAL PAGE IS  
OF POOR QUALITY

11/14/83 - 12/10/83

Bartels Solar Rotation Period = 2054

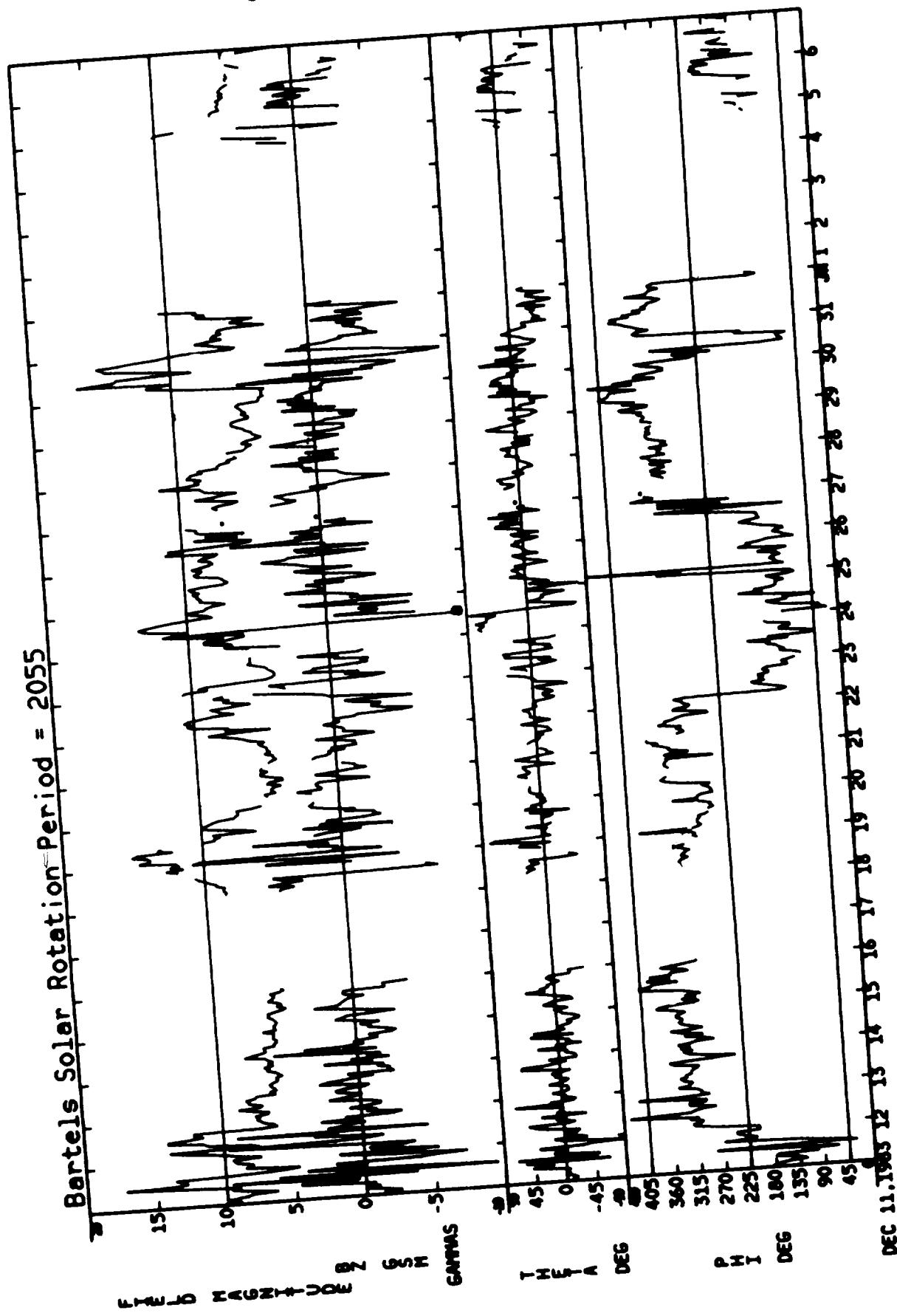


12/11/83 – 01/06/84

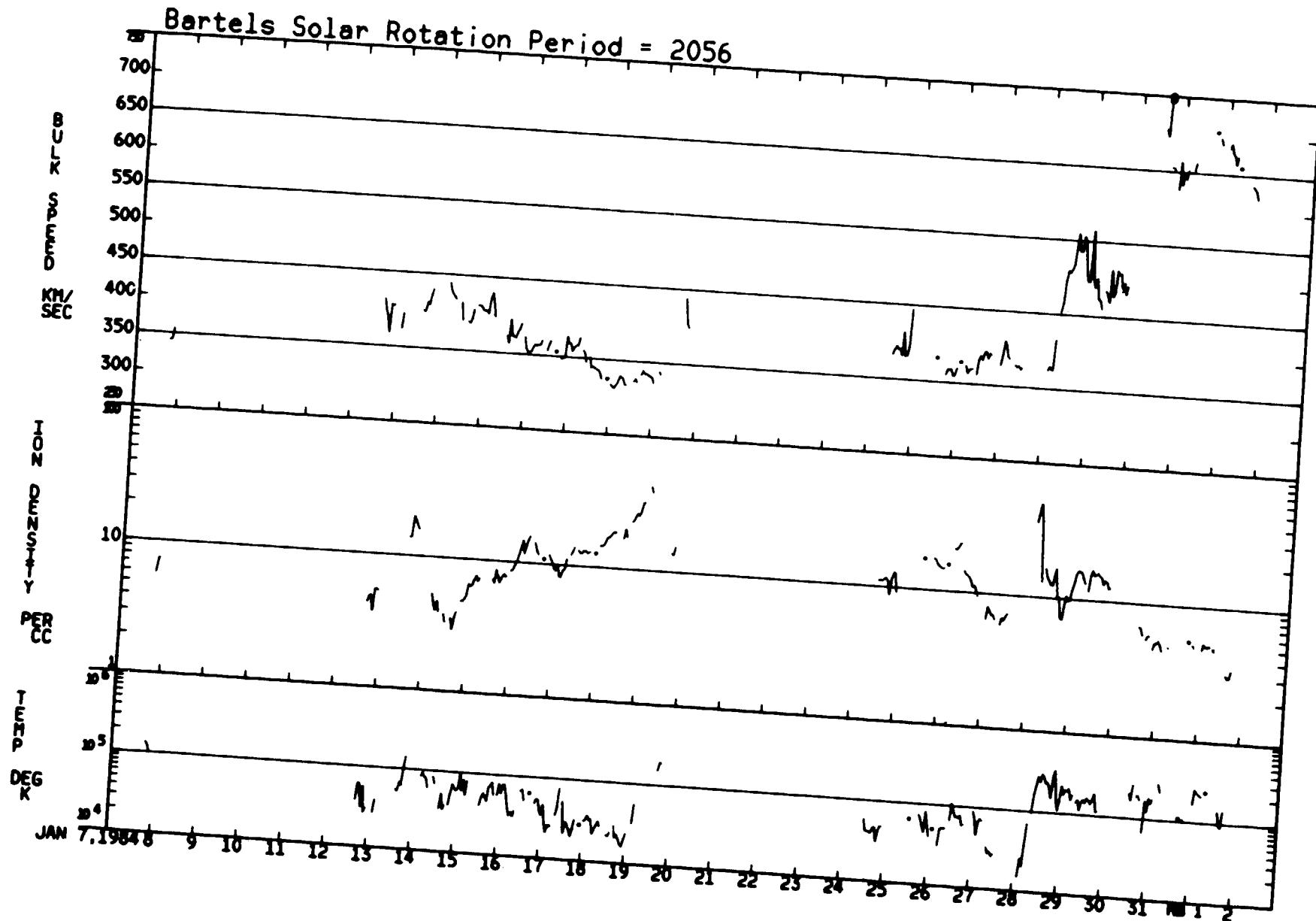


ORIGINAL PAGE IS  
OF POOR QUALITY

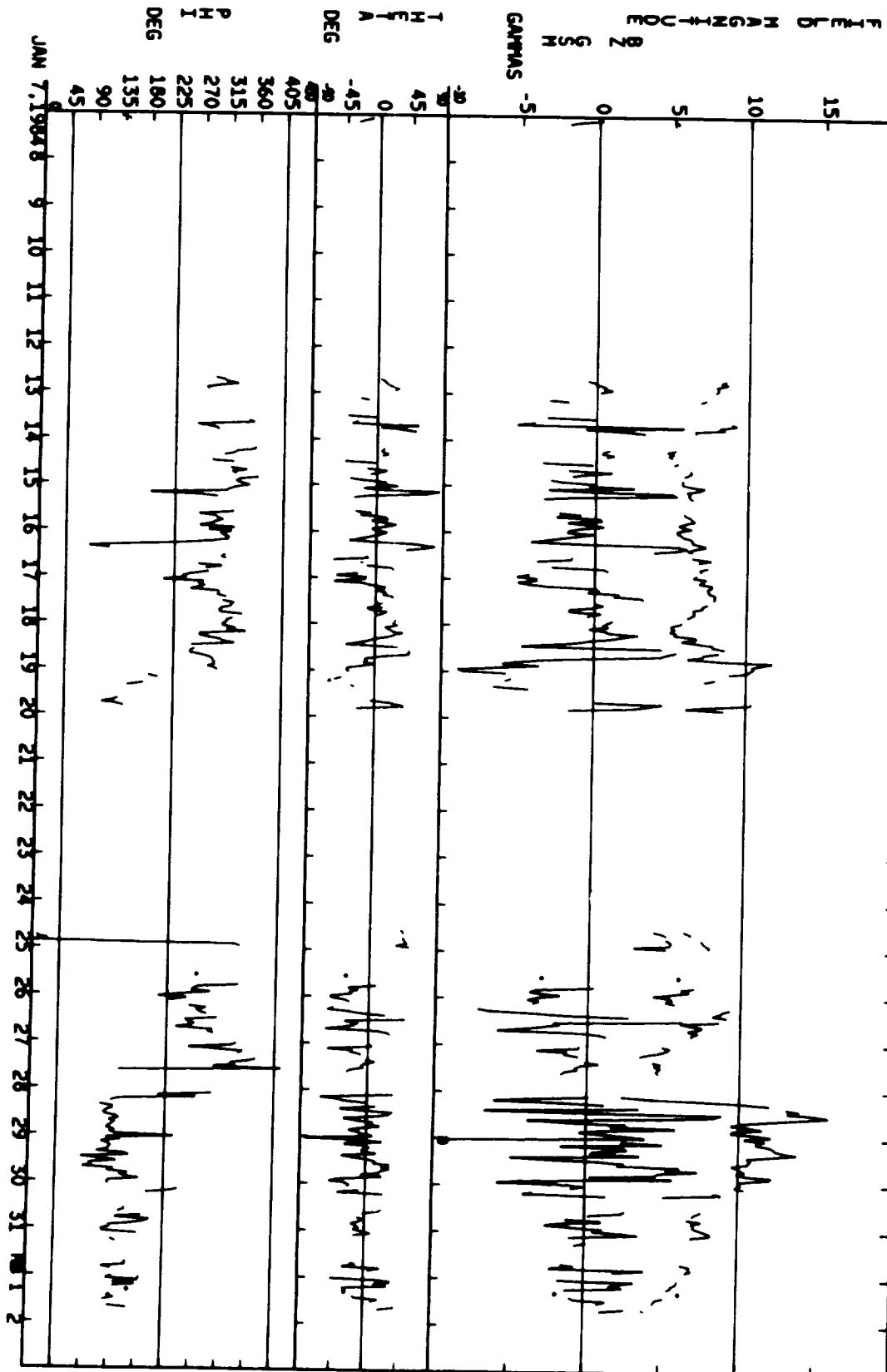
12/11/83 - 01/06/84



01/07/84 - 02/02/84



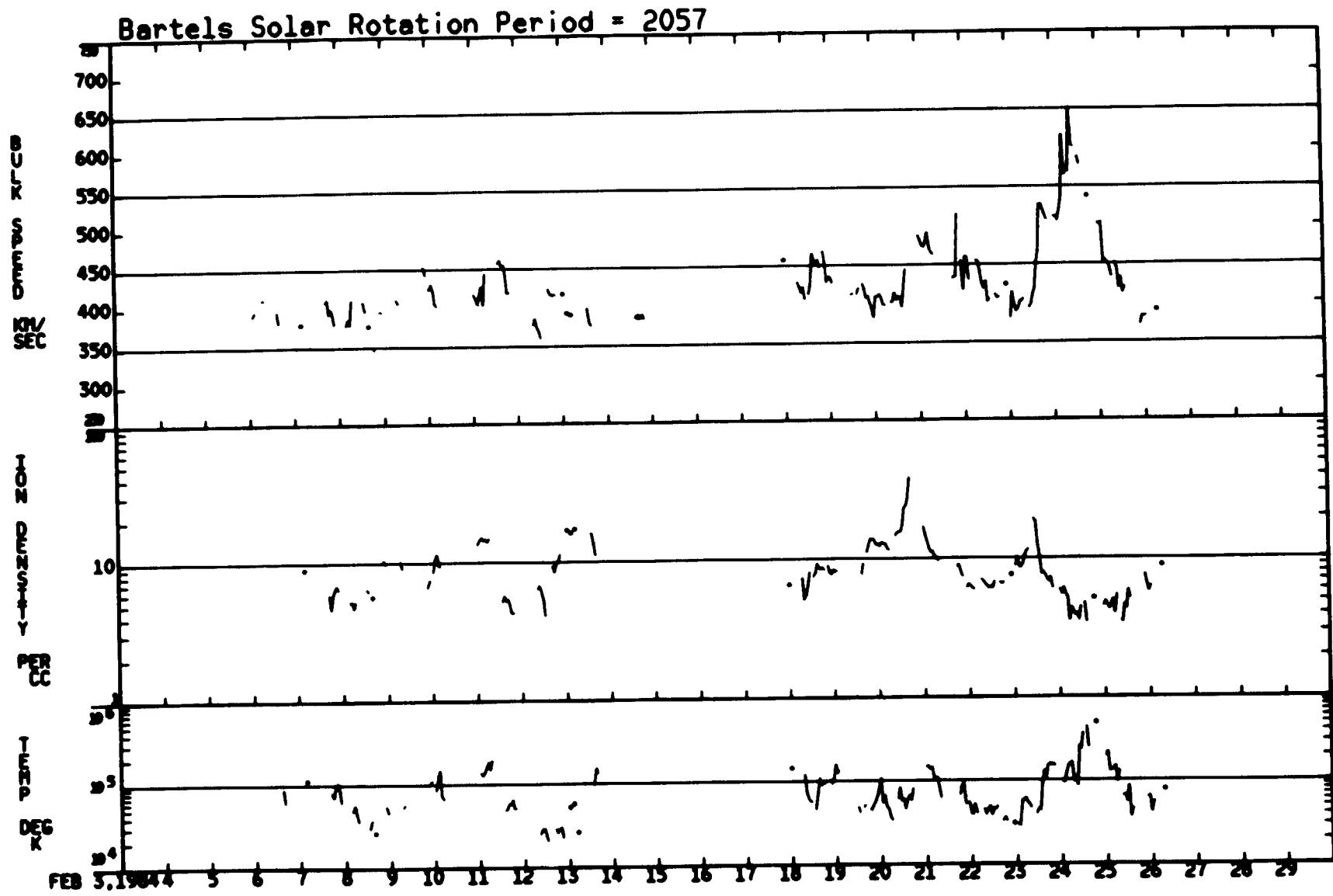
Bartels Solar Rotation Period = 2056



01/07/84 — 02/02/84

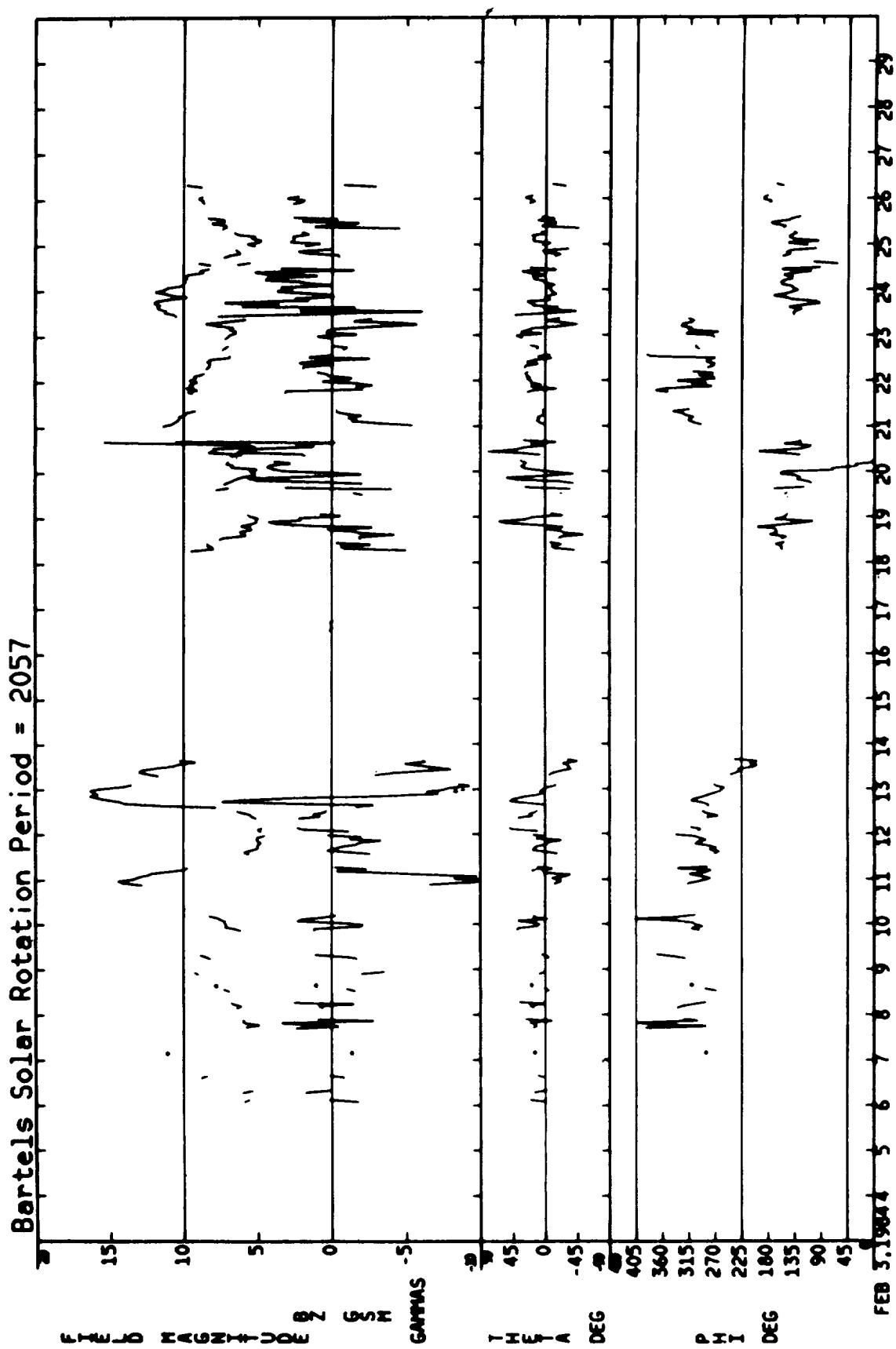
ORIGINAL PAGE IS  
OF POOR QUALITY

02/03/84 - 02/29/84

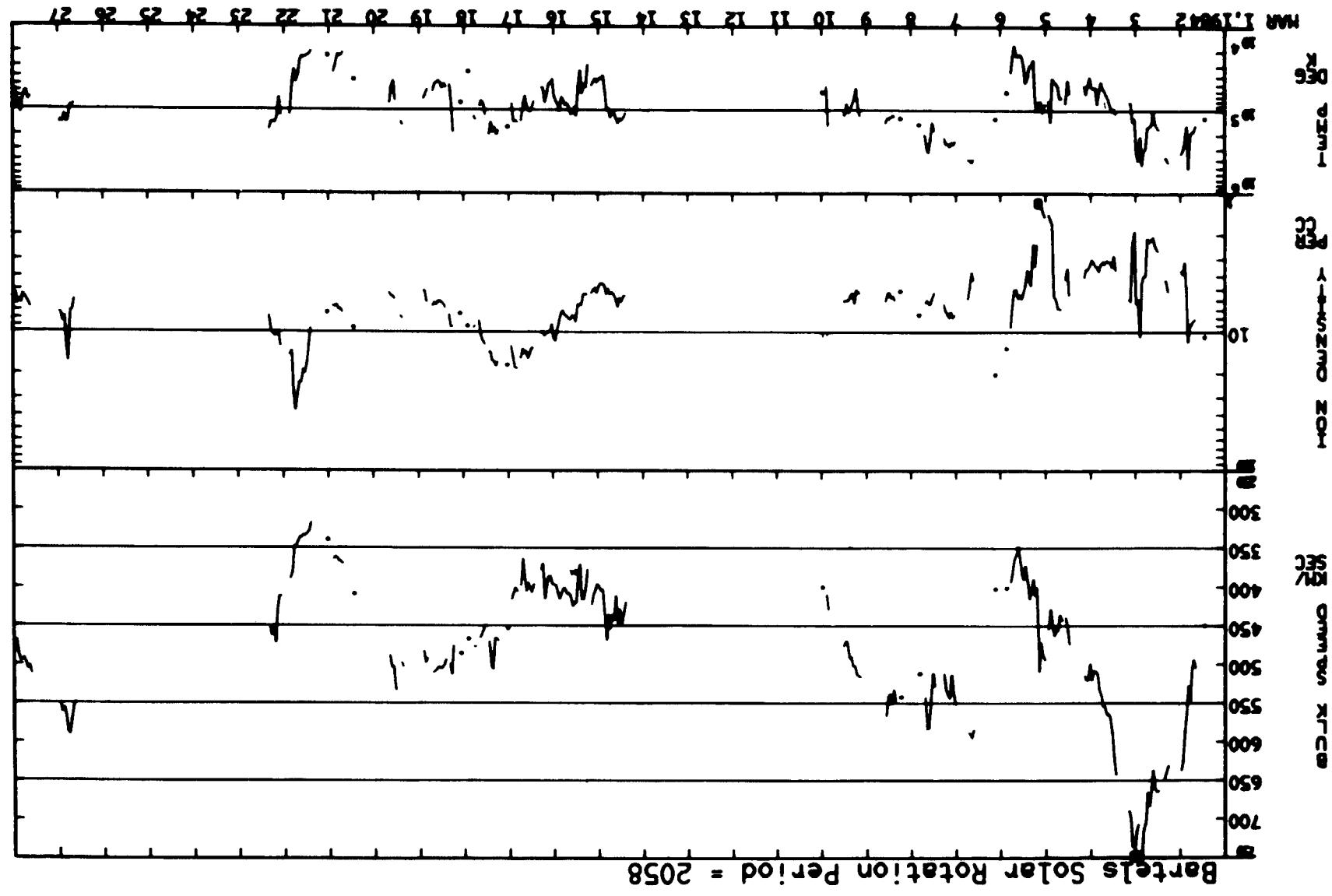


ORIGINAL PAGE IS  
OF POOR QUALITY

02/03/84 — 02/29/84



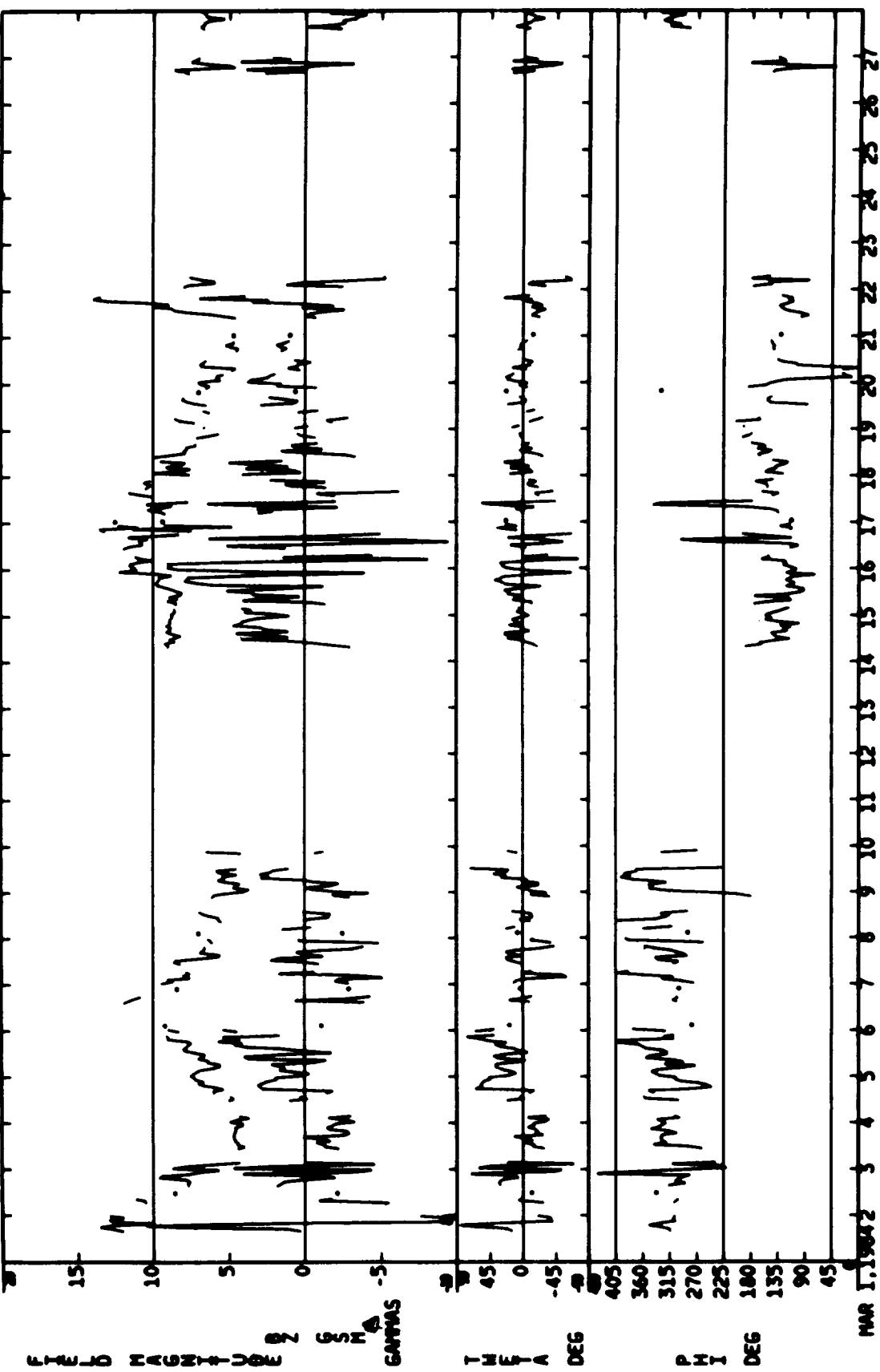
03/01/84 - 03/27/84



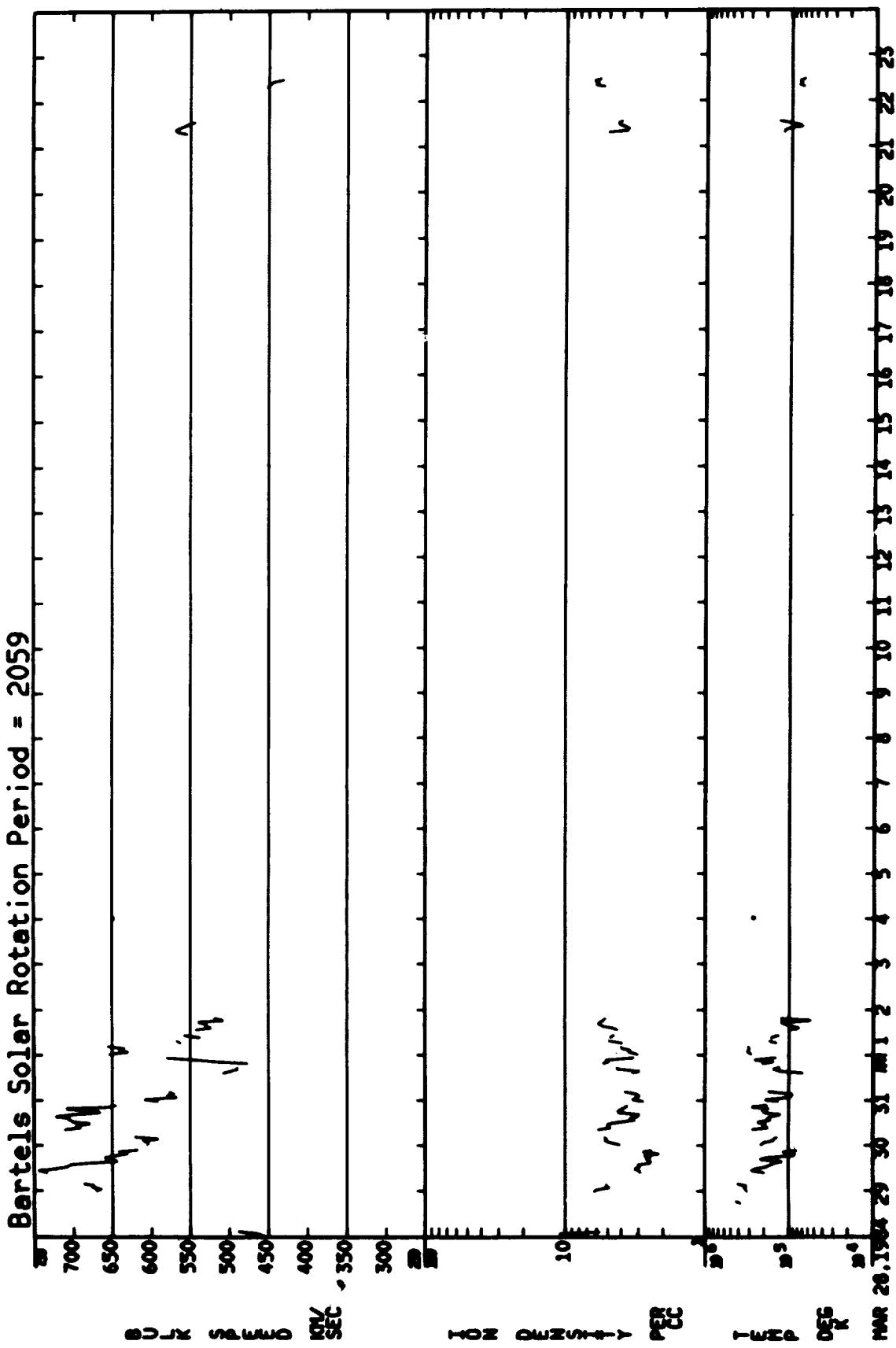
ORIGINAL PAGE IS  
OF POOR QUALITY

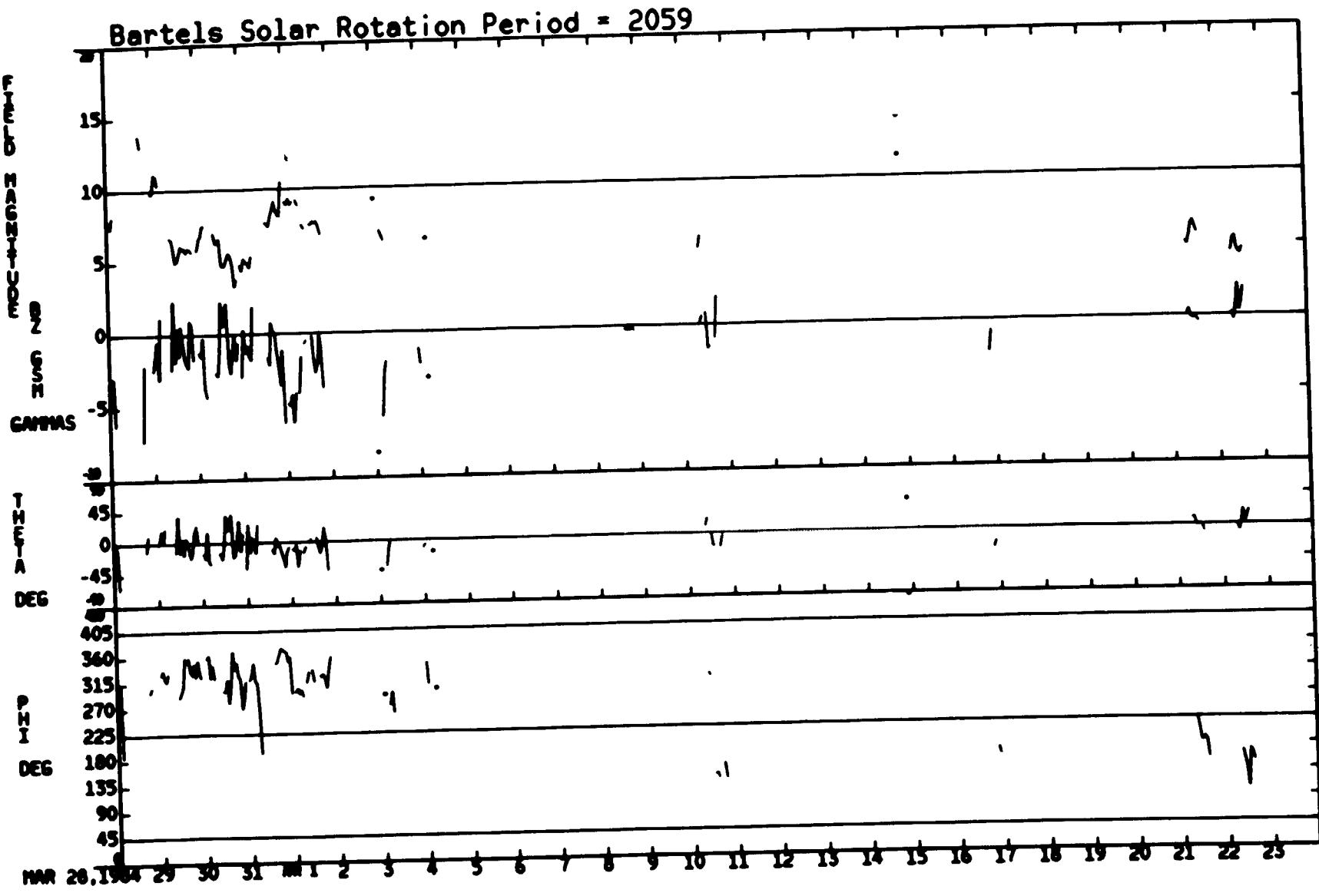
03/01/84 — 03/27/84

Bartels Solar Rotation Period = 2058



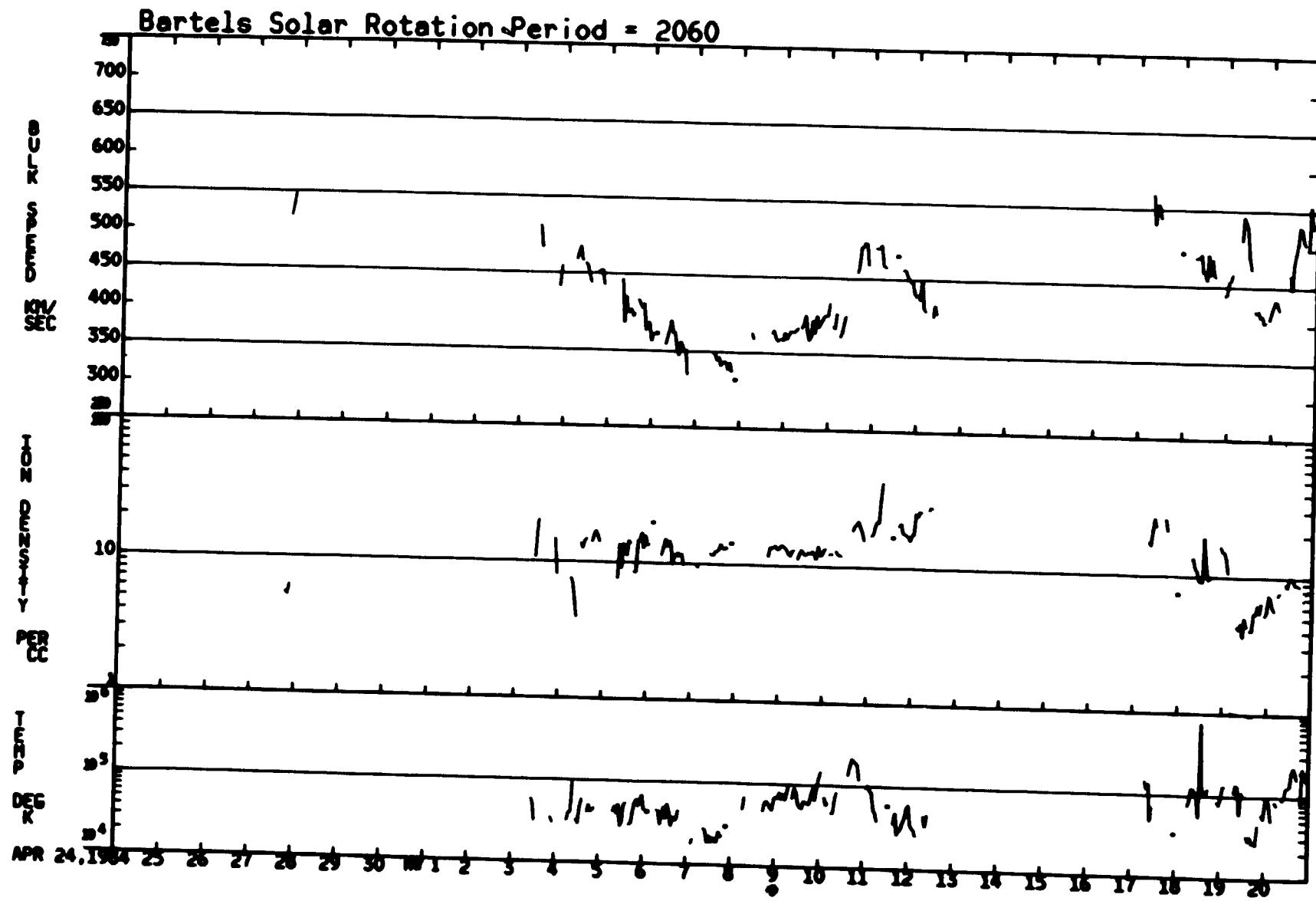
03/28/84 — 04/23/84





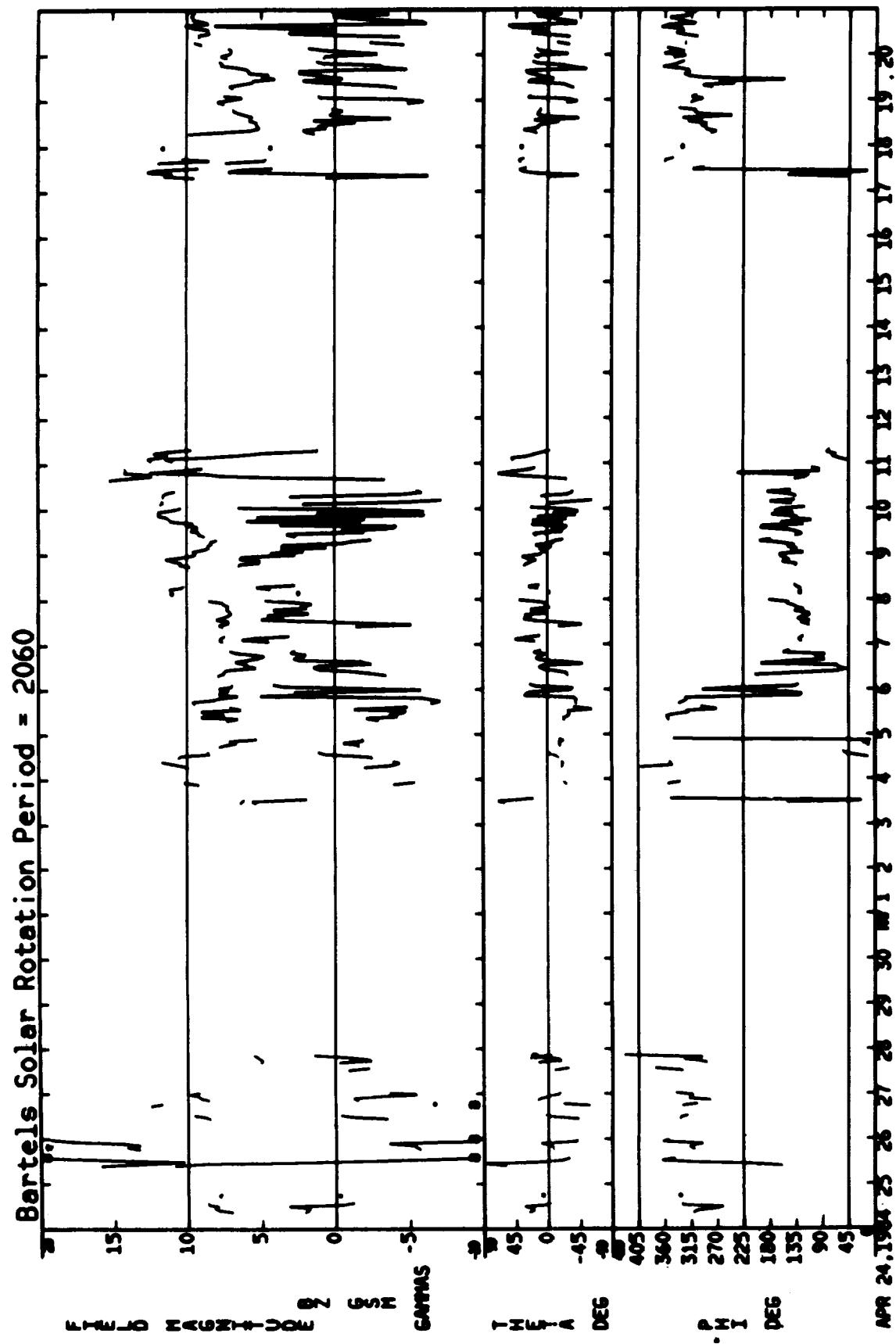
ORIGINAL PAGE IS  
OF POOR QUALITY  
03/28/84 – 04/23/84

04/24/84 — 05/20/84

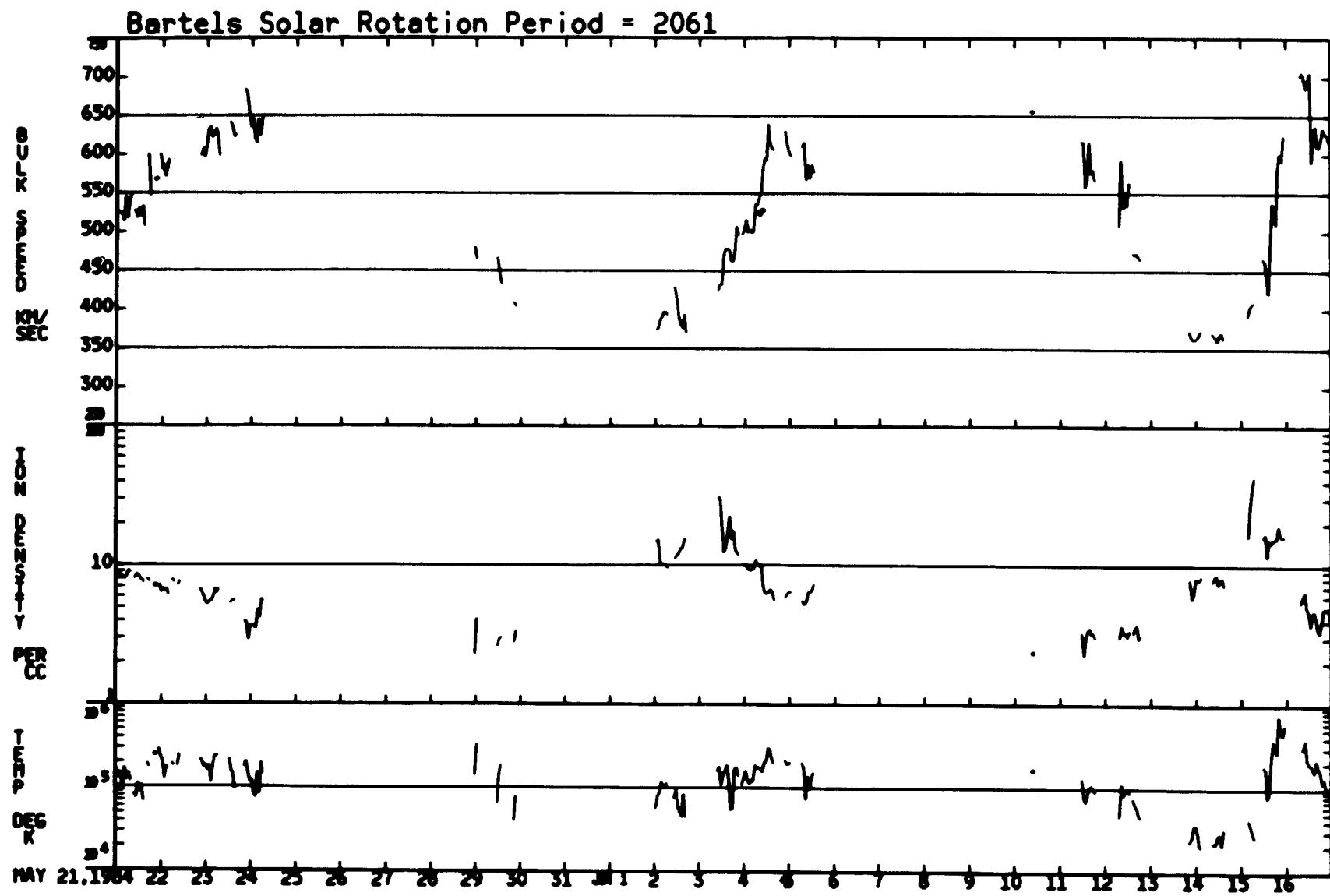


ORIGINAL PAGE IS  
OF POOR QUALITY

04/24/84 — 05/20/84

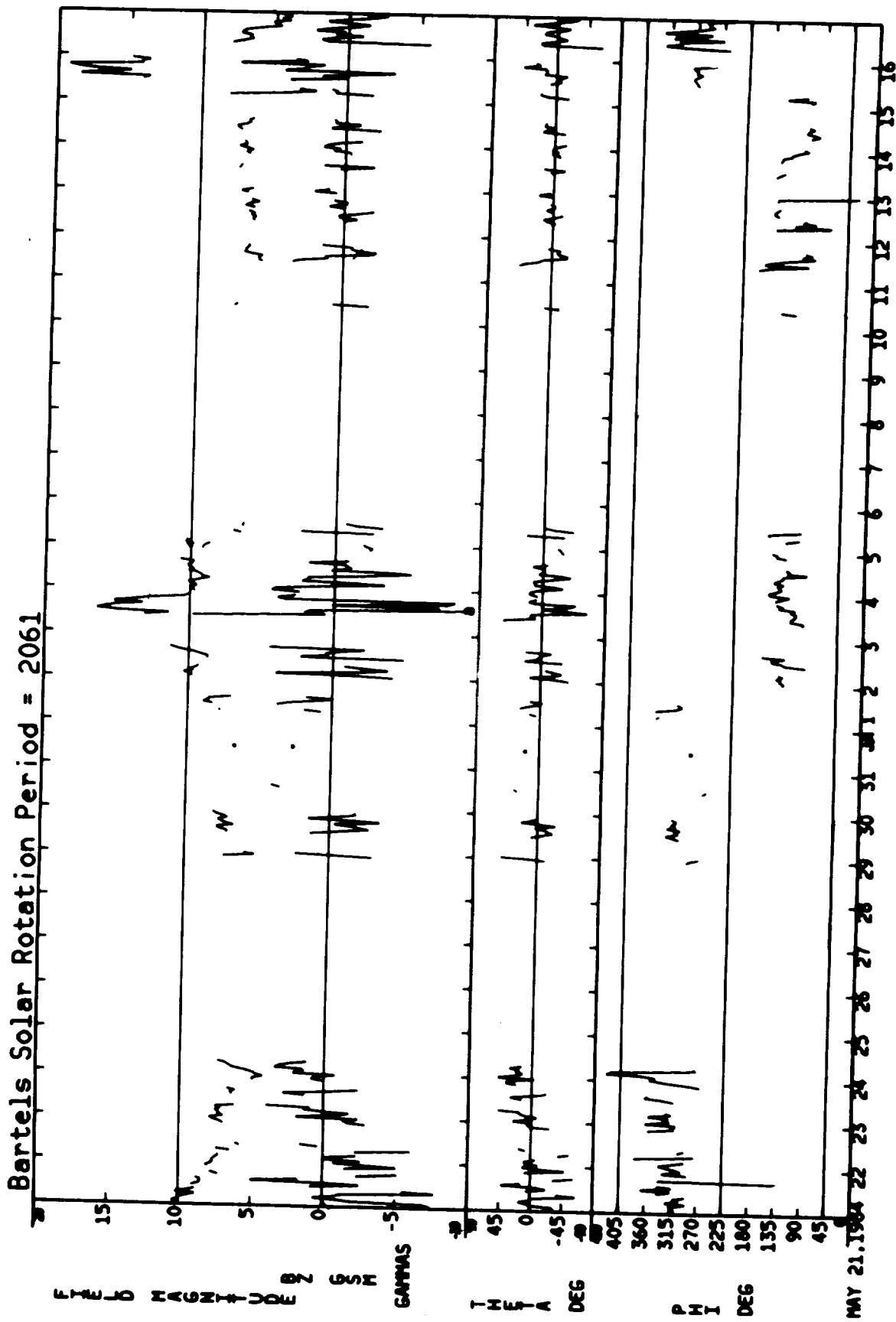


05/21/84 – 06/16/84

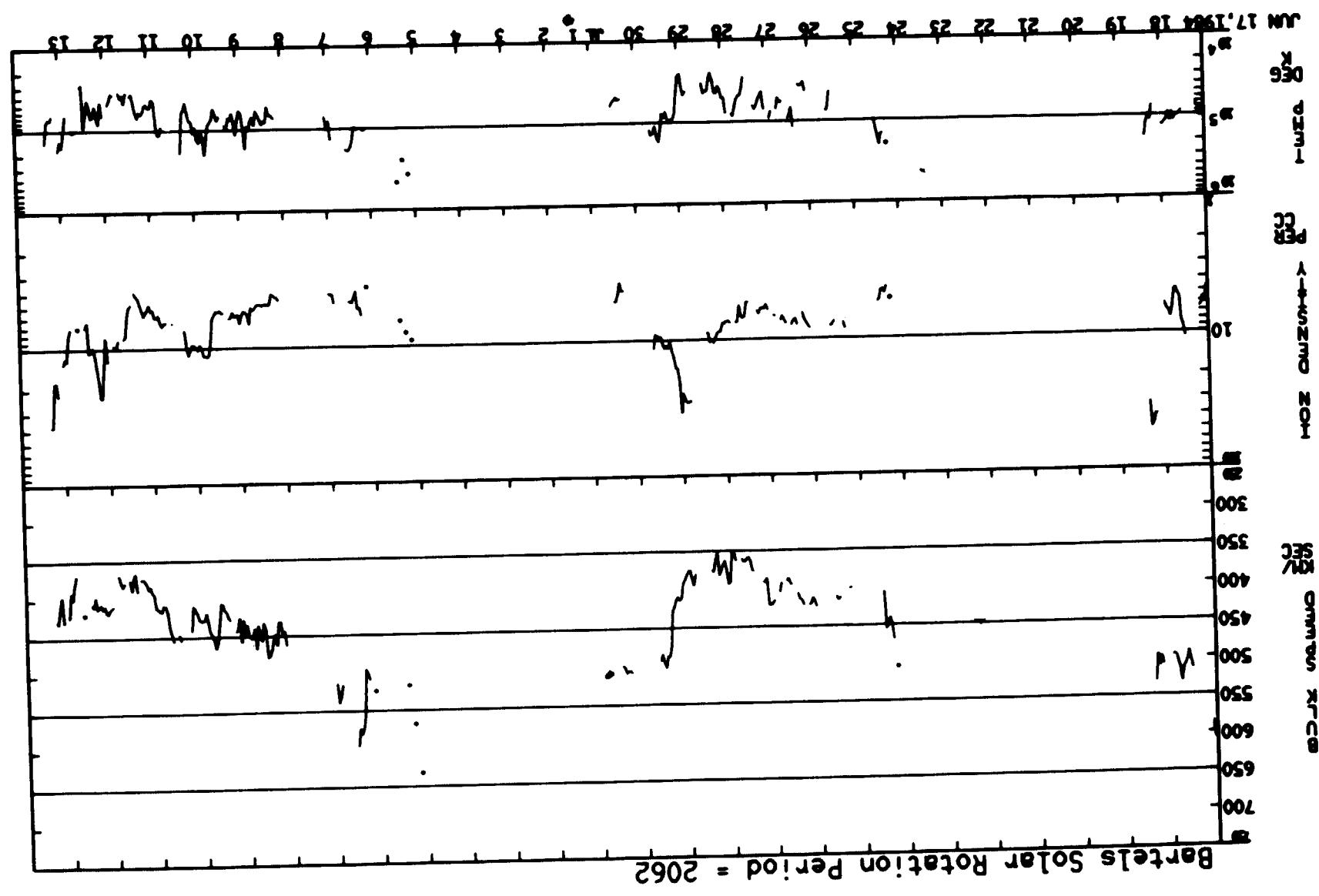


ORIGINAL PAGE IS  
OF POOR QUALITY

05/21/84 — 06/16/84



06/17/84 - 07/13/84



ORIGINAL PAGE IS  
OF POOR QUALITY

06/17/84 – 07/13/84

Bartels Solar Rotation Period = 2062

NUCLEAR COUNTS IN GREEK

15  
10  
5  
0  
-5

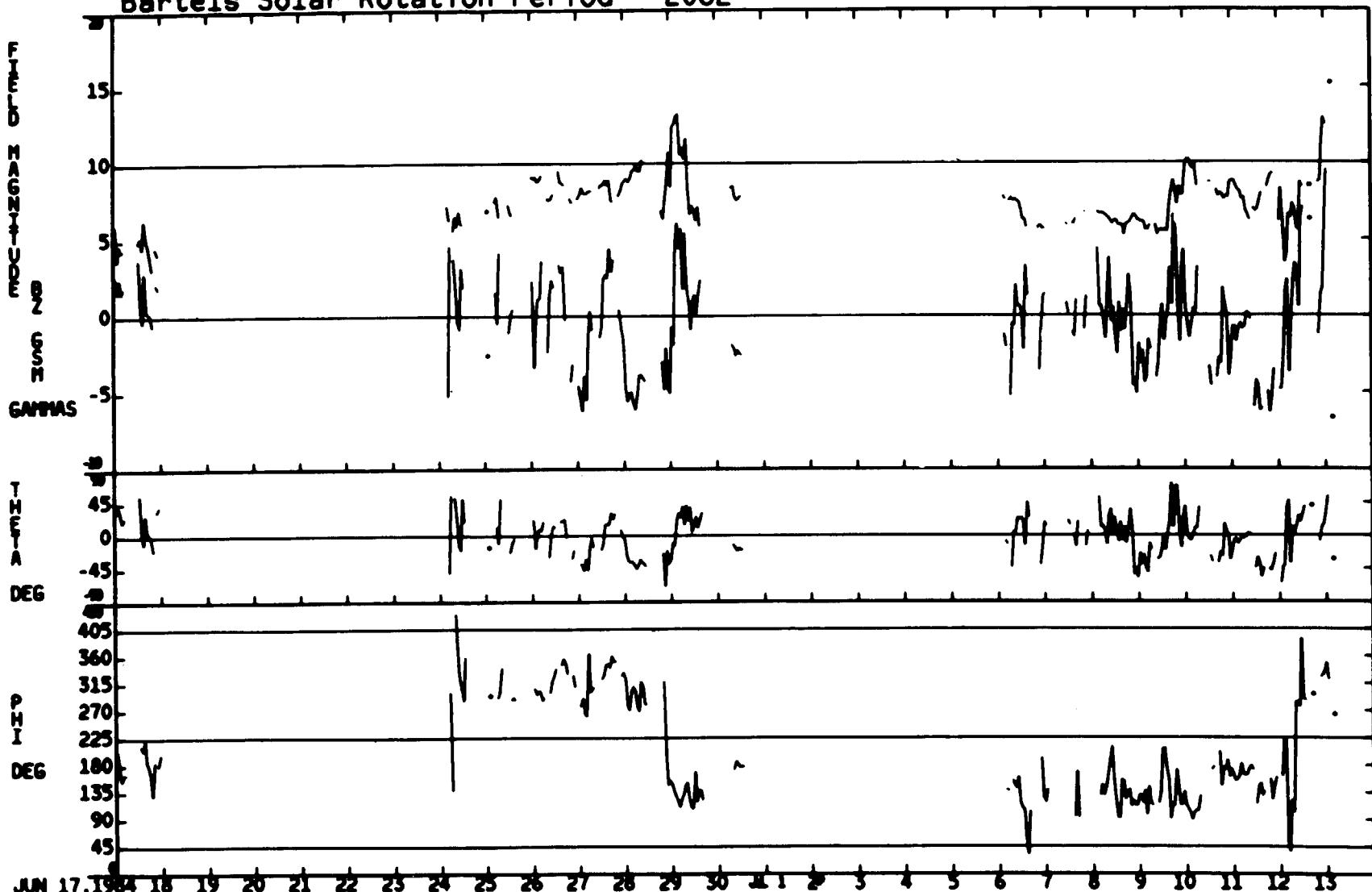
THETA DEG

45  
0  
-45

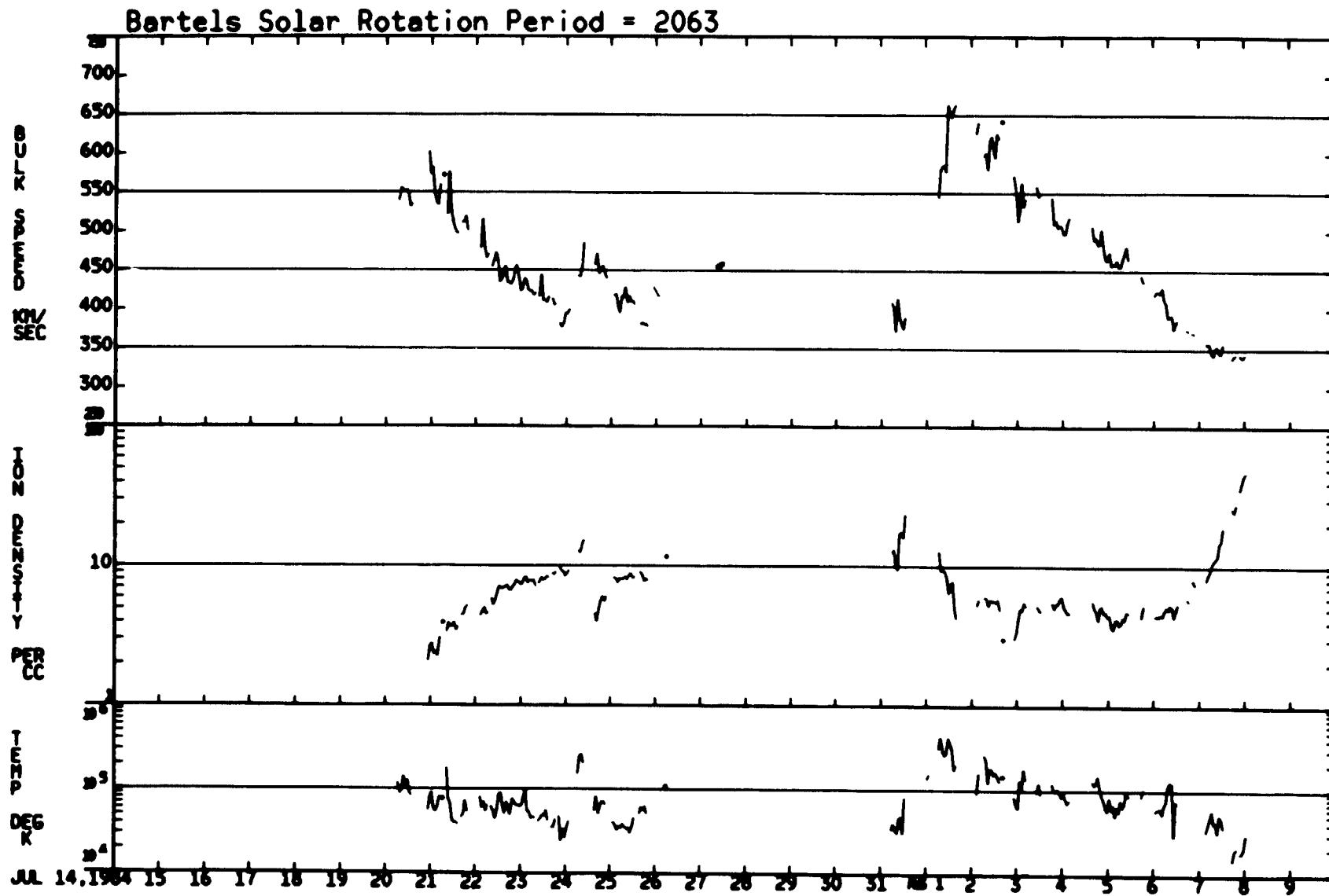
PHI DEG

405  
360  
315  
270  
225  
180  
135  
90  
45

JUN 17, 1984 18 19 20 21 22 23 24 25 26 27 28 29 30 31 1 2 3 4 5 6 7 8 9 10 11 12 13

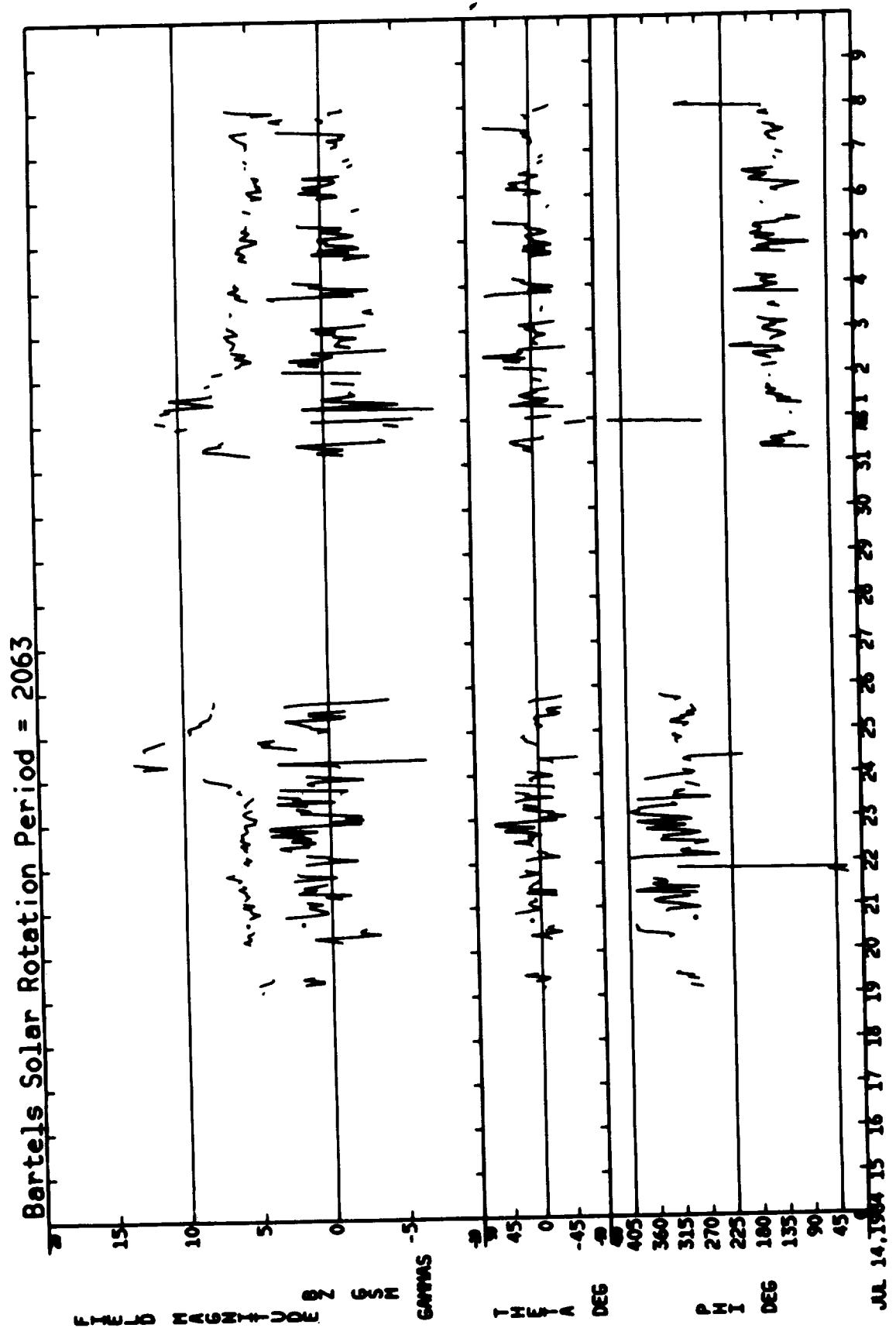


07/14/84 - 08/09/84

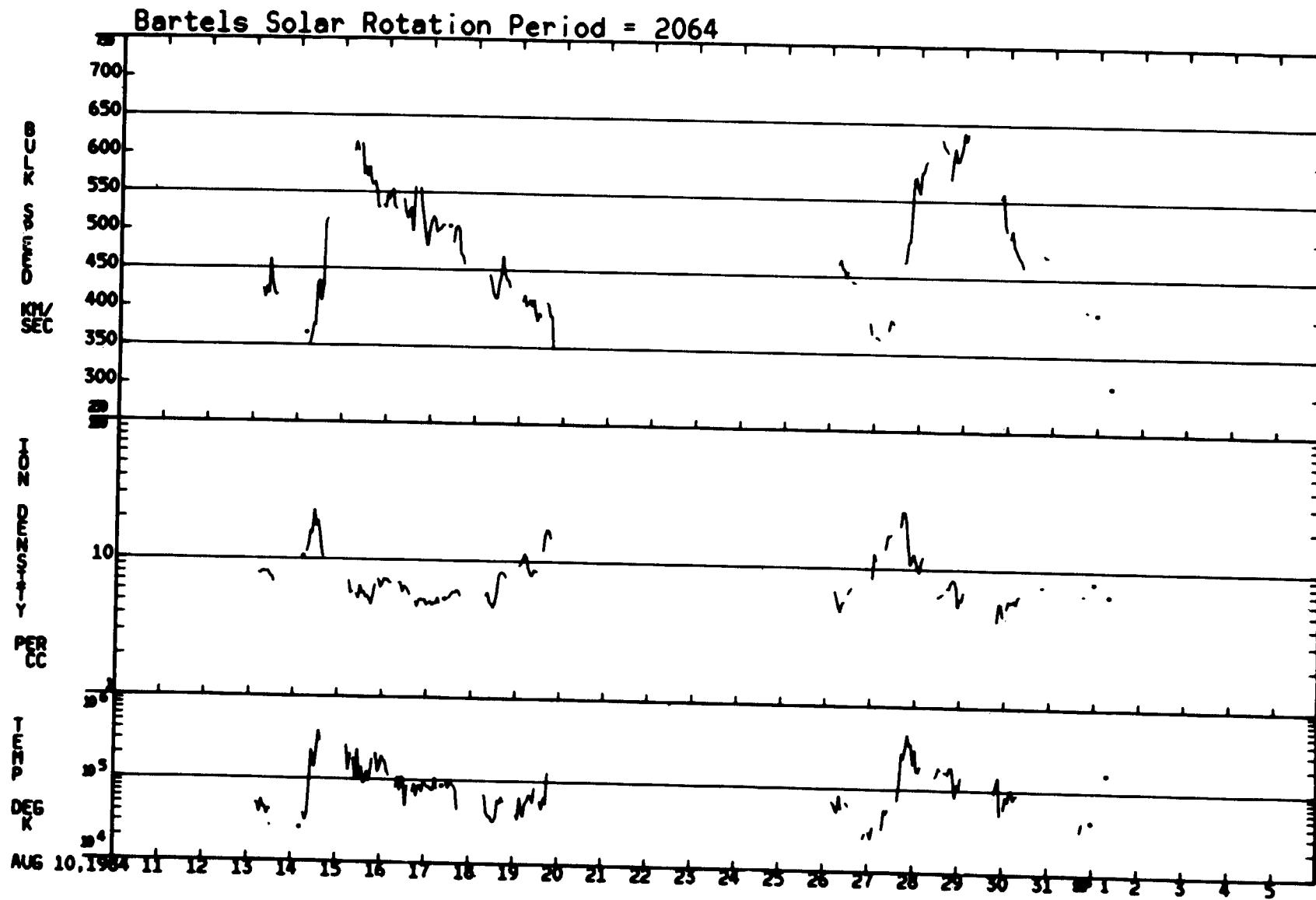


**ORIGINAL PAGE IS  
OF POOR QUALITY**

07/14/84 - 08/09/84

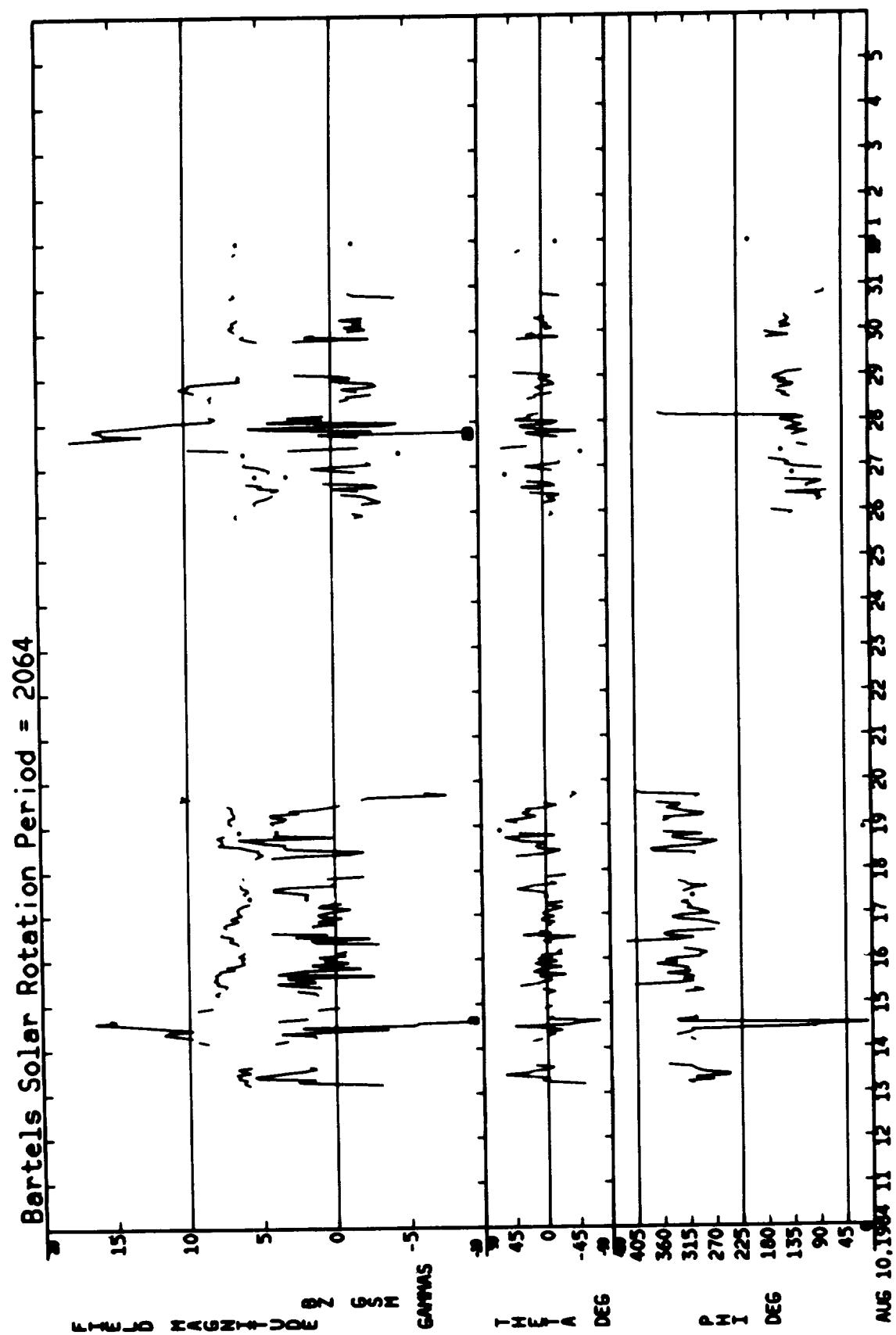


08/10/84 – 09/05/84

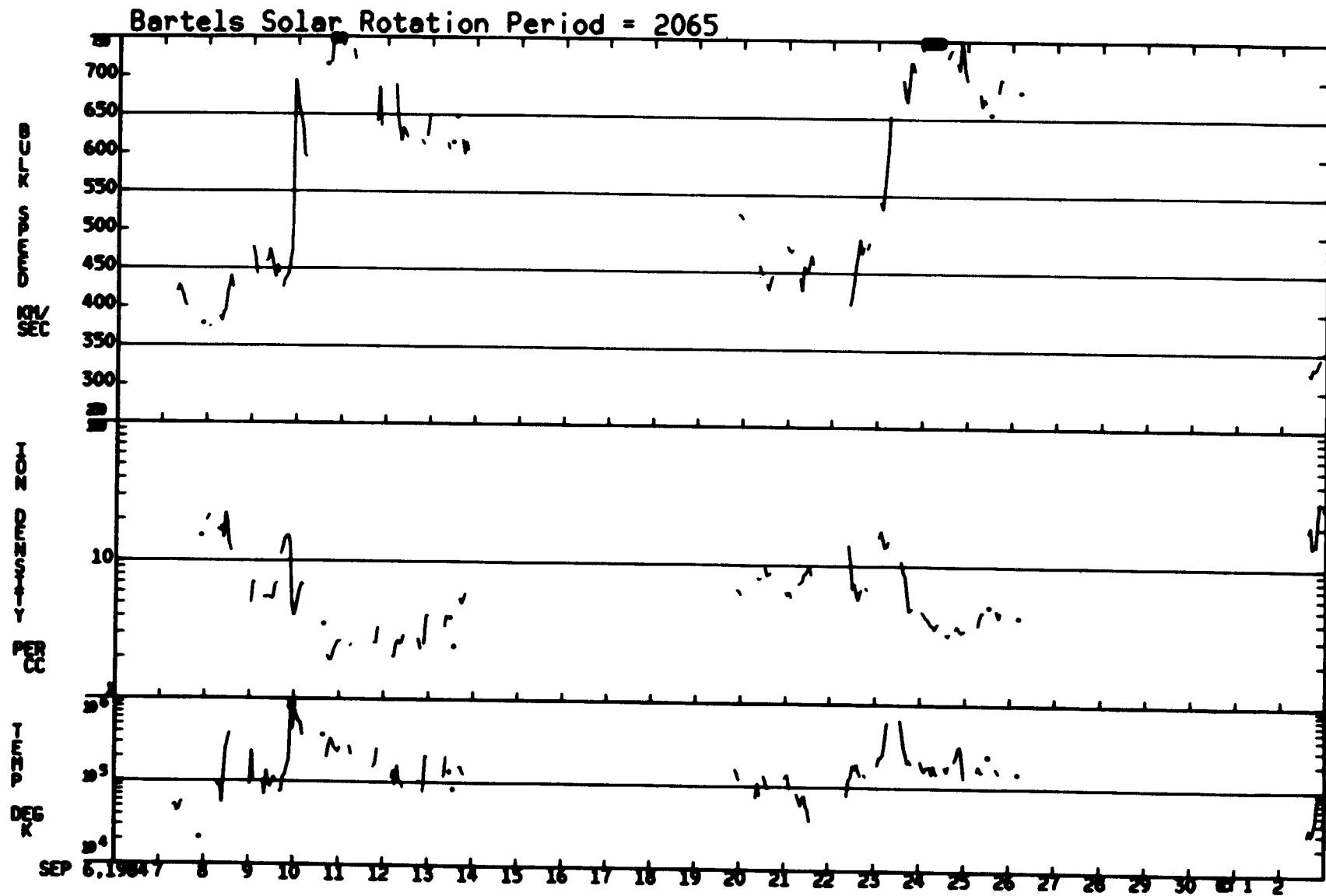


ORIGINAL PAGE IS  
OF POOR QUALITY

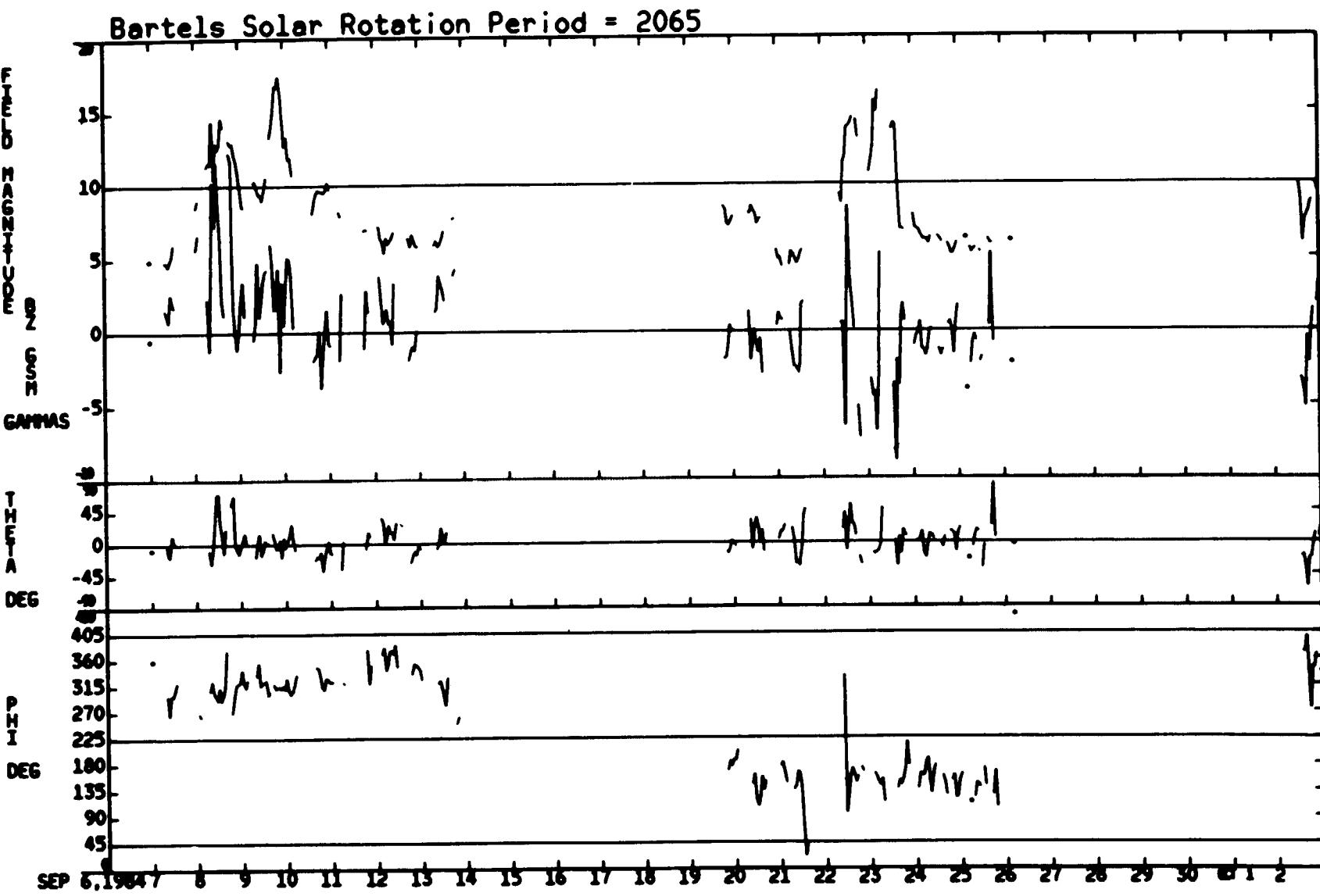
08/10/84 — 09/05/84



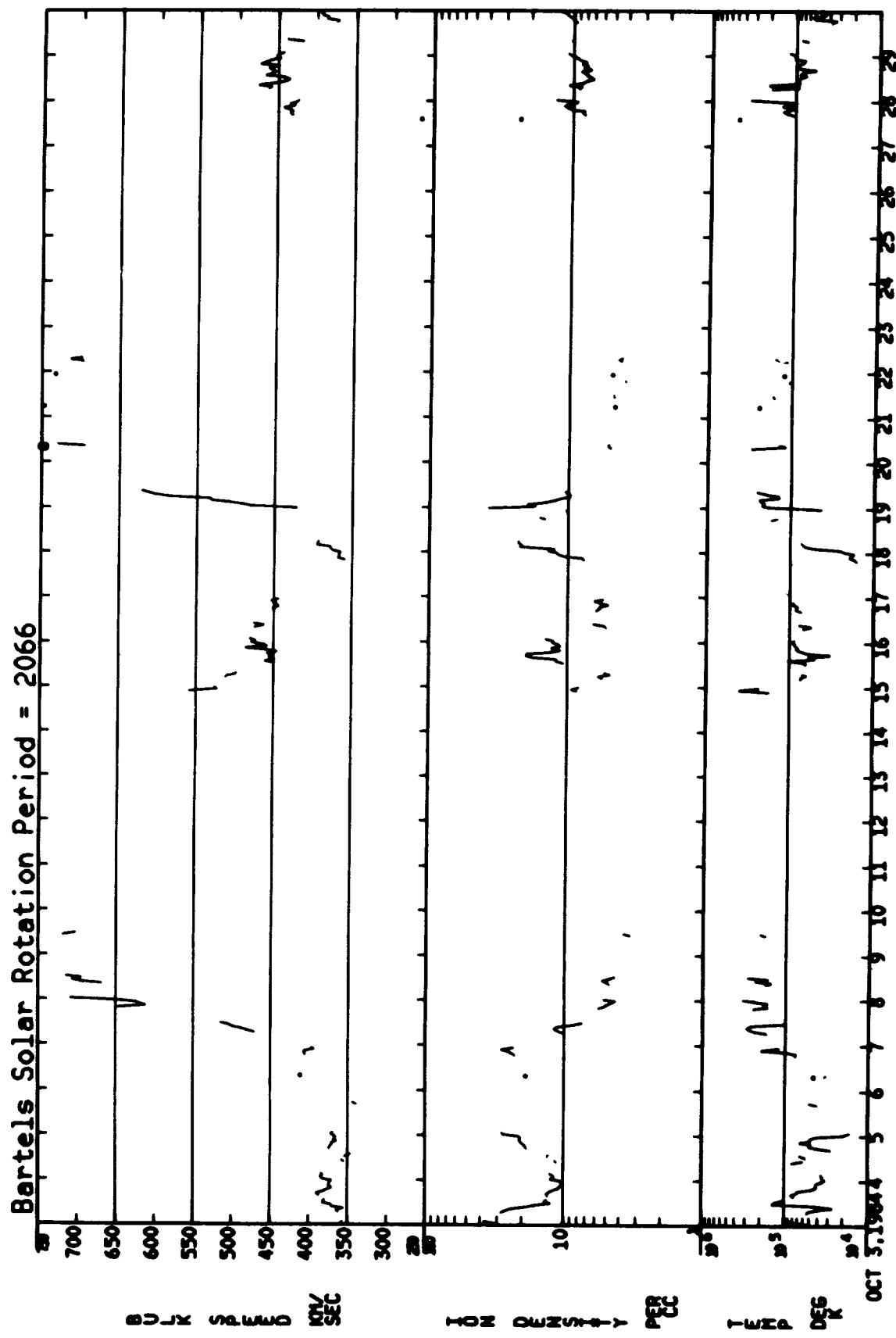
09/06/84 - 10/02/84



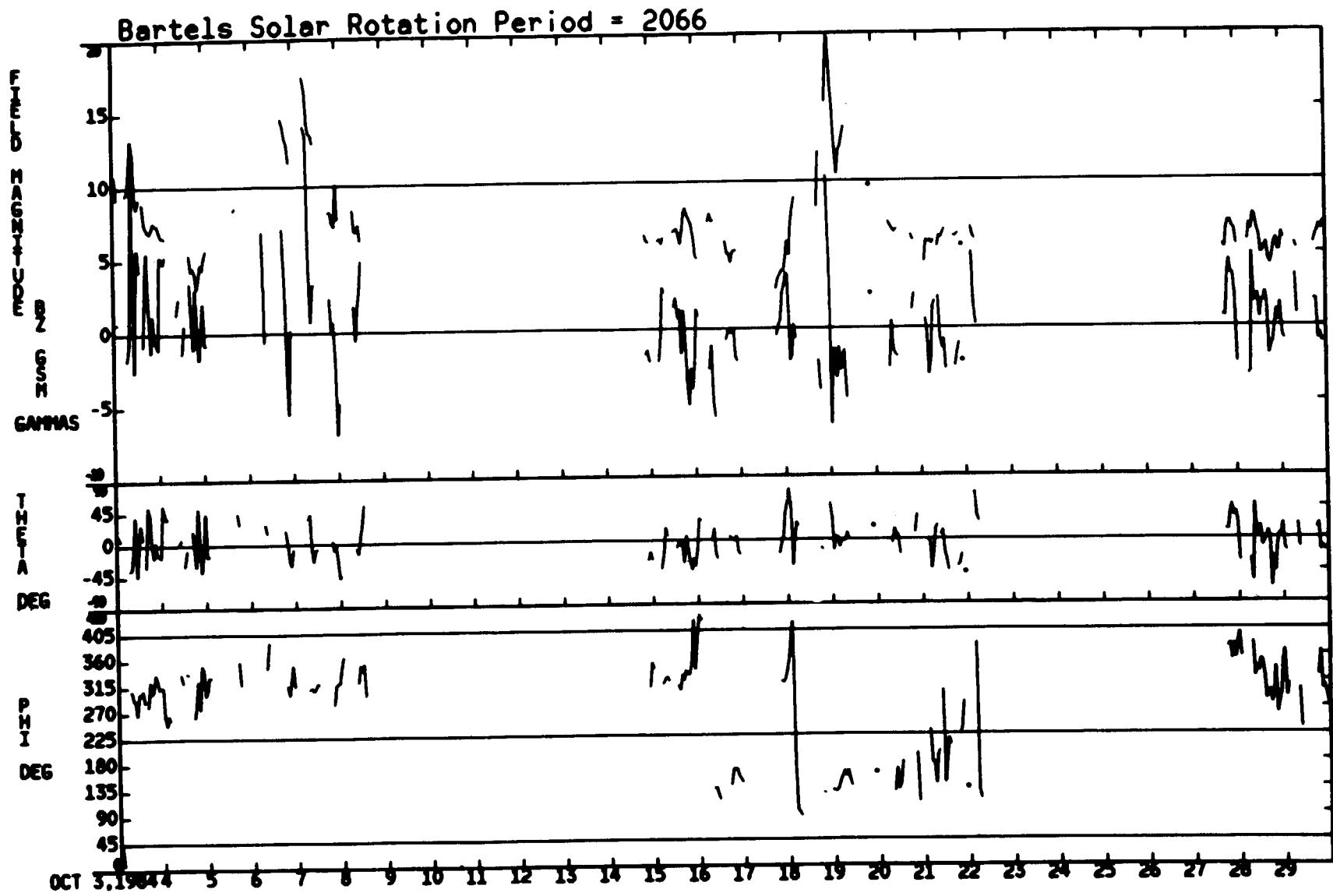
ORIGINAL PAGE IS  
OF POOR QUALITY  
09/06/84 - 10/02/84



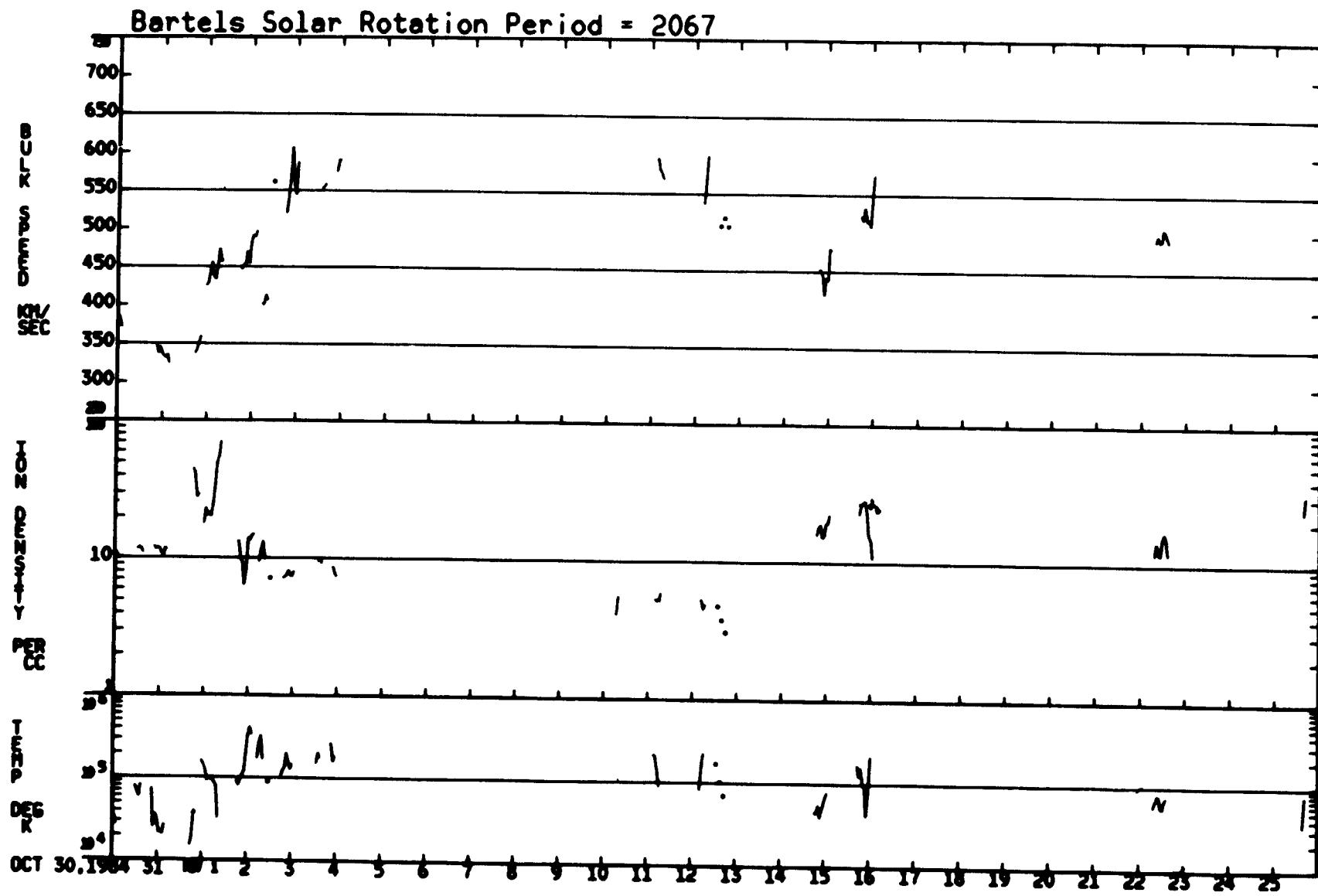
10/03/84 — 10/25/84



ORIGINAL PAGE IS  
OF POOR  
QUALITY  
10/03/84 – 10/25/84

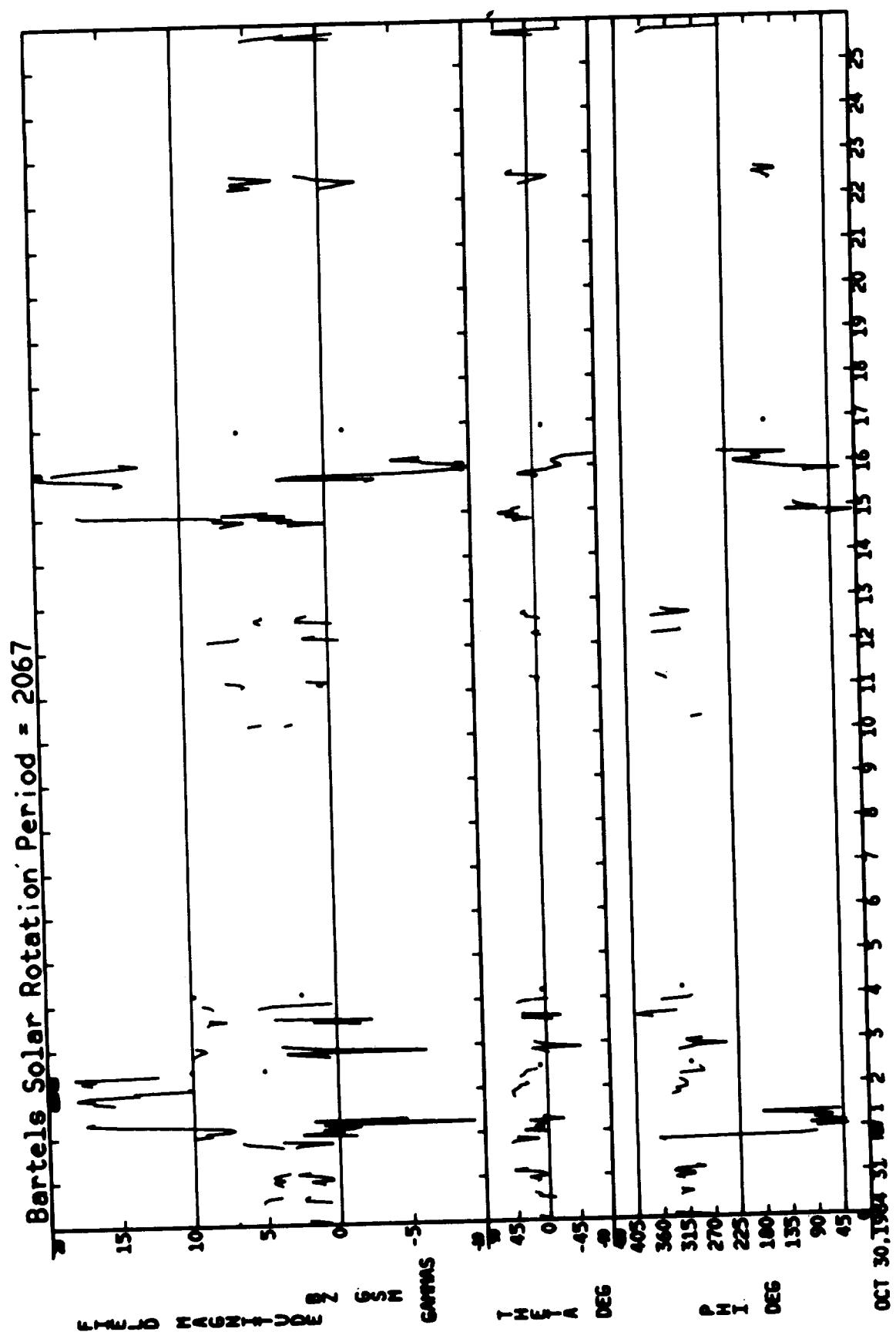


10/30/84 – 11/25/84

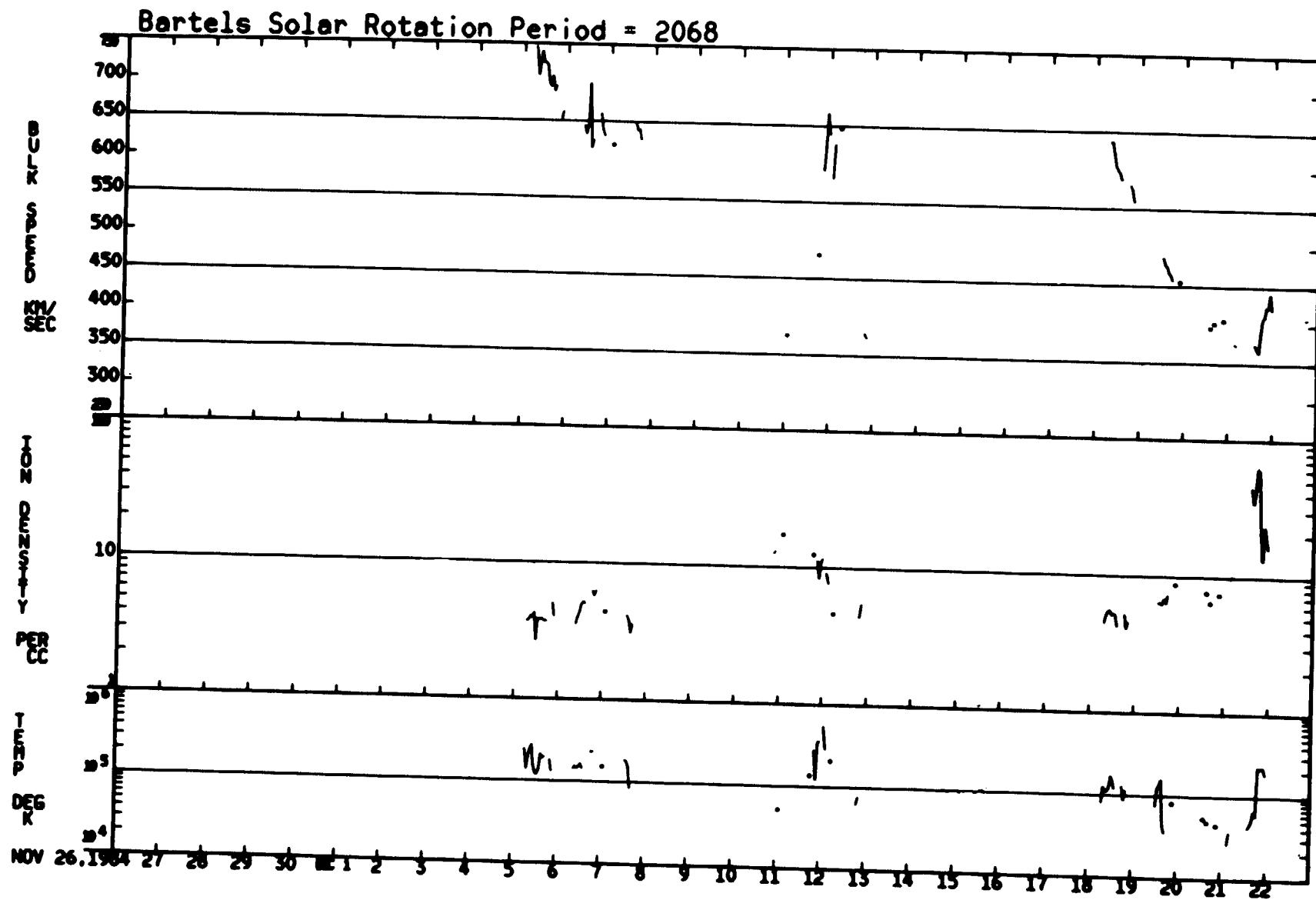


ORIGINAL PAGE IS  
OF POOR QUALITY

10/30/84 — 11/25/84



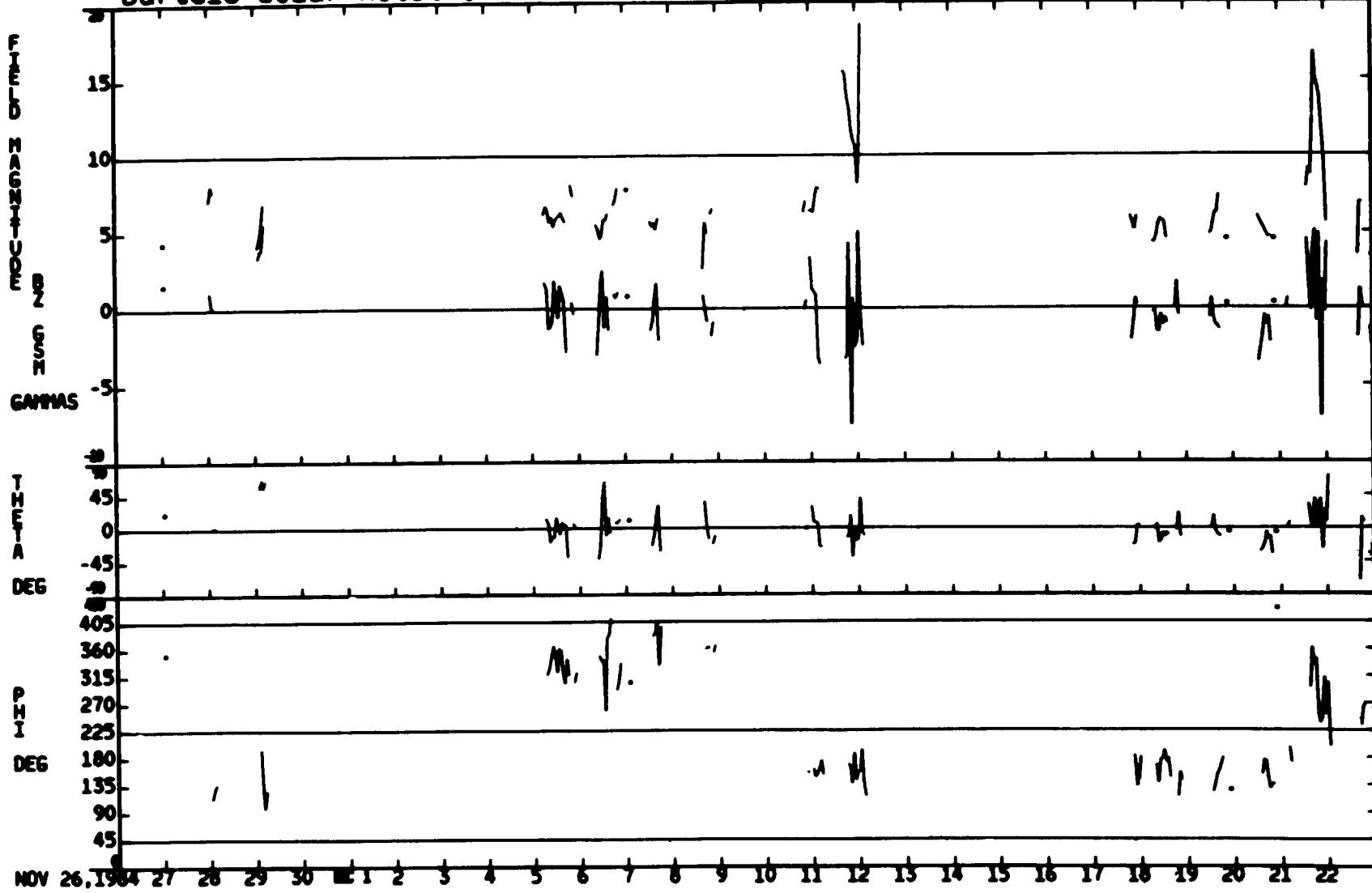
11/26/84 - 12/22/84



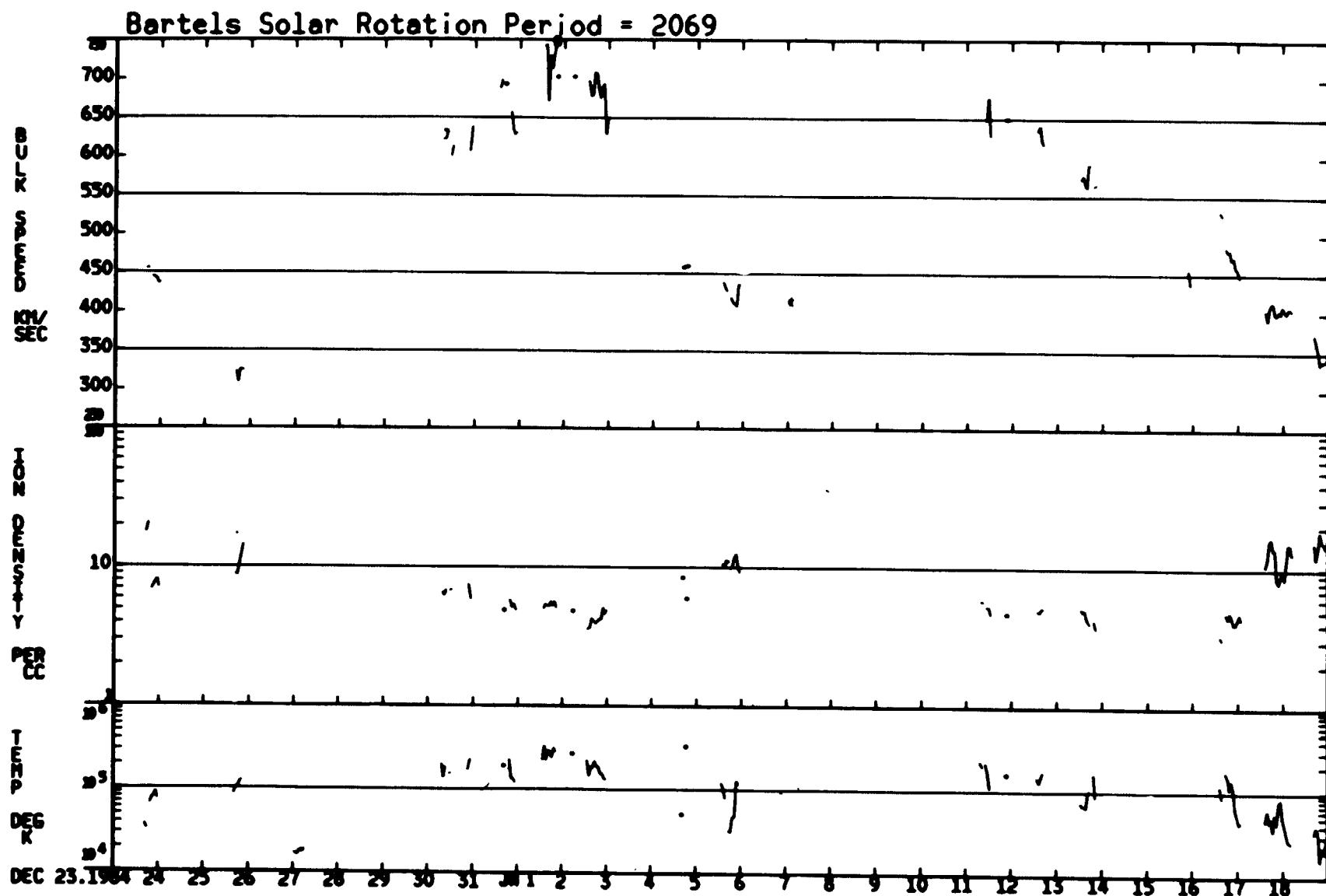
ORIGINAL PAGE IS  
OF POOR QUALITY

11/26/84 - 12/22/84

Bartels Solar Rotation Period = 2068

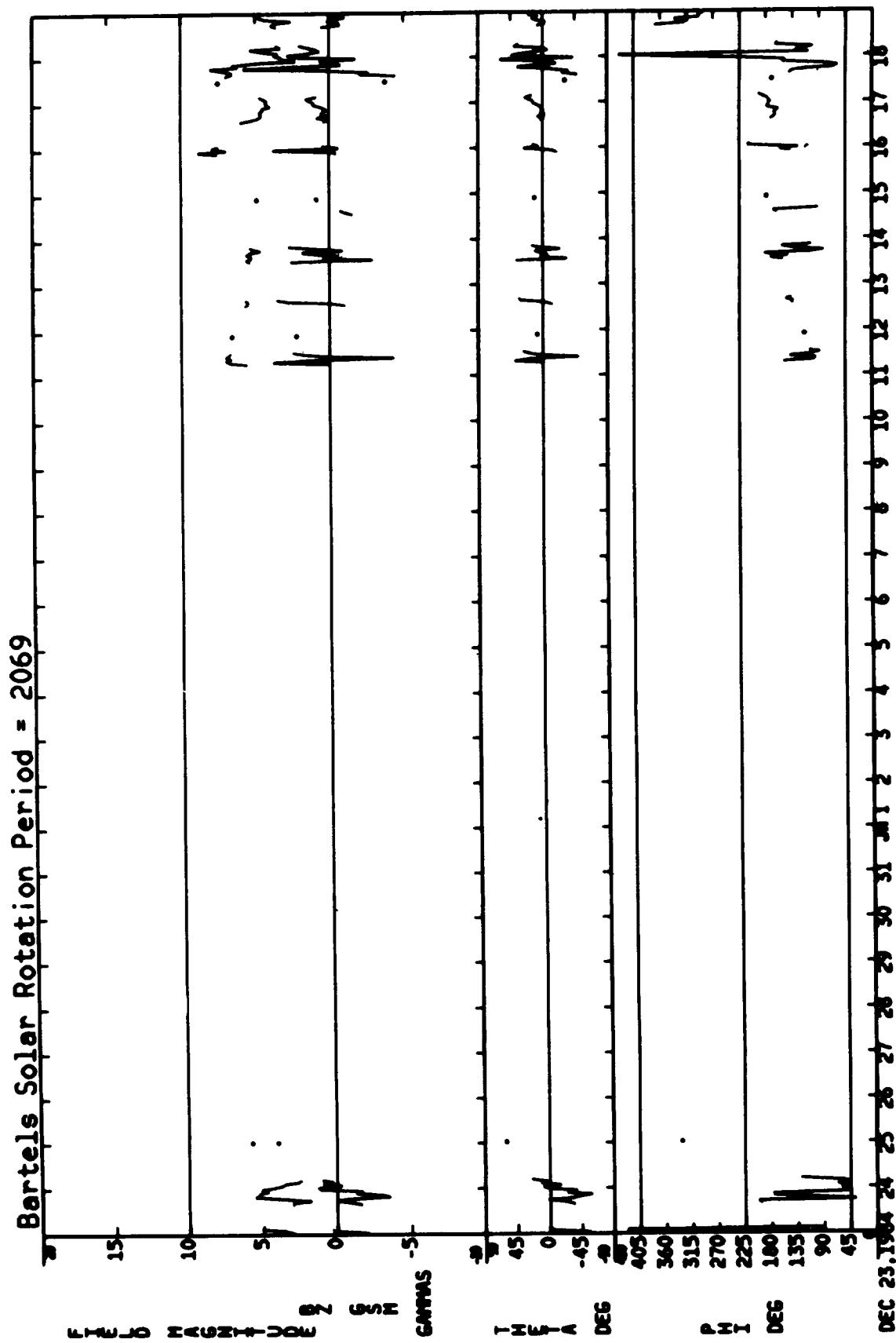


12/23/84 – 01/18/85

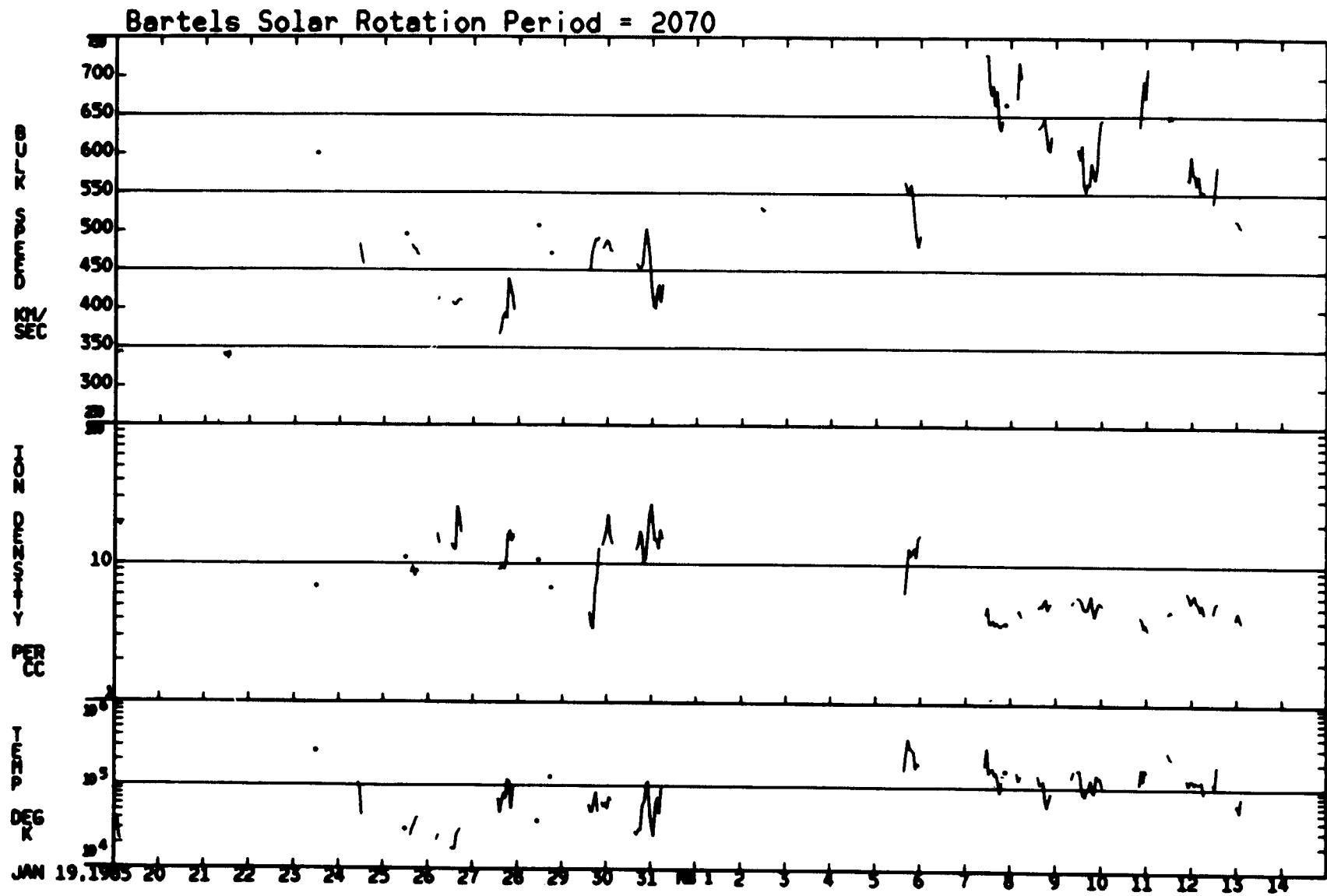


ORIGINAL PAGE IS  
OF POOR QUALITY

12/23/84 – 01/18/85

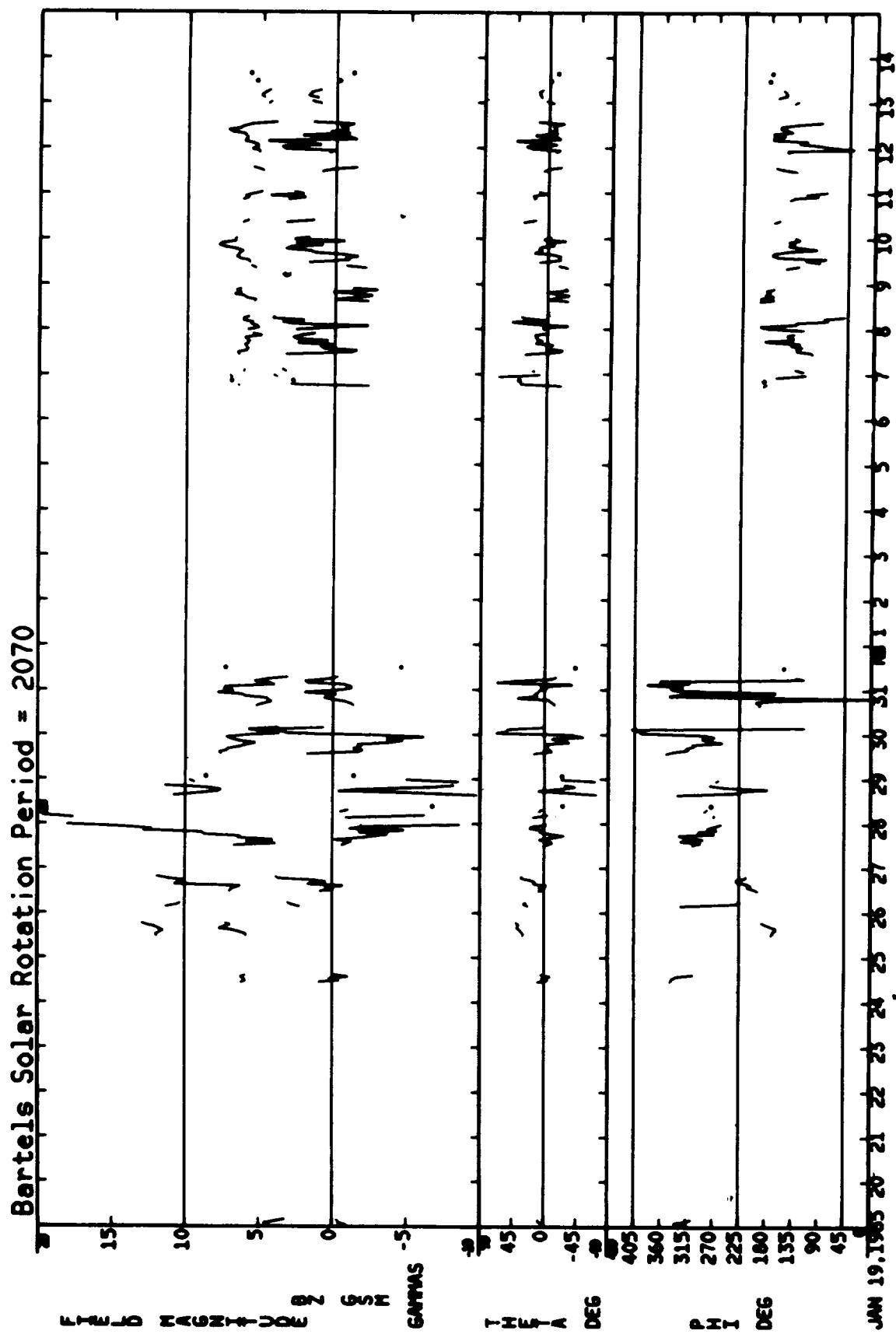


01/19/85 – 02/14/85

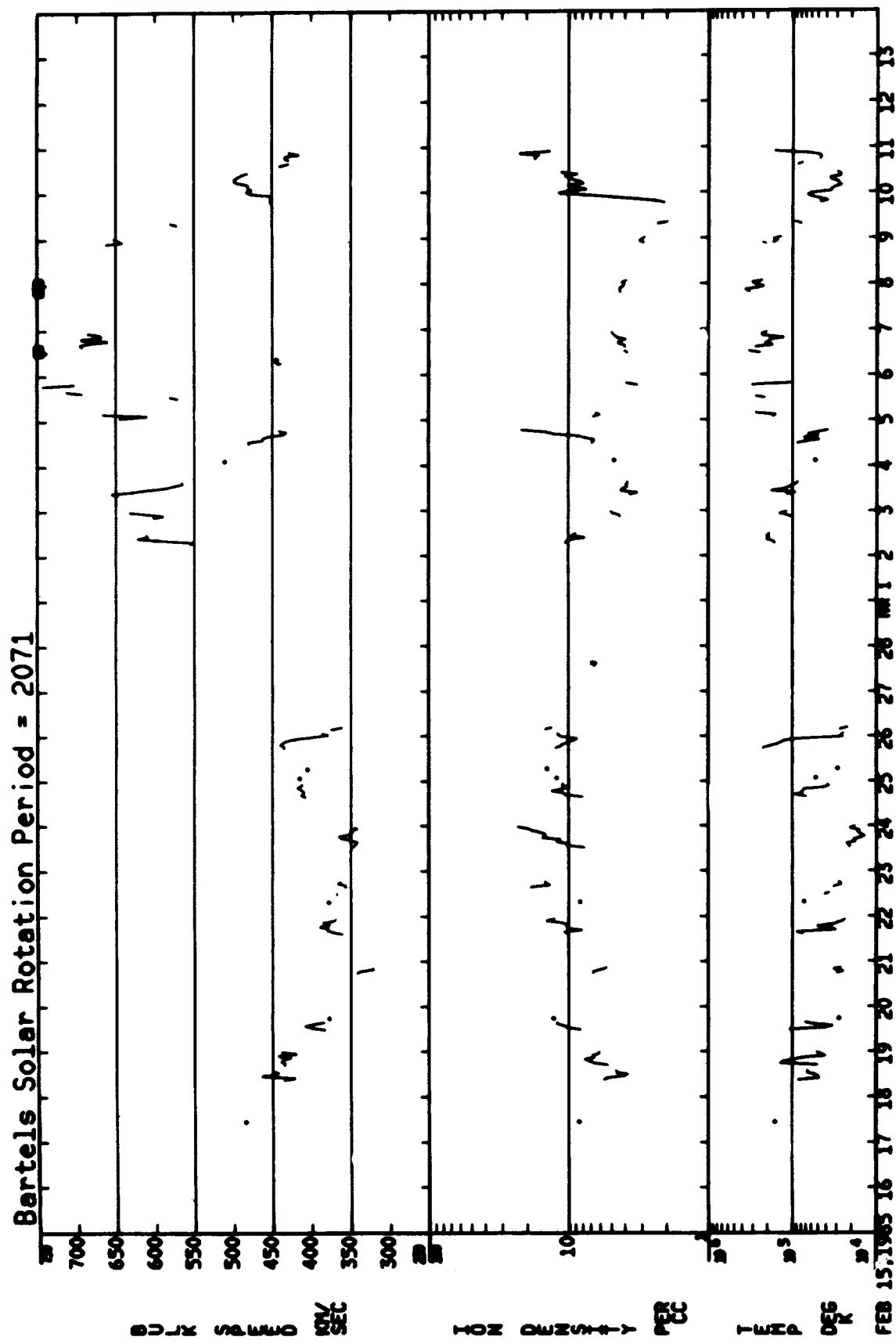


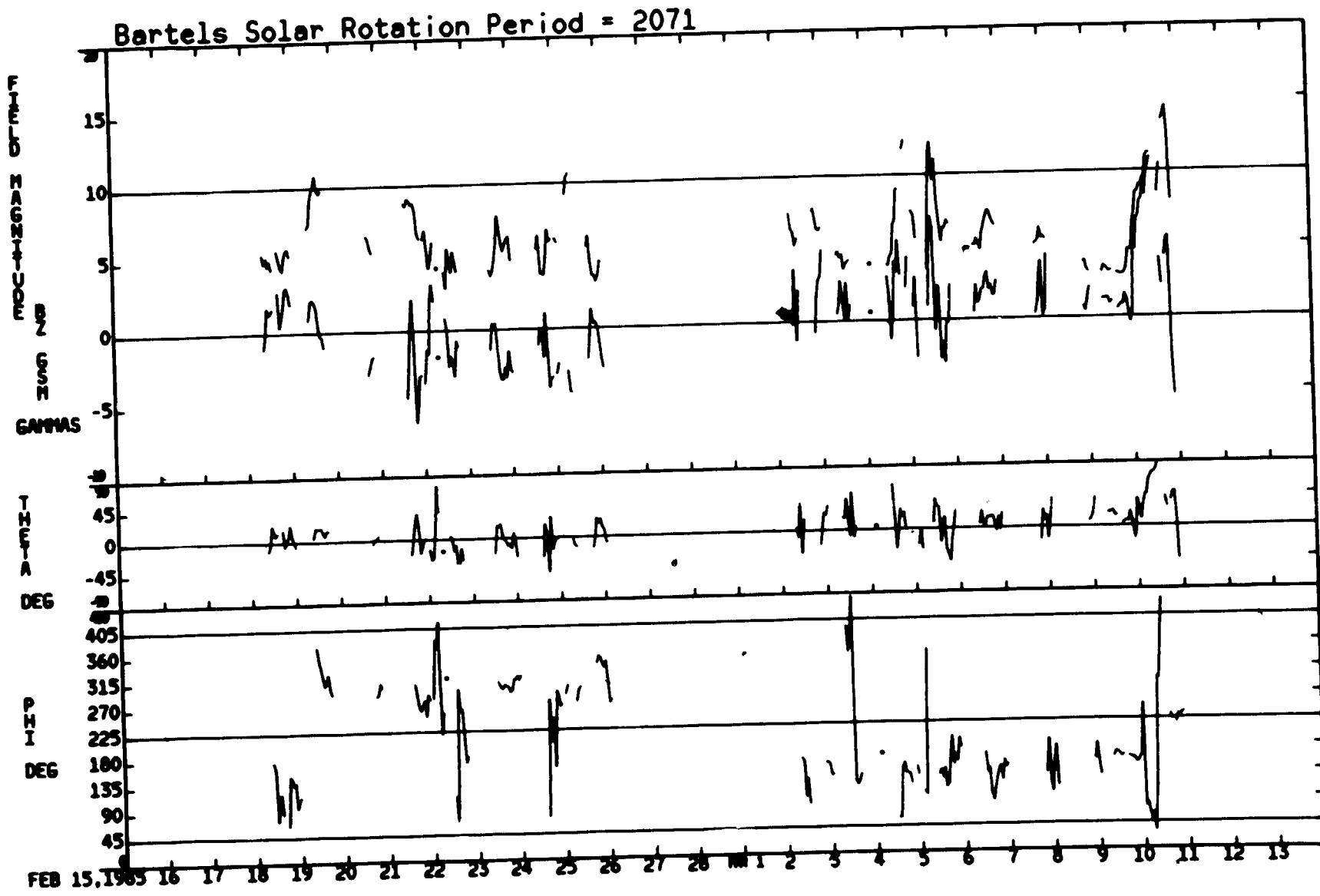
ORIGINAL PAGE IS  
OF POOR QUALITY

01/19/85 - 02/14/85



02/15/85 – 03/13/85

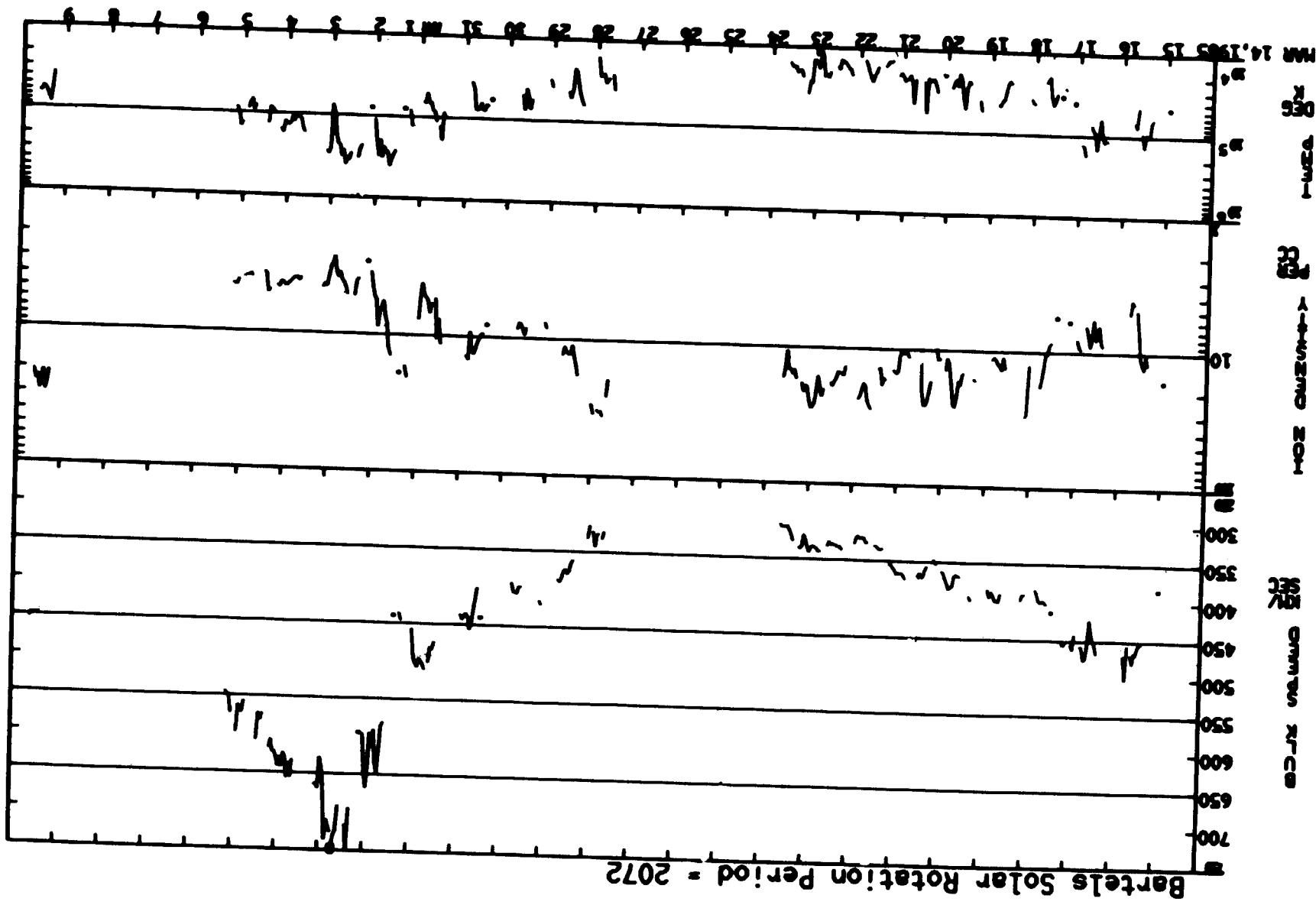




ORIGINAL PAGE IS  
OF POOR QUALITY

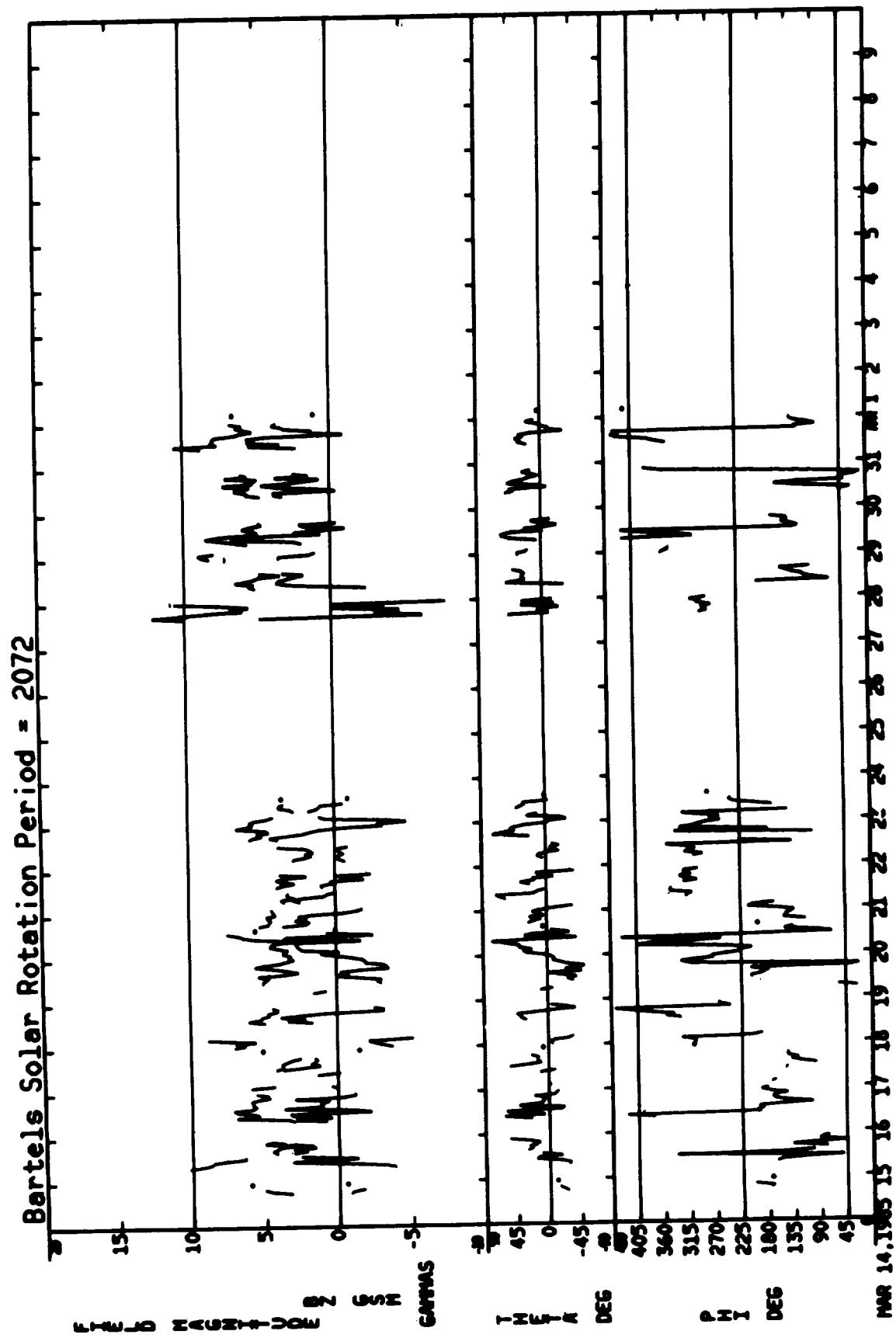
02/15/85 – 03/13/85

03/14/85 - 04/09/85

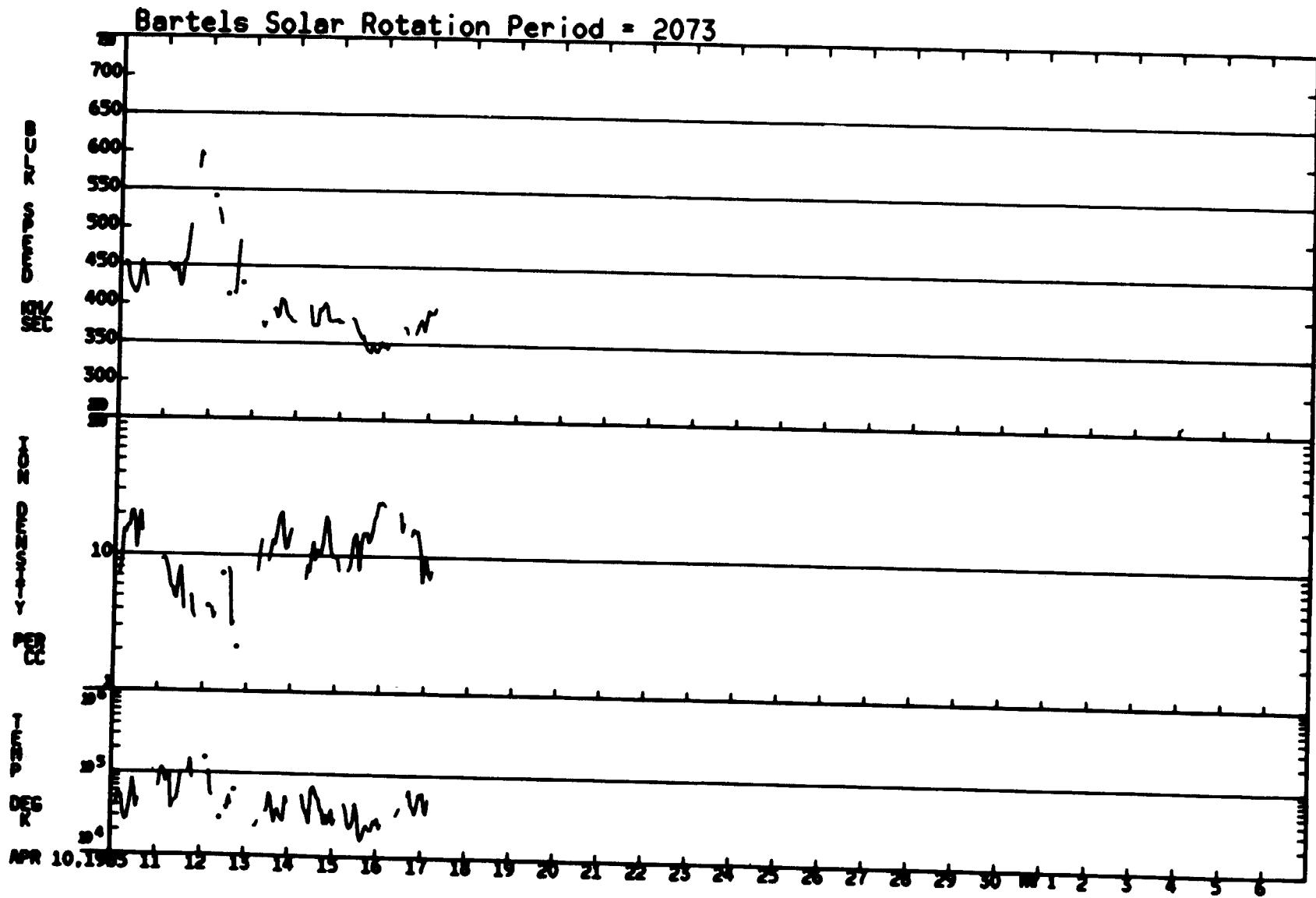


ORIGINAL PAGE IS  
OF POOR QUALITY

03/14/85 - 04/09/85



04/10/85 – 05/06/85



ORIGINAL PAGE IS  
OF POOR QUALITY

04/10/85 - 05/06/85

